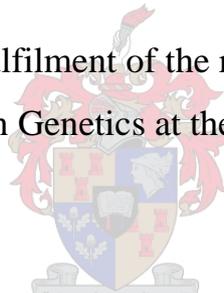


**The role of renin-angiotensin-aldosterone system
(RAAS) genes in the development of hypertrophy in
hypertrophic cardiomyopathy (HCM)**

N Carstens

Thesis presented in partial fulfilment of the requirements for the degree of
Master of Science (MSc) in Genetics at the University of Stellenbosch



Promoter: Prof JC Moolman-Smook

Co-promoter: Prof L van der Merwe

March 2009

DECLARATION

By submitting this thesis electronically, I declare that the entirety of the work contained therein is my own, original work, that I am the owner of the copyright thereof (unless to the extent explicitly otherwise stated) and that I have not previously in its entirety or in part submitted it for obtaining any qualification.

Date: 24 February 2009

Copyright © 2009 Stellenbosch University

All rights reserved

ABSTRACT

Hypertrophic cardiomyopathy (HCM), an inherited primary cardiac disorder mostly caused by defective sarcomeric proteins, is considered a model for studying left ventricular hypertrophy (LVH) in the absence of increased external loading conditions. The disease manifests extreme variability in the degree and pattern of LVH, even in HCM patients with the same causal mutation. The clinical phenotype of HCM can therefore be viewed as a product of the effect of sarcomere dysfunction and of additional genetic modifiers. Components of the renin-angiotensin-aldosterone system (RAAS) are plausible candidate modifiers because of their effect on blood pressure and their direct hypertrophic effect on cardiomyocytes.

The present study investigated genes encoding components of the RAAS for association with cardiac hypertrophy traits, in 353 individuals comprised of genetically and echocardiographically affected and unaffected family members, belonging to 22 HCM families with HCM founder mutations by employing a multi-SNP approach with TaqMan allelic discrimination technology. Gene-gene interaction analysis was also performed to investigate the effect of epistasis on hypertrophy. Candidate genes for analysis included the angiotensin II type 2 receptor (AT₂ receptor), renin, renin-binding protein (RnBP), the (pro)renin receptor, the mineralocorticoid receptor as well as genes encoding subunits of the epithelial sodium channels (ENaC) and Na⁺/K⁺-ATPase that showed evidence for cardiac expression.

The present study demonstrates for the first time that variations in the renin and RnBP genes play a role in modulating hypertrophy in HCM, independent of blood pressure and confirms the involvement of the AT₂ receptor in hypertrophy in HCM. Additionally we report an association between Na⁺/K⁺-ATPase α 1- and β 1-subunits as well as the ENaC α - and β -subunits and hypertrophy. Significant evidence for epistasis was found between renin and downstream RAAS effectors, suggesting a complex interplay between these RAAS variants and the hypertrophic phenotype in HCM. The identification of such modifiers for HCM may offer novel targets for hypertrophy research and ultimately anti-hypertrophic therapy.

OPSOMMING

Hipertrofiese kardiomiopatie (HKM), 'n oorerflike hartsiekte wat meestal veroorsaak word deur defektiewe sarkomeer proteïene, word beskou as 'n model vir die bestudering van linker ventrikulêre hipertrofie (LVH). Hierdie siekte toon groot variasie in die graad en verspreiding van LVH, selfs in individue met dieselfde HKM-veroorsakende mutasie. Die kliniese fenotipe van HKM kan dus gesien word as 'n produk van die effek van 'n defektiewe sarkomeer en addisionele genetiese modifiserende faktore. Komponente van die renien-angiotensien-aldosteron sisteem (RAAS) is moontlike kandidaat modifiserende faktore vir hipertrofie as gevolg van hul effek op bloeddruk en hul direkte hipertrofiese effek op kardiomiosiete.

Die huidige studie het gene wat kodeer vir RAAS komponente ondersoek vir assosiasie met hart hipertrofie metings in 'n kohort van 353 individue wat bestaan uit echokardiografies geaffekteerde en ongeaffekteerde familie lede uit 22 HKM families deur gebruik te maak van 'n multi-SNP benadering met TaqMan alleliese diskriminasie tegnologie. Geen-geen interaksie analise is ook gedoen om die effek van epistase op hipertrofie te ondersoek. Kandidaat gene vir analise het die volgende ingesluit: die angiotensien II tipe 2 reseptor (AT_2 reseptor), renien, renien-bindings proteïen (RnBP), die (pro)renien reseptor, die mineralokortikoïed reseptor sowel as gene wat kodeer vir subeenhede van die epiteel natrium kanale (ENaK) en Na^+/K^+ -ATPase wat wel in die hart uitgedruk word.

Die huidige studie demonstreer vir die eerste keer dat variasies in die renien en RnBP gene 'n rol speel in die ontwikkeling van hipertrofie, onafhanklik van hul effek op bloeddruk en bevestig die betrokkenheid van die AT_2 reseptor by hipertrofie in HKM. Ons rapporteer ook 'n assosiasie tussen Na^+/K^+ -ATPase α 1- and β 1-subeenhede sowel as ENaK α - and β -subeenhede en hipertrofie. Betekenisvolle bewyse vir epistase is gevind tussen renien en RAAS effektors wat dui op 'n komplekse interaksie tussen RAAS polimorfismes en die hipertrofiese fenotipe van HKM. Die identifikasie van modifiserende faktore vir HKM soos hierdie mag lei tot nuwe teikens vir hipertrofie navorsing en uiteindelik anti-hipertrofiese terapie.

INDEX	PAGE
ACKNOWLEDGEMENTS	iv
LIST OF ABBREVIATIONS	v
LIST OF FIGURES	xi
LIST OF TABLES	xiii
1. INTRODUCTION	1
2. MATERIALS AND METHODS	22
3. RESULTS	39
4. DISCUSSION	89
APPENDIX I	110
APPENDIX II	112
REFERENCES	141

ACKNOWLEDGEMENTS

I would like to express my sincere gratitude to the following people who assisted me during the course of this degree:

Prof Hanlie Moolman-Smook and Prof Lize van der Merwe for their invaluable guidance, expertise, time and effort. I am truly blessed to have the opportunity to work with you.

Dr Craig Kinnear and Ms Kashefa Carelse-Tofa for their emotional and technical support with the TaqMan allelic discrimination analysis. Mr Ruben Cloete and the whole MAGIC lab team for their assistance, support and two wonderful, unforgettable years.

My family and friends: for your support, understanding and putting up with my absence and mood swings. Lehani, for being there every step of the way. Adriaan, for your incredible support and understanding these past few months.

My Lord and Saviour, for giving me hope and strength when I so desperately needed it.

LIST OF ABBREVIATIONS

α	alpha
β	beta
γ	gamma
$^{\circ}\text{C}$	degrees Celsius
11 β -HSD2	11 β -hydroxysteroid-dehydrogenase type 2
2-D	two-dimensional
3'	three prime
5'	five prime
A	adenine
ABI	Applied Biosystems Incorporated
ACE	angiotensin-converting enzyme
ACE2	angiotensin-converting enzyme 2
ACTC1	α -cardiac actin
AGT	angiotensinogen
AGTR1	Angiotensin II type I receptor gene
AGTR2	Angiotensin II type II receptor gene
aIVSmit	anterior interventricular septum thickness at the mitral valve
aIVSpap	anterior interventricular septum thickness at the papillary level
Ang	angiotensin
ARB	Angiotensin II receptor blocker
ASREA	allele specific restriction enzyme analysis
AT ₁ receptor	Angiotensin II type I receptor
AT ₂ receptor	Angiotensin II type II receptor
ATP1A1	ATPase, Na ⁺ /K ⁺ transporting, alpha 1 polypeptide
ATP1A2	Na ⁺ /K ⁺ transporting, alpha 2 polypeptide
ATP1B1	Na ⁺ /K ⁺ transporting, beta 1 polypeptide
ATP1B3	Na ⁺ /K ⁺ transporting, beta 3 polypeptide
ATP6AP2	ATPase, H ⁺ transporting, lysosomal accessory protein 2
ATPase	adenosine triphosphatase

AV	aortic valve
AWapx	anterior wall thickness at the supra-apex level
AWmit	anterior wall thickness at the mitral valve
AWpap	anterior wall thickness at the papillary level
BP	blood pressure
BSA	body surface area
C	cytosine
Ca ²⁺	calcium
CEU	HapMap population: parent-offspring trios with northern and western European ancestry
CHB	HapMap population: unrelated Han Chinese individuals from Beijing, China
<i>CMA</i>	cardiac chymase
Comp1	Principle component score
CWT	cumulative wall thickness
<i>CYP11B2</i>	aldosterone synthase
DNA	Deoxyribo Nucleic Acid
EDTA	ethylene-diamine-tetra-acetic acid
ENaC	epithelial Na ⁺ channels
EPHESUS	eplerenone post acute myocardial infarction efficacy and survival study
G	guanine
GLAECO	Glasgow Heart Scan
GLAEOLD	Glasgow Heart Scan Old
H ⁺	Hydrogen
HCM	hypertrophic cardiomyopathy
HF	heart failure
HOPE	Heart Outcomes Prevention Evaluation
HR	heart rate
HSP27	heat-shock protein 27
HWE	Hardy-Weinberg equilibrium

Hz	Hertz
I/D	insertion/deletion
IBD	identity-by-descent
IVS	interventricular septum
IVSapx	interventricular septum thickness at the supra-apex level
IWmit	inferior wall thickness at the mitral valve
IWpap	inferior wall thickness at the papillary level
JAK	janus kinase
JPT	HapMap population: unrelated Japanese individuals from Tokyo, Japan
K ⁺	potassium
kb	kilo bases
LA	left atrium
<i>LAMP2</i>	lysosomal-associated membrane protein 2
LD	linkage disequilibrium
LDU	linkage disequilibrium unit
LIFE	Losartan Intervention for Endpoint reduction
LOD	logarith of odds
LV	left ventricle
LVH	left ventricular hypertrophy
LVM	left ventricular mass
LVOT	left ventricular outflow tract
LVWT	left ventricular wall thickness
LWapx	lateral wall thickness at the supra-apex level
LWmit	lateral wall thickness at the mitral valve
LWpap	lateral wall thickness at the papillary level
M6P	Mannose-6-Phosphate
MAF	minor allele frequency
MAPK	mitogen-activated protein kinase
MC	mutation carrier
MGB	minor groove binder

min	minute
mIVST	maximal interventricular septum thickness
mIVSTmit	maximal interventricular septum thickness at the mitral valve
mIVSTpap	maximal interventricular septum thickness at the papillary level
mLVWT	maximal left ventricular wall thickness
mLVWTapx	maximal left ventricular wall thickness at the supra-apex level
mLVWTmit	maximal left ventricular wall thickness at the mitral valve
mLVWTpap	maximal left ventricular wall thickness at the papillary level
mPWT	maximal posterior wall thickness
MR	mineralocorticoid receptor
mRNA	messenger ribonucleic acid
MV	mitral valve
<i>MYBPC3</i>	cardiac myosin-binding protein C
<i>MYH6</i>	α -myosin heavy chain
<i>MYH7</i>	β -myosin heavy chain
<i>MYL2</i>	regulatory myosin light chains
<i>MYL3</i>	essential myosin light chains
Na ⁺	sodium
Na ⁺ /Ca ²⁺ exchanger	sodium calcium exchanger
Na ⁺ /K ⁺ -ATPase	sodium-potassium pump
NaCl	sodium chloride
NAGE	N-acetyl-D-glucosamine 2-epimerase
NC	non-carrier
NCBI	National Center for Bioinformatics
<i>NCX3</i>	sodium-calcium exchanger 3
Nedd4-2	neural precursor cell expressed, developmentally downregulated-4-2
NFQ	nonfluorescent quencher
<i>NR3C2</i>	nuclear receptor subfamily 3, group C, member 2
PAI-1	plasminogen activator inhibitor-1
PCR	polymerase chain reaction

pIVSmit	posterior interventricular septum thickness at the mitral valve
pIVSpap	posterior interventricular septum thickness at the papillary level
PRA	plasma renin activity
<i>PRKAG2</i>	AMP-dependant protein kinase
PWapx	posterior wall thickness at the supra-apex level
PWmit	posterior wall thickness at the mitral valve
PWpap	posterior wall thickness at the papillary level
QTDT	quantitative transmission disequilibrium test
QTL	quantitative trait locus
RAAS	renin-angiotensin-aldosterone system
RALES	randomized aldactone evaluation study
<i>REN</i>	renin
<i>RENBP</i>	renin binding protein
RnBP	renin-binding protein
ROS	reactive oxygen species
RSA	Republic of South Africa
RVOT	right ventricular outflow tract
SB	di-sodium tetraborate-decahydrate
SCD	sudden cardiac death
<i>SCNN1A</i>	sodium channel, nonvoltage-gated 1 alpha
<i>SCNN1B</i>	sodium channel, nonvoltage-gated 1 beta
<i>SCNN1G</i>	sodium channel, nonvoltage-gated 1 gamma
SDS	Sequence Detection Systems
sec	second
SNP	single nucleotide polymorphism
STAT	Signal transducers and activators of transcription
STR	short tandem repeat
T	thymine
TGF	transforming growth factor
TGF- β	transforming growth factor beta
T _m	melting temperature

<i>TNNC1</i>	cardiac troponin C
<i>TNNI3</i>	cardiac troponin I
<i>TNNT2</i>	cardiac troponin T
t-PA	tissue-type plasminogen activator
<i>TPM1</i>	α -tropomyosin
<i>TTN</i>	titin
UK	United Kingdom
USA	United States of America
UV	ultra-violet
V	Volts
v	version
YRI	HapMap population: parent-offspring trios from the Yoruba people in Ibadan, Nigeria

LIST OF FIGURES

FIGURE	PAGE
CHAPTER 1	
Figure 1.1. The pathology of hypertrophic cardiomyopathy.	4
Figure 1.2. Diagram of the sarcomere, showing the thick and thin filaments.	6
Figure 1.3. An overview of the renin-angiotensin-aldosterone system (RAAS).	11
Figure 1.4. The renin-angiotensin-aldosterone system (RAAS) in the heart.	14
 CHAPTER 2	
Figure 2.1. Graphical representative example of the heart being divided into 3 levels.	25
Figure 2.2. Overview of TaqMan allelic discrimination technology.	33
 CHAPTER 3	
Figure 3.1. Representative genotyping result for TaqMan allelic discrimination.	44
Figure 3.2. A representation of the eight alleles observed in the present study for the AGAT repeat STR.	46
Figure 3.3. Allele frequencies for the AGAT repeat in <i>NR3C2</i> .	49
Figure 3.4. Allele frequencies for SNPs in <i>AGTR2</i> .	50
Figure 3.5. Allele frequencies for SNPs in <i>RENBP</i> .	51
Figure 3.6. Allele frequencies for SNPs in <i>ATP6AP2</i> .	52
Figure 3.7. Allele frequencies for SNPs in <i>REN</i> .	53
Figure 3.8. Allele frequencies for SNPs in <i>ATP1A1</i> .	54
Figure 3.9. Allele frequencies for SNPs in <i>ATP1A2</i> .	54
Figure 3.10. Allele frequencies for SNPs in <i>ATP1B1</i> .	55
Figure 3.11. Allele frequencies for the SNP in <i>ATP1B3</i> .	56

Figure 3.12. Allele frequencies for SNPs in <i>SCNNIA</i> .	57
Figure 3.13. Allele frequencies for SNPs in <i>SCNNIG</i> .	58
Figure 3.14. Allele frequencies for SNPs in <i>SCNNIB</i> .	59
Figure 3.15. Pairwise LD structure for <i>AGTR2</i> .	61
Figure 3.16. Pairwise LD structure for <i>REN</i> (A), <i>RENBP</i> (B) and <i>ATP6AP2</i> (C).	62
Figure 3.17. Pairwise LD structure for <i>ATPIA1</i> (A), <i>ATPIA2</i> (B) and <i>ATP1B1</i> (C).	62
Figure 3.18. Pairwise LD structure for <i>SCNNIA</i> (A), <i>SCNNIB</i> (B) and <i>SCNNIG</i> (C).	63
Figure 3.19. An illustration of the interaction between rs2269370 in <i>RENBP</i> and rs1464816 in <i>REN</i> on mLVWT.	81
Figure 3.20. An illustration of the interaction between rs10900555 in <i>REN</i> and rs2303153 in <i>SCNNIB</i> on mLVWT.	82
Figure 3.21. An illustration of the interaction between rs1040503 in <i>ATP1B1</i> and rs1464816 and rs5705 in <i>REN</i> on mLVWT and LVM.	83
Figure 3.22. An illustration of the interaction between rs2968917 in <i>ATP6AP2</i> and rs250563 in <i>SCNNIB</i> on mLVWT.	84
Figure 3.23. An illustration of the interaction between a subset of the ENaC subunit genes on mLVWT.	85
Figure 3.24. An illustration of the interaction between rs1358714 in <i>ATP1B1</i> and rs11614164 and rs3782726 in <i>SCNNIA</i> on LVM and mLVWT.	86
Figure 3.25. An illustration of the interaction between rs2068230 in <i>ATP1B3</i> and three SNPs on LVM and mLVWT: rs11614164 in <i>SCNNIA</i> and rs238547 and rs250563 in <i>SCNNIB</i> .	88

LIST OF TABLES

TABLE	PAGE
CHAPTER 1	
Table 1.1. Sarcomere protein genes identified as causal genes for HCM.	7
CHAPTER 2	
Table 2.1. South African HCM-affected families of Caucasian and Mixed Ancestry descent that were analysed in the present study.	24
Table 2.2. Summary of echocardiographically determined hypertrophy traits and composite scores used to describe the degree and distribution of cardiac hypertrophy.	27
Table 2.3. Candidate genes chosen for investigation.	29
Table 2.4. SNPs chosen for investigation as well as the respective TaqMan assays used for genotyping each polymorphism.	31
CHAPTER 3	
Table 3.1. Basic characteristics of the study cohort stratified into mutation carrier (MC) and non-carrier (NC) groups according to HCM mutation status.	41
Table 3.2. Minor allele frequencies (MAF) of each SNP covered in the present study in the HapMap YRI, CEU and JPT + CHB population groups.	43
Table 3.3. Exact Hardy-Weinberg equilibrium p-values calculated for unrelated individuals.	48
Table 3.4. Results from the association analysis: p-values for association between the AGAT repeat in <i>NR3C2</i> and hypertrophy traits.	65
Table 3.5. Results from the association analysis: p-values for association between variants in <i>AGTR2</i> and hypertrophy traits.	67
Table 3.6. Effect sizes for the significant associations obtained in the association analysis of <i>AGTR2</i> .	68

Table 3.7. Results from the association analysis: p-values for association between variants in <i>REN</i> , <i>RENBP</i> and <i>ATP6AP2</i> and hypertrophy traits.	69
Table 3.8. Effect sizes for the significant associations obtained in the association analysis of <i>REN</i> and <i>RENBP</i> .	70
Table 3.9. Results from the association analysis: p-values for association between variants in <i>ATPIA1</i> , <i>ATPIA2</i> , <i>ATP1B1</i> and <i>ATP1B3</i> and hypertrophy traits.	72
Table 3.10. Effect sizes for the significant associations obtained in the association analysis of <i>ATPIA1</i> and <i>ATP1B1</i> .	73
Table 3.11. Results from the association analysis: p-values for association between variants in <i>SCNNIA</i> and <i>SCNNIG</i> and hypertrophy traits.	74
Table 3.12. Results from the association analysis: p-values for association between variants in <i>SCNNIB</i> and hypertrophy traits.	76
Table 3.13. Effect sizes for the significant associations obtained in the association analysis of <i>SCNNIA</i> and <i>SCNNIB</i> .	77
Table 3.14. Results from the gene-gene interaction analysis between all the SNPs for the various hypertrophy traits.	78
Table 3.15. Results from the gene-gene interaction analysis between all the SNPs for the various hypertrophy traits.	79
Table 3.16. The distribution of the number of hypertrophy traits that were affected by highly significant interactions ($p < 0.01$).	80
Table 3.17. Highly significant SNP interactions.	80

CHAPTER 1
INTRODUCTION

INDEX	PAGE
1.1 LEFT VENTRICULAR HYPERTROPHY (LVH)	2
1.2 HYPERTROPHIC CARDIOMYOPATHY (HCM)	3
1.2.1 Molecular genetics of HCM	5
1.2.2 Clinical variability in HCM	7
1.2.3 Candidate gene modifiers of HCM	9
1.3 RENIN-ANGIOTENSIN-ALDOSTERONE SYSTEM (RAAS)	10
1.3.1 RAAS genes in the heart	13
1.3.2 RAAS genes in hypertension	14
1.3.3 RAAS genes in LVH	15
1.3.3.1 <i>In vitro</i> studies	15
1.3.3.2 Animal models	16
1.3.3.3 RAAS activity in human cardiovascular pathologies	17
1.3.3.4 Clinical studies	17
1.3.3.5 Genetic association studies	18
1.3.4 RAAS genes implicated in HCM: previous association studies	18
1.4 THE PRESENT STUDY	19
1.4.1 AT₂ Receptor	20
1.4.2 Renin and renin-associated genes	20
1.4.3 MR	20
1.4.4 ENaC subunits	21
1.4.5 Na⁺/K⁺-ATPase subunits	21

CHAPTER 1: INTRODUCTION

1.1 LEFT VENTRICULAR HYPERTROPHY (LVH)

Left ventricular hypertrophy (LVH) is acknowledged as a major risk factor for cardiovascular morbidity and mortality. Increased LVH has been shown to predict the development of congestive heart failure (HF) (Mathew et al., 2001), coronary heart disease (Devereux and Roman, 1993), stroke (Verdecchia et al., 2001), cardiac arrhythmias (McLenachan et al., 1987) and sudden cardiac death (SCD) (Haider et al., 1998).

Regression of LVH is associated with a higher life expectancy (Sharp and Mayet, 2002) and better clinical prognosis (Verdecchia et al., 1998). This is also evident from the Heart Outcomes Prevention Evaluation (HOPE) and Losartan Intervention for Endpoint reduction (LIFE) studies. In the HOPE trial, cardiovascular morbidity and mortality was significantly reduced by regression of LVH with ramipril (Mathew et al., 2001). In the LIFE study, the risk for SCD, myocardial infarction and stroke was significantly reduced with reduction in left ventricular mass (LVM), an indicator of LVH, independent of systolic blood pressure (BP) or treatment administered (Devereux et al., 2004).

Previous studies have shown that LVH is the most common cardiac complication caused by hypertension (Levy et al., 1990). However, antihypertensive treatment has not reduced morbidity and mortality from cardiovascular disease associated with LVH as would be expected for the degree of BP reduction (Koren et al., 1991) and LVH has also been observed in normotensive subjects (Levy et al., 1990; Schunkert et al., 1999). LVH is consequently not only attributable to pressure overload, but also to non-haemodynamic factors (Lijnen and Petrov, 1999).

It is therefore evident that understanding the underlying determinants of LVH is vital to facilitate more effective therapeutic intervention. Identifying molecular markers associated with LVH would enable improved risk stratification for cardiac morbidity in susceptible individuals. Identifying such markers, particularly genetic markers, is more easily achieved by means of family-based studies. Hypertrophic cardiomyopathy (HCM), an inherited disease characterised by LVH, has proven to be a valuable model to investigate the molecular mechanisms involved in hypertrophy development (Watkins et al., 1995a).

1.2. HYPERTROPHIC CARDIOMYOPATHY (HCM)

HCM is a primary cardiac disorder characterized clinically by primary LVH that occurs in the absence of increased external loading conditions (Marian 2002), as well as diastolic dysfunction, arrhythmias and sudden death (Kaufman et al., 2007). The prevalence of HCM has been shown to be as 0.002% in young adults through population-based clinical studies (Maron et al., 1995). However, a much higher prevalence is expected in older individuals, based on the fact that HCM penetrance is age dependant (Niimura et al., 2002).

In HCM, the cardiac mass is increased due to left ventricular wall thickening that is frequently asymmetric most often involves thickening of the interventricular septum (Seidman and Seidman, 2001). As a consequence of this hypertrophy, the left ventricular chamber volumes are severely decreased as illustrated in figure 1.1A. However, the myocardial hypertrophy observed in HCM is extremely variable in extent and localisation (Wigle, 1995). Ventricular septal hypertrophy is the most frequently observed type of asymmetrical hypertrophy, with midventricular, apical, right ventricular and concentric hypertrophy being less common (Wigle et al., 1995).

Histopathology of HCM shows abnormal hypertrophic growth of the individual myocytes as well as myocyte disarray and interstitial fibrosis, as shown in figure 1.1B (Chung et al., 2003).

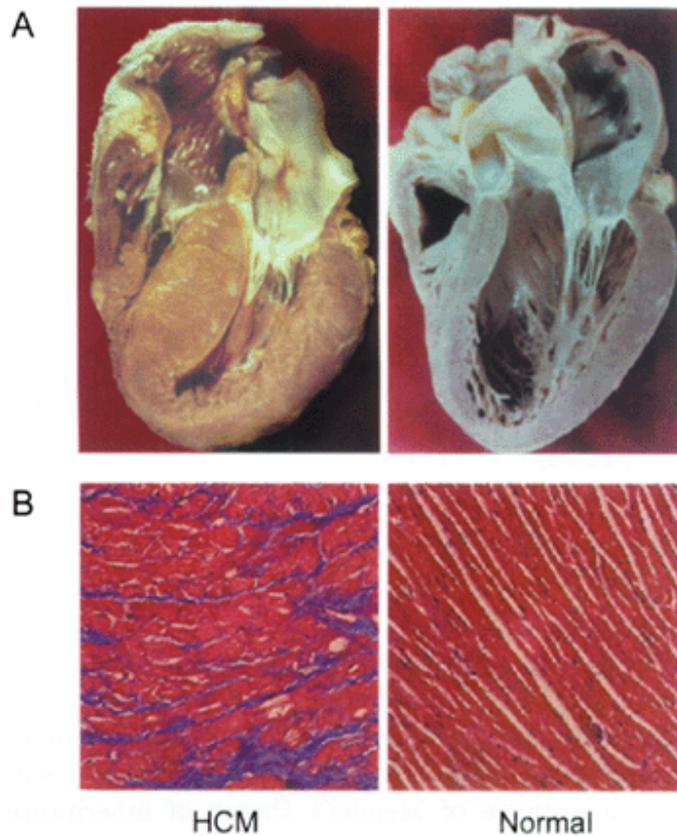


Figure 1.1. The pathology of hypertrophic cardiomyopathy. A. Post-mortem examination of a heart from an individual with HCM illustrating massive asymmetric left ventricular hypertrophy with an associated reduction in left ventricular cavity size, compared to a normal heart. **B.** Histopathology of heart sections stained with Masson's trichrome demonstrating the significant myofibre disarray and interstitial fibrosis observed in HCM (taken from Chung et al., 2003).

Clinical diagnosis of HCM is established most easily with two-dimensional (2-D) echocardiography by imaging the hypertrophied but nondilated LV chamber (Maron and McKenna et al., 2003). Clinical presentation in patients with HCM varies greatly, some patients present with minimal or no symptoms and have a benign, asymptomatic course, while others develop more serious complications, such as cardiac arrhythmias and HF, with one of the most severe endpoints being sudden death (Tsoutsman et al., 2006).

The HCM phenotype is not stagnant; LVH can develop at virtually any age and increase or decrease dynamically throughout life (Maron, 2002). This is confirmed by the fact that a small subset of HCM patients progress to the “burned-out” phase, with characteristic features being LV wall thinning, cavity enlargement, systolic dysfunction and HF (Maron et al., 1987; Spirito et al.,

1997) and the fact that some patients experience slight regression in left ventricular (LV) wall thickness with aging, reflecting progressive cardiac remodelling (Spirito and Maron, 1989).

1.2.1 Molecular genetics of HCM

HCM is classically described as a disease of the sarcomere (Thierfelder et al., 1994). Primary HCM is inherited as an autosomal dominant trait and to date 450 different causal mutations have been identified within 13 sarcomere- and myofilament-related genes (reviewed in Alcalai et al., 2008). Sarcomeres, as part of myofibrils, constitute the contractile elements in cardiac muscle. The sarcomere is comprised of thick and thin filaments. The thick filament primarily consists of myosin-binding protein C and the myosin heavy and light chains, while the thin filament consists primarily of actin, α -tropomyosin and troponins I, C and T (figure 1.2).

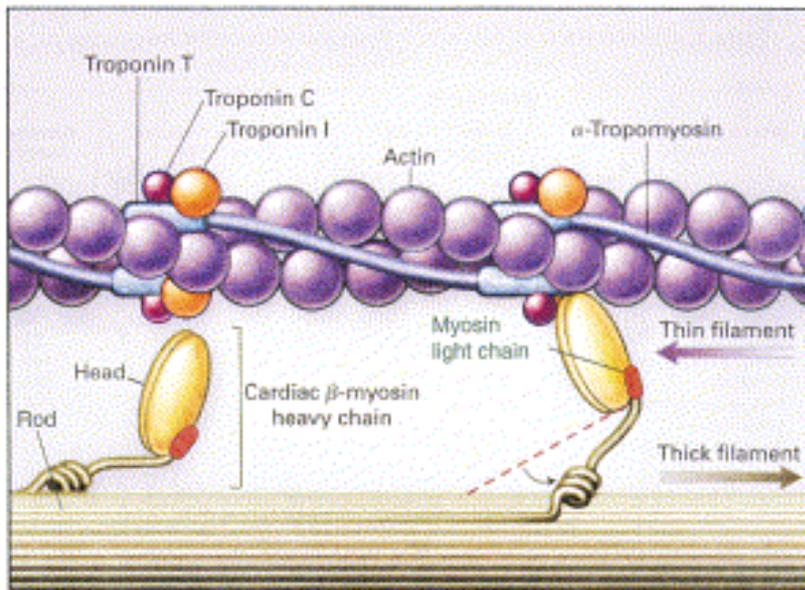


Figure 1.2. Diagram of the sarcomere, showing the thick and thin filaments (taken from Seidman and Seidman, 2001).

The first causal mutation identified for HCM was a missense mutation in the β -myosin heavy chain gene (*MYH7*) on chromosome 14q12 (Geisterfer-Lowrance et al., 1990). Identification of HCM causal mutations in other genes soon followed and to date more than 400 different causal mutations have been identified within sarcomeric genes. These include *MYH7* (Watkins et al., 1992), cardiac troponin T (*TNNT2*), α -tropomyosin (*TPM1*) (Thierfelder et al., 1994), cardiac myosin-binding protein C (*MYBPC3*) (Watkins et al., 1995b), regulatory (*MYL2*) and essential (*MYL3*) myosin light chains (Poetter et al., 1996), cardiac troponin I (*TNNI3*) (Kimura et al., 1997), α -cardiac actin (*ACTC1*) (Mogensen et al., 1999) and titin (*TTN*) (Sato et al., 1999).

Table 1.1 lists the various genes coding for sarcomere proteins that have been identified as causal genes for HCM through molecular genetic studies, as well as their respective chromosomal locations and number of mutations that has been implicated in the pathogenesis of HCM. Mutations in the *MYH7*, *MYBPC3* and *TNNT2* genes account for the majority of HCM cases. Watkins et al. (1995a) reported that ~35% of HCM cases are caused by mutations in *MYH7*, ~20% caused by mutations in *MYBPC3*, ~15% caused by mutations in *TNNT2*. Mutations in the *TNNI3*, *MYL2*, *MYL*, *TPM1* and *ACTC1* are considered less prevalent in HCM. Rare HCM causal variants have also been reported in cardiac troponin C (*TNNC1*) (Hoffmann et al., 2001), α -myosin heavy

chain (*MYH6*) (Niimura et al., 2002), as well as Z-disc proteins that are responsible for connecting sarcomere units to each other (Geier et al., 2003; Osio et al., 2007).

Table 1.1. Sarcomere protein genes identified as causal genes for HCM.

Gene	Chromosomal location	Sarcomere component	Number of mutations
<i>MYH7</i>	14q12	Thick filament	194
<i>MYBPC3</i>	11p11	Thick filament	149
<i>TNNT2</i>	1q32	Thin filament	31
<i>TNNI3</i>	19q13	Thin filament	27
<i>TPM1</i>	15q22	Thin filament	11
<i>MYL2</i>	12q23-q24	Thick filament	10
<i>ACTC1</i>	15q14	Thin filament	7
<i>MYL3</i>	3p21	Thick filament	5
<i>TTN</i>	2q31	Thick filament	2

Abbreviations: *ACTC1* - actin; *MYBPC3* - myosin-binding protein C; *MYH7*- β -myosin heavy chain; *MYL2*- myosin regulatory light chain; *MYL3* – myosin essential light chain; *TNNI3* - troponin I; *TNNT2* - troponin T; *TPM1* – α -tropomyosin; *TTN* - titin. (Compiled from the Sarcomere Protein Gene Mutation Database, <http://genetics.med.harvard.edu/~seidman/cg3/index.html>)

However, sarcomeric and sarcomere-related gene mutations cannot be identified as the causative mutation in approximately all HCM patients (Richard et al., 2003; Van Driest et al., 2005). Mutations in non-sarcomeric genes have also been identified as causing a HCM-like phenotype at the gross morphological level, although the histopathology differs from sarcomeric HCM, for example, mutations in the $\gamma 2$ subunit of AMP-dependant protein kinase (*PRKAG2*) and in the lysosomal-associated membrane protein 2 (*LAMP2*) (Arad et al., 2005). Additionally, mutations in the mitochondrial genome (Simon and Johns; 1999) and certain triplet repeat syndromes, such as Friedreich ataxia and myotonic muscular dystrophy (Marian, 2002) have been implicated in an HCM-like phenotype.

1.2.2 Clinical variability in HCM

The cardiac phenotype of HCM is extremely heterogeneous. Previous studies have shown that the clinical presentation observed in HCM varies greatly between individuals from the same and different families, with intrafamilial and interfamilial variability being similar (Epstein et al., 1992; Fananapazir et al., 1994; Posen et al., 1995). This clinical variability is particularly observed in the

extent and distribution of hypertrophy, ranging from extensive and diffuse to mild and segmental, with no particular pattern considered typical (Klues et al., 1995).

Asymmetrical hypertrophy is observed most frequently and regularly affects the interventricular septum (IVS) and, to some extent, the posterior walls of the LV, resulting in a narrow outflow tract. Concentric (i.e. symmetric) and apical hypertrophy is regarded as relatively uncommon (reviewed by Maron, 2002). In addition to the vast array of patterns, the extent of hypertrophy in individuals carrying HCM-causing mutations ranges from none or minimal (less than 13 mm in adults regarded as normal), to massive hypertrophy (defined as maximum ventricular wall thickness of 35 mm or more in adults), which is adjusted for age in children (Spirito et al., 1997). However, the diagnostic criteria for hypertrophy is lower (11 mm) in families with HCM-probands as the familial occurrence of HCM increases the probability that even marginal hypertrophy might be significant. The phenotypic variability of HCM is also observed in age of onset, penetrance and clinical course, particularly regarding predisposition to HF and SCD (Arad et al., 2002).

The variability in the clinical course of HCM can be explained to some extent by the causal mutation of an individual, particularly regarding the magnitude of hypertrophy and SCD. Cardiac troponin T mutations are usually associated with mild hypertrophy, but a high incidence of SCD and more extensive myofibrillar disarray (Moolman et al., 1997; Varnava et al., 2001). Mutations in the *MYBPC3* gene are typically associated with low penetrance, late onset of disease, mild hypertrophy and low incidence of SCD (Niimura et al., 1998; Erdmann et al., 2001; Niimura et al., 2002). In contrast, mutations in the *MYH7* gene are often associated with severe hypertrophy, an early onset of disease and higher susceptibility to SCD (Charron et al., 1998); however, some point mutations are associated with a relatively benign outcome (V606M) and others with a high incidence of SCD (R403Q, R453C, R719W) (Anan et al., 1994; Marian and Roberts, 1998). However, it must be mentioned that gene-phenotype studies are confounded by the occurrence of familial mutations, intragenic heterogeneity and the small number of HCM-affected individuals used in most studies.

It has been suggested that the prognostic significance of a given causal mutation is related to their influence on the magnitude of hypertrophy (Abchee and Marian, 1997) and the dose of mutant proteins in an individual has been shown to have a strong impact on the clinical course of HCM. Individuals with homozygous or compound heterozygous mutations in sarcomere protein genes

exhibit more severe clinical phenotypes (Ho et al., 2000; Mohiddin et al., 2003; Lekanne Deprez et al., 2006). This double heterozygosity complicates the interpretation of genetic screening results as the contribution of each mutation is influenced its contribution to disease penetrance and expressivity. This is especially true in studies where the initial genetic screening did not target all known HCM-causal genes (Andersen et al., 2008). Furthermore, Moolman et al., (1997) suggested that the position of the mutation within the causal gene affects the phenotype. However, it has been proven that the diverse spectrum of clinical presentations seen in HCM can only be explained in part by the causal mutation (Marian, 2001). This suggests that the clinical heterogeneity of HCM can be viewed as a product of the causal mutation as well as additional genetic and environmental factors.

1.2.3 Candidate gene modifiers for HCM

Modifier genes are neither essential nor adequate to cause HCM, but may significantly affect the severity of the disease phenotype (Alcalai et al., 2008). The case for genetic modifiers of HCM is predicated on the fact that a discrepancy exists between sarcomere-related mutations and the resulting cardiac phenotype. Fananapazir and Epstein (1994) provided conclusive evidence for modifier genes in HCM. They described a Caucasian and Korean kindred with an identical disease causing mutation (R403Q) in the *MYH7* gene. The R403Q mutation was associated with 100% disease penetrance and a high incidence of SCD in the Caucasian kindred, while no SCD was observed in the Korean kindred and the clinical presentation of HCM differed significantly between the two families, leading the authors to conclude that the genetic background of the individuals along with environmental factors are responsible for the phenotypic diversity. This phenotypic variability in HCM was confirmed by other studies (Epstein et al., 1992; Solomon et al., 1993; Marian et al., 1995).

Epidemiological studies in monozygotic and dizygotic twins have found that LVH is influenced by the genetic background of an individual in addition to the known biological causes of LVH (Adams et al., 1985; Harshfield et al., 1990; Verhaaren et al., 1991).

Transgenic animal models have also proven helpful in confirming a role for genetic modifiers on the cardiac phenotype in HCM, due to the ability to control environmental influences and the genetic background of the animals (Geisterfer-Lowrance et al., 1996). By performing a genome-wide search, Innes et al. (1998) found a quantitative trait locus (QTL) on chromosome 2 of

spontaneously hypertensive rats that affects relative LVM independent of BP. In addition, Sebkhii et al. (1999) identified a QTL on the rat chromosome 3 that is significantly linked to LVM through a whole genome linkage scan in two normotensive inbred rat strains. Other researchers confirmed the presence of genetic loci that influence cardiac hypertrophy, independent of BP, in a number of chromosomal regions in rats (Pravenec et al., 1995; Kato et al., 1999; Tsujita et al., 2000). Semsarian and co-workers (2001) studied a mouse model of HCM that they designated α -MHC^{403/+}. The α -MHC^{403/+} missense mutation in mice is equivalent to the human *MYH7* R403Q mutation. By breeding the α -MHC^{403/+} mice in different genetic backgrounds, they were able to identify a range of phenotypic differences in terms of hypertrophy, histopathology and exercise capacity, providing confirmation for the presence of genetic modifiers in HCM. It can therefore be argued that similar genetic loci (QTLs) to the ones observed in animal studies influence hypertrophy in humans. However, the exact identity of the genetic factors within these animal QTLs remains largely unknown at present.

Although HCM is regarded as a monogenic disease due to the necessity of causative mutations to trigger the development of the phenotype, it can also be regarded as a complex trait due to involvement of additional genetic loci and environmental factors. Various genetic mapping approaches have been employed to identify the QTLs that alter the hypertrophic phenotype of HCM, the most common being candidate gene association analysis. Components of the renin-angiotensin-aldosterone system (RAAS) are particularly plausible candidate modifiers due to their effect on BP and their direct hypertrophic effect on cardiomyocytes (Griendling et al., 1993).

1.3 RENIN-ANGIOTENSIN-ALDOSTERONE SYSTEM (RAAS)

The RAAS is critical in regulating BP as well as maintaining fluid and Na⁺ balance, with the main effector being angiotensin (Ang) II. Ang II is generated from angiotensinogen in two sequential steps (figure 1.3).

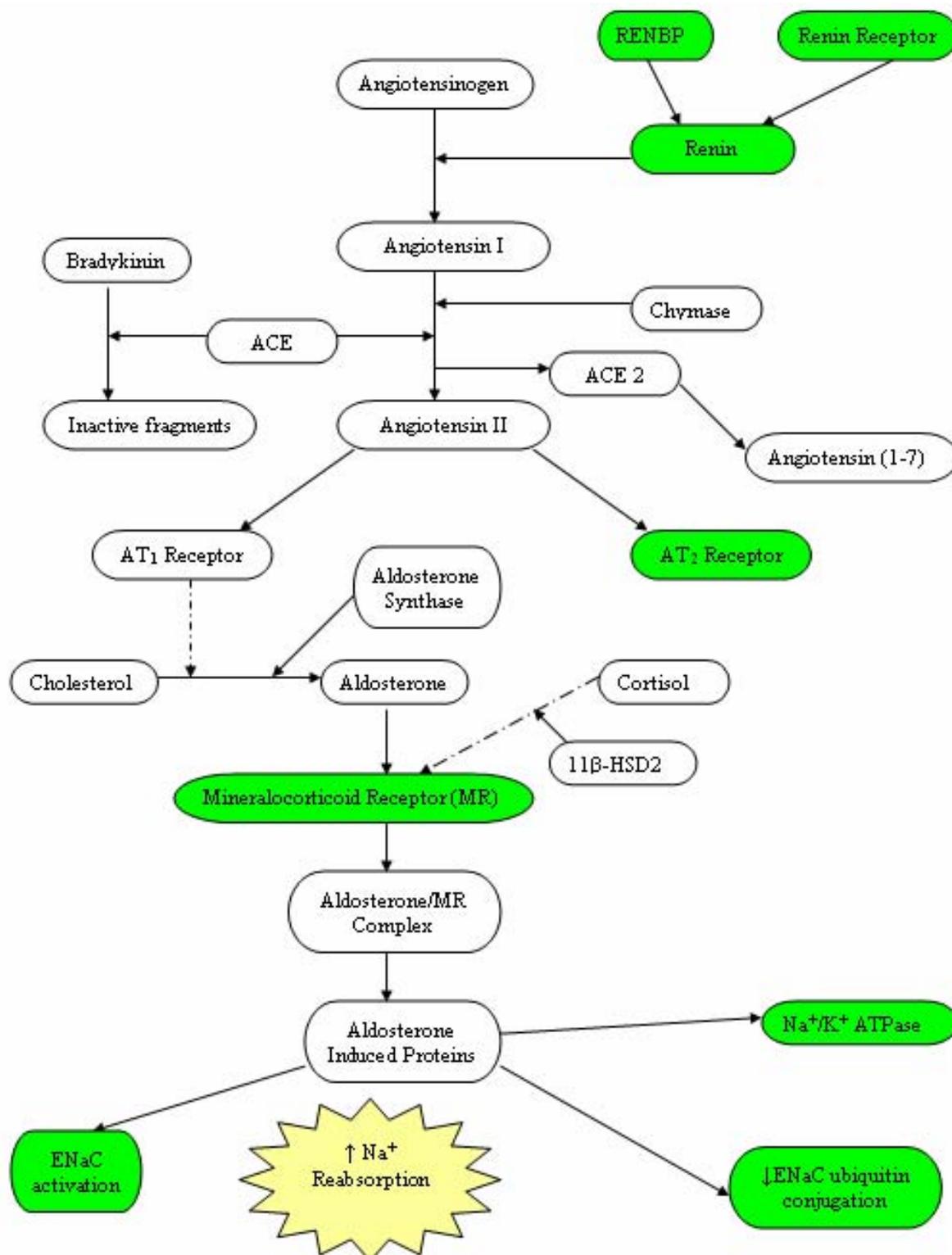


Figure 1.3. An overview of the renin-angiotensin-aldosterone system (RAAS). Components indicated in green are of particular interest in the present study.

Initially, the biologically inert decapeptide Ang I is cleaved from angiotensinogen by the aspartyl protease renin. Angiotensinogen is primarily synthesized in the liver and is found in large quantities within the circulation, while renin is synthesized and released from the juxtaglomerular cells within the wall of the renal afferent arterioles. Ang I is subsequently hydrolyzed to the active octapeptide Ang II by angiotensin-converting enzyme (ACE) within the circulation or by ACE-independent mechanisms, such as chymase. ACE is also responsible for breaking down various peptides, such as bradykinin, to inactive fragments. A second ACE, ACE2, has also been discovered, which converts Ang I to Ang-(1-7). Ang-(1-7) has been shown to counteract the vasoconstrictive effects of ACE. Ang II exerts its main biological effects by binding to the highly specific Ang II receptors. Two main receptors have been characterized to date in humans: the Ang II type I (AT₁ receptor) and Ang II type II (AT₂ receptor), each with their own signalling cascade and physiological function (De Gasparo et al., 2000; Chai and Danser, 2006).

The main functions of the AT₁ receptor include vasoconstriction, AT₁ receptor-induced growth responses, vasopressin and aldosterone release as well as Na⁺ reabsorption (Unger 2002; Booz 2004). This receptor is primarily coupled to a guanosine triphosphate-binding protein and operates through a signalling pathway that involves phospholipases A, C, D, calcium channels, inositol phosphates and a variety of serine/threonine and tyrosine kinases (De Gasparo et al., 2000). Binding of Ang II to the AT₁ receptor, triggers the synthesis of aldosterone via aldosterone synthase (*CYP11B2*) (Mehta and Griendling 2007).

Aldosterone is a mineralocorticoid that exerts its function by binding to the mineralocorticoid receptor (MR) and increases the transcription of MR-responsive genes (Lemarié et al., 2008). The MR binds aldosterone and glucocorticoids, such as cortisol, with equal affinity. However, the enzyme 11 β-hydroxysteroid-dehydrogenase type 2 (11β-HSD2) increases the MR specificity for aldosterone by inactivating the glucocorticoids (Tannin et al., 1991). The MR/aldosterone complex exerts its Na⁺-regulating effects in three phases (Eaton et al., 2001; Kamynina and Staub, 2002). The first is a latent period that lasts for about an hour, during which aldosterone-induced transcription and translation takes place. The second is an “early response” phase of up to three hours during which Na⁺ transport is increased, mainly by increasing the open probability and number of active epithelial Na⁺ channels (ENaC). A further increase in Na⁺ transport is observed during the “late response” of about 24 hours and expression of ENaC as well as Na⁺/K⁺-ATPase subunits are increased at this stage (Rossier et al., 2002; Stockland 2002).

The exact function of AT₂ receptor still remains somewhat unclear. Previous studies have shown that AT₂ receptor stimulation causes vasodilation and it counteracts the trophic responses of the AT₁ receptor by affecting cell proliferation and differentiation (Unger 2002; Booz 2004). The signalling pathways of the AT₂ receptor are quite different from the AT₁ receptor and it includes serine and tyrosine phosphatases, phospholipase A₂, cyclic guanosine monophosphate, nitric oxide as well as bradykinin stimulation (De Gasparo et al., 2000; Berry et al., 2001).

A large body of evidence suggests that Ang II has the ability to act as a systemic hormone (circulating RAAS) and as a local factor (tissue RAAS) (reviewed in Paul et al., 2006).

1.3.1 RAAS genes in the heart

Various studies have identified RAAS components (Dzau and Re, 1987; Lindpainter et al., 1990; Paul et al., 1990) in the heart. However, their mere presence in cardiac tissue does not provide conclusive evidence for local synthesis and more studies were necessary to determine whether a local tissue RAAS system exists or whether these cardiac RAAS components are present in the heart due to the circulating RAAS within the body's blood system.

The presence of renin in the heart is a matter of great controversy as evidence for local renin synthesis has not been conclusive. It is now widely accepted that cardiac renin is taken up from circulation due to diffusion into the interstitium (De Lannoy et al., 1997; Danser and Saris, 2002) or through specific functional binding sites or the (pro)renin receptor (Nguyen et al., 2004; Catanzaro 2005). Previous studies have also shown that the Mannose-6-Phosphate (M6P) receptor is able to bind prorenin and renin on cardiomyocytes (Saris et al., 2001).

The local production of ACE and its homologue ACE2 within the heart is however not as controversial. ACE mRNA has been detected in rat (Schunkert et al., 1990) and human hearts (Paul et al., 1993) and further mRNA studies have provided evidence for ACE expression in cardiomyocytes (Paul et al., 1996). The AT₁ receptor as well as AT₂ receptor expression in cardiac tissue has been confirmed and they appear to be localised on cardiomyocytes (Rogers et al., 1986; Urata et al., 1990; De Gasparo et al., 2000). *In situ* hybridization techniques were also used to successfully identify the expression of angiotensinogen (Dostal et al., 1992), MR and 11 β -HSD2 in human cardiac tissue (Bonvalet et al., 1995; Lombes et al., 1995).

The cardiac tissue RAAS seems to be principally involved in maintaining a balance between stimuli responsible for inducing and inhibiting cell growth and proliferation as well as mediating adaptive responses to myocardial stressors (Paul et al., 2006), largely through the opposing actions of the AT₁ receptor and AT₂ receptor. Figure 1.4 depicts the cardiac tissue RAAS.

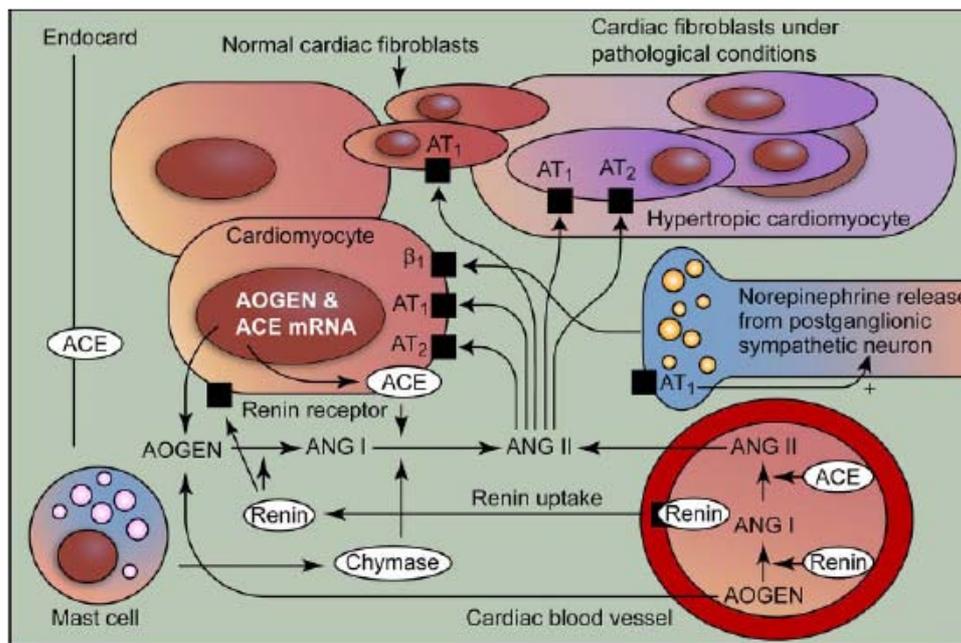


Figure 1.4. The renin-angiotensin-aldosterone system (RAAS) in the heart. Renin and angiotensinogen (Aogen) are mostly taken up from the plasma or formed locally. Ang II synthesis occurs extracellularly and acts on cell-specific receptors on different cell types such as cardiomyocytes and fibroblasts (taken from Paul et al., 2006).

1.3.2 RAAS genes in hypertension

A large number of RAAS components have been implicated in salt-sensitive and essential hypertension. Previous studies have implicated angiotensinogen (Kunz et al., 1997), renin (Ahmad et al., 2005), ACE (O' Donnell et al., 1998; Poch et al., 2001), AT₁ receptor (Mottl et al., 2008), AT₂ receptor (Zhang et al., 2003), aldosterone synthase (Brand et al., 1998), the MR (Geller et al., 2000; Stowasser and Gordon, 2006) and ENaCs (Ambrosius et al., 1999) in the pathogenesis of hypertension. Angiotensin II receptor blockers (ARBs) and ACE inhibitors are currently used as part of therapeutic interventions to manage hypertension and have been proven to cause a reduction in BP and other BP-associated cardiovascular morbidities (Neal et al., 2000; Ram 2008). Recent clinical trials have provided evidence that the renin inhibitor Aliskiren is a potent

antihypertensive as it is able to cause a dose-dependent BP reduction (reviewed by Gradman and Kad, 2008).

Dietary salt (NaCl) intake has been shown to be an important factor in essential hypertension. Interestingly, a number of studies have found that dietary NaCl intake as assessed by 24-hour urinary Na⁺ excretion to be a BP-independent determinant of LVM and a reduction in dietary Na⁺ has been proven to reduce LVH (reviewed by Messerli et al., 1997).

Hypertension has a well documented effect on cardiac hypertrophy development (Koren et al., 1991). Cardiac hypertrophy has however been shown to develop independently of BP and LVH has been witnessed in normotensive individuals as mentioned previously. The present study is therefore particularly concerned with the BP-independent effects of RAAS genes.

1.3.3 RAAS genes in LVH

Evidence from *in vitro* and clinical studies, animal models, and genetic association studies suggests an undeniable involvement of RAAS components in the progression of LVH.

1.3.3.1 *In vitro* studies

The main effector peptide of the RAAS, Ang II, has been shown to cause hypertrophy in *in vitro* studies of rat neonatal (Baker and Aceto, 1990; Sadoshima and Izumo, 1993) and adult (Schunkert et al., 1995; Wada et al., 1996; Ritchie et al., 1998) cardiomyocytes. Schunkert et al. (1990) found that Ang I to Ang II conversion rates were elevated in rat hearts with adaptive LVH, indicating increased RAAS activity in cardiac hypertrophy. In addition, Dostal and Baker (1992) demonstrated that infusion of rats with Ang II induced cardiac hypertrophy. This effect was prevented when an AT₁ receptor antagonist was administered, but not with a reduction in BP, leading the authors to conclude that this effect was BP-independent. It is now recognised that Ang II mediates cardiomyocyte hypertrophy through activation of the AT₁ receptor.

Further studies in rat cardiomyocytes showed that the antihypertrophic effects of AT₁ receptor antagonists is partly explained by the upregulated AT₂ receptor-mediated antiproliferative effects, suggesting that the net hypertrophic effect of Ang II depends on the cellular AT₁ receptor/ AT₂ receptor ratio (Van Kesteren, 1997; Booz and Baker 1998). This was complemented by studies on

adult rat hearts where AT₂ receptor blockade was shown to diminish the antihypertrophic effects of AT₁ receptor antagonists (Bartunek et al., 1999; Mukawa et al., 2003).

1.3.3.2 Animal models

Transgenic rat models in which human RAAS components, such as the AT₁ receptor gene (*AGTR1*) (Hoffmann et al., 2001a; Hoffmann, 2005), *ACE* (Pokharel et al., 2004; Tian et al., 2004) and renin and angiotensinogen (Muller et al., 1998) were overexpressed, provided clear proof of LVH caused by enhanced cardiac Ang II generation. These effects on LVH occurred independently of Ang II's influence on BP. In a 94-week longitudinal study on mice that develop Ang II-mediated cardiac hypertrophy in absence of elevated BP, Domenighetti et al. (2005) demonstrated that chronic myocardial Ang II stimulation caused cardiomyocyte hypertrophy and eventual heart failure independent of BP. Studies on rats have shown that the hypertrophic changes brought on by Ang II is mediated by a number of intracellular pathways, including MAPK and JAK/STAT pathways (Marrero et al., 1995; Unger et al., 1996; Schieffer et al., 1997).

Interestingly, rats expressing a prorenin transgene, which encodes the inactive precursor of renin, exclusively in the liver demonstrate severe liver fibrosis as well cardiac and aortic hypertrophy in the absence of hypertension (Veniant et al., 1996). A study by Saris et al. (2006) demonstrated that when prorenin bound to the (pro)renin receptor, it activated the p38 MAPK/HSP27 pathway in neonatal rat cardiomyocytes. They postulated that activation of this pathway is responsible for the severe cardiac hypertrophy that was observed by Veniant and colleagues (1996). This and other studies (Nguyen et al., 1996; Methot et al., 1999; Prescott et al., 2002; Huang et al., 2006) suggest that renin *per se* exerts hypertrophic cellular effects, independent of Ang II generation.

Nagata et al. (2006) investigated the effect of MR-blockade on cardiac hypertrophy in rats with salt-sensitive hypertension and concluded that MR-blockade attenuates LVH, in the absence of an antihypertensive effect. The involvement of the downstream effectors of the MR in hypertrophy development has also been reported. Previous studies on rat hypertrophy models have showed that the expression of Na⁺/K⁺-ATPase α - and β -subunit isoforms are altered in hypertrophied ventricles (Xie et al., 1999; Baek and Weis, 2005; Zwadlo and Borlak, 2005). Nedd4-2 is an ubiquitin ligase protein that is directly related to and extremely critical in the regulation of ENaC activity. Shi et al. (2008) demonstrated that mice deficient in Nedd4-2 developed cardiac hypertrophy and had noticeably depressed cardiac function.

1.3.3.3 RAAS activity in human cardiovascular pathologies

In a study on 84 individuals with a predisposition to hypertrophy, Harrap et al. (1996) found that plasma Ang II, renin and ACE were significantly associated with LVM, independent of BP and body size. This led the authors to conclude that Ang II exerts a direct effect on cardiac hypertrophy. A number of studies have provided evidence of increased RAAS activity in cardiac pathologies that results from or are directly related to hypertrophy.

Wharton et al. (1998) as well as Tsutumi et al. (1998) reported an increased expression of the AT₂ receptor gene (*AGTR2*) in cardiac pathologies such as heart failure and cardiac fibrosis. Schunkert et al. (1997) showed that serum aldosterone levels are associated with LVM in hypertensive and normotensive individuals. A study on patients with primary aldosteronism, a condition caused by hypersecretion of aldosterone, found that LVM index adjusted for BP and other confounding factors was significantly increased in this condition (Matsumura et al., 2006). Additionally, a case-control study by Malmqvist and colleagues (2002) on hypertensive patients found that plasma renin activity (PRA) and aldosterone was related to LVM and left ventricular wall thickness (LVWT), independent of BP and body surface area (BSA). Ribonuclease protection assays demonstrated increased expression of the renin-binding protein (RnBP) in human cardiomyocytes from hearts with HF due to end-stage cardiomyopathies (Bohlmeyer et al., 2003).

In accordance with results obtained from animal models, several researchers reported a decrease in the expression of Na⁺/K⁺-ATPase α- and β-subunit isoforms in failing human hearts (reviewed in Schwinger et al., 2003).

1.3.3.4 Clinical studies

Treatment of 9193 patients with hypertension and LVH in the LIFE study with AT₁ receptor antagonists resulted in a significant reduction in LVH and other cardiovascular morbidities. This led the investigators to the conclusion that AT₁ receptor antagonists confer cardiovascular benefits beyond a reduction in BP (Dahlof et al., 2002; Okin et al., 2003). ACE inhibition has been shown to ameliorate LVH in clinical and experimental studies (Weinberg et al., 1994; Schmieder et al., 1998; Devereux et al., 2001; Palmieri and Devereux, 2002). The randomized aldactone evaluation study (RALES) and eplerenone post acute myocardial infarction efficacy and survival study (EPHESUS) clinical trials have shown that MR antagonists are able to reduce ventricular

remodelling and myocardial fibrosis in patients with systolic LV dysfunction, independent of the MR antagonist's effect on BP (Pitt et al., 1999; Pitt et al., 2003).

1.3.3.5 Genetic association studies

Additional evidence for the involvement of RAAS genes in the development of LVH comes from genetic association studies. A study by Herrmann et al. (2002) on 1968 individuals from the Glasgow Heart Scan (GLAECO) and Glasgow Heart Scan Old (GLAEOLD) studies revealed that a +1675 G/A polymorphism in *AGTR2* is significantly associated with LVH and coronary ischemia.

Polymorphisms in *ACE*, *AGTR1*, cardiac chymase (*CMA*), angiotensinogen (*AGT*) and *CYP11B2* and their association with electrocardiographically and echocardiographically determined LVH have been studied intensively in the past. Five RAAS polymorphisms (the so-called pro-LVH-polymorphisms) have been particularly associated with LVH: this includes an insertion/deletion (I/D) polymorphism in intron 16 of *ACE* (Schunkert et al., 1994; Iwai et al., 1994), a +1666 A/C variant in *AGTR1* (Osterop et al., 1998), a -1903G/A variant in *CMA* (Pfeufer et al., 1996), a M235T missense mutation in *AGT* (Ishanov et al., 1997) and a +344 C/T variant in *CYP11B2* (Delles et al., 2001).

1.3.4 RAAS genes implicated in HCM: previous association studies

Lechin et al. (1995) assessed the effect of *ACE* polymorphisms on LVM index and the extent of hypertrophy in 183 HCM patients and reported that the I/D polymorphism significantly influences the phenotypic expression of hypertrophy in HCM. Previously Marian et al. (1993) reported that this polymorphism is associated with LVH and SCD in HCM. Lieb et al. (2006) examined the association between polymorphisms in *ACE2* and echocardiographically determined cardiac hypertrophy parameters in a study population of 1674 German residents of the Augsburg area and reported that *ACE2* polymorphisms are significantly associated with LVH in men. A recent study from our laboratory on 227 South African HCM patients found that variants in *ACE2* modulate cardiac hypertrophy in HCM patients, independent of BP and other known hypertrophy covariates (Van der Merwe et al., 2008).

Osterop et al. (1998) reported that a +1166 A/C *AGTR1* polymorphism modulates the phenotypic expression of cardiac hypertrophy in HCM, independently of plasma renin and the I/D *ACE*

polymorphism. Later, Deinum et al. (2001) investigated the effect of an *AGTR2* +3123 A/C polymorphism on LVH in 103 unrelated HCM patients. Multiple regression analysis showed that the *AGTR2* +3123 C-allele decreased LVM index in female subjects, independently of plasma renin, the +1166 A/C *AGTR1* variant or the I/D *ACE* variant. They concluded that *AGTR2* modulates cardiac hypertrophy in HCM, independently of circulating RAAS activity.

A study by Perkins et al. (2005) on 389 unrelated HCM-patients found association between the pro-LVH polymorphisms and LVH parameters. Ortlepp et al., (2002) investigated the effects of the five pro-LVH polymorphisms in a single family with HCM due to a *MYBPC* mutation. They were particularly interested to find out whether the compound effect of the five pro-LVH polymorphisms significantly affects cardiac hypertrophy. The study cohort consisted of 48 family members (26 affected and 22 unaffected) and 100 unrelated healthy controls. The authors concluded that RAAS pro-LVH polymorphisms individually or collectively influence the penetrance and extent of LVH in HCM. Recently, a study by Kaufman et al. (2007) corroborated these findings. They demonstrated that children with two or more pro-LVH polymorphisms exhibited a greater increase in LVM and septal thickness in a study on 65 paediatric HCM patients.

1.4 THE PRESENT STUDY

The present study forms part of a South African HCM investigation in which the ultimate aim is to investigate whether genes encoding components of the RAAS modulate the development of hypertrophy in 22 South African mixed ancestry HCM families. Previously, Mr. Ruben Cloete investigated the effect of polymorphisms in *ACE1*, *AGT*, *CYP11B2*, *AGTR1*, *CMA* and *ACE2* in this cohort (Cloete REA, M.Sc). The present study was aimed at expanding our current knowledge of the influence of RAAS genes in the modulation of hypertrophy in a South African HCM cohort as well as to elucidate the influence of RAAS gene polymorphisms on hypertrophy development *per se* using a family-based association and multi-SNP approach.

One of three unique HCM-causing founder mutations segregates in these families: two *MYH7* mutations (A797T and R403W) and a R92W *TNNT2* mutation. Haplotype analysis performed by Moolman-Smook et al. (1999) confirmed that individuals harbouring the same HCM-causal mutation inherited that mutation from a common ancestor.

In the present study, quantitative measures of the hypertrophic phenotype, such as maximal wall thickness, a variety of wall thickness indexes and LVM, were tested for association with single polymorphisms using family-based statistical genetic analysis. We used a high-throughput genotyping approach employing ABI Validated TaqMan genotyping assays, in contrast to the polymerase chain reaction (PCR) -based genotyping approach that was used in the previous study, i.e. SNaPshot primer extension analysis and allele specific restriction enzyme analysis (ASREA).

Twelve genes known to be involved in RAAS, which had not previously been studied in our laboratory, were selected from the literature to be investigated, based on their functions within the RAAS.

1.4.1 AT₂ receptor

The AT₂ receptor binds the main effector peptide of the RAAS, AngII, and is known to exert antihypertensive and antiproliferative effects. The AT₂ receptor gene (*AGTR2*) is located on chromosome Xq22-q23 and consists of three exons and two introns and the entire open reading frame of the gene is situated in exon 3.

1.4.2 Renin and renin-associated genes

Renin is a rate-limiting component of the RAAS as it controls the initial conversion of angiotensinogen to Ang I. Two additional proteins have been identified to be directly related to renin activity. Binding of renin and its inactive precursor, prorenin, to the (pro)renin receptor elicits Ang II-dependent and –independent signalling. Several researchers have proposed that the (pro)renin receptor gene (*ATP6AP2*) plays an integral role in cardiac renin levels. The RnBP is a potent cellular renin inhibitor, and significantly affects renin activity. The gene responsible for this protein, *RENBP*, is located on chromosome Xq28, consists of 11 exons and ten introns and spans about 10 kb of DNA. Renin maps to chromosome 1q32, spans about 12 kb and contains 8 introns. The (pro)renin receptor gene maps to chromosome Xp11.4, spans about 25 kb and consists of 9 exons.

1.4.3 MR

The MR, encoded by *NR3C2*, is responsible for the downstream RAAS function as it bind to aldosterone to form a MR/aldosterone complex, which then activates aldosterone-induced early and late response gene transcription and signalling cascades to mediate cellular Na⁺ homeostasis

via its downstream effectors. *NR3C2* maps to chromosome 4q31 spans about 360 kb and contains 10 exons.

1.4.4 ENaC subunits

The ENaCs are important downstream effectors of the MR/aldosterone. Each ENaC consists of an α -, β -, and γ -subunit, encoded by the *SCNNIA*, *SCNNIB*, and *SCNNIG* genes respectively. The ENaCs are responsible for mediating electrodiffusion of Na^+ through epithelial cells. *SCNNIA* maps to chromosome 12p13 and consists of 13 exons spanning 28 kb. *SCNNIB* maps to chromosome 16p12.2-p12.1 and spans about 80 kb, while *SCNNIG* maps to 16p12 and spans about 30 kb.

1.4.5 Na^+/K^+ -ATPase subunits

The Na^+/K^+ -ATPase catalyzes the exchange of Na^+ and K^+ ions across plasma membranes and are also essential downstream effectors of the MR/aldosterone complex. Each Na^+/K^+ -ATPase consists of an α - and a β -subunit. A number of Na^+/K^+ -ATPase subunit isoforms have been described in the literature. In the present study we only investigated the isoforms that showed evidence for cardiac expression, i.e. *ATP1A1*, *ATP1A2*, *ATP1B1* and *ATP1B3*. *ATP1A1* maps to chromosome 1p21 and spans about 30 kb, while *ATP1A2* also spans about 30 kb and maps to 1q21-q23. *ATP1B1* maps to chromosome 1q24, spans about 26 kb and consists of 6 exons and 5 introns, while *ATP1B3* chromosome 3q23 and spans about 50kb, split into 7 exons and 6 introns.

CHAPTER 2
MATERIALS AND METHODS

INDEX	PAGE
2.1 STUDY SUBJECTS	23
2.2 BLOOD COLLECTION AND DNA EXTRACTION	28
2.3 BIOINFORMATICS	28
2.3.1 Selection of candidate genes	28
2.3.2 SNP Selection	30
2.4 TAQMAN SNP GENOTYPING	32
2.4.1 Real-time PCR amplification	33
2.4.2 Allelic discrimination	34
2.5 STR GENOTYPING	34
2.5.1 PCR amplification	34
2.5.2 Agarose gel electrophoresis	34
2.5.3 STR analysis	35
2.6 STATISTICAL ANALYSIS	36
2.6.1 Descriptive statistics and trait distribution	36
2.6.2 Linkage disequilibrium (LD) determination	36
2.6.3 Quantitative transmission disequilibrium test	37
2.6.4 Linear mixed effects models	37

CHAPTER 2: MATERIALS AND METHODS

2.1. STUDY SUBJECTS

The University of Stellenbosch Ethics Committee reviewed and granted approval for the present study (N04/03/062). Subjects entered into the study gave written informed consent and blood samples were collected from each subject for molecular genetic testing. During routine mutation screening for HCM-causing mutations, a panel of HCM probands was screened for disease-causing mutations in 11 sarcomeric genes that account for 95% of all HCM cases. In the process, 22 probands carrying one of three mutations that occur as founder mutations in South Africa, i.e. R92W in *TNNT2*, R403W in *MYH7*, and A797T in *MYH7* were identified. These mutations have previously been described within a South African population by Moolman-Smook et al. (1999).

Pedigree tracing was performed for these index individuals and their family members asked to participate in this modifier gene study. These families were of South African Caucasian or of Mixed Ancestry descent (table 2.1). Thus, a panel of 353 individuals that included genetically and clinically affected and unaffected family members was identified; these individuals were all screened for the presence or absence of all three founder mutations.

Table 2.1. South African HCM-affected families of Caucasian and Mixed Ancestry descent that were analysed in the present study.

Pedigree	Ethnic group	n	Gene	Mutation	Location
101	Caucasian	22	<i>MYH7</i>	A797T	exon 21
104	Mixed Ancestry	14	<i>MYH7</i>	A797T	exon 21
123	Mixed Ancestry	16	<i>MYH7</i>	A797T	exon 21
124	Caucasian	4	<i>MYH7</i>	A797T	exon 21
131	Caucasian	25	<i>MYH7</i>	A797T	exon 21
138	Caucasian	32	<i>MYH7</i>	A797T	exon 21
145	Mixed Ancestry	4	<i>MYH7</i>	A797T	exon 21
147	Mixed Ancestry	10	<i>MYH7</i>	A797T	exon 21
158	Caucasian	5	<i>MYH7</i>	A797T	exon 21
159	Mixed Ancestry	11	<i>MYH7</i>	A797T	exon 21
163	Caucasian	9	<i>MYH7</i>	A797T	exon 21
172	Caucasian	8	<i>MYH7</i>	A797T	exon 21
106	Mixed Ancestry	69	<i>MYH7</i>	R403W	exon 13
134	Mixed Ancestry	9	<i>MYH7</i>	R403W	exon 13
157	Mixed Ancestry	4	<i>MYH7</i>	R403W	exon 13
100	Mixed Ancestry	43	<i>TNNT2</i>	R92W	exon 9
103	Mixed Ancestry	5	<i>TNNT2</i>	R92W	exon 9
109	Mixed Ancestry	8	<i>TNNT2</i>	R92W	exon 9
139	Mixed Ancestry	41	<i>TNNT2</i>	R92W	exon 9
137	Mixed Ancestry	7	<i>TNNT2</i>	R92W	exon 9
149	Mixed Ancestry	10	<i>TNNT2</i>	R92W	exon 9
173	Mixed Ancestry	2	<i>TNNT2</i>	R92W	exon 9

Abbreviations: n = number of individuals screened for SNPs in the present study - includes mutation and non-mutation carriers, *MYH7* -myosin heavy chain gene 7; *TNNT2*- troponin T gene 2.

The subjects in the present study are 18 years and older and were comprehensively clinically characterised by 2-D echocardiography performed by a single cardiologist (Dr Miriam Revera from Pavia University, Italy) who was unaware of the mutation status of each subject. Analyses included echocardiographic recordings in M-mode, 2-D and Doppler blood-flow imaging using a 2.5 Hz transducer in standard parasternal long-axis and short-axis, apical four- and two-chamber views using a GE Healthcare Vivid7 cardiovascular ultrasound system. To determine the maximal LVWT, the heart muscle was divided into three levels, namely, mitral valve, papillary muscle and supra-apex level (figure 2.1). 2-D-echocardiographic measurements were performed in six

segments of the LV wall at the mitral valve and papillary muscle levels and in four segments at the smaller supra-apex level, thus a total of 16 segments were measured.

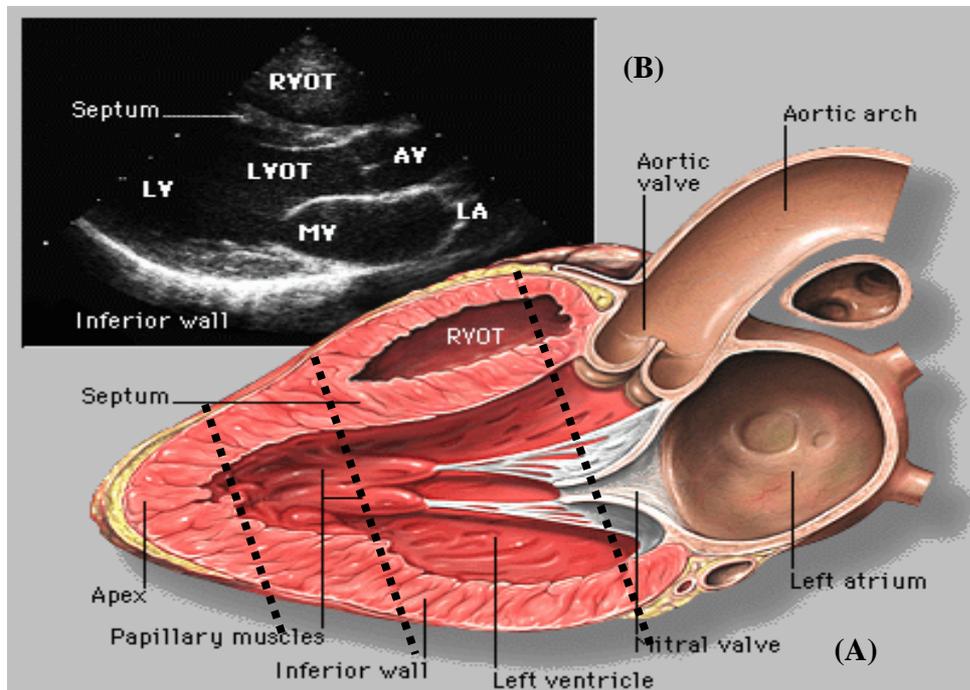


Figure 2.1. Graphical representative example of the heart being divided into 3 levels. A) Long-axis view of left ventricle, taken at level of mitral valve, papillary muscles as well as just above apex (levels indicated by dotted lines). B) An example of a 2D echocardiographic ultrasound of the left ventricle. Abbreviations: AV- aortic valve, LA-left atrium, LV-left ventricle, LVOT-left ventricular outflow tract, MV- mitral valve, RVOT-right ventricular outflow tract. Taken from (http://www.med.yale.edu/.../aortic_regurgitation.html) with minor modifications by JC Moolman-Smook.

The six measurements at the mitral valve and papillary muscle levels were taken at the anterior interventricular septum (aIVS), posterior interventricular septum (pIVS) and anterior wall (AW), lateral wall (LW), inferior wall (IW) and posterior wall (PW) of the left ventricle. Evaluation of the supra-apex level consisted of segments IVS, AW, LW and PW as per four chamber view. All these variables were measured according to the recommendation of the American Society of Echocardiography (<http://www.asecho.org/guidelines.php>). Covariates of cardiac structure were noted for each participant; these included systolic BP, diastolic BP, age, sex, BSA and heart rate (HR).

Echocardiographically determined LVM and Maron-Spirito score (Spirito and Maron, 1990) was calculated to better describe the extent of hypertrophy. LVM was calculated using the formula for the estimation of LVM from 2-D LV linear dimensions recommended by the American Society of Echocardiography:

$$LVM = 0.8 \times (1.04 [(LVIDd + PWTD + SWTd)^3 - (LVIDd)^3]) + 0.6g .$$

Additionally, a new cumulative wall thickness score (CWT) was determined by adding the 16 wall thickness measurements in all three levels of the heart. We also used principal component analysis to statistically define a composite score that reflects ventricle-wide hypertrophy. One component, hereafter referred to as Comp1, explained 76% of the variance in the 16 wall thickness measurements. Comp1 showed significant heritability and was therefore used in the association analysis. Table 2.2 lists the various hypertrophy traits and composite scores used to describe the degree and distribution of cardiac hypertrophy.

Table 2.2. Summary of echocardiographically determined hypertrophy traits and composite scores used to describe the degree and distribution of cardiac hypertrophy.

Level	Hypertrophy trait	Description
Mitral valve level	mLVWTmit	maximal left ventricular wall thickness at the mitral valve
	mIVSTmit	maximal interventricular septum thickness at the mitral valve
	pIVSmit	posterior interventricular septum thickness at the mitral valve
	aIVSmit	anterior interventricular septum thickness at the mitral valve
	AWmit	anterior wall thickness at the mitral valve
	LWmit	lateral wall thickness at the mitral valve
	IWmit	inferior wall thickness at the mitral valve
	PWmit	posterior wall thickness at the mitral valve
Papillary level	mLVWTpap	maximal left ventricular wall thickness at the papillary level
	mIVSTpap	maximal interventricular septum thickness at the papillary level
	pIVSpap	posterior interventricular septum thickness at the papillary level
	aIVSpap	anterior interventricular septum thickness at the papillary level
	AWpap	anterior wall thickness at the papillary level
	LWpap	lateral wall thickness at the papillary level
	IWpap	inferior wall thickness at the papillary level
	PWpap	posterior wall thickness at the papillary level
Apex level	mLVWTapx	maximal left ventricular wall thickness at the supra-apex level
	IVSapx	interventricular septum thickness at the supra-apex level
	AWapx	anterior wall thickness at the supra-apex level
	LWapx	lateral wall thickness at the supra-apex level
	PWapx	posterior wall thickness at the supra-apex level
Overall	LVM	left ventricular mass
	mIVST	maximal interventricular septum thickness
	mLVWT	maximal left ventricular wall thickness
	mPWT	maximal posterior wall thickness
Composite scores	Maron-Spirito score	as defined by Spirito and Maron, 1990
	CWTscore	cumulative wall thickness score
	Comp1	principal component score

2.2. BLOOD COLLECTION AND DNA EXTRACTION

Blood from each individual was collected in 2x 5 ml ethylene-diamine-tetra-acetic acid (EDTA) tubes (Vacutainer, RSA) for DNA extraction and in 1x 10 ml heparin tube (Vacutainer, RSA) to establish permanent lymphoblastoid cell lines using the method described by Neitzel (1986). Blood that was drawn from patients at other centres in South Africa was couriered to the research laboratory within 24 hours of sampling.

DNA was extracted from nucleated blood cells using the method previously described by Corfield et al. (1993) with minor modifications. The DNA extractions, cell transformations and maintenance were performed by Mrs I le Roux. A list of the solutions used for DNA extractions is provided in Appendix I.

2.3. BIOINFORMATICS

2.3.1. Selection of Candidate Genes

Twelve genes known to be involved in the RAAS, and which had not previously been studied in our laboratory, were selected to be investigated from the literature. Public databases (Pubmed/Medline <http://www.pubmed.gov>) were searched for information on the reported association status of these genes in hypertrophy, hypertension and HCM. Table 2.3 shows the candidate genes chosen for investigation as well as their respective protein functions.

Table 2.3. Candidate genes chosen for investigation.

Gene	Localisation	Size (kb)	Protein function
<i>AGTR2</i>	Xq22-q23	3.82	receptor for angiotensin II
<i>ATPIA1</i>	1p21	31.51	alpha subunit of Na ⁺ /K ⁺ -ATPase, catalyzes exchange of Na ⁺ and K ⁺ ions across plasma membrane
<i>ATPIA2</i>	1q21-q23	27.83	alpha subunit of Na ⁺ /K ⁺ -ATPase, catalyzes exchange of Na ⁺ and K ⁺ ions across plasma membrane
<i>ATPIB1</i>	1q24	25.95	beta subunit of Na ⁺ /K ⁺ -ATPase, catalyzes exchange of Na ⁺ and K ⁺ ions across plasma membrane
<i>ATPIB3</i>	3q23	49.74	beta subunit of Na ⁺ /K ⁺ -ATPase, catalyzes exchange of Na ⁺ and K ⁺ ions across plasma membrane
<i>ATP6AP2</i>	Xp11.4	25.66	receptor for renin
<i>NR3C2</i>	4q31.1	363.6	receptor for aldosterone
<i>REN</i>	1q32	11.52	converts angiotensinogen to angiotensin I
<i>RENBP</i>	Xq28	9.51	inhibits renin activity
<i>SCNNIA</i>	12p13	28.07	alpha subunit of ENaC, mediates electrodiffusion of Na ⁺ through epithelial cells
<i>SCNNIB</i>	16p12.2-p12.1	78.98	beta subunit of ENaC, mediates electrodiffusion of Na ⁺ through epithelial cells
<i>SCNNIG</i>	16p12	30.61	gamma subunit of ENaC, mediates electrodiffusion of Na ⁺ through epithelial cells

Abbreviations: *AGTR2*-angiotensin II receptor, type 2; *ATPIA1*-ATPase, Na⁺/K⁺ transporting, alpha 1 polypeptide; *ATPIA2*-ATPase, Na⁺/K⁺ transporting, alpha 2 polypeptide; *ATPIB1*-ATPase, Na⁺/K⁺ transporting, beta 1 polypeptide; *ATPIB3*-ATPase, Na⁺/K⁺ transporting, beta 3 polypeptide; *ATP6AP2*-ATPase, H⁺ transporting, lysosomal accessory protein 2; ENaC- epithelial sodium channel; K⁺-potassium; kb-kilo-bases; Na⁺-sodium; Na⁺/K⁺-ATPase-sodium-potassium pump; *REN*-renin; *RENBP*-renin binding protein; *SCNNIA*-sodium channel, nonvoltage-gated 1 alpha; *SCNNIB*-sodium channel, nonvoltage-gated 1, beta; *SCNNIG*-sodium channel, nonvoltage-gated 1, gamma; *NR3C2*-nuclear receptor subfamily 3, group C, member 2

2.3.2. SNP Selection

Maniatis et al. (2002) defined genetic map distance in terms of linkage disequilibrium units (LDUs). LDUs define a metric coordinate system where locations are additive and distances are proportional to the allelic association between markers (Maniatis et al. (2002). These LD maps are analogous to the genetic map expressed in centi-Morgans and can be used to efficiently position markers for population-based disease association studies (Collins et al., 2004).

For the present study, SNPs were selected using the SNPbrowser v 3.5.3 software (De La Vega et al., 2006) to achieve an even spacing of 0.5 LDUs on the metric LD map for the HapMap CEU and YRI populations (table 2.4) using the default parameters of the software (De La Vega, 2007).

SNPbrowser utilises a set of metric LD maps constructed from the HapMap NCBI b36 assembly using the LDMAP software (Kuo et al., 2007). The LDMAP software places SNPs on an additive coordinate system, for example, SNPs in perfect LD have zero distance between them, whereas SNPs with no significant correlation are separated by over three LDUs in this map (De La Vega et al., 2006).

Table 2.4. SNPs chosen for investigation as well as the respective TaqMan assays used for genotyping each polymorphism.

Gene	Chromosome	SNP	Chromosomal Position (bp)	Nucleotide Change	ABI TaqMan Assay
<i>AGTR2</i>	Xq22-q23	rs1403543	115216220	G/A	C__7481825_10
		rs5194	115218858	G/A	C__1841567_20
		rs11091046	115219154	C/A	C__1841568_10
<i>ATP6AP2</i>	Xp11.4	rs2968915	40324378	A/G	C__15881558_20
		rs2968917	40327762	C/T	C__15881550_10
		rs10536	40350712	G/A	C__8789353_10
<i>RENBP</i>	Xq28	rs762656	152864846	A/G	C__13880_10
		rs2269372	152860739	A/G	C__15876539_10
		rs2269370	152849623	A/C	C__15876550_10
<i>REN</i>	1q32	rs10900555	202398933	A/G	C__31567082_10
		rs5705	202397809	G/T	C__11451777_10
		rs11571082	202397654	C/T	C__31567075_10
		rs1464816	202395477	G/T	C__8687919_1_
<i>ATPIA1</i>	1p21	rs10924074	116722542	A/G	C__3072256_10
		rs850609	116734086	A/T	C__8696039_10
<i>ATPIA2</i>	1q21-q23	rs7548116	158361751	A/T	C__1843215_10
		rs11585375	158380967	A/G	C__31909450_10
<i>ATP1B1</i>	1q24	rs1200130	167345196	C/T	C__8919154_10
		rs1358714	167346043	A/G	C__8919160_10
		rs1040503	167352845	A/G	C__8919179_10
<i>ATP1B3</i>	3q23	rs2068230	143106062	A/T	C__15861969_10
<i>SCNNIA</i>	12p13	rs11614164	6334123	A/G	C__2981241_20
		rs3782726	6339932	G/T	C__2981240_10
		rs7973914	6346984	C/T	C__31787955_10
		rs10849446	6349553	A/C	C__31787949_10
		rs2286600	6353047	A/G	C__1249946_1_
<i>SCNNIB</i>	16p12.2-p12.1	rs11074555	23231527	C/T	C__3188761_10
		rs9930640	23239801	A/G	C__30539119_10
		rs239345	23253439	A/T	C__2387896_30
		rs238547	23267700	C/T	C__2387909_1_
		rs8044970	23269331	G/T	C__3280856_10
		rs152740	23276591	A/T	C__2387921_10
		rs250563	23286780	C/T	C__2387939_10
		rs2303153	23297702	G/C	C__15971133_10
<i>SCNNIG</i>	16p12	rs5735	23108349	C/T	C__11894747_10
		rs4247210	23113158	C/G	C__11190190_10

Abbreviations: A-adenine; ABI-Applied Biosystems Incorporated; *AGTR2*-angiotensin II receptor, type 2; *ATPIA1*-ATPase, Na⁺/K⁺ transporting, alpha 1 polypeptide; *ATPIA2*-ATPase, Na⁺/K⁺ transporting, alpha 2 (+) polypeptide; *ATP1B1*-ATPase, Na⁺/K⁺ transporting, beta 1 polypeptide; *ATP1B3*-ATPase, Na⁺/K⁺ transporting, beta 3 polypeptide; *ATP6AP2*-ATPase, H⁺ transporting, lysosomal accessory protein 2; Bp- base pairs; C-cytosine; G-guanine; *REN*-renin; *RENBP*-renin binding protein; *SCNNIA*-sodium channel, nonvoltage-gated 1 alpha; *SCNNIB*-sodium channel, nonvoltage-gated 1, beta; *SCNNIG*-sodium channel, nonvoltage-gated 1, gamma; SNP- single nucleotide polymorphism ; T-thymine

2.4. TAQMAN SNP GENOTYPING

Genotypes were determined on all DNA samples using TaqMan allelic discrimination technology with ABI TaqMan Validated SNP Genotyping Assays (Applied Biosystems, Foster City CA, USA). Each SNP genotyping assay consists of two primers for amplification of the sequence of interest as well as two TaqMan MGB probes for allele detection. Each TaqMan probe contains a reporter dye at the 5' end of each allele specific probe (VIC for the Allele 1 probe and FAM for the Allele 2 probe), a minor groove binder (MGB) and a nonfluorescent quencher (NFQ) at the 3' end of each probe. The MGB increases the probe melting temperature (T_m) without increasing probe length resulting in greater differences in T_m values between matched and mismatched probes, thereby producing more accurate allelic discrimination (Kutyavin et al., 2000). Detection is achieved with proven 5' nuclease chemistry by means of exonuclease cleavage of a 5' allele-specific dye label, which generates the permanent assay signal by removal of the effect of the 3' quencher (figure 2.2).

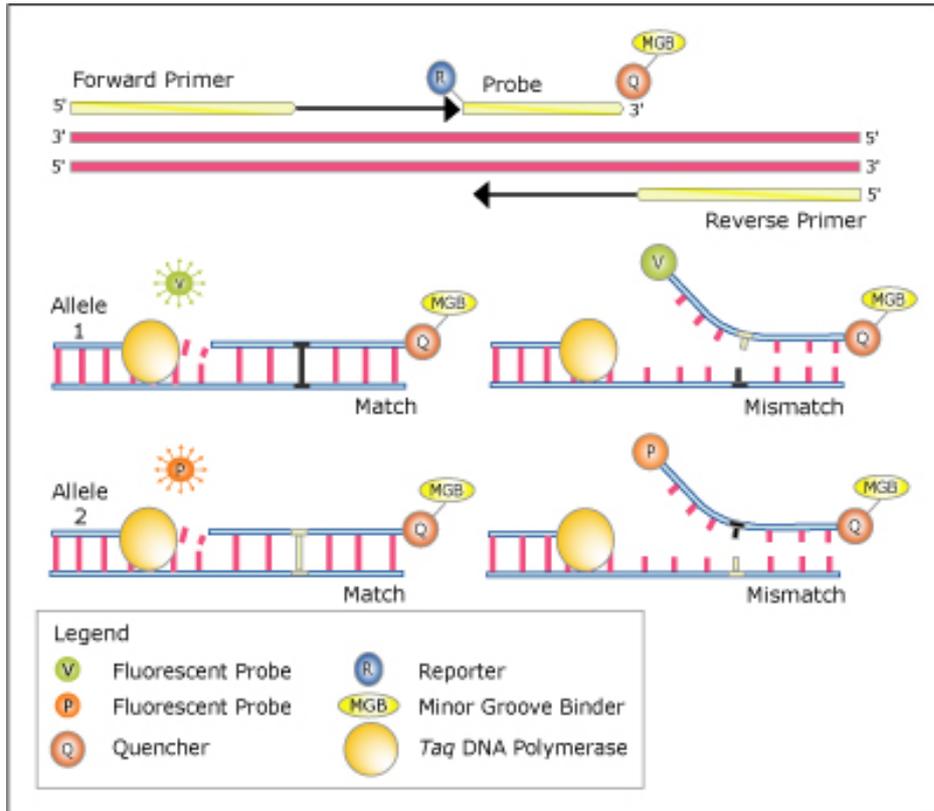


Figure 2.2. Overview of TaqMan allelic discrimination technology. Allelic discrimination is achieved by the selective annealing of the TaqMan probes and exonuclease cleavage of a 5' allele-specific dye label, which generates the assay signal (Taken from www.servicexs.com/.../TaqMan_AD_SNP_assay.jpg).

2.4.1. Real-time PCR amplification

PCR amplification for each SNP was performed in a single reaction tube on a thermostable 384-well plate on an ABI Prism 7900HT Sequence Detection System (Applied Biosystems Inc, Foster City CA, USA) following the manufacturer's instructions. All 384-well plates were prepared with an EpMotion pipetting robot (Eppendorf, Hamburg, Germany). A 5 µl reaction consisted of 2.5 µl ABI TaqMan Universal PCR Master Mix with the passive reference ROX (Perkin Elmer), 20 ng of genomic DNA, 0.25 µl TaqMan primer and probe dye mix and 1.25 µl DNase-free, sterile-filtered water. Each plate contained 330 PCR amplification reactions and 54 non-template control reactions, which contained all the above-mentioned reagents except genomic DNA, to test for contamination. PCR conditions were 2 min at 50°C, 10 min at 95°C, followed by 40 cycles of 15 sec at 92°C and 1 min 30 sec at 60°C.

2.4.2 Allelic discrimination

Allele discrimination was accomplished by running end point detection using ABI Prism 7900HT and the Sequence Detection Systems (SDS) 2.3 software (autocaller confidence level 95%). The SDS software reads fluorescence and performs automatic allele calling by generating allelic discrimination plots. A text file containing the genotyping results is then generated and directly incorporated into a database, minimizing transfer errors. In addition, all results were confirmed by visual inspection of the real-time PCR multicomponent analysis plots.

2.5. STR GENOTYPING

The *NR3C2* gene is relatively large (363.60kb) when compared to the other genes covered in the present study and therefore we decided to first perform an preliminary association study using short tandem repeat (STR) analysis and follow with a multi-SNP based association study, should sufficient evidence for association of this genomic region to hypertrophy in HCM be found. Subjects were genotyped according to the length of the tetranucleotide AGAT repeat in intron 2 of *NR3C2* as previously described by Munoz-Brauning et al. (2005).

2.5.1. PCR amplification

PCR amplification was performed in 10 µl reactions, which contained 2x KapaTaq ReadyMix (Kapa Biosystems Inc, RSA), 5 pmol of 5` FAM labelled forward primer (5' AAC CCC TGG GTG AAG AGA AT 3'), 5 pmol of reverse primer (5' TTG AGG TCA CTC AGT ATT TGC C 3') and 20ng of genomic DNA. A non-template control reaction which contained all the above-mentioned reagents except genomic DNA was included in each PCR amplification run to test for contamination.

PCR conditions were 3 min at 94°C, followed by 35 cycles of 40 sec at 94°C, 40 sec at 60°C and 40 sec at 72°C and a final extension step of 10 min at 72°C. Amplification was performed in a Perkin-Elmer 2700 thermal cycler (Applied Biosystems Inc, Foster City CA, USA). The samples were then analyzed on a 1.5 % agarose gel to determine the presence of PCR product.

2.5.2. Agarose gel electrophoresis

Verification of the STR PCR-amplification was performed by gel electrophoresis, allowing visualisation of DNA bands on an agarose gel. The agarose gel was prepared by mixing 1.5 g of agarose powder (Whitehead Scientific, RSA) with 100 ml 1x di-sodium tetraborate-decahydrate

buffer (SB) for a 1% agarose gel (Appendix I). The mixture was then heated until the agarose was completely dissolved and 5 μ l of (10 mg/ml) ethidium bromide (Whitehead Scientific, RSA) was added to the agarose solution, which was subsequently poured into a casting tray containing a well-forming sample comb and allowed to solidify at room temperature.

After solidification, the gel was placed horizontally into the electrophoresis chamber and covered with 1x SB buffer solution (Appendix I). Electrophoresis was performed as follows: 5 μ l of each amplification product was mixed with 3 μ l of bromophenol blue loading dye (Appendix I) and then pipetted into the sample wells. A 100 bp DNA ladder (Promega Corp, Madison Wisconsin, USA) was co-electrophoresed with PCR products and used as a molecular size marker.

Electrophoresis of samples occurred at 200 V for 15-20 min in 1x SB buffer solution. Electrophoretically separated PCR samples were then visualised under ultra-violet (UV) light using the Syngene gel documentation G-box HR (Frederick, MD, USA). A permanent photographic record of the gel analysis was obtained again using the Syngene gel documentation G-box HR (Frederick, MD, USA).

2.5.3. STR analysis

To enable the AGAT repeat analysis, 0.5 μ l of Liz 500 size standard (Applied Biosystems Inc, Foster City CA, USA) and 9 μ l HiDi Formamide (Applied Biosystems Inc, Foster City CA, USA) was added to 1 μ l of each PCR product. All the samples were then denatured for 2 min at 94°C and placed on ice for 5 min. Subsequently, samples were run on the 3130xl Genetic Analyzer (Applied Biosystems Inc, Foster City CA, USA) and analysed with Genemapper v. 3.5 software (Applied Biosystems Inc, Foster City CA, USA).

2.6 STATISTICAL ANALYSIS

Genotypic and phenotypic data were captured onto family trees using Cyrillic 2.1 (Cherwell Scientific, UK) and subsequently exported in MLINK format and combined with an Excel sheet containing the echocardiographic and covariate data to create a pedigree file for statistical analysis.

Family-based tests for association were utilized to investigate the association between the abovementioned polymorphisms and hypertrophic traits. Family-based association tests have the advantage that they allow tracing of the transmission of the alleles associated with hypertrophic

phenotypes from parent to offspring in multiple generations. Linear mixed-effects models were used, because they enable us to adjust for various known confounders, as well as for the specific relatedness between family members in estimating the various variance components (environment, polygenic, specific genes). For all single autosomal polymorphisms, we used the orthogonal test from a program, QTDT (quantitative transmission disequilibrium test), developed by Abecasis et al. (2002), which incorporates the specific relationship between pairs of individuals in assessing the phenotype-genotype association. Because QTDT does not cover these yet, we used an R package, kinship, to test association with X-linked markers as well as for estimating and testing interactions between pairs of markers.

QTDT enables both linkage and association analysis of quantitative traits depending on the model implemented in the program. R is an environment for statistical computing and graphics, which is freely available from www.r-project.org. The R package, kinship, was designed for linear mixed-effects models for data from large pedigrees and is also available from www.r-project.org.

2.6.1 Descriptive statistics and trait distribution

Validation of input files and Mendelian inheritance within families was verified with Pedstats v. 6.11 (Wigginton and Abecasis, 2005) and genotyping inconsistencies were resolved by re-genotyping. X-chromosome settings were used throughout for the analyses of X-linked genes, i.e. *AGTR2*, *ATP6AP2* and *RENBP*. Furthermore, Pedstats was used to test conformance of genotypes with Hardy-Weinberg equilibrium (HWE) and graphical summaries were generated of allele and genotype frequencies as well as the distribution and familial correlations of quantitative traits and covariates. Pedstats selected unrelated individuals from the families for both Hardy-Weinberg testing and frequency estimation.

Linear models and variance components analyses are sensitive to kurtosis and skewness in trait distribution and various trait values in the present study were positively skewed. Quantile normalization was therefore used to transform each trait to approximate normality (Pilia et al., 2006) prior to association analysis.

2.6.2 Linkage disequilibrium (LD) determination

Haploview v. 4.1 (Barrett et al., 2005) was used to compute pairwise LD statistics for our study cohort using the genotype data generated in the present study. The pairwise LD is analysed in

terms of D' values and each pair of SNPs is labelled as being in strong LD, uncertain or in strong recombination. Haploview also enables haplotype analysis by constructing haplotypes using a common block definition from Gabriel et al., (2002). A haplotype block is created if a D' value indicates strong LD.

2.6.3 Quantitative transmission disequilibrium test

The orthogonal test from QTDT is ideally suited for this study as it is applicable to the analysis of quantitative traits in families of any size and is robust to population stratification. The transformed dataset was used to construct pedigree and data files as specified by the QTDT tutorial (<http://www.sph.umich.edu/csg/abecasis/QTDT/>) for the subsequent analyses of all the quantitative hypertrophic traits listed in table 2.2. The specific relationship between family members was integrated in the analyses using identity-by-descent (IBD) probabilities estimated with simwalk2 (Sobel et al., 2001). The following covariates were also included: systolic BP, diastolic BP, age, sex, BSA and HR. Furthermore, the three mutation founder groups (A797T, R403W and R92W) were included to adjust for ancestral relatedness within each founder group and to correct for the possible influence of the distinct HCM causal mutation on variability of the hypertrophic phenotype.

The initial step was to build a variance component model by dividing trait variance into environmental and heritable polygenic components without modelling association (Abecasis et al., 2002; Iles 2002). The variance component analysis and heritability testing of the various hypertrophy traits for this dataset were already performed by Mr. R Cloete and is reported in his thesis (Cloete REA, M.Sc). The association of autosomal gene variants with heritable hypertrophy traits were assessed with QTDT's orthogonal model, adjusting for all covariates and environmental and polygenic variance components. Exact p-values for all QTDT significant associations were determined using Monte-Carlo permutation tests (McIntyre et al., 2000). For alleles that showed significant association with the hypertrophy traits, effect sizes were estimated in the original units of measurement, using the untransformed dataset.

2.6.4 Linear mixed-effects models

The linear mixed-model analyses were done with function `lmekin` from R package: kinship (www.r-project.org). The function enables linear mixed-effects modeling for data from large pedigrees using per-individual random effects which are correlated according to kinship

coefficients. The transformed dataset was used to construct pedigree data files for the subsequent analyses of all the quantitative hypertrophic traits listed in table 2.2. The specific relationship between family members was integrated in the analyses using kinship probabilities estimated with function `makekinship` in `kinship`. The following covariates were also included: systolic BP, diastolic BP, age, sex, BSA and HR. Furthermore, the three mutation founder groups (A797T, R403W and R92W) were included to adjust for ancestral relatedness within each founder group and to correct for the possible influence of the distinct HCM causal mutation on variability of the hypertrophic phenotype. This was used for assessing association with X-linked genes, as well as gene-gene interactions. For markers that showed significant association with the hypertrophy traits, effect sizes were estimated in the original units of measurement, using the untransformed dataset.

We found 1006 significant interactions between pairs of markers on traits. We calculated, for each pair of markers, the number of traits for which they showed significant interactions. Because describing and discussing them all would be beyond the scope of this thesis, we decided to concentrate on those pairs of markers showing significant interactions on more than 4 of the hypertrophy traits. Line plots are used to illustrate the interactions of pairs of SNPs on selected traits. The two SNPs would show parallel graphs for all the genotypes if there is no evidence for interaction.

CHAPTER 3
RESULTS

INDEX	PAGE
3.1 BASELINE CHARACTERISTICS FOR THE STUDY COHORT	40
3.2 CANDIDATE GENES SELECTED	42
3.3 PRIORITIZING SNPS FOR INVESTIGATION	42
3.4 GENOTYPING RESULTS	44
3.4.1 TaqMan allelic discrimination	44
3.4.2 STR genotyping	45
3.5 STATISTICAL ANALYSES	47
3.5.1 Descriptive statistics	47
3.5.2 LD assessment	60
3.5.3 Association tests	63
3.5.3.1 MR	64
3.5.3.2 AT ₂ Receptor	66
3.5.3.3 Renin and renin-associated genes	68
3.5.3.4 Na ⁺ /K ⁺ -ATPase subunits	71
3.5.3.5 ENaC subunits	73
3.6 GENE-GENE INTERACTION ANALYSIS	77
3.6.1 <i>REN</i> and <i>RENBP</i>	81
3.6.2 <i>REN</i> and <i>SCNN1B</i>	81
3.6.3 <i>REN</i> and <i>ATP1B1</i>	82
3.6.4 <i>ATP6AP2</i> and <i>SCNN1B</i>	84
3.6.5 ENaC subunits	84
3.6.6 Na⁺/K⁺-ATPase subunits and ENaC subunits	86

3.1 BASELINE CHARACTERISTICS FOR THE STUDY COHORT

The basic characteristics of the study subjects as well as selected hypertrophy traits are presented in table 3.1, stratified into mutation carrier (MC) and non-carrier (NC) groups for the three HCM causal mutations present in the study cohort. Data are summarised here as median (interquartile range) due to the skewness of some of the trait distributions. In total, we identified 127 individuals with HCM causal mutations in the study cohort.

Table 3.1. Basic characteristics of the study cohort stratified into mutation carrier (MC) and non-carrier (NC) groups according to HCM mutation status.

	A797T		R92W		R403W	
	MC	NC	MC	NC	MC	NC
Total:	56	50	41	29	30	21
Males (%)	32 (57)	27 (54)	18 (44)	11 (38)	19 (63)	8 (38)
Age	43.5 (14-81)	36.5 (14-68)	37 (14-78)	33 (17-60)	39.5 (18-72)	35 (16-58)
BSA (m²)	1.9 (1.3-2.5)	1.9 (1.5-2.3)	1.7 (1.3-2.2)	1.8 (1.3-2.1)	1.8 (1.3-2.3)	2.0 (1.5-2.3)
SBP (mm Hg)	120 (100-180)	120 (90-180)	120 (90-200)	120 (90-160)	122.5 (100-170)	125 (100-230)
DBP (mm Hg)	80 (60-100)	80 (60-120)	77.5 (60-100)	80 (60-90)	80 (60-110)	80 (60-110)
HR (bpm)	65 (44-120)	65 (50-95)	68 (45-110)	70 (45-83)	65 (52-96)	72 (53-90)
LVM (g)	200.8 (71.4-476.6)	133.3 (61.1-272)	133.7 (48.2-295.4)	113.7 (58.4-246.1)	173.9 (77.4-273.8)	141.9 (59.1-290.5)
mIVSTmit (mm)	14 (8-34)	9.6 (5.6-20.5)	13.8 (6.3-27)	9.3 (6.8-16.5)	13.1 (7.2-27)	10.7 (6.6-16.1)
mIVSTpap (mm)	15.4 (8-38.7)	9.6 (6.5-27)	13.7 (6.7-30)	8.6 (6.8-15.5)	13.4 (7.7-27.8)	10.5 (7-18.5)
mIVSTapx (mm)	12.1 (8.3-37.4)	9.3 (5.6-20.6)	10.4 (6.5-25.6)	8.7 (6.3-11.9)	10.7 (7.2-24.9)	10.1 (6.8-12.6)
PWmit (mm)	9.1 (6-15.1)	8.6 (5.4-13)	8.1 (5.7-13.2)	7.5 (4.3-9.6)	8.8 (6-13.7)	8.8 (5.4-13.6)
PWpap (mm)	9.8 (6.3-16)	8.6 (5-15)	8.5 (6.6-12.7)	7.6 (5.6-10)	9.3 (6.5-16)	8.8 (5.2-11)
PWapx (mm)	9.6 (6.7-17.5)	8.3 (6.2-13.5)	9 (6.1-15.3)	7.8 (5.6-10.3)	10.1 (6.7-17.9)	9.3 (6-10.3)

*Data summarised as median (Q₁, Q₃)

Abbreviations: BSA-body surface area; DBP-diastolic blood pressure; HCM-hypertrophic cardiomyopathy; HR-heart rate; LVM-left ventricular mass; MC-HCM mutation carrier; mIVST-maximal interventricular septum thickness; mIVSTmit-maximal interventricular septum thickness at the mitral valve; mIVSTpap-maximal interventricular septum thickness at the papillary level; NC-non-carrier; PWapx-posterior wall thickness at the supra-apex level; PWmit-posterior wall thickness at the mitral valve; PWpap-posterior wall thickness at the papillary level; SBP-systolic blood pressure

3.2 CANDIDATE GENES SELECTED

Bioinformatic-based literature searches identified twelve candidate genes which encode key components of the RAAS. A literature search was subsequently performed to find evidence for their involvement in HCM, LVH or EH. Although hypertension can be viewed as an indirect link to HCM, its role in hypertrophy can not be ignored as discussed in section 1.3.2. A detailed discussion of these findings within the context of the present study will follow in the Discussion chapter.

3.3 PRIORITIZING SNPS FOR INVESTIGATION

For the present study, SNPs were selected to achieve an even spacing of 0.5 LDUs on the metric LD map for the HapMap CEU and YRI populations. Only SNPs for which validated TaqMan assays could be obtained were chosen for investigation.

The YRI population sample consisted of 30 parent-offspring trios from the Yoruba people in Ibadan, Nigeria while the CEU population consisted of 30 parent-offspring trios with northern and western European ancestry (obtained from the Centre d'Etude du Polymorphisme Humain). The HapMap data also contains two additional populations: 45 unrelated Han Chinese individuals from Beijing, China (CHB) and 45 unrelated Japanese individuals from Tokyo, Japan (JPT). For the purposes of the present study, we combined the JPT and CHB data, resulting in three groups: YRI, CEU and JPT + CHB. Table 3.2 depicts the minor allele frequency (MAF) of each SNP covered in the present study in each of the three groups.

Table 3.2. Minor allele frequencies (MAF) of each SNP covered in the present study in the HapMap YRI, CEU and JPT + CHB population groups.

Gene	Chromosome	SNP	Nucleotide Change	MAF*		
				CEU	YRI	JPT + HCB
<i>AGTR2</i>	Xq22-q23	rs1403543	G/A	0.433 (G)	0.425 (A)	0.284 (G)
		rs5194	G/A	0.457 (A)	0.375 (G)	0.340 (A)
		rs11091046	C/A	0.391 (A)	0.386 (C)	0.417 (A)
<i>ATP6AP2</i>	Xp11.4	rs2968915	A/G	0.075 (G)	0.142 (G)	0.118 (G)
		rs2968917	C/T	0.075 (C)	0.142 (C)	0.128 (C)
		rs10536	G/A	0.000 (G)	0.474 (G)	0.143 (G)
<i>RENBP</i>	Xq28	rs762656	A/G	0.242 (G)	0.333 (A)	0.191 (A)
		rs2269372	A/G	0.242 (G)	0.308 (A)	0.189 (A)
		rs2269370	A/C	0.217 (A)	0.350 (A)	0.312 (C)
<i>REN</i>	1q32	rs10900555	C/T	0.258 (C)	0.483 (T)	0.433 (C)
		rs5705	A/C	0.150 (C)	0.333 (C)	0.028 (C)
		rs11571082	A/G	0.150 (A)	0.275 (A)	0.017 (A)
		rs1464816	G/T	0.433 (T)	0.228 (T)	0.293 (T)
<i>ATPIA1</i>	1p21	rs10924074	A/G	0.034 (G)	0.275 (G)	0.000 (G)
		rs850609	A/T	0.233 (T)	0.000 (T)	0.343 (T)
<i>ATPIA2</i>	1q21-q23	rs7548116	A/T	0.367 (T)	0.449 (A)	0.444 (T)
		rs11585375	A/G	0.408 (G)	0.250 (G)	0.300 (G)
<i>ATPIB1</i>	1q24	rs1200130	C/T	0.133 (T)	0.308 (T)	0.143 (T)
		rs1358714	A/G	0.500 (G)	0.292 (A)	0.157 (G)
		rs1040503	A/G	0.383 (G)	0.155 (A)	0.139 (A)
<i>ATPIB3</i>	3q23	rs2068230	A/T	0.433 (A)	0.183 (T)	0.433 (T)
<i>SCNNIA</i>	12p13	rs11614164	A/G	0.500 (G)	0.053 (G)	0.194 (G)
		rs3782726	G/T	0.483 (G)	0.085 (G)	0.209 (G)
		rs7973914	C/T	0.433 (T)	0.358 (T)	0.449 (T)
		rs10849446	A/C	0.450 (A)	0.044 (C)	0.052 (C)
		rs2286600	A/G	0.475 (C)	0.025 (T)	0.045 (T)
<i>SCNNIB</i>	16p12.2-p12.1	rs11074555	C/T	0.288 (C)	0.242 (T)	0.217 (C)
		rs9930640	A/G	0.000 (A)	0.342 (A)	0.000 (A)
		rs239345	A/T	0.325 (A)	0.433 (A)	0.213 (A)
		rs238547	C/T	0.432 (T)	0.017 (T)	0.022 (T)
		rs8044970	G/T	0.158 (G)	0.275 (G)	0.406 (G)
		rs152740	A/T	0.305 (T)	0.347 (A)	0.184 (A)
		rs250563	C/T	0.025 (T)	0.283 (T)	0.000 (T)
		rs2303153	G/C	0.467 (C)	0.175 (C)	0.145 (C)
<i>SCNNIG</i>	16p12	rs5735	C/T	0.283 (C)	0.042 (C)	0.185 (C)
		rs4247210	C/G	0.300 (C)	0.483 (G)	0.300 (C)

*Allele in brackets indicates minor allele

Abbreviations: A-adenine; *AGTR2*-angiotensin II receptor, type 2; *ATPIA1*-ATPase, Na⁺/K⁺ transporting, alpha 1 polypeptide; *ATPIA2*-ATPase, Na⁺/K⁺ transporting, alpha 2 (+) polypeptide; *ATPIB1*-ATPase, Na⁺/K⁺ transporting, beta 1 polypeptide; *ATPIB3*-ATPase, Na⁺/K⁺ transporting, beta 3 polypeptide; *ATP6AP2*-ATPase, H⁺ transporting, lysosomal accessory protein 2; C-cytosine; G-guanine; MAF-minor allele frequency; *REN*-renin; *RENBP*-renin binding protein; *SCNNIA*-sodium channel, nonvoltage-gated 1 alpha; *SCNNIB*-sodium channel, nonvoltage-gated 1, beta; *SCNNIG*-sodium channel, nonvoltage-gated 1, gamma; SNP- single nucleotide polymorphism ; T-thymine

3.4 GENOTYPING RESULTS

3.4.1 TaqMan allelic discrimination

All TaqMan PCR amplification runs were completed successfully and no amplification was observed in the non-template controls, ruling out the possibility of contamination. Results from the end point analyses were exported to a database file for further statistical analysis. Figure 3.1 depicts the genotyping results for the rs239345 polymorphism as a representation of the allelic discrimination plots obtained with the SDS software during end point analyses.

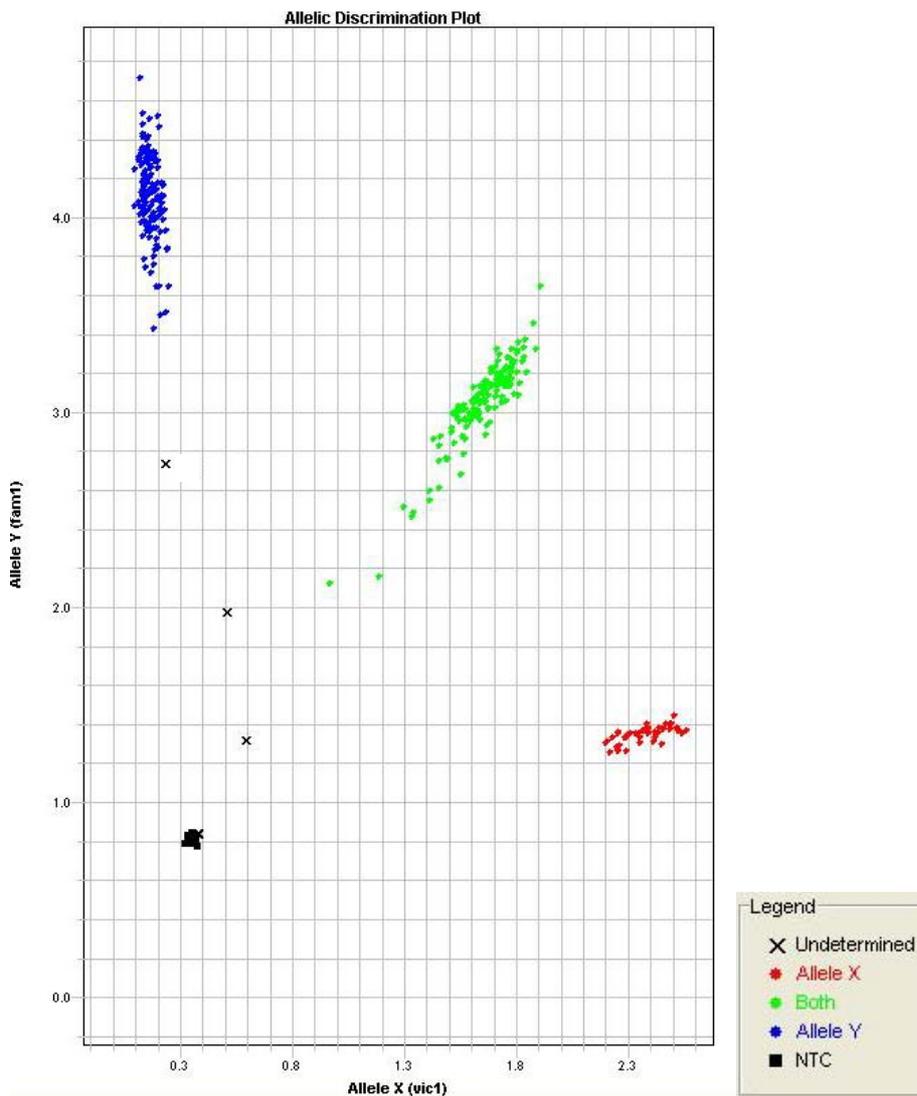


Figure 3.1. Representative genotyping result for TaqMan allelic discrimination. Genotyping results for the rs239345 polymorphism as a representation of the allelic discrimination plots obtained with the SDS software during end point analyses. Allele X = A; Allele Y = T

3.4.2 STR genotyping

PCR amplification runs were completed successfully and no amplification was observed in the non-template controls, indicating the absence of contamination. Figure 3.2 depicts a representation of the various alleles observed for the *NR3C2* AGAT repeat in the present study. Eight alleles were observed in total: 178, 182, 186, 190, 194, 198, 202 and 206 base pairs (bp) lengths, hereafter referred to as a₁, a₂, a₃, a₄, a₅, a₆, a₇ and a₈ respectively.

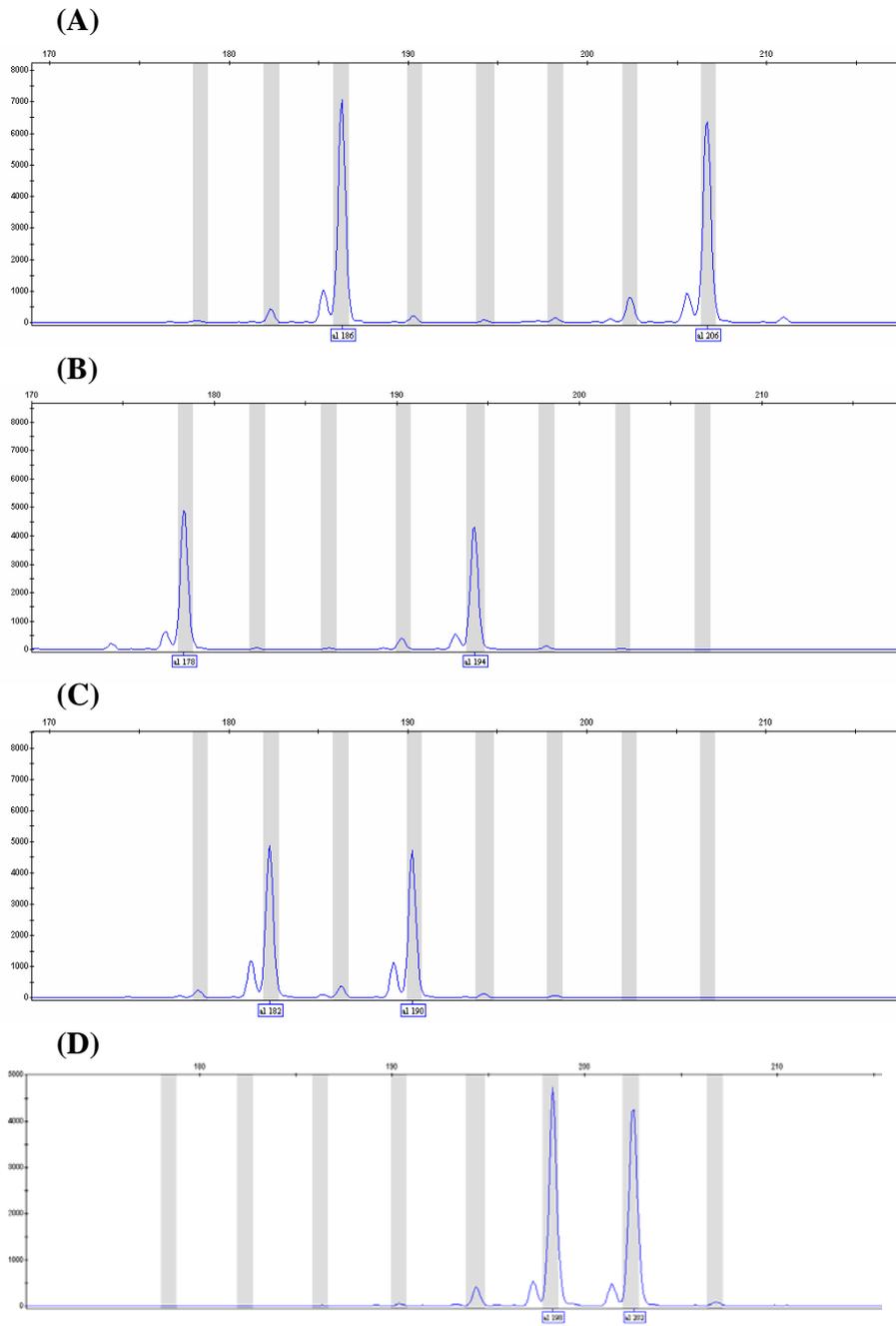


Figure 3.2. A representation of the eight alleles observed in the present study for the AGAT repeat STR. (A) Representation of the a_3/a_8 genotype. (B) Representation of the a_1/a_5 genotype. (C) Representation of the a_2/a_4 genotype. (D) Representation of the a_6/a_7 genotype.

3.5 STATISTICAL ANALYSES

3.5.1 Descriptive statistics

All genotypes shown to be inconsistent with expected Mendelian inheritance patterns as determined with Pedstats, were re-genotyped and included in the subsequent analysis. Table 3.3 shows the exact p-values obtained from an exact HWE test among unrelated individuals within the families as determined with Pedstats. Only the female population was used to test HWE for the X-linked markers. Genotype frequencies for all markers were in agreement with HWE.

Table 3.3. Exact Hardy-Weinberg equilibrium p-values calculated for unrelated individuals.

Gene	Chromosome	Marker	HWE exact p-value
<i>AGTR2</i>	Xq22-q23	rs1403543	0.455
		rs5194	0.133
		rs11091046	0.133
<i>ATP6AP2</i>	Xp11.4	rs2968915	0.390
		rs2968917	1.000
		rs10536	1.000
<i>RENBP</i>	Xq28	rs762656	0.060
		rs2269372	0.060
		rs2269370	0.639
<i>REN</i>	1q32	rs10900555	0.515
		rs5705	1.000
		rs11571082	1.000
<i>ATPIA1</i>	1p21	rs1464816	0.744
		rs10924074	0.124
		rs850609	0.548
<i>ATPIA2</i>	1q21-q23	rs7548116	0.514
		rs11585375	0.275
<i>ATPIB1</i>	1q24	rs1200130	0.231
		rs1358714	1.000
		rs1040503	0.740
<i>ATPIB3</i>	3q23	rs2068230	0.051
<i>SCNNIA</i>	12p13	rs11614164	0.304
		rs3782726	0.333
		rs7973914	0.523
		rs10849446	1.000
		rs2286600	1.000
		rs11074555	0.448
<i>SCNNIB</i>	16p12.2-p12.1	rs9930640	1.000
		rs239345	1.000
		rs238547	0.082
		rs8044970	0.067
		rs152740	0.528
		rs250563	1.000
		rs2303153	0.616
		rs5735	0.093
<i>SCNNIG</i>	16p12	rs4247210	0.150
		AGAT repeat	0.075

Abbreviations: *AGTR2*-angiotensin II receptor, type 2; *ATPIA1*-ATPase, Na⁺/K⁺ transporting, alpha 1 polypeptide; *ATPIA2*-ATPase, Na⁺/K⁺ transporting, alpha 2 polypeptide; *ATPIB1*-ATPase, Na⁺/K⁺ transporting, beta 1 polypeptide; *ATPIB3*-ATPase, Na⁺/K⁺ transporting, beta 3 polypeptide; *ATP6AP2*-ATPase, H⁺ transporting, lysosomal accessory protein 2; HWE-Hardy-Weinberg Equilibrium; *REN*-renin; *RENBP*-renin binding protein; *SCNNIA*-sodium channel, nonvoltage-gated 1 alpha; *SCNNIB*-sodium channel, nonvoltage-gated 1, beta; *SCNNIG*-sodium channel, nonvoltage-gated 1, gamma; *NR3C2*-nuclear receptor subfamily 3, group C, member 2

Pedstats was used to generate graphical outputs of the allele frequencies for each marker. Figures 3.3 to 3.14 depict the allele frequencies of each marker for the whole cohort (indicated in blue) and unrelated individuals (indicated in green): allele frequencies are plotted on the y-axis, while the allele name is plotted in the x-axis. The allele frequencies for the unrelated individuals present a

better estimate of the actual allele frequency within this South African mixed ancestry study population due to the familial nature of the study cohort.

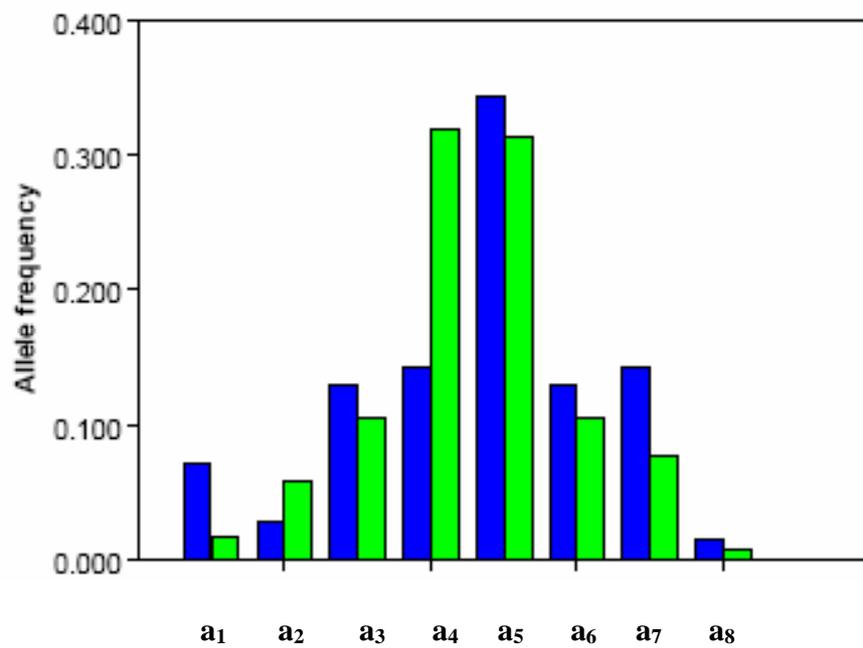


Figure 3.3. Allele frequencies for the AGAT repeat in NR3C2. Allele frequencies for the whole cohort are indicated in blue and in green for the unrelated individuals.

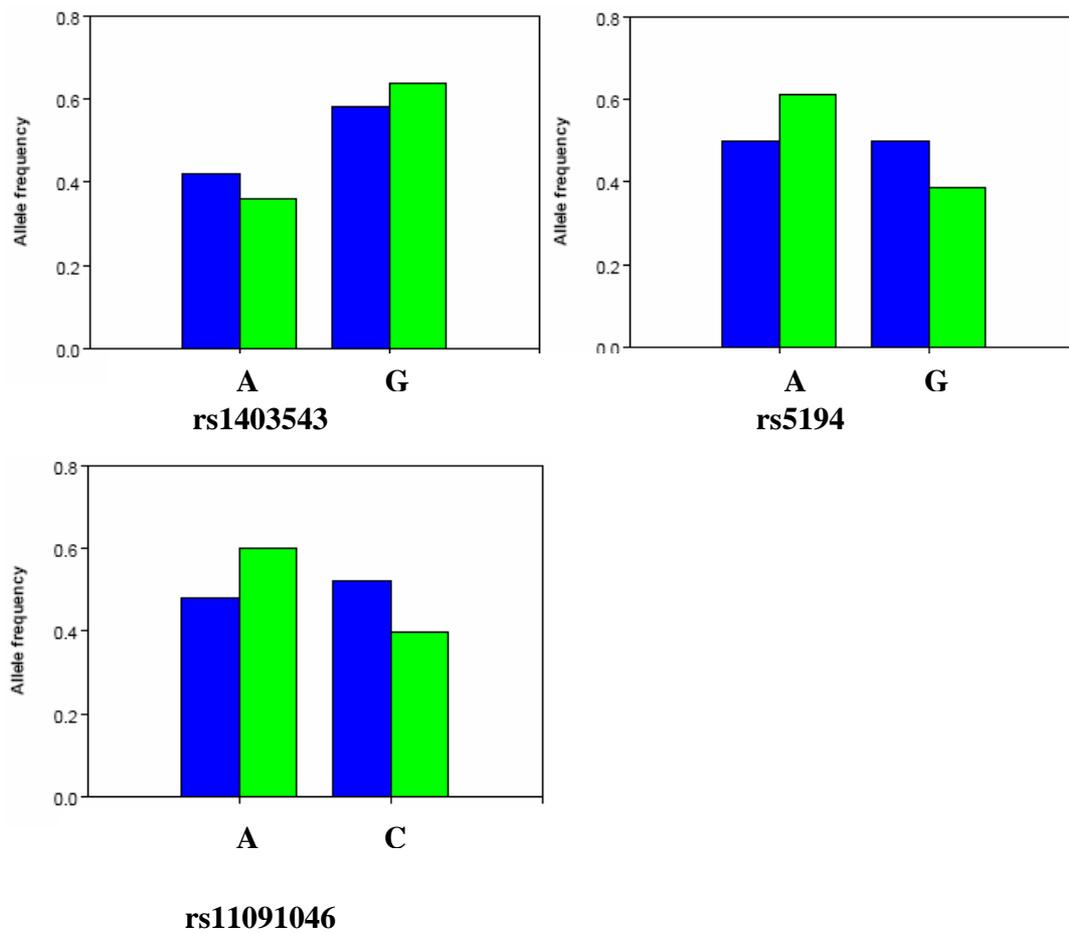


Figure 3.4. Allele frequencies for SNPs in *AGTR2*. Allele frequencies for the whole cohort are indicated in blue and in green for the unrelated individuals.

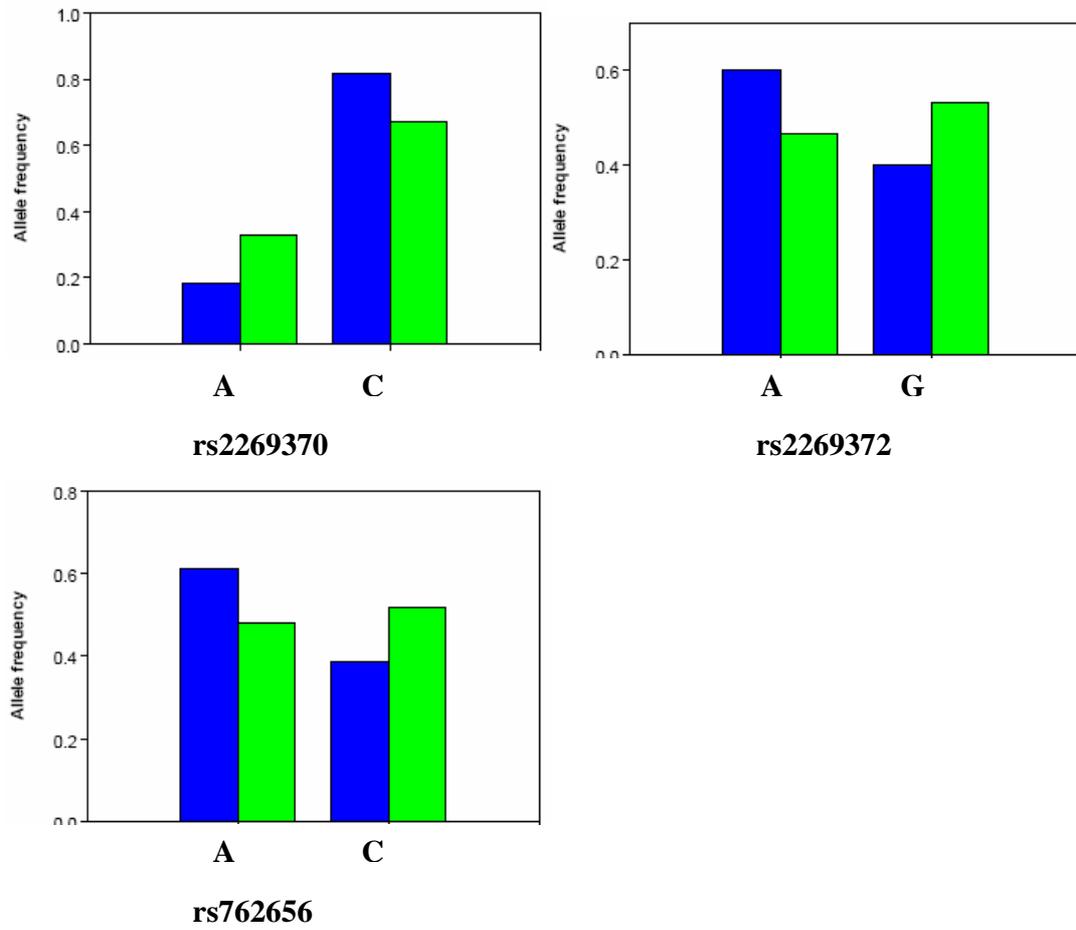


Figure 3.5. Allele frequencies for SNPs in *RENBP*. Allele frequencies for the whole cohort are indicated in blue and in green for the unrelated individuals.

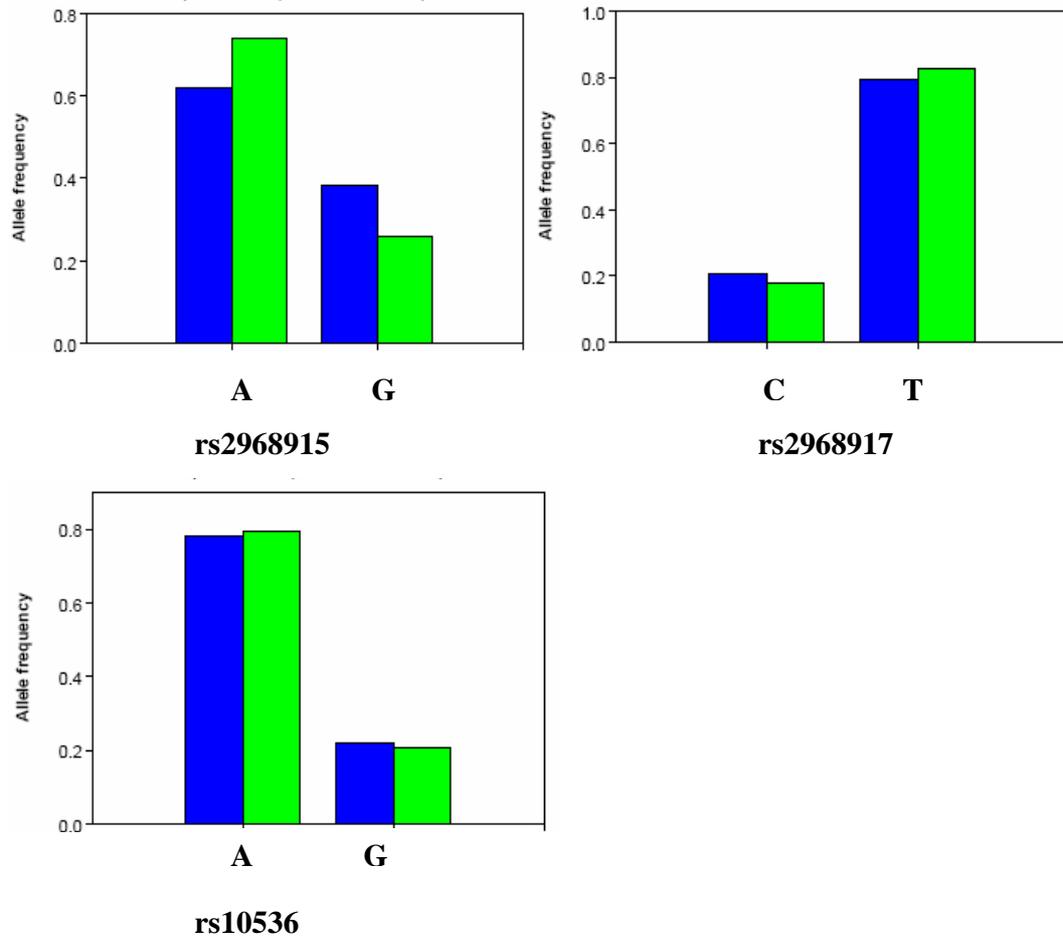


Figure 3.6. Allele frequencies for SNPs in *ATP6AP2*. Allele frequencies for the whole cohort are indicated in blue and in green for the unrelated individuals.

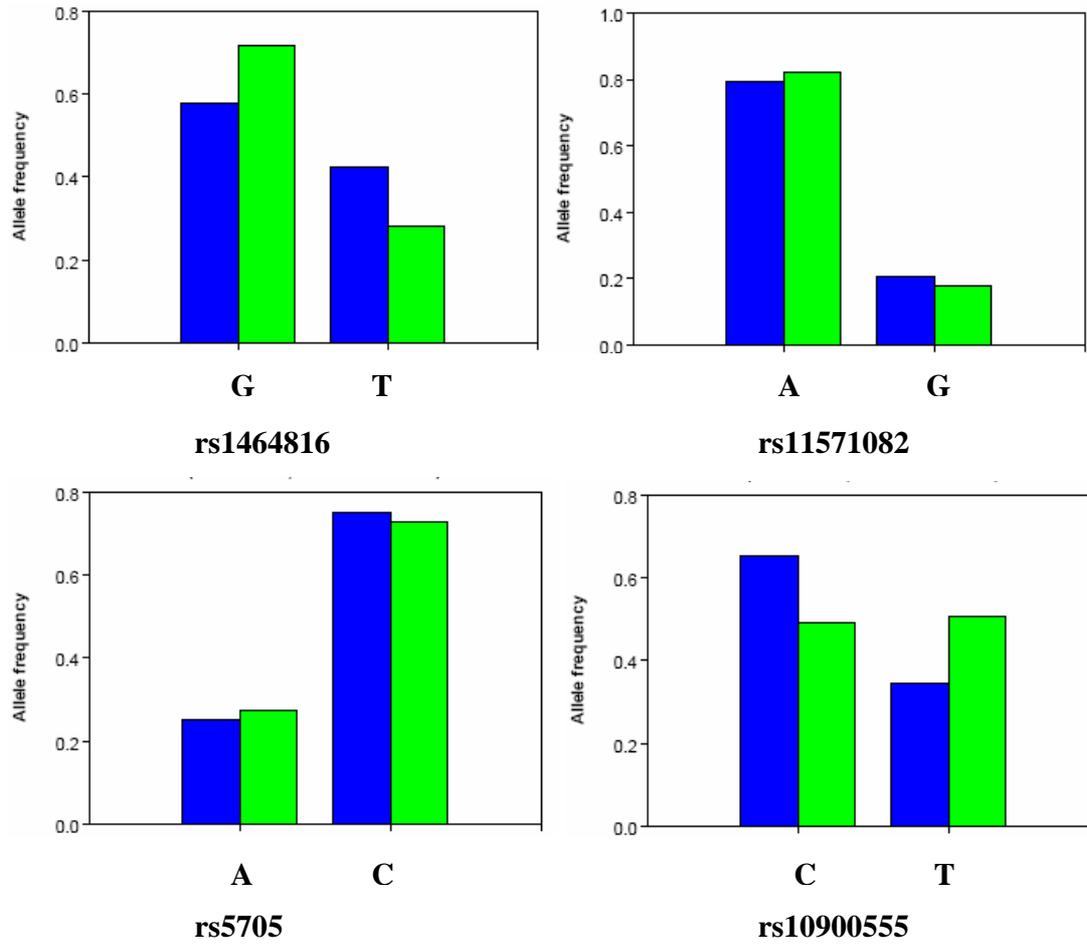


Figure 3.7. Allele frequencies for SNPs in *REN*. Allele frequencies for the whole cohort are indicated in blue and in green for the unrelated individuals.

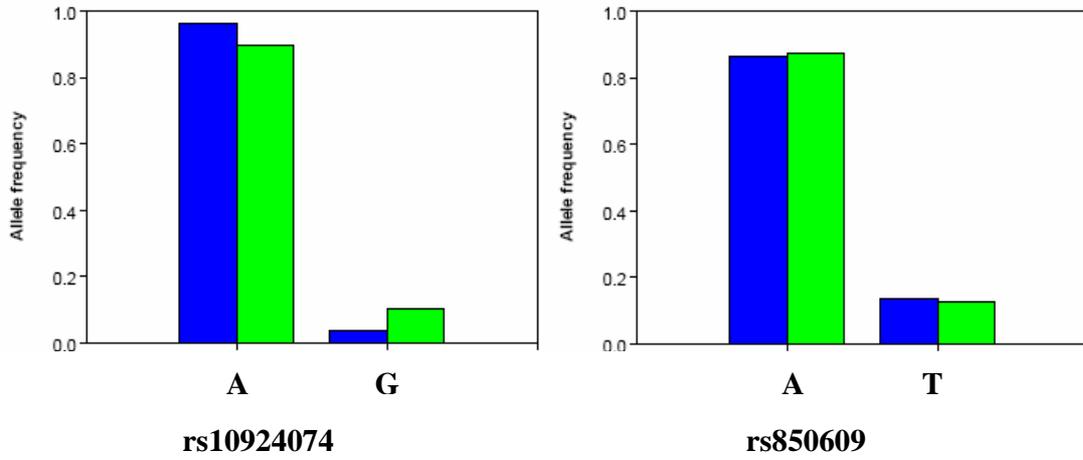


Figure 3.8. Allele frequencies for SNPs in *ATP1A1*. Allele frequencies for the whole cohort are indicated in blue and in green for the unrelated individuals.

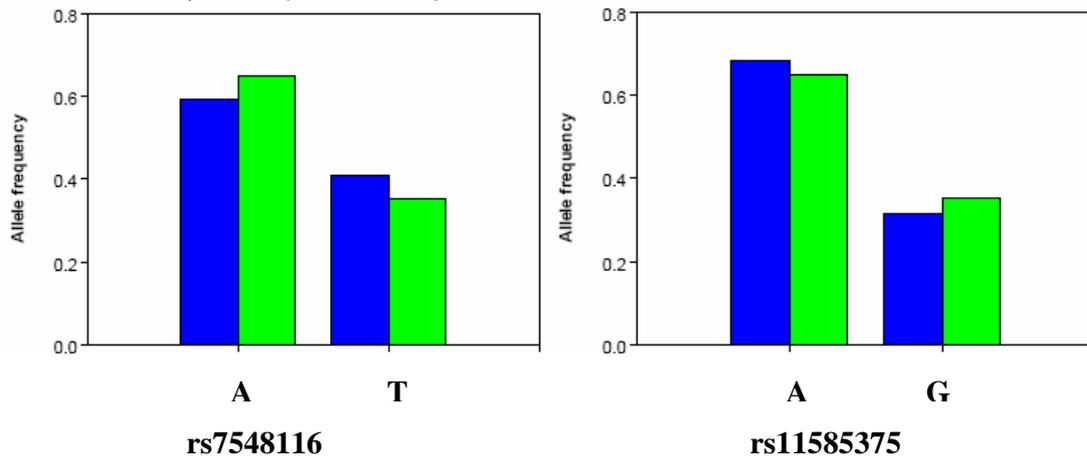


Figure 3.9. Allele frequencies for SNPs in *ATP1A2*. Allele frequencies for the whole cohort are indicated in blue and in green for the unrelated individuals.

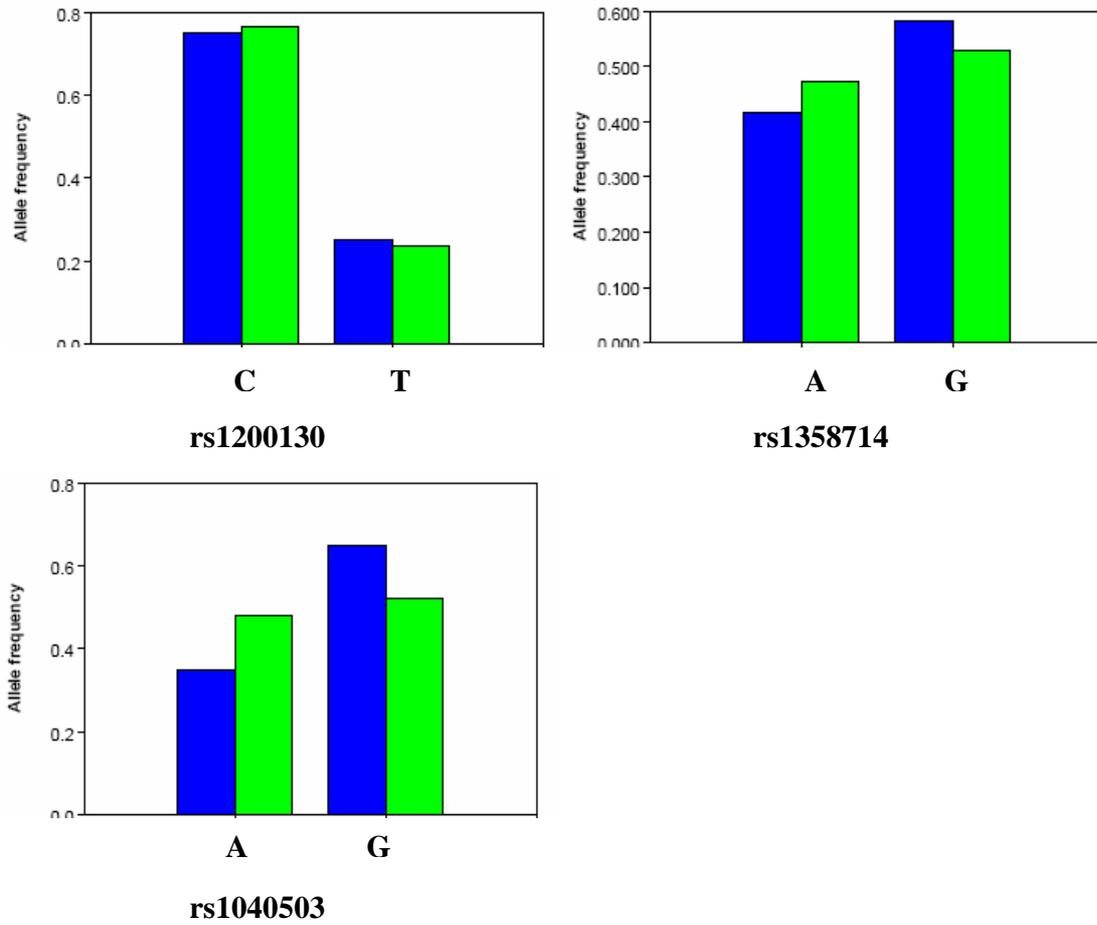


Figure 3.10. Allele frequencies for SNPs in *ATP1B1*. Allele frequencies for the whole cohort are indicated in blue and in green for the unrelated individuals.

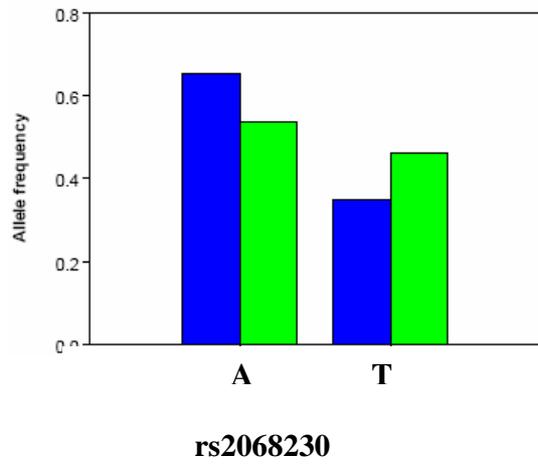


Figure 3.11. Allele frequencies for the SNP in *ATP1B3*. Allele frequencies for the whole cohort are indicated in blue and in green for the unrelated individuals.

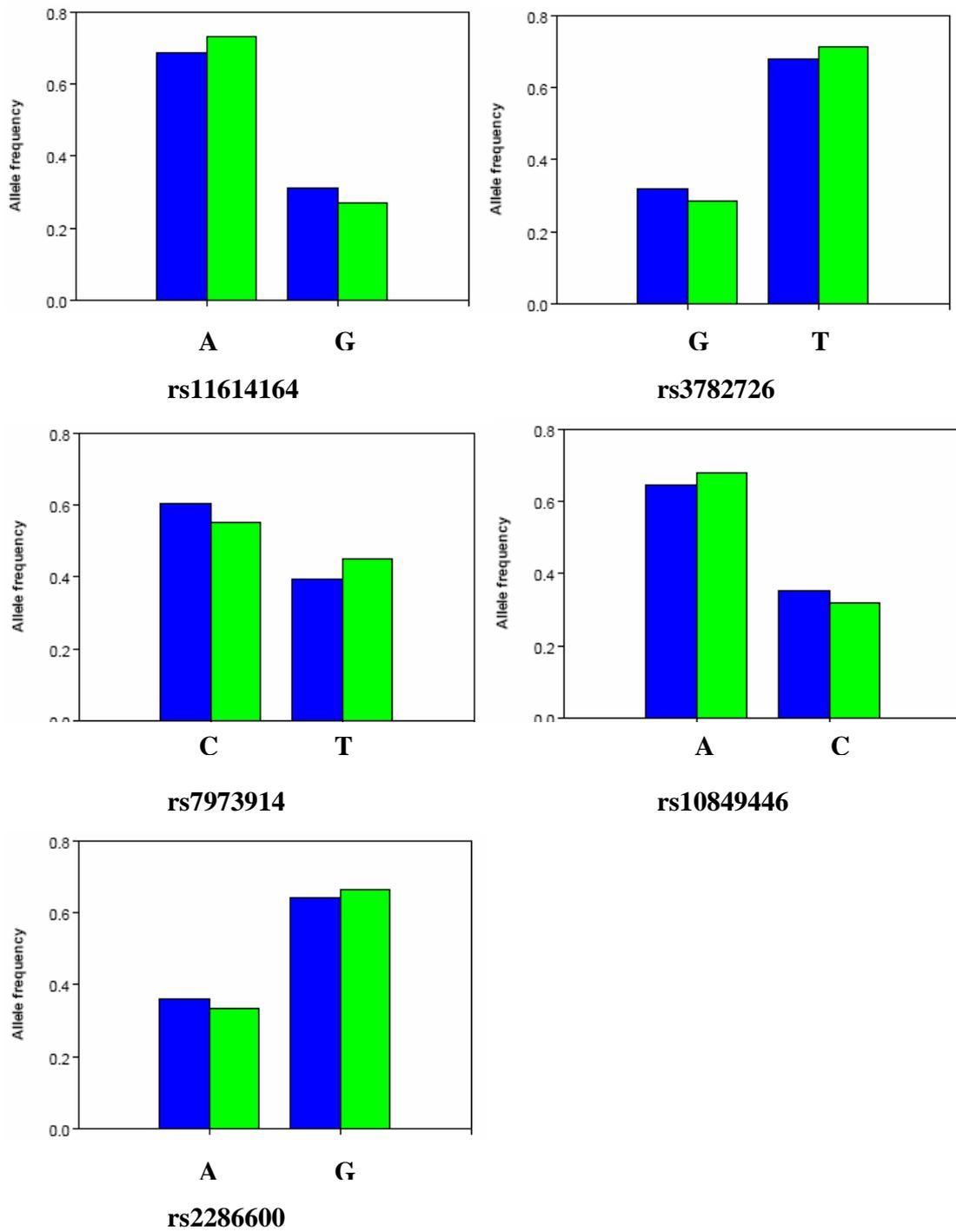


Figure 3.12. Allele frequencies for SNPs in *SCNN1A*. Allele frequencies for the whole cohort are indicated in blue and in green for the unrelated individuals.

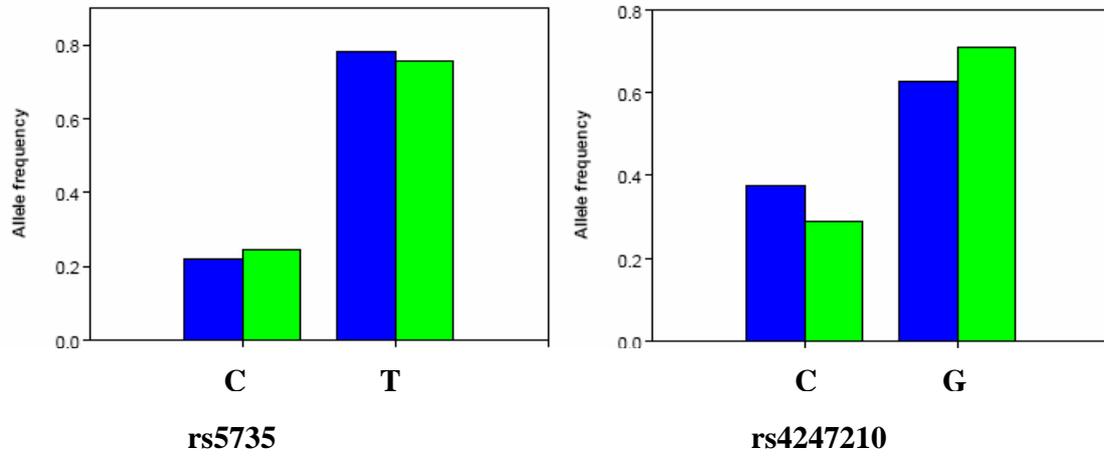


Figure 3.13. Allele frequencies for SNPs in *SCNN1G*. Allele frequencies for the whole cohort are indicated in blue and in green for the unrelated individuals.

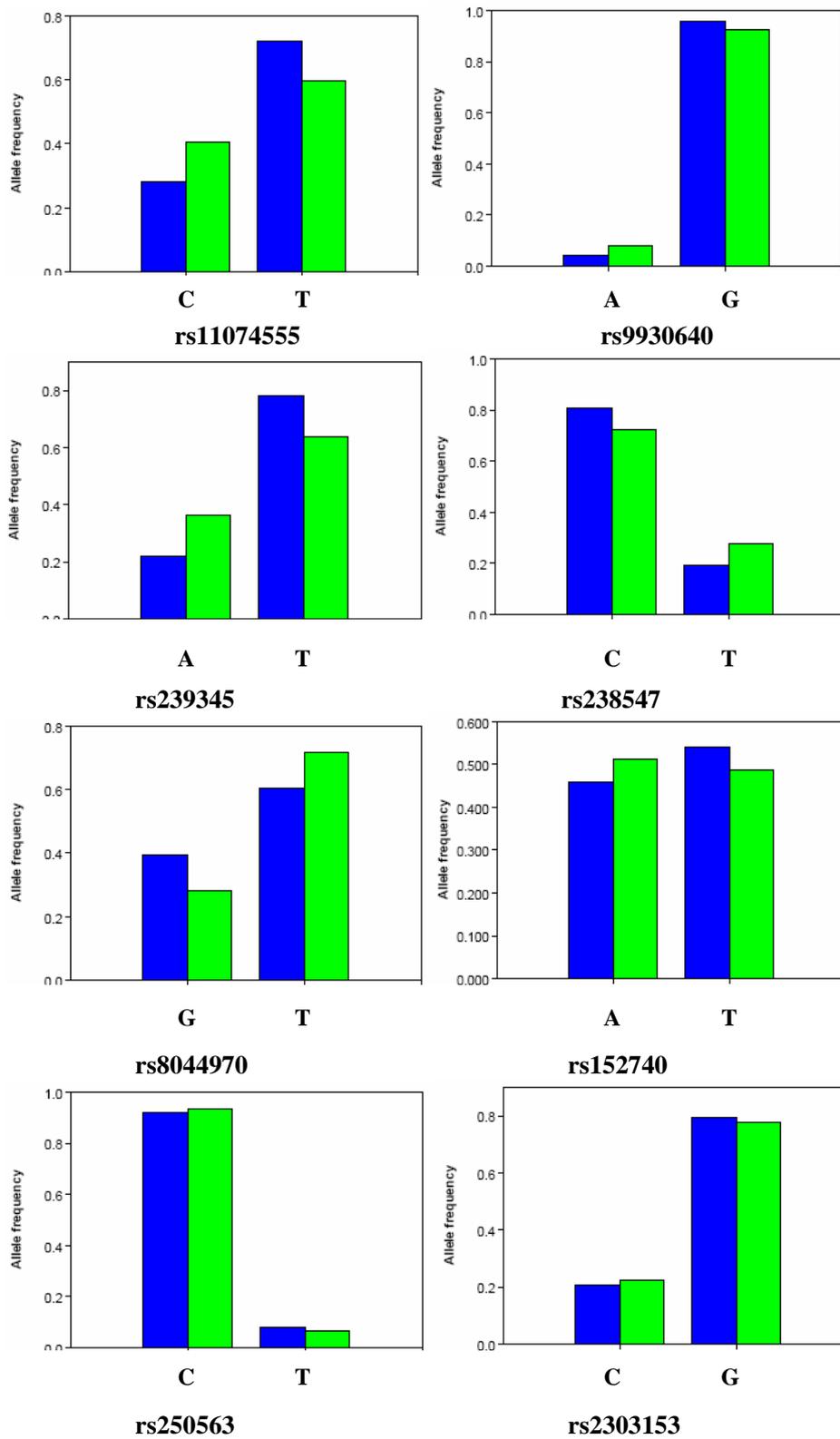


Figure 3.14. Allele frequencies for SNPs in *SCNN1B*. Allele frequencies for the whole cohort are indicated in blue and in green for the unrelated individuals.

3.5.2 LD assessment

Pairwise LD analyses were performed and haplotype blocks defined for the candidate genes for which two or more variants were genotyped and graphical representations, heatmaps, were obtained with Haploview.

Haploview provides unique estimates with case-control data and family trios, however, we observed minor inconsistencies in estimates of LD measures for different analysis runs with the same data in the present study cohort. Haploview attempts to define a set of maximally informative unrelated individuals to use in subsequent analyses as a sample of related individuals will give an incorrect estimate of LD, because related individuals are in tight LD by definition.. This task is relatively simple for nuclear- and trio family data. However, the present cohort consists of extended families. In situations like these Haploview uses a routine to define a sample of unrelated individuals, but there are sometimes multiple, equally valid unrelated sample sets, which can result in different LD estimates from the same family data. However, these differences are minor and can be safely ignored (Barrett JC, personal communication). Additionally, Haploview was the standard program that was used to estimate LD plots for the CEU and YRI populations in the HapMap project. We therefore include the results from the Haploview analyses as an estimate of LD between the investigated SNPs.

The following key was used to indicate the various D' values and LOD scores. a red block indicates a $D'=1$ and $\text{LOD} \geq 2$, while a blue block indicates $D'=1$ and $\text{LOD} < 2$. For $\text{LOD} \geq 2$, with D' values decrease gradually with lighter shades of red; white indicates a low D' and a low LOD score, $\text{LOD} < 2$. D' values are written as a percentage.

Figure 3.15 depicts the pairwise LD structure for the *AGTR2* in the present HCM cohort. Complete LD was observed between rs5194 and rs11091046 within *AGTR2* ($D'=1$) as indicated by the haplotype block in figure 3.15, while incomplete LD was observed between rs1403543 and rs5194 ($D'=0.68$) and rs11091046 ($D'=0.665$).

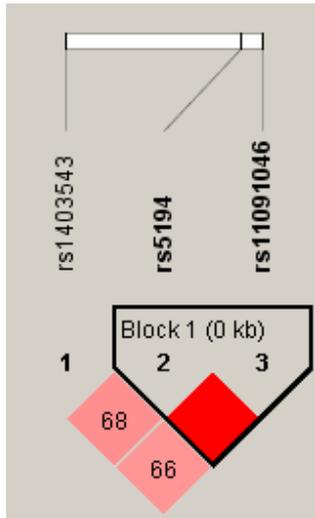


Figure 3.15. Pairwise LD structure for *AGTR2*.

Figure 3.16 depicts the pairwise LD structure for the *REN*, *RENBP* and *ATP6AP2*. Complete LD was observed between rs11571082 and rs5705 ($D' = 1$) and between rs1464816 and rs11571082 ($D' = 0.815$) within *REN*. Incomplete LD was observed between rs1464816 and rs5705 ($D' = 0.603$), rs1464816 and rs10900555 ($D' = 0.784$), rs5705 and rs10900555 ($D' = 0.722$) and rs11571082 and rs10900555 ($D' = 0.709$).

Complete LD was also observed between all the polymorphisms studied within *RENBP*, particularly between rs2269370 and rs762656 ($D' = 1$). As seen in figure 3.16 (C), complete LD was observed between rs2968915 and rs2968917 ($D' = 0.89$) while little evidence for pairwise LD was observed between rs2968915 and rs10536 ($D' = 0.486$), and rs2968917 and rs10536 ($D' = 0.39$) within *ATP6AP2*.

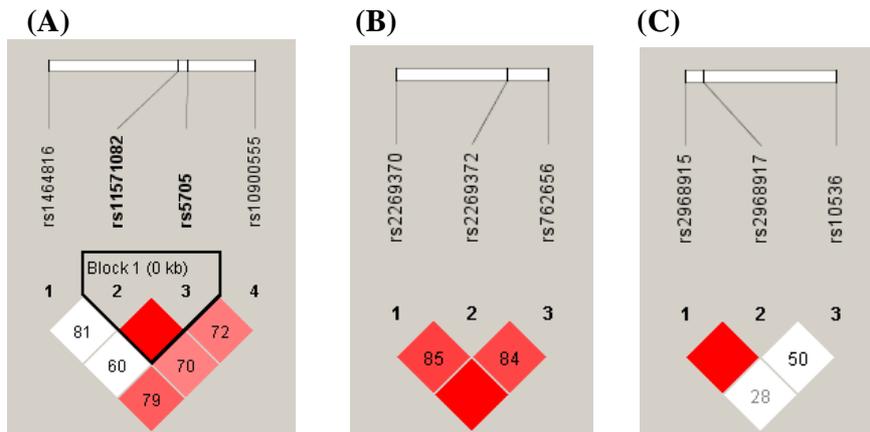


Figure 3.16. Pairwise LD structure for *REN* (A), *RENBP* (B) and *ATP6AP2* (C).

Figure 3.17 depicts the pairwise LD structure for *ATPIA1*, *ATPIA2* and *ATPIB1*. Overall, very little pairwise LD was observed between the polymorphisms studied within *ATPIA1*, *ATPIA2* and *ATPIB1*. The highest D' -value was observed between rs1200130 and rs1040503 ($D'=0.438$) within *ATPIB1*.

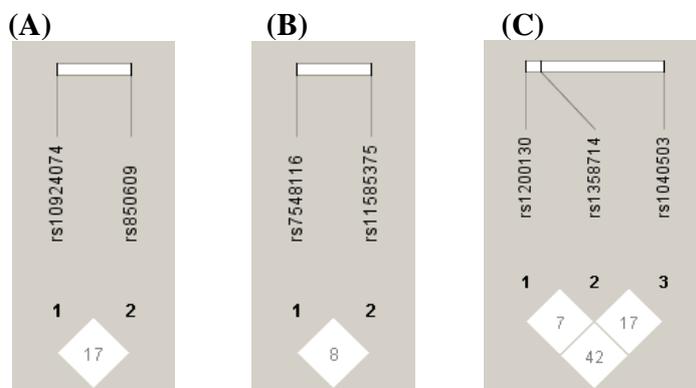


Figure 3.17. Pairwise LD structure for *ATPIA1* (A), *ATPIA2* (B) and *ATPIB1* (C).

Figure 3.18 depicts the pairwise LD structure for *SCNNIA*, *SCNNIB* and *SCNNIG*. Complete LD was observed between rs11614164 and rs3782726 ($D'=0.825$), rs11614164 and rs7973914 ($D'=0.835$) and rs10849446 and rs2286600 ($D'=0.938$) within *SCNNIA*. Incomplete LD was observed between rs3782726 and rs7973914 ($D'=0.739$), rs11614164 and rs10849446 ($D'=0.486$), rs11614164 and rs2286600 ($D'=0.473$) and rs3782726 and rs10849446 ($D'=0.473$). However, weaker evidence for LD was observed between the rest of the variants within *SCNNIA*, with the lowest D' -value observed between rs7973914 and rs2286600 ($D'=0.03$).

Complete LD was observed between rs11074555 and rs9930640 ($D' = 1$) as well as between rs238547 and rs8044970 ($D' = 1$) within *SCNN1B*. Incomplete LD was observed between rs11074555 and rs239345 ($D' = 0.591$) and rs238547 and rs152740 ($D' = 0.766$). Progressively weaker evidence for pairwise LD between the remaining markers studied within this gene was observed, starting at a D' -value of 0.461 between rs152740 and rs8044970 and the lowest D' -value was observed between rs9930640 and rs250563 ($D' = 0.027$).

Very little evidence for pairwise LD was observed between the two SNPs covered in *SCNN1G* ($D' = 0.124$).

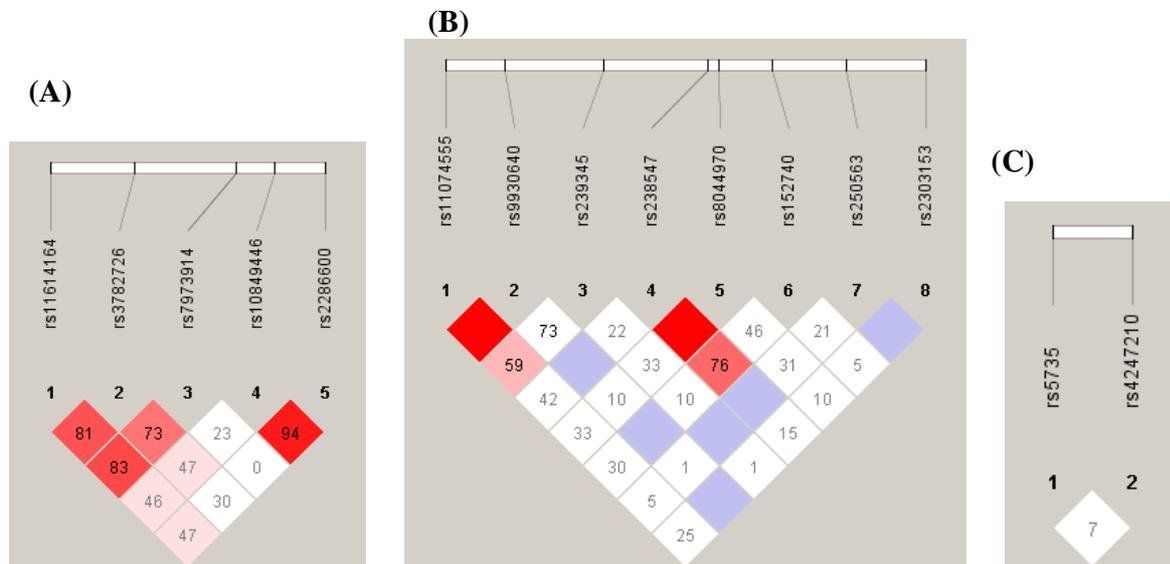


Figure 3.18. Pairwise LD structure for *SCNN1A* (A), *SCNN1B* (B) and *SCNN1G* (C).

3.5.3 Association tests

All markers were assessed under an additive model of association. Exact p-values for all significant associations detected with QTDT were determined using Monte-Carlo permutation tests. Effect sizes were calculated on untransformed covariate-adjusted traits and are thus given in terms of the original measurements. Effects sizes are reported as the average effect cause by the addition of an effect allele. For all X-linked variants, the effect allele refers to the minor allele and for autosomal variants this refers to the first allele in terms of alphabetical order. Note that if one allele causes a decrease in effect size, the other allele at that locus will cause an increase in effect size.

3.5.3.1 MR

QTDT requires at least 30 informative individuals, i.e. phenotyped individuals with at least one heterozygous parent to enable association analysis and two alleles of the AGAT repeat (i.e. a_1 and a_8) did not have the sufficient number of genotyped informative individuals, due to their very low allele frequency in our study population, and could therefore not be tested for association. Table 3.4 reports the results from the within-family tests of association. Significant association was found between the a_2 and a_7 alleles of the AGAT repeat and LW thickness at the apex level (p-values of 0.040 and 0.049, respectively). However, accurate echocardiographic measurements at the apex is difficult and the fact that association could only be found with a single hypertrophy trait at the apex level does not provide strong evidence for the involvement of the AGAT repeat within *NR3C2* in hypertrophy development in the current study cohort.

Table 3.4. Results from the association analysis: p-values for association between the AGAT repeat in NR3C2 and hypertrophy traits. P-values for the a₁ and a₈ alleles are not shown as they did not have the sufficient number of genotyped informative individuals to enable QTDT analysis. Significant p-values are indicated in bold red.

	<i>NR3C2</i>					
	a ₂	a ₃	a ₄	a ₅	a ₆	a ₇
mLVWTmit	0.970	0.972	0.945	0.273	0.400	0.221
mIVSTmit	0.822	0.844	0.910	0.590	0.303	0.709
pIVSmit	0.920	0.593	0.746	0.217	0.918	0.156
aIVSmit	0.411	0.404	0.650	0.324	0.607	0.559
AWmit	0.608	0.693	0.496	0.090	0.601	0.421
LWmit	0.428	0.071	0.992	0.052	0.870	0.976
IWmit	0.275	0.773	0.234	0.890	0.839	0.472
PWmit	0.756	0.051	0.202	0.493	0.358	0.287
mLVWtpap	0.263	0.559	0.707	0.426	0.467	0.284
mIVSpap	0.545	0.592	0.860	0.340	0.216	0.599
pIVSpap	0.558	0.315	0.771	0.243	0.071	0.679
aIVSpap	0.811	0.883	0.873	0.314	0.240	0.497
AWpap	0.129	0.760	0.345	0.390	0.620	0.128
LWpap	0.106	0.749	0.398	0.465	0.661	0.323
IWpap	0.514	0.932	0.733	0.791	0.746	0.652
PWpap	0.224	0.599	0.951	0.812	0.642	0.329
mLVWTapx	0.633	0.670	0.737	0.389	0.481	0.242
IVSapx	0.821	0.247	0.871	0.434	0.462	0.258
AWapx	0.953	0.828	0.630	0.529	0.138	0.326
LWapx	0.040	0.543	0.567	0.551	0.386	0.049
PWapx	0.287	0.579	0.883	0.817	0.508	0.227
LVM	0.913	0.558	0.705	0.673	0.264	0.239
mIVST	0.665	0.786	0.896	0.648	0.431	0.401
mLVWT	0.473	0.963	0.668	0.522	0.512	0.302
mPWT	0.261	0.795	0.735	0.660	0.566	0.371
Maron-Sprito score	0.529	0.379	0.663	0.263	0.390	0.322
CWT score	0.991	0.461	0.879	0.276	0.293	0.307
Comp1	0.601	0.482	0.869	0.347	0.239	0.300

Abbreviations: aIVSmit-anterior interventricular septum thickness at the mitral valve; aIVSpap-anterior interventricular septum thickness at the papillary level; AWapx-anterior wall thickness at the supra-apex level; AWmit-anterior wall thickness at the mitral valve; AWpap-anterior wall thickness at the papillary level; Comp1-principal component score; CWTscore-cumulative wall thickness score; IVSapx-interventricular septum thickness at the supra-apex level; IWmit-inferior wall thickness at the mitral valve; IWpap-inferior wall thickness at the papillary level; LVM-left ventricular mass; LWapx-lateral wall thickness at the supra-apex level; LWmit-lateral wall thickness at the mitral valve; LWpap-lateral wall thickness at the papillary level; Maron-Spirito score-as defined by Spirito and Maron (1990); mIVST-maximal interventricular septum thickness; mIVSTmit-maximal interventricular septum thickness at the mitral valve; mIVSTpap-maximal interventricular septum thickness at the papillary level; mLVWT-maximal left ventricular wall thickness; mLVWTapx-maximal left ventricular wall thickness at the supra-apex level; mLVWTmit-maximal left ventricular wall thickness at the mitral valve; mLVWTpap-maximal left ventricular wall thickness at the papillary level; mPWT-maximal posterior wall thickness; NR3C2-nuclear receptor subfamily 3, group C, member 2; pIVSmit-posterior interventricular septum thickness at the mitral valve; pIVSpap-posterior interventricular septum thickness at the papillary level; PWapx-posterior wall thickness at the supra-apex level; PWmit-posterior wall thickness at the mitral valve; PWpap-posterior wall thickness at the papillary level

3.5.3.2 AT₂ Receptor

Table 3.5 contains the p-values obtained from the association analysis for *AGTR2*. Highly significant evidence for association between rs1403543 and hypertrophy traits was found in the present study cohort. Significant association was observed between rs1403543 and a total of 16 heritable hypertrophy traits, these include LVM ($p = 0.033$), mIVST ($p = 0.015$), mLVWT ($p = 0.027$) as well as the Maron-Spirito ($p = 0.038$) and Comp1 ($p = 0.012$) scores, among others. However, no evidence for association was observed between the other two SNPs covered in *AGTR2*, i.e. rs5194 and rs11091046, and any of the hypertrophy traits.

Table 3.6 depicts the effects sizes for the significant associations ($p < 0.05$) obtained in the association analysis of *AGTR2*. Among others, the A-allele of rs1403543 was found to decrease LVM by 11.36 g, mIVST by 1.18 mm and mLVWT by 1.00 mm.

Table 3.5. Results from the association analysis: p-values for association between variants in *AGTR2* and hypertrophy traits. Significant p-values are indicated in bold red.

	<i>AGTR2</i>		
	rs1403543	rs5194	rs11091046
mLVWTmit	0.037	0.114	0.140
mIVSTmit	0.009	0.154	0.188
pIVSmit	0.010	0.165	0.223
aIVSmit	0.024	0.077	0.090
AWmit	0.338	0.427	0.466
LWmit	0.100	0.084	0.093
IWmit	0.006	0.114	0.131
PWmit	0.188	0.365	0.408
mLVWTpap	0.016	0.116	0.157
mIVSpap	0.017	0.165	0.219
pIVSpap	0.011	0.152	0.222
aIVSpap	0.019	0.291	0.263
AWpap	0.139	0.360	0.484
LWpap	0.014	0.095	0.071
IWpap	0.153	0.457	0.518
PWpap	0.172	0.387	0.421
mLVWTapx	0.059	0.293	0.298
IVSapx	0.021	0.134	0.162
AWapx	0.053	0.208	0.236
LWapx	0.144	0.456	0.501
PWapx	0.346	0.854	0.762
LVM	0.033	0.099	0.103
mIVST	0.015	0.084	0.101
mLVWT	0.027	0.192	0.216
mPWT	0.229	0.538	0.553
Maron-Spirito score	0.038	0.153	0.190
CWT score	0.052	0.318	0.372
Comp1	0.012	0.239	0.276

Abbreviations: *AGTR2*-angiotensin II receptor, type 2; aIVSmit-anterior interventricular septum thickness at the mitral valve; aIVSpap-anterior interventricular septum thickness at the papillary level; AWapx-anterior wall thickness at the supra-apex level; AWmit-anterior wall thickness at the mitral valve; AWpap-anterior wall thickness at the papillary level; Comp1-Principal component score; CWTscore-cumulative wall thickness score; IVSapx-interventricular septum thickness at the supra-apex level; IWmit-inferior wall thickness at the mitral valve; IWpap-inferior wall thickness at the papillary level; LVM-left ventricular mass; LWapx-lateral wall thickness at the supra-apex level; LWmit-lateral wall thickness at the mitral valve; LWpap-lateral wall thickness at the papillary level; Maron-Spirito score-as defined by Spirito and Maron (1990); mIVST-maximal interventricular septum thickness; mIVSTmit-maximal interventricular septum thickness at the mitral valve; mIVSTpap-maximal interventricular septum thickness at the papillary level; mLVWT-maximal left ventricular wall thickness; mLVWTapx-maximal left ventricular wall thickness at the supra-apex level; mLVWTmit-maximal left ventricular wall thickness at the mitral valve; mLVWTpap-maximal left ventricular wall thickness at the papillary level; mPWT-maximal posterior wall thickness; pIVSmit-posterior interventricular septum thickness at the mitral valve; pIVSpap-posterior interventricular septum thickness at the papillary level; PWapx-posterior wall thickness at the supra-apex level; PWmit-posterior wall thickness at the mitral valve; PWpap-posterior wall thickness at the papillary level

Table 3.6. Effect sizes for the significant associations obtained in the association analysis of *AGTR2*. Effect sizes are given in terms of the original measurements.

Gene	SNP	Effect Allele	Hypertrophy Trait	p-value	Effect size
<i>AGTR2</i>	rs1403543	A	LVM	0.033	-11.358 g
			mIVST	0.015	-1.176 mm
			mLVWT	0.027	-0.998 mm
			Maron score	0.038	-2.603 mm
			mLVWTmit	0.037	-1.060 mm
			mIVSmit	0.007	-1.253 mm
			pIVSmit	0.010	-0.857 mm
			aIVSmit	0.024	-1.149 mm
			IWmit	0.006	-0.508 mm
			mLVWTpap	0.016	-0.970 mm
			mIVSpap	0.017	-1.038 mm
			pIVSpap	0.011	-0.900 mm
			aIVSpap	0.019	-1.040 mm
			LWpap	0.014	-0.316 mm
			IVSapx	0.021	-0.587 mm
			Comp1	0.012	-0.894 mm

Abbreviations: A-adenine; *AGTR2*-angiotensin II receptor, type 2; aIVSmit-anterior interventricular septum thickness at the mitral valve; aIVSpap-anterior interventricular septum thickness at the papillary level; Comp1-Principal component score; IVSapx-interventricular septum thickness at the supra-apex level; IWmit-inferior wall thickness at the mitral valve; LVM-left ventricular mass; LWpap-lateral wall thickness at the papillary level; Maron score-as defined by Spirito and Maron (1990); mIVSpap-maximal interventricular septum thickness at the papillary level; mIVST-maximal interventricular septum thickness; mIVSTmit-maximal interventricular septum thickness at the mitral valve; mLVWT-maximal left ventricular wall thickness; mLVWTmit-maximal left ventricular wall thickness at the mitral valve; mLVWTpap-maximal left ventricular wall thickness at the papillary level; pIVSmit-posterior interventricular septum thickness at the mitral valve; pIVSpap-posterior interventricular septum thickness at the papillary level; SNP-single nucleotide polymorphism

3.5.3.3 Renin and renin-associated genes

Table 3.7 depicts the p-values obtained from the association analysis for *REN*, *RENBP* and *ATP6AP2* and table 3.8 contains the effects sizes for the significant associations. Strong evidence for association was found between hypertrophy traits and variants in *REN*. In particular, rs1464816 was found to have a significant effect on eight of the investigated hypertrophy traits, including LVM ($p = 0.043$) and mPWT ($p = 0.038$). The G-allele of rs1464816 was found to decrease LVM by 28.013 g and mPWT by 0.72 mm (table 3.8). Furthermore, rs11571082 was found to be associated with seven hypertrophy traits, while rs5705 was associated with five and rs10900555 with two hypertrophy traits. Both rs1464816 and rs11571082 were significantly associated with Comp1, with p-values of 0.013 and 0.036 respectively.

Table 3.7. Results from the association analysis: p-values for association between variants in *REN*, *RENBP* and *ATP6AP2* and hypertrophy traits. Significant p-values are indicated in bold red.

	<i>REN</i>				<i>RENBP</i>			<i>ATP6AP2</i>		
	rs1464816	rs11571082	rs5705	rs10900555	rs2269370	rs2269372	rs762656	rs2968915	rs2968917	rs10536
mLVWTmit	0.306	0.284	0.191	0.551	0.499	0.129	0.025	0.609	0.394	0.665
mIVSmit	0.294	0.430	0.304	0.121	0.529	0.241	0.076	0.518	0.298	0.936
pIVSmit	0.243	0.072	0.041	0.125	0.907	0.071	0.013	0.555	0.430	0.996
aIVSmit	0.106	0.374	0.382	0.153	0.257	0.272	0.112	0.791	0.541	0.878
AWmit	0.289	0.078	0.037	0.976	0.356	0.686	0.158	0.431	0.360	0.451
LWmit	0.007	0.177	0.831	0.073	0.994	0.871	0.246	0.349	0.384	0.420
IWmit	0.082	0.219	0.698	< 0.001	0.881	0.233	0.078	0.382	0.551	0.168
PWmit	0.012	0.638	0.578	0.044	0.828	0.276	0.269	0.582	0.584	0.396
mLVWTpap	0.161	0.063	0.192	0.878	0.943	0.549	0.258	0.941	0.709	0.966
mIVSpap	0.225	0.312	0.371	0.562	0.983	0.621	0.166	0.793	0.867	0.938
pIVSpap	0.135	0.713	0.901	0.185	0.763	0.692	0.164	0.981	0.915	0.611
aIVSpap	0.276	0.073	0.175	0.686	0.528	0.626	0.170	0.847	0.655	0.613
AWpap	0.107	0.165	0.499	0.961	0.620	0.694	0.353	0.518	0.375	0.501
LWpap	0.024	0.012	0.070	0.433	0.728	0.463	0.168	0.920	0.848	0.123
IWpap	0.119	0.345	0.655	0.078	0.441	0.079	0.006	0.398	0.638	0.062
PWpap	0.048	0.169	0.831	0.100	0.461	0.069	0.039	0.481	0.677	0.089
mLVWTapx	0.140	0.008	0.020	0.619	0.026	0.054	0.007	0.732	0.915	0.477
IVSapx	0.078	0.042	0.032	0.775	0.025	0.060	0.012	0.481	0.841	0.459
AWapx	0.216	0.007	0.008	0.504	0.221	0.131	0.010	0.569	0.577	0.432
LWapx	0.161	0.014	0.085	0.390	0.248	0.132	0.024	0.681	0.997	0.304
PWapx	0.091	0.057	0.183	0.606	0.575	0.198	0.096	0.774	0.832	0.281
LVM	0.043	0.406	0.521	0.746	0.238	0.091	0.039	0.552	0.779	0.451
mIVST	0.308	0.148	0.217	0.624	0.404	0.226	0.055	0.962	0.551	0.932
mLVWT	0.174	0.239	0.265	0.936	0.490	0.238	0.067	0.906	0.606	0.936
mPWT	0.038	0.306	0.709	0.129	0.469	0.033	0.010	0.814	0.928	0.427
Maron-Spirito score	0.037	0.117	0.250	0.304	0.638	0.570	0.181	0.964	0.681	0.587
CWT score	0.085	0.032	0.064	0.598	0.469	0.362	0.061	0.794	0.795	0.685
Comp1	0.013	0.036	0.291	0.328	0.466	0.275	0.049	0.673	0.972	0.767

Abbreviations: aIVSmit-anterior interventricular septum thickness at the mitral valve; aIVSpap-anterior interventricular septum thickness at the papillary level; *ATP6AP2*-ATPase, H⁺ transporting, lysosomal accessory protein 2; AWapx-anterior wall thickness at the supra-apex level; AWmit-anterior wall thickness at the mitral valve; AWpap-anterior wall thickness at the papillary level; Comp1-Principal component score; CWTscore-cumulative wall thickness score; IVSapx-interventricular septum thickness at the supra-apex level; IWmit-inferior wall thickness at the mitral valve; IWpap-inferior wall thickness at the papillary level; LVM-left ventricular mass; LWapx-lateral wall thickness at the supra-apex level; LWmit-lateral wall thickness at the mitral valve; LWpap-lateral wall thickness at the papillary level; Maron-Spirito score-as defined by Spirito and Maron (1990); mIVST-maximal interventricular septum thickness; mIVSTmit-maximal interventricular septum thickness at the mitral valve; mIVSTpap-maximal interventricular septum thickness at the papillary level; mLVWT-maximal left ventricular wall thickness; mLVWTapx-maximal left ventricular wall thickness at the supra-apex level; mLVWTmit-maximal left ventricular wall thickness at the mitral valve; mLVWTpap-maximal left ventricular wall thickness at the papillary level; mPWT-maximal posterior wall thickness; pIVSmit-posterior interventricular septum thickness at the mitral valve; pIVSpap-posterior interventricular septum thickness at the papillary level; PWapx-posterior wall thickness at the supra-apex level; PWmit-posterior wall thickness at the mitral valve; PWpap-posterior wall thickness at the papillary level; *REN*-renin; *RENBP*-renin binding protein

Table 3.8. Effect sizes for the significant associations obtained in the association analysis of *REN* and *RENBP*. Effect sizes are given in terms of the original measurements.

Gene	SNP	Effect Allele	Hypertrophy Trait	p-value	Effect size
<i>REN</i>	rs1464816	G	LVM	0.043	-28.013 g
			mPWT	0.038	-0.720 mm
			Maronscore	0.037	-5.509
			LWmit	0.007	-1.053 mm
			PWmit	0.012	-0.981 mm
			LWpap	0.024	-1.014 mm
			PWpap	0.048	-0.777 mm
	rs11571082	A	CWT score	0.032	-14.111 mm
			LWpap	0.012	-0.399 mm
			mLVWTapx	0.008	-1.971 mm
			IVSapx	0.042	-1.731 mm
			AWapx	0.007	-2.043 mm
			LWapx	0.014	-0.474 mm
			rs5705	A	pIVSmit
	AWmit	0.037			-0.843 mm
	mLVWTapx	0.020			-2.017 mm
	IVSapx	0.032			-1.774 mm
	AWapx	0.008			-2.069 mm
	IWmit	< 0.001			0.768 mm
	<i>RENBP</i>	rs2269370	A	PWmit	0.044
mLVWTapx				0.026	1.439 mm
rs2269372		A	IVSapx	0.025	1.482 mm
			mPWT	0.033	-0.460 mm
rs762656		A	LVM	0.039	-14.769 g
			mPWT	0.010	-0.572 mm
			mLVWThit	0.025	-1.319 mm
			pIVSmit	0.013	-1.234 mm
			IWpap	0.006	-0.544 mm
			PWpap	0.039	-0.477 mm
			mLVWTapx	0.007	-1.645 mm
			IVSapx	0.012	-1.496 mm
			AWapx	0.010	-1.282 mm
LWapx	0.024	-0.599 mm			
Comp1	0.049	-0.694 mm			

Abbreviations: A-adenine; *ATP6AP2*-ATPase, H⁺ transporting, lysosomal accessory protein 2; AWapx-anterior wall thickness at the supra-apex level; AWmit-anterior wall thickness at the mitral valve; C-cytosine; Comp1-Principal component score; CWTscore-cumulative wall thickness score; IVSapx-interventricular septum thickness at the supra-apex level; IWmit-inferior wall thickness at the mitral valve; IWpap-inferior wall thickness at the papillary level; LVM-left ventricular mass; LWapx-lateral wall thickness at the supra-apex level; LWmit-lateral wall thickness at the mitral valve; LWpap-lateral wall thickness at the papillary level; Maron-Spirito score-as defined by Spirito and Maron (1990); mLVWTapx-maximal left ventricular wall thickness at the supra-apex level; mLVWThit-maximal left ventricular wall thickness at the mitral valve; mPWT-maximal posterior wall thickness; pIVSmit-posterior interventricular septum thickness at the mitral valve; PWmit-posterior wall thickness at the mitral valve; PWpap-posterior wall thickness at the papillary level; *REN*-renin; *RENBP*-renin binding protein

Variants within *RENBP* were also found to have a significant effect on a number of heritable hypertrophy traits. One SNP, rs762656, was found to be associated with 11 hypertrophy traits, including LVM ($p = 0.039$), mPWT ($p = 0.010$) and Comp1 ($p = 0.049$) (table 3.7). The A-allele of rs762656 was found to be responsible for an average decrease of 14.769 g in LVM and 0.572 mm in mPWT (table 3.8). Association was also found between the rs2269372 SNP in *RENBP* and mPWT ($p = 0.033$). Interestingly, the A-allele of rs2269370 was found to significantly increase two hypertrophy traits at the apex level, i.e. mLWVTapx ($p = 0.026$) and IVSapx ($p = 0.025$). No evidence for association was found between the three SNPs covered in *ATP6AP2* and hypertrophy traits.

3.5.3.4 Na⁺/K⁺-ATPase subunits

Table 3.9 depicts the p-values obtained from the association analysis for *ATP1A1*, *ATP1A2*, *ATP1B1* and *ATP1B3*. While there was no evidence for association between SNPs in *ATP1A2* and *ATP1B3* and hypertrophy traits, the rs850609 in *ATP1A1* and rs1200130 in *ATP1B1*, was found to be significantly associated with hypertrophy traits.

In *ATP1A1*, the A-allele of rs850609 was found to significantly increase IWmit ($p = 0.022$) and LWpap ($p = 0.019$) by 0.936 mm and 1.156 mm, respectively (table 3.10). However, rs10924074 in *ATP1A1* was not significantly associated with any hypertrophy traits.

Table 3.9. Results from the association analysis: p-values for association between variants in *ATPIA1*, *ATPIA2*, *ATPIB1* and *ATPIB3* and hypertrophy traits. Significant p-values are indicated in bold red.

	<i>ATPIA1</i>		<i>ATPIA2</i>		<i>ATPIB1</i>			<i>ATPIB3</i>
	rs10924074	rs850609	rs7548116	rs11585375	rs1200130	rs1358714	rs1040503	rs2068230
mLVWTmit	0.583	0.130	0.209	0.584	0.509	0.400	0.625	0.835
mIVSTmit	1.000	0.082	0.336	0.745	0.508	0.318	0.904	0.360
pIVSmit	0.972	0.135	0.188	0.340	0.415	0.367	0.344	0.203
aIVSmit	0.735	0.176	0.207	0.892	0.316	0.398	0.587	0.624
AWmit	0.582	0.158	0.136	0.709	0.364	0.340	0.651	0.660
LWmit	0.680	0.158	0.638	0.329	0.312	0.185	0.762	0.715
IWmit	0.589	0.022	0.754	0.197	0.035	0.526	0.595	0.693
PWmit	0.807	0.054	0.733	0.606	0.014	0.430	0.492	0.607
mLVWTpap	0.627	0.147	0.148	0.510	0.483	0.410	0.489	0.434
mIVSpap	0.955	0.299	0.246	0.267	0.637	0.510	0.265	0.558
pIVSpap	0.927	0.303	0.223	0.150	0.980	0.387	0.653	0.286
aIVSpap	0.436	0.357	0.153	0.404	0.271	0.628	0.202	0.623
AWpap	0.586	0.199	0.053	0.392	0.905	0.302	0.896	0.284
LWpap	0.700	0.019	0.152	0.576	0.198	0.721	0.929	0.054
IWpap	0.708	0.663	0.785	0.734	0.589	0.108	0.401	0.798
PWpap	0.740	0.604	0.722	0.911	0.180	0.809	0.202	0.856
mLVWTapx	0.304	0.154	0.154	0.727	0.268	0.161	0.736	0.897
IVSapx	0.436	0.136	0.091	0.638	0.203	0.125	0.387	0.497
AWapx	0.436	0.604	0.096	0.758	0.436	0.236	0.799	0.762
LWapx	0.431	0.326	0.130	0.924	0.973	0.138	0.603	0.851
PWapx	0.672	0.963	0.209	0.935	0.870	0.685	0.826	0.167
LVM	0.312	0.298	0.234	0.640	0.136	0.635	0.915	0.066
mIVST	0.345	0.170	0.210	0.383	0.672	0.387	0.662	0.749
mLVWT	0.455	0.057	0.223	0.729	0.592	0.445	0.551	0.812
mPWT	0.918	0.697	0.442	0.711	0.508	0.590	0.837	0.302
Maron-Spirito score	0.558	0.134	0.091	0.461	0.303	0.467	0.424	0.743
CWT score	0.927	0.344	0.111	0.973	0.207	0.306	0.393	0.895
Comp1	0.847	0.196	0.198	0.408	0.298	0.361	0.725	0.442

Abbreviations: aIVSmit-anterior interventricular septum thickness at the mitral valve; aIVSpap-anterior interventricular septum thickness at the papillary level; *ATPIA1*-ATPase, Na⁺/K⁺ transporting, alpha 1 polypeptide; *ATPIA2*-ATPase, Na⁺/K⁺ transporting, alpha 2 (+) polypeptide; *ATPIB1*-ATPase, Na⁺/K⁺ transporting, beta 1 polypeptide; *ATPIB3*-ATPase, Na⁺/K⁺ transporting, beta 3 polypeptide; AWapx-anterior wall thickness at the supra-apex level; AWmit-anterior wall thickness at the mitral valve; AWpap-anterior wall thickness at the papillary level; Comp1-Principal component score; CWTscore-cumulative wall thickness score; IVSapx-interventricular septum thickness at the supra-apex level; IWmit-inferior wall thickness at the mitral valve; IWpap-inferior wall thickness at the papillary level; LVM-left ventricular mass; LWapx-lateral wall thickness at the supra-apex level; LWmit-lateral wall thickness at the mitral valve; LWpap-lateral wall thickness at the papillary level; Maron-Spirito score-as defined by Spirito and Maron (1990); mIVST-maximal interventricular septum thickness; mIVSTmit-maximal interventricular septum thickness at the mitral valve; mIVSTpap-maximal interventricular septum thickness at the papillary level; mLVWT-maximal left ventricular wall thickness; mLVWTapx-maximal left ventricular wall thickness at the supra-apex level; mLVWTmit-maximal left ventricular wall thickness at the mitral valve; mLVWTpap-maximal left ventricular wall thickness at the papillary level; mPWT-maximal posterior wall thickness; pIVSmit-posterior interventricular septum thickness at the mitral valve; pIVSpap-posterior interventricular septum thickness at the papillary level; PWapx-posterior wall thickness at the supra-apex level; PWmit-posterior wall thickness at the mitral valve; PWpap-posterior wall thickness at the papillary level

Table 3.10. Effect sizes for the significant associations obtained in the association analysis of *ATPIA1* and *ATPIB1*. Effect sizes are given in terms of the original measurements.

Gene	SNP	Effect Allele	Hypertrophy Trait	p-value	Effect size
<i>ATPIA1</i>	rs850609	A	IWmit	0.022	0.936 mm
			LWpap	0.019	1.156 mm
<i>ATPIB1</i>	rs1200130	C	IWmit	0.035	-0.418 mm
			PWmit	0.014	-0.639 mm

Abbreviations: A-adenine; *ATPIA1*-ATPase, Na⁺/K⁺ transporting, alpha 1 polypeptide; *ATPIB1*-ATPase, Na⁺/K⁺ transporting, beta 1 polypeptide; C-cytosine; IWmit-inferior wall thickness at the mitral valve; LWpap-lateral wall thickness at the papillary level; PWmit-posterior wall thickness at the mitral valve; SNP-single nucleotide polymorphism

The C-allele of rs1200130 in *ATPIB1* was found to be significantly associated with a decrease in IWmit ($p = 0.035$) and PWmit ($p = 0.014$) by 0.418 mm and 0.639 mm, respectively (table 3.10). No association was found between the two other SNPs investigated in *ATPIB1*, namely rs1358714 and rs1040503 and heritable hypertrophy traits.

3.5.3.5 ENaC subunits

Table 3.11 reports the p-values for association between variants in *SCNNIA* and *SCNNIG* and hypertrophy traits. A significant association was found between a single hypertrophy trait, IWmit, and rs2286600 in *SCNNIA* ($p = 0.044$). However, no further evidence for association between the rest of the variants investigated in *SCNNIA* and any heritable hypertrophy traits was found. No evidence for association was found between the SNPs investigated in *SCNNIG* and hypertrophy traits (table 3.11).

Table 3.11. Results from the association analysis: p-values for association between variants in *SCNNIA* and *SCNNIG* and hypertrophy traits. Significant p-values are indicated in bold red.

	<i>SCNNIA</i>					<i>SCNNIG</i>	
	rs11614164	rs3782726	rs7973914	rs10849446	rs2286600	rs5735	rs4247210
mLVWTmit	0.792	0.142	0.600	0.442	0.916	0.916	0.755
mIVSTmit	0.662	0.171	0.812	0.446	0.886	0.643	0.708
pIVSmit	0.943	0.200	0.988	0.700	0.554	0.820	0.651
aIVSmit	0.413	0.129	0.433	0.570	0.852	0.803	0.515
AWmit	0.744	0.058	0.488	0.299	0.667	0.789	0.507
LWmit	0.733	0.267	0.551	0.525	0.234	0.975	0.539
IWmit	0.987	0.746	0.723	0.438	0.044	0.147	0.908
PWmit	0.717	0.729	0.543	0.758	0.166	0.232	0.891
mLVWTapx	0.859	0.495	0.712	0.343	0.83	0.919	0.642
mIVSpap	0.949	0.368	0.606	0.486	0.762	0.782	0.638
pIVSpap	0.903	0.225	0.786	0.403	0.849	0.702	0.789
aIVSpap	0.739	0.161	0.179	0.359	0.572	0.893	0.718
AWpap	0.835	0.097	0.304	0.238	0.693	0.597	0.622
LWpap	0.916	0.302	0.298	0.579	0.359	0.251	0.098
IWpap	0.814	0.352	0.277	0.645	0.224	0.529	0.991
PWpap	0.249	0.249	0.382	0.108	0.053	0.132	0.435
mLVWTapx	0.708	0.375	0.492	0.793	0.749	0.489	0.810
IVSapx	0.669	0.345	0.985	0.897	0.798	0.400	0.514
AWapx	0.911	0.530	0.682	0.707	0.886	0.816	0.933
LWapx	0.751	0.901	0.419	0.583	0.710	0.075	0.574
PWapx	0.167	0.074	0.222	0.325	0.366	0.867	0.987
LVM	0.576	0.434	0.270	0.960	0.105	0.740	0.372
mIVST	0.605	0.207	0.511	0.755	0.471	0.898	0.739
mLVWT	0.759	0.165	0.505	0.653	0.611	0.855	0.822
mPWT	0.261	0.303	0.311	0.892	0.289	0.827	0.820
Maron-Spirito score	0.651	0.234	0.662	0.510	0.704	0.738	0.562
CWT score	0.773	0.102	0.483	0.485	0.897	0.679	0.476
Comp1	0.665	0.102	0.394	0.382	0.812	0.336	0.421

Abbreviations: aIVSmit-anterior interventricular septum thickness at the mitral valve; aIVSpap-anterior interventricular septum thickness at the papillary level; *ATP1A1*-ATPase, Na⁺/K⁺ transporting, alpha 1 polypeptide; *ATP1A2*-ATPase, Na⁺/K⁺ transporting, alpha 2 (+) polypeptide; *ATP1B1*-ATPase, Na⁺/K⁺ transporting, beta 1 polypeptide; *ATP1B3*-ATPase, Na⁺/K⁺ transporting, beta 3 polypeptide; AWapx-anterior wall thickness at the supra-apex level; AWmit-anterior wall thickness at the mitral valve; AWpap-anterior wall thickness at the papillary level; Comp1-Principal component score; CWTscore-cumulative wall thickness score; IVSapx-interventricular septum thickness at the supra-apex level; IWmit-inferior wall thickness at the mitral valve; IWpap-inferior wall thickness at the papillary level; LVM-left ventricular mass; LWapx-lateral wall thickness at the supra-apex level; LWmit-lateral wall thickness at the mitral valve; LWpap-lateral wall thickness at the papillary level; Maron-Spirito score-as defined by Spirito and Maron (1990); mIVST-maximal interventricular septum thickness; mIVSTmit-maximal interventricular septum thickness at the mitral valve; mIVSTpap-maximal interventricular septum thickness at the papillary level; mLVWT-maximal left ventricular wall thickness; mLVWTapx-maximal left ventricular wall thickness at the supra-apex level; mLVWTmit-maximal left ventricular wall thickness at the mitral valve; mLVWTapx-maximal left ventricular wall thickness at the papillary level; mPWT-maximal posterior wall thickness; pIVSmit-posterior interventricular septum thickness at the mitral valve; pIVSpap-posterior interventricular septum thickness at the papillary level; PWapx-posterior wall thickness at the supra-apex level; PWmit-posterior wall thickness at the mitral valve; PWpap-posterior wall thickness at the papillary level; *SCNNIA*-sodium channel, nonvoltage-gated 1 alpha; *SCNNIG*-sodium channel, nonvoltage-gated 1, gamma

Table 3.12 depicts the p-values obtained from the association analysis for *SCNN1B* and table 3.13 contains the effects sizes for the significant associations. One SNP within *SCNN1B*, rs11074555, was found to be significantly associated with five cardiac wall thickness measurements. The C-allele of this SNP was shown to significantly decrease LW thickness at the mitral and apex levels as well as PW thickness at the papillary and apex levels (table 3.13). Another SNP in *SCNN1B*, rs9930640, was found to significantly increase mLVWTmit ($p = 0.030$), aIVSpap ($p = 0.046$) and LWpap ($p = 0.035$) (table 3.13). However, no further evidence for association between the rest of the variants investigated in *SCNN1B* and hypertrophy traits was found.

Table 3.12. Results from the association analysis: p-values for association between variants in *SCNN1B* and hypertrophy traits. Significant p-values are indicated in bold red.

	<i>SCNN1B</i>							
	rs11074555	rs9930640	rs239345	rs238547	rs8044970	rs152740	rs250563	rs2303153
mLVWTmit	0.161	0.294	0.139	0.281	0.258	0.815	0.178	0.876
mIVSTmit	0.203	0.265	0.208	0.168	0.221	0.985	0.116	0.858
pIVSmit	0.226	0.287	0.237	0.390	0.489	0.592	0.261	0.612
aIVSmit	0.235	0.256	0.125	0.212	0.140	0.703	0.233	0.700
AWmit	0.193	0.309	0.113	0.289	0.380	0.757	**	0.783
LWmit	0.019	0.138	0.888	0.908	0.070	0.553	**	0.255
IWmit	0.287	0.995	0.701	0.446	0.669	0.825	**	0.528
PWmit	0.359	0.416	0.408	0.702	0.796	0.637	**	0.529
mLVWTpap	0.098	0.030	0.434	0.357	0.133	0.345	0.192	0.926
mIVSpap	0.135	0.071	0.338	0.224	0.100	0.333	0.464	0.642
pIVSpap	0.093	0.266	0.380	0.412	0.140	0.462	0.264	0.715
aIVSpap	0.259	0.046	0.343	0.273	0.153	0.410	0.390	0.813
AWpap	0.208	0.107	0.474	0.454	0.054	0.379	**	0.598
LWpap	0.120	0.035	0.863	0.650	0.190	0.522	**	0.543
IWpap	< 0.001	0.805	0.547	0.143	0.434	0.525	**	0.441
PWpap	0.009	0.737	0.486	0.634	0.065	0.572	**	0.962
mLVWTapx	0.128	0.393	0.547	0.199	0.210	0.213	0.208	0.572
IVSapx	0.580	0.318	0.598	0.180	0.147	0.194	0.269	0.492
AWapx	0.100	0.966	0.768	0.373	0.419	0.502	**	0.750
LWapx	0.003	0.465	0.248	0.920	0.113	0.318	**	0.942
PWapx	0.001	0.668	0.871	0.753	0.087	0.708	**	0.836
LVM	0.576	0.733	0.689	0.929	0.269	0.528	0.977	0.378
mIVST	0.380	0.109	0.557	0.230	0.056	0.548	0.571	0.761
mLVWT	0.329	0.170	0.376	0.250	0.116	0.625	0.282	0.828
mPWT	0.068	0.351	0.744	0.986	0.138	0.984	0.328	0.516
Maron-Spirito score	0.094	0.208	0.543	0.507	0.155	0.347	**	0.983
CWT score	0.295	0.140	0.150	0.386	0.171	0.280	**	0.369
Comp1	0.085	0.441	0.816	0.485	0.095	0.282	0.130	0.416

** Not sufficient number of genotyped informative individuals to perform analysis

Abbreviations: aIVSmit-anterior interventricular septum thickness at the mitral valve; aIVSpap-anterior interventricular septum thickness at the papillary level; *ATP1A1*-ATPase, Na⁺/K⁺ transporting, alpha 1 polypeptide; *ATP1A2*-ATPase, Na⁺/K⁺ transporting, alpha 2 (+) polypeptide; *ATP1B1*-ATPase, Na⁺/K⁺ transporting, beta 1 polypeptide; *ATP1B3*-ATPase, Na⁺/K⁺ transporting, beta 3 polypeptide; AWapx-anterior wall thickness at the supra-apex level; AWmit-anterior wall thickness at the mitral valve; AWpap-anterior wall thickness at the papillary level; Comp1-Principal component score; CWTscore-cumulative wall thickness score; IVSapx-interventricular septum thickness at the supra-apex level; IWmit-inferior wall thickness at the mitral valve; IWpap-inferior wall thickness at the papillary level; LVM-left ventricular mass; LWapx-lateral wall thickness at the supra-apex level; LWmit-lateral wall thickness at the mitral valve; LWpap-lateral wall thickness at the papillary level; Maron-Spirito score-as defined by Spirito and Maron (1990); mIVST-maximal interventricular septum thickness; mIVSTmit-maximal interventricular septum thickness at the mitral valve; mIVSTpap-maximal interventricular septum thickness at the papillary level; mLVWT-maximal left ventricular wall thickness; mLVWTapx-maximal left ventricular wall thickness at the supra-apex level; mLVWTmit-maximal left ventricular wall thickness at the mitral valve; mLVWTpap-maximal left ventricular wall thickness at the papillary level; mPWT-maximal posterior wall thickness; pIVSmit-posterior interventricular septum thickness at the mitral valve; pIVSpap-posterior interventricular septum thickness at the papillary level; PWapx-posterior wall thickness at the supra-apex level; PWmit-posterior wall thickness at the mitral valve; PWpap-posterior wall thickness at the papillary level; *SCNN1B*-sodium channel, nonvoltage-gated 1 beta

Table 3.13. Effect sizes for the significant associations obtained in the association analysis of *SCNNIA* and *SCNNIB*. Effect sizes are given in terms of the original measurements.

Gene	SNP	Effect Allele	Hypertrophy Trait	p-value	Effect size
<i>SCNNIA</i>	rs2286600	A	IWmit	0.044	-0.219 mm
<i>SCNNIB</i>	rs11074555	C	LWmit	0.019	-0.547 mm
			IWpap	< 0.001	-0.921 mm
			PWpap	0.009	-0.593 mm
			LWapx	0.003	-0.717 mm
			PWapx	0.001	-0.602 mm
	rs9930640	A	mLVWTpap	0.030	1.592 mm
			aIVSpap	0.046	1.725 mm
			LWpap	0.035	0.729 mm

Abbreviations: A-adenine; aIVSpap-anterior interventricular septum thickness at the papillary level; C-cytosine ;IWmit-inferior wall thickness at the mitral valve; IWpap-inferior wall thickness at the papillary level; LWapx-lateral wall thickness at the supra-apex level; LWmit-lateral wall thickness at the mitral valve; LWpap-lateral wall thickness at the papillary level; mLVWTpap-maximal left ventricular wall thickness at the papillary level; PWapx-posterior wall thickness at the supra-apex level; PWpap-posterior wall thickness at the papillary level; *SCNNIA*-sodium channel, nonvoltage-gated 1 alpha; *SCNNIB*-sodium channel, nonvoltage-gated 1, beta; SNP-single nucleotide polymorphism

3.6 GENE-GENE INTERACTION ANALYSIS

The p-values for the gene-gene interaction analysis between all the SNPs for the hypertrophy traits are reported in Appendix II. Table 3.14 shows the number of traits for which a significant interactions ($p < 0.05$) was observed between each pair of SNPs investigated in this study while table 3.15 shows the number of highly significant interactions ($p < 0.01$).

Due to the large number, 1006, of SNP pairs that indicated significant interactions ($p < 0.05$) to influence hypertrophy traits, we decided to limit our investigation to the 228 highly significant interactions ($p < 0.01$) for the purpose of the present study. Table 3.15 shows the distribution of the number of hypertrophy traits that were influenced by highly significant interactions. Taking this into account, we decided to describe highly significant SNP interactions ($p < 0.01$) that affect five or more hypertrophy traits (indicated in green). These interactions are listed in table 3.16.

Table 3.16. The distribution of the number of hypertrophy traits that were affected by highly significant interactions ($p < 0.01$).

Number of hypertrophy traits	Number of highly significant SNP interactions
0	559
1 - 4	58
5 - 9	5
10 -14	4
15 -19	3
≥ 20	1

Table 3.17. Highly significant SNP interactions.

SNP1	Gene	SNP2	Gene
rs1040503	<i>ATP1B1</i>	rs1464816	<i>REN</i>
rs1040503	<i>ATP1B1</i>	rs5705	<i>REN</i>
rs1358714	<i>ATP1B1</i>	rs11614164	<i>SCNNIA</i>
rs1358714	<i>ATP1B1</i>	rs3782726	<i>SCNNIA</i>
rs2269370	<i>RENBP</i>	rs1464816	<i>REN</i>
rs10900555	<i>REN</i>	rs2303153	<i>SCNNIB</i>
rs2068230	<i>ATP1B3</i>	rs11614164	<i>SCNNIA</i>
rs2068230	<i>ATP1B3</i>	rs238547	<i>SCNNIB</i>
rs2068230	<i>ATP1B3</i>	rs250563	<i>SCNNIB</i>
rs11614164	<i>SCNNIA</i>	rs2303153	<i>SCNNIB</i>
rs3782726	<i>SCNNIA</i>	rs2303153	<i>SCNNIB</i>
rs5735	<i>SCNNIG</i>	rs250563	<i>SCNNIB</i>
rs250563	<i>SCNNIB</i>	rs2968917	<i>ATP6AP2</i>

Abbreviations: *ATP1B1*-ATPase, Na⁺/K⁺ transporting, beta 1 polypeptide; *ATP1B3*-ATPase, Na⁺/K⁺ transporting, beta 3 polypeptide; *ATP6AP2*-ATPase, H⁺ transporting, lysosomal accessory protein 2; *REN*-renin; *RENBP*-renin binding protein; *SCNNIA*-sodium channel, nonvoltage-gated 1 alpha; *SCNNIB*-sodium channel, nonvoltage-gated 1, beta; *SCNNIG*-sodium channel, nonvoltage-gated 1, gamma; SNP- single nucleotide polymorphism

Line plots are used to illustrate the interactions on selected traits. The two SNPs would show parallel graphs for all the genotypes if there is no evidence for interaction.

3.6.1 *REN* and *RENBP*

Highly significant interaction was found between rs2269370 in *RENBP* and rs1464816 in *REN* in five traits. These two SNPs were found to significantly interact to influence mLVWT ($p = 0.0062$), mIVST ($p = 0.0046$), mIVSpap ($p = 0.0067$), pIVSpap ($p = 0.0095$) and aIVSpap ($p = 0.0032$). Figure 3.19 illustrates the interaction between these two SNPs to influence mLVWT. Males and females were analyzed separately as *RENBP* is an X-linked gene. The graphs show that a male individual will have a significantly increased mLVWT if he is hemizygous for the A-allele for rs2269370 and homozygous for the T-allele for rs1464816. Females who are homozygous for the A-allele for rs2269370 and possess at least one T-allele for rs1464816, exhibit a significant increase in mLVWT.

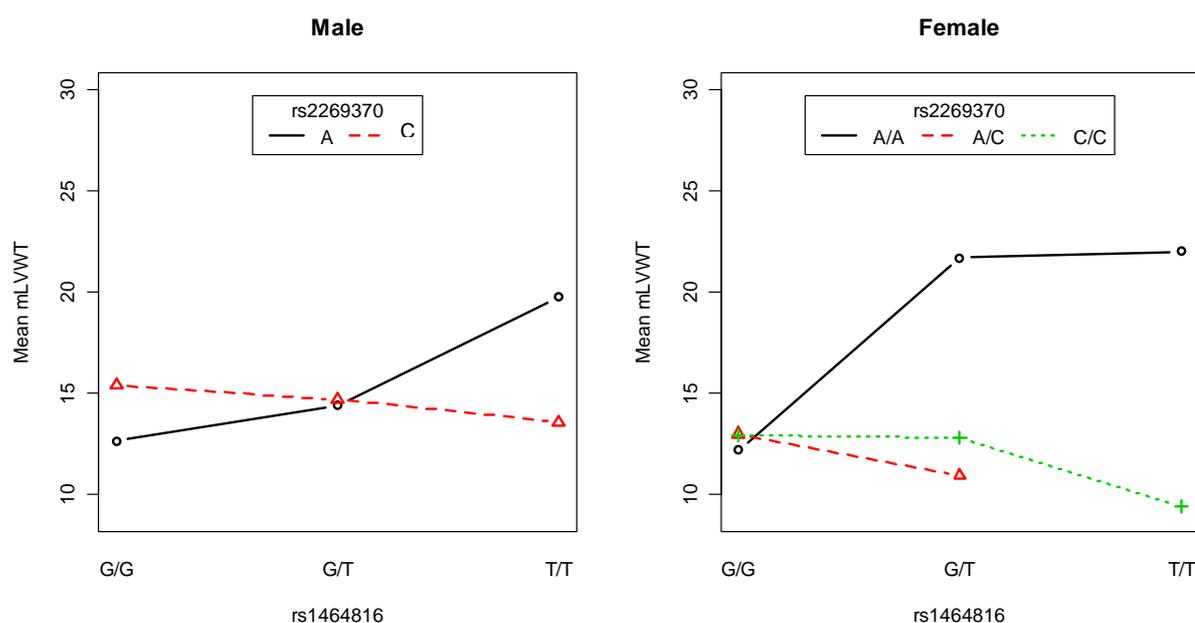


Figure 3.19. An illustration of the interaction between rs2269370 in *RENBP* and rs1464816 in *REN* on mLVWT.

3.6.2 *REN* and *SCNN1B*

Strong evidence was found for interaction between rs10900555 in *REN* and rs2303153 in *SCNN1B*. Highly significant interaction between these two SNPs was found to influence

ten hypertrophy traits, including mIVST ($p = 0.0006$) and mLVWT ($p = 0.0004$). Figure 3.20 illustrates the interaction between these two SNPs to influence mLVWT. The two SNPs would show two parallel graphs there is no evidence for interaction, however, the addition of a G-allele for the rs10900555 variant in *REN* alters this pattern, signifying interaction.

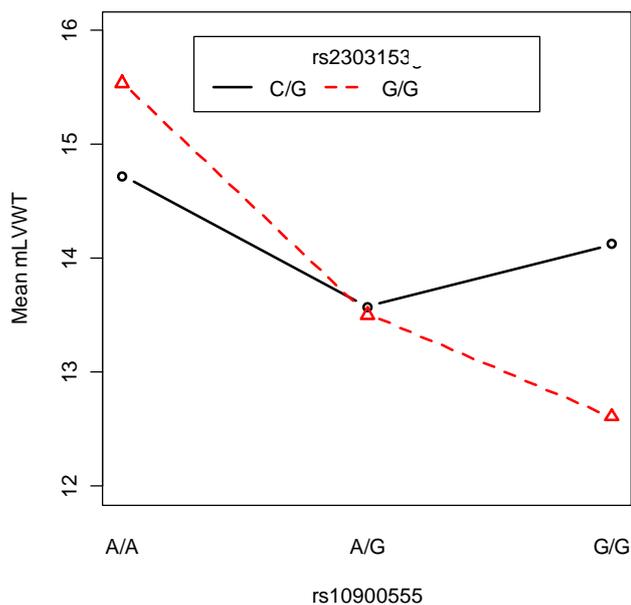


Figure 3.20. An illustration of the interaction between rs10900555 in *REN* and rs2303153 in *SCNN1B* on mLVWT.

3.6.3 *REN* and *ATP1B1*

Figure 3.21 depicts a representation of the highly significant interactions observed between rs1040503 in *ATP1B1* and two SNPs in *REN*. Highly significant evidence for interaction was found between rs1040503 in *ATP1B1* and rs1464816 in *REN* for 18 hypertrophy traits, including LVM ($p = 0.0006$), mIVST ($p = 0.0008$) and mLVWT ($p = 0.0005$). Significant interaction was also found between rs1040503 in *ATP1B1* and rs5705 in *REN* for 22 hypertrophy traits, including LVM ($p < 0.0001$), mIVST ($p = 0.0005$), mLVWT ($p = 0.0002$) and mPWT ($p = 0.0026$).

Ideally, two SNPs would show two parallel graphs there is no evidence for interaction, however, a deviation from this pattern signifies interaction between the two SNPs. Note that a decrease in mLVWT and LVM is observed for individuals who are homozygous for the G-allele of the *REN* rs1464816 variant and heterozygous for the G-allele of the *ATP1B1* rs1040503 variant. Conversely, a significant increase is observed for individuals who are homozygous for the G-allele in rs1040503 and homozygous for the T-allele in rs1464816. Individuals who are homozygous for the *REN* rs5705 variant G-allele, shows a decrease in mLVWT and LVM with the addition of at least one T-allele of the *ATP1B1* rs1040503 variant.

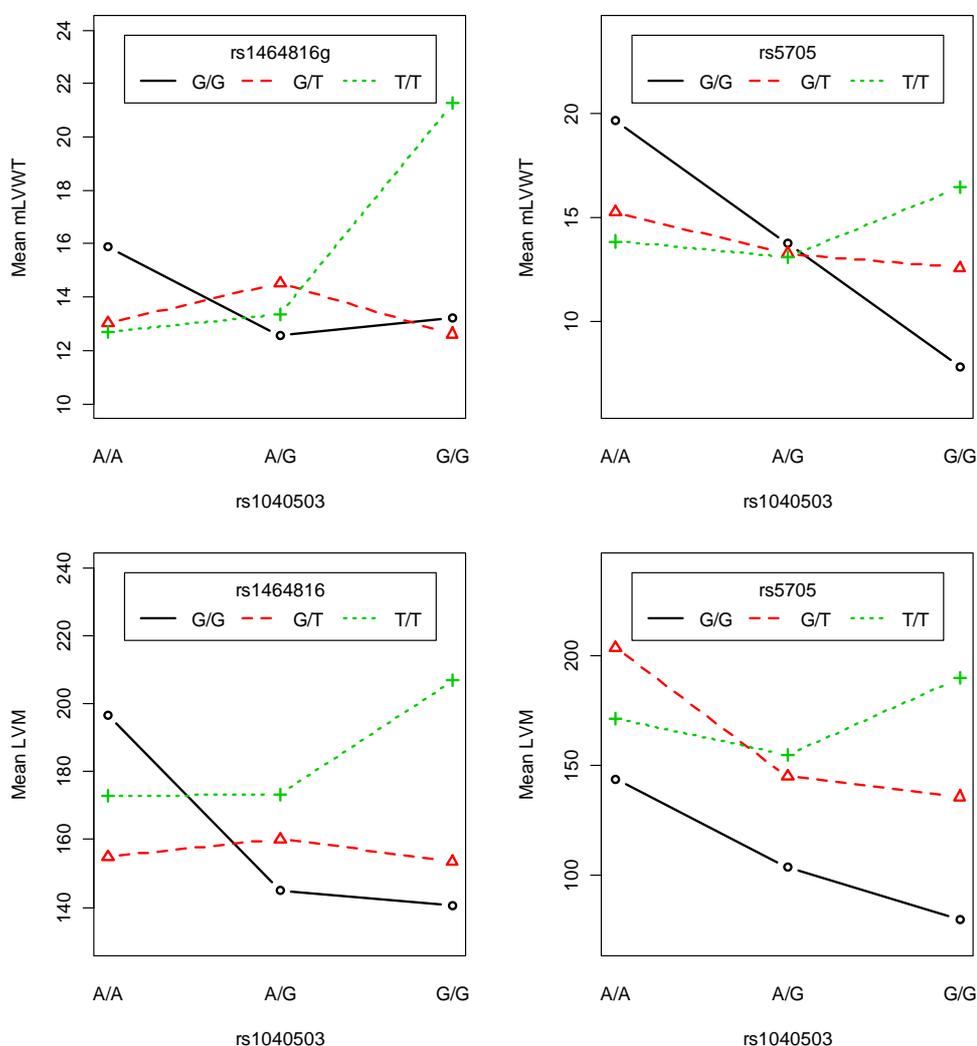


Figure 3.21. An illustration of the interaction between rs1040503 in *ATP1B1* and rs1464816 and rs5705 in *REN* on mLVWT and LVM.

3.6.4 *ATP6AP2* and *SCNN1B*

Figure 3.22 illustrates the interaction between rs2968917 in *ATP6AP2* and rs250563 in *SCNN1B* to influence mLVWT. Males and females were analyzed separately as *ATP6AP2* is an X-linked gene. Highly significant interaction was found between these two SNPs for five hypertrophy traits. Ideally, two SNPs would show two parallel graphs there is no evidence for interaction, however, these two SNPs shows a deviation from this pattern, signifying interaction between the two SNPs. Note the significant increase in mLVWT caused by the addition of a T-allele in rs2968917 in females who are heterozygous for the rs250563 variant.

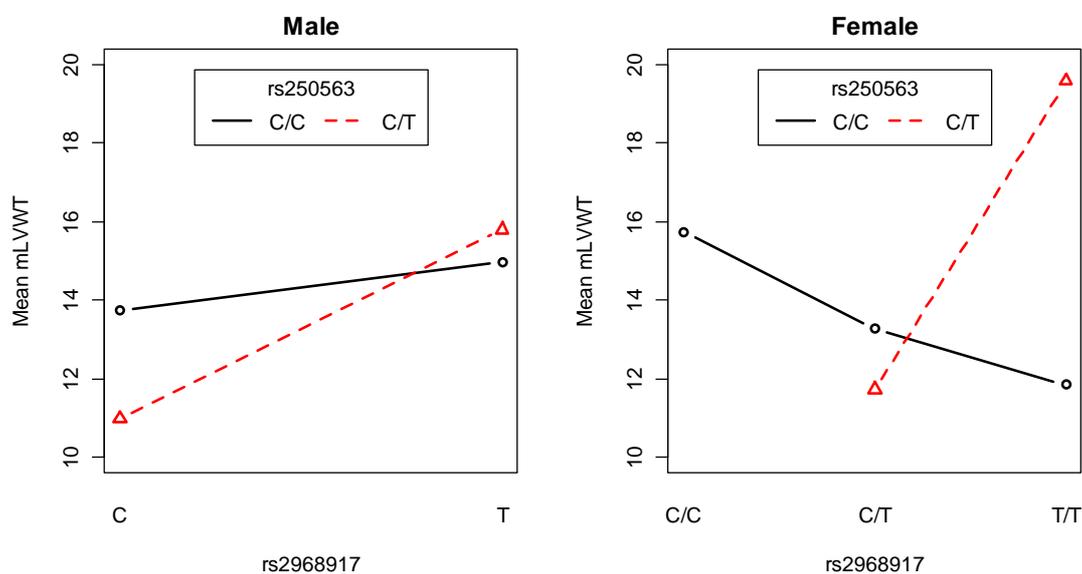


Figure 3.22. An illustration of the interaction between rs2968917 in *ATP6AP2* and rs250563 in *SCNN1B* on mLVWT.

3.6.5 ENaC subunits

Three highly significant interactions were observed between the ENaC subunit genes. One SNP in *SCNN1B*, rs2303153, showed evidence of interaction with two SNPs in *SCNN1A*, i.e. rs11614164 and rs378726. The interaction between rs2303153 and rs11614164 influences 16 hypertrophy traits, including mIVST ($p = 0.0023$), mLVWT ($p = 0.0051$) and mPWT ($p = 0.0001$). Similarly, the interaction between rs2303153 and rs378726 influences 12 hypertrophy traits, also including mIVST ($p = 0.0050$), mLVWT

($p = 0.0074$) and mPWT ($p < 0.001$). Interaction was also observed between rs250563 in *SCNN1B* and rs5735 in *SCNN1G* for nine hypertrophy traits (figure 3.23). Ideally, two SNPs would show two parallel graphs there is no evidence for interaction, however, the deviation from this pattern in all three SNP-pairs signifies interaction.

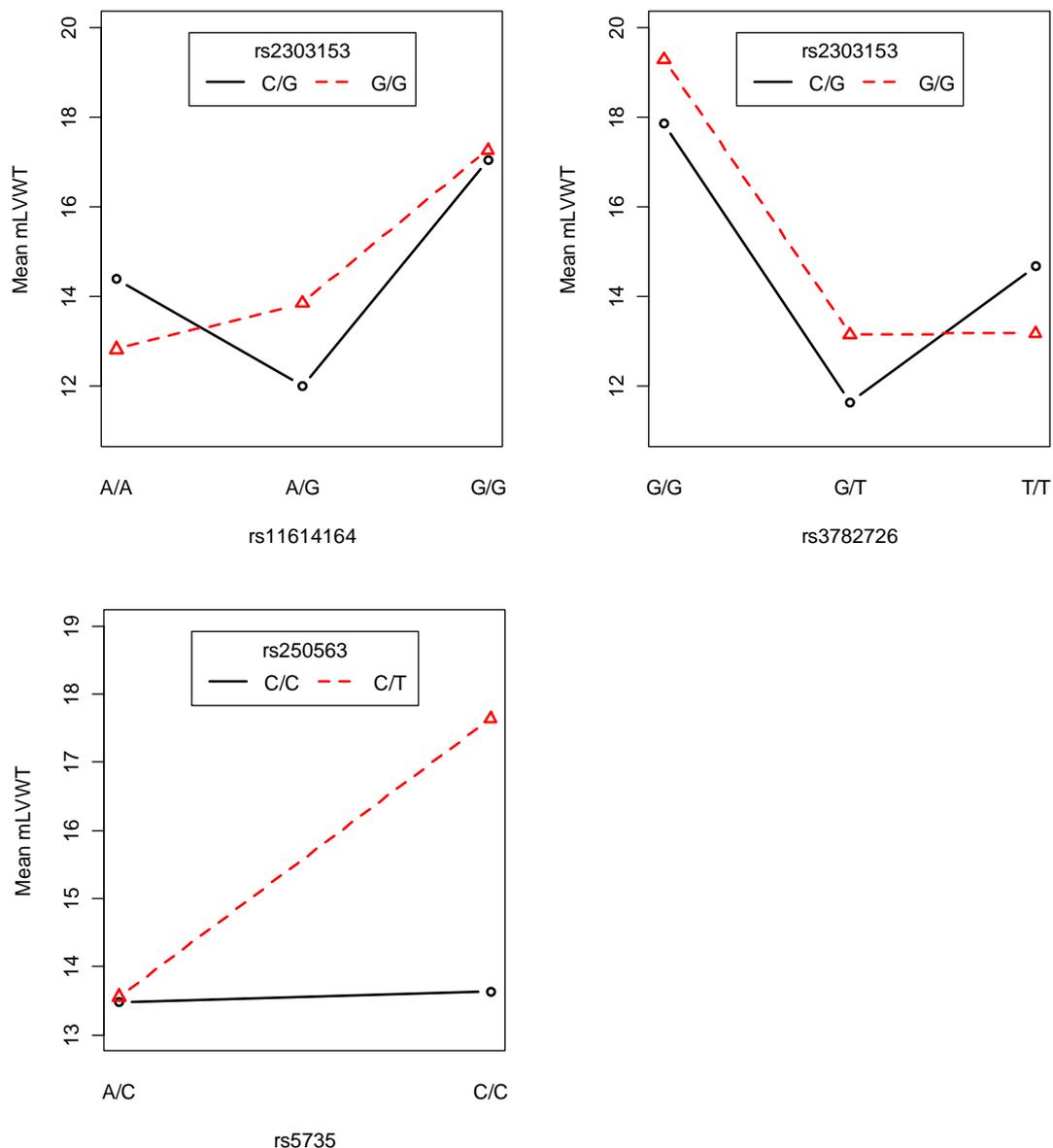


Figure 3.23. An illustration of the interaction between a subset of the ENaC subunit genes on mLVWT.

3.6.6 Na⁺/K⁺-ATPase subunits and ENaC subunits

Highly significant evidence for interaction was found between SNPs in genes coding for β -subunit isoforms of the Na⁺/K⁺-ATPase and SNPs coding for ENaC subunits. One SNP in *ATP1B1*, rs1358714, showed significant evidence for interaction with rs11614164 and rs3782726 in *SCNNIA*. The interaction between rs1358714 and rs11614164 influenced ten hypertrophy traits, including LVM ($p = 0.0046$), mIVST ($p = 0.0021$) and mLVWT ($p = 0.0064$). Similarly, the interaction between rs1358714 and rs3782726 influenced seven hypertrophy traits, including LVM ($p = 0.0072$) and mIVST ($p = 0.0012$) (figure 3.24).

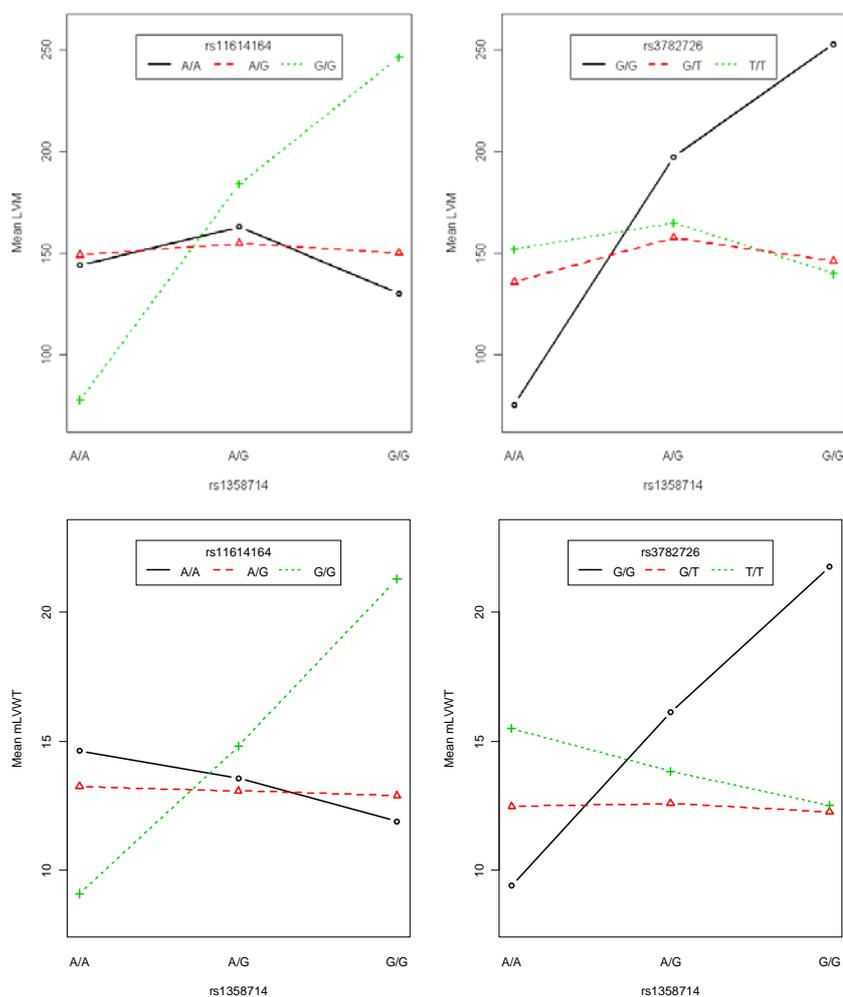


Figure 3.24. An illustration of the interaction between rs1358714 in *ATP1B1* and rs11614164 and rs3782726 in *SCNNIA* on LVM and mLVWT.

Interestingly, these two SNP-pairs show strikingly similar interaction patterns. Individuals who are homozygous for the G-allele of rs11614164 show a significant increase in mLVWT an LVM with the addition of at least one G-allele of rs1358714. Similarly, individuals who are homozygous for the G-allele of rs3782726 show a significant increase in mLVWT an LVM with the addition of at least one G-allele of rs1358714.

One SNP in *ATP1B3*, rs2068230, showed significant interaction with three SNPs: rs11614164 in *SCNN1A* and rs238547 and rs250563 in *SCNN1B*. The interaction between rs2068230 and rs11614164 influenced six hypertrophy traits, while the two *ATP1B3*-*SCNN1B* interactions influenced 17 and 13 hypertrophy traits respectively. These interactions are illustrated in figure 3.25.

An interesting interaction was observed between rs11614164 and rs2068203, which is seen best in the graph for LVM. An individual who is homozygous for the G-allele of rs11614164, will exhibit a decreased LVM if homozygous for the A-allele of rs2068203, but an increase in LVM if homozygous for the T-allele of rs2068230.

Ideally, two SNPs would show two parallel graphs there is no evidence for interaction, however, a deviation from this pattern signifies interaction between the two SNPs as seen in the interaction between rs238547 and rs2068230. Individuals who are heterozygous for the rs250563 variant will exhibit a decrease in mLVWT with the addition of at least one T-allele in rs2068230 and a similar trend is observed for LVM.

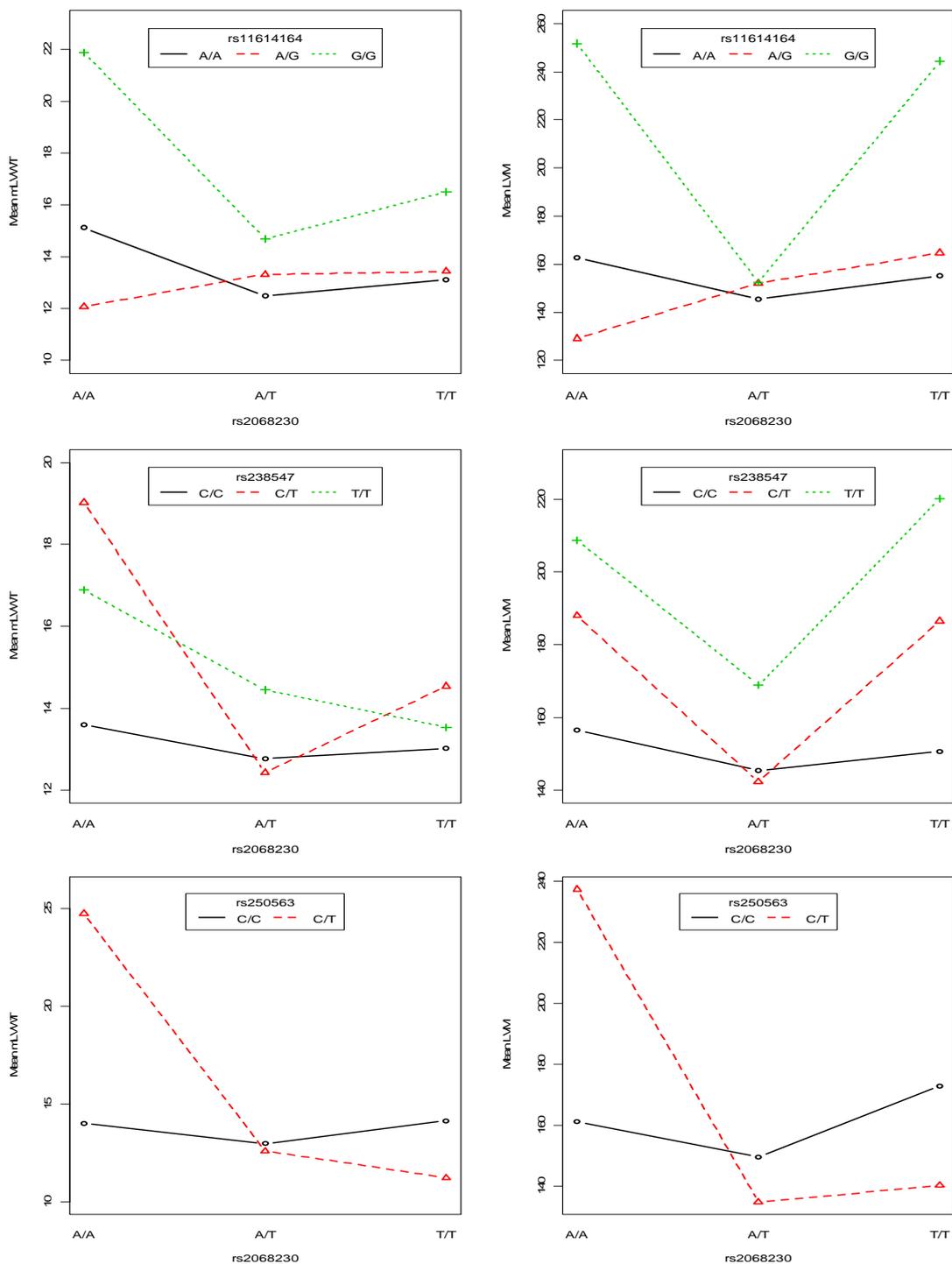


Figure 3.25. An illustration of the interaction between rs2068230 in *ATP1B3* and three SNPs on LVM and mLVWT: rs11614164 in *SCNNIA* and rs238547 and rs250563 in *SCNNIB*.

CHAPTER 4 DISCUSSION

INDEX	PAGE
4.1 PREVIOUS HCM STUDIES	90
4.2 SNP SELECTION	90
4.3 GENOTYPING APPROACH	91
4.4 CAVEATS IN ASSOCIATION STUDIES	93
4.4.1 Population stratification	93
4.4.2 Phenotypic definition	93
4.4.3 Power	94
4.4.4 Multiple testing	95
4.4.5 Confounding variables	95
4.5 RESULTS FROM ASSOCIATION ANALYSES IN THE PRESENT STUDY	96
4.5.1 AT₂ receptor	96
4.5.2 Renin and renin-associated genes	98
4.5.3 MR	100
4.5.4 Na⁺/K⁺-ATPase subunits	102
4.5.5 ENaC subunits	104
4.6 GENE-GENE INTERACTION ANALYSIS	106
4.6.1 Renin and RnBP	106
4.6.2 Renin and the ENaC β-subunit	106
4.6.3 Renin and the Na⁺/K⁺-ATPase β1-subunit	107
4.6.4 (Pro)renin receptor and the ENaC β-subunit	107
4.6.5 ENaC subunits	107
4.6.6 Na⁺/K⁺-ATPase and ENaC subunits	108
4.7 FUTURE STUDIES	108
4.8 CONCLUSION	109

CHAPTER 4: DISCUSSION

4.1 PREVIOUS HCM STUDIES

Previous investigations on the influence of RAAS gene polymorphisms on the development of hypertrophy within the context of HCM were largely focussed on a small subset of so-called pro-LVH polymorphisms as mentioned in section 1.3.4. These polymorphisms and other polymorphisms within the *ACE1*, *AGTR1*, *CMA*, *AGT* and *CYP11B2* genes have been the main focus in HCM studies of hypertrophy to date. A study by Ortlepp and colleagues (2002) concluded that polymorphisms within these RAAS genes significantly influence the hypertrophic phenotype in HCM. This was later confirmed by other association studies in different population groups (Perkins et al., 2005; Kaufman et al., 2007).

The effect of polymorphisms in the *ACE1*, *ACE2*, *AGTR1*, *CMA*, *AGT* and *CYP11B2* genes on hypertrophy in the HCM cohort investigated in the present study, have been studied previously. The present study was therefore aimed at expanding our current knowledge of the influence of RAAS gene polymorphisms in the modulation of hypertrophy in a South African HCM cohort, using a family-based association and multi-SNP approach. Moreover, we investigated polymorphisms within genes that are not considered classical RAAS modifiers of HCM in an attempt to identify new avenues for hypertrophy research.

4.2 SNP SELECTION

The number of SNPs required for a genetic association study depends on the pattern of LD in the area of interest (Zhang et al., 2004). Recent studies showed that LD patterns vary greatly across the human genome with some regions of low LD interspersed with regions of high LD (Johnson et al., 2001; Gabriel et al., 2002; Zhang et al., 2004). Johnson et al. (2001) and Patil et al. (2001) proposed that only a small number of tag SNPs are required to capture most of the haplotype structure in high LD regions of the human genome. This method reduces genotyping effort in association studies, without much loss of power (Zhang et al., 2002a).

In the present study, we selected SNPs using the SNPbrowser software to achieve an even spacing of 0.5 LDUs on the metric LD map for the HapMap CEU and YRI populations. The SNPbrowser programme offers a user-friendly interface to browse HapMap data and minimizes the effort associated with SNP selection.

The metric LD map with additive distances in LDUs was first developed by Maniatis et al. (2002). Zhang et al. (2002) examined the properties of these maps and found a remarkable agreement between LDU steps and meiotic recombination sites. Later, Maniatis et al. (2004) investigated the application of LDU maps in the context of association mapping. They concluded that the LDU maps have greater power when compared to the centi-Morgan/kb map. Further studies revealed that LDU maps are a powerful tool for disease gene association mapping using LD (Collins et al., 2004; Maniatis et al., 2005).

The theoretical number of SNPs needed to cover a gene is significantly reduced with this LDU method, when compared to a tag SNP selection method. For example, to sufficiently cover the 80 kb *SCNN1B* gene as in the present study using the tag SNP approach would require 11 SNPs for the HapMap CEU population and 19 SNPs for the YRI population, with 5 SNPs overlapping. Thus, a total of 25 SNPs is required to cover *SCNN1B* in these populations using the tag SNP approach. In contrast, a total of eight SNPs is required to cover *SCNN1B* in the HapMap CEU and YRI populations using the LDU approach.

4.3 GENOTYPING APPROACH

Previous studies from our laboratory on the present cohort utilized PCR-based genotyping approaches, such as ASREA and SNaPshot primer extension analysis. ASREA has the advantage of being relatively simple and cheap. However, only a small subset of polymorphisms is located within an endonuclease restriction site and the effectiveness of this system relies on the completeness of digestion in all samples (Kristensen et al., 2001). Moreover, additional confirmation, such as sequencing or re-genotyping, is needed to confirm the accuracy of ASREA genotyping. The SNaPshot

system is moderately priced primarily because it allows for multiplex reactions in which several polymorphisms can be genotyped simultaneously (Makridakis and Reichardt, 2001). Accurate and effective primer design is crucial to the success of this method and this could be a potential drawback (Kaderali, 2007) and additional confirmation is also needed to confirm genotyping accuracy.

Both these methods are labour intensive, potentially time-consuming and require a large amount of optimization and post-PCR handling. Additionally, genotype data must be transferred to the database manually, creating opportunities for human typographical error.

The ABI Validated TaqMan genotyping system was extremely effective in the present study. This high-throughput system, although more expensive, offers many advantages. Firstly, time is saved on assay design, testing and optimization. The TaqMan assays used in the present study are pre-designed and validated by ABI; no additional confirmation or optimization was therefore considered requisite. It must be mentioned that validated predesigned assays are not available for all SNPs, but the researcher is able to custom design TaqMan assays, if the available assays are not suitable for their purpose. However, additional sequencing would be needed to confirm accuracy in such a situation.

The ABI TaqMan assays are optimized to operate with low DNA concentrations (5-20 ng), sparing precious DNA samples. As was done in the present study, reactions can be set up by an automatic pipetting robot and performed in 384-well plates in 5 µl reaction volumes, which reduces costs, human error and allows for quicker genotyping. No post-PCR transfer or handling is needed and the SDS software performs automatic allele-calling based on fluorescence signals. All genotypes with a confidence level of lower than 95 % are marked as undetermined, ensuring that dubious genotypes are not entered into the data analyses. Genotyping results are exported as a text file, which can subsequently be directly imported into the database, minimizing the likelihood of human typographical error.

4.4 CAVEATS IN ASSOCIATION STUDIES

Statistical evidence for association between a specific allele and a phenotypic trait can arise from three situations (Cardon and Palmer, 2003). Firstly, the allele itself might be functional and exert a direct effect on the expression of the phenotype. Secondly, the allele might be correlated with or in LD with a functional allele. However, a possibility exists that the association is purely due to chance.

It is therefore vital to ensure the reproducibility of a study. There are many factors that affect the reproducibility of an association study on complex genetic traits. Factors such as genetic and phenotypic heterogeneity and failure to account for confounding variables directly influence the reproducibility of a particular study (Cardon and Palmer, 2003). The responsibility of the researcher is, therefore, to minimize the chance for spurious results through careful study design and relevant statistical methods.

4.4.1 Population stratification

Theoretically, spurious association might originate from undetected population substructure in any association study. Association between a specific genotype and disease trait could be confounded by population stratification in a study population consisting of a mixture of two or more subpopulations with different allele frequencies and disease risks, leading to a false positive association between a certain variant and a particular disease trait (Colhoun et al., 2003). The use of TDT tests like the QTDT test used in the present study protects against this population stratification by matching each “case-control” pair within a family, this renders any population-level differences in allele frequency irrelevant (Cardon and Palmer, 2003).

4.4.2 Phenotypic definition

Phenotypic definition contributes significantly to the reproducibility of a particular study and is thus vital to any association study. It is of the utmost importance that all measurements are relevant to the disease phenotype and taken with the same precision.

In HCM phenotypic definition poses a potential problem. As discussed in section 1.2.2, the phenotypic expression of HCM varies greatly between individuals, particularly regarding the extent and distribution of hypertrophy. Cardiac hypertrophy in HCM is mostly asymmetrical and HCM patients rarely exhibit uniform concentric hypertrophy. It is therefore difficult to quantify the extent of hypertrophy in a whole cohort with a single measurement. One way to address this issue is to measure composite scores that encompass a number of hypertrophy measurements to describe the extent of hypertrophy. However, it is still uncertain which composite score offers the best estimate of the extent of hypertrophy.

In the present study we addressed these issues as follows. All the individuals in this cohort were clinically characterised by 2-D and M-mode echocardiography by a single cardiologist. In total, 16 wall thickness measurements were taken at three levels of the heart to estimate the distribution of hypertrophy. Additionally, we determined LVM by echocardiography as an indication of the extent of hypertrophy. It must be mentioned that a possibility exists that LVM as determined by echocardiography could not be an appropriate estimate of hypertrophy due to left ventricular geometry in the presence of LVH; however, it is still a commonly used trait in similar studies and was therefore determined for comparison. We therefore performed a principal component analysis and two composite scores (CWT and Spirito-Marón) were measured to obtain a comprehensive indication of the extent of hypertrophy.

4.4.3 Power

Statistical power in an association study refers to the probability that a test statistic reflects a true association (or lack thereof) between a genomic variant and a specific disease trait (Gordon and Finch, 2005). Traditionally, the power of a study relies on the disease allele frequency as well as sample and effect size (Colhoun et al., 2003; Donahue and Allen, 2005). In addition, errors in phenotypic classification and genotype errors contribute significantly to the power of an association study (Gordon and Finch, 2005). Presently, no comprehensive method for calculating the power of an association study in extended families exists.

The present study was conducted in the context of an explorative study and while every effort was taken to minimize these effects that conventionally decrease power, no formal calculations were done to estimate the power of the present study. Additionally, we included every individual who gave consent within these 22 families, including all HCM-mutation carriers 18 years and older. There is therefore no possibility of increasing the number of study subjects at this time, which is an accepted method of increasing power.

4.4.4 Multiple testing

Multiple testing in any cohort can result in an increased probability of obtaining a false positive result (type I error). A popular solution for this is to use a Bonferroni adjustment. This method assumes that all the performed tests are independent and each p-value is subsequently multiplied with the number of tests performed. However, Bonferroni corrections can be overly stringent in family-based association studies (Perneger, 1998). Additionally, Bayesian methods for correction require prior knowledge of the probability of involvement, which is presently unknown for most genetic variants (Campbell and Rudan, 2002).

In the present study we determined exact p-values for QTDT analyses with Monte-Carlo permutations to reduce the probability of type I errors as this method provides an overall appraisal of significance (McIntyre et al., 2000). However, it must be mentioned that no formal corrections for multiple testing were made as the present study was conducted as an explorative study. Moreover, the LVH measurements in this study are highly correlated and LD, although incomplete, exists between some of the SNPs and it is therefore not appropriate to use Bonferroni corrections under these circumstances.

4.4.5 Confounding variables

It is important to ensure that the association observed between a specific variant and a phenotypic trait is due to the effect of that variant and not due to an unrelated covariate or trait. For example, BP has an acknowledged independent effect on hypertrophy and if this aspect is not accounted for in a specific association study, one cannot be sure whether variation in hypertrophy is due to variation in BP or the genomic variant in question. In

the present study all analyses were adjusted for known hypertrophy covariates, i.e. systolic BP, diastolic BP, age, sex, BSA and HR.

4.5 RESULTS FROM ASSOCIATION ANALYSES IN THE PRESENT STUDY

HCM was initially viewed as a monogenic disease, as a single mutation within a sarcomeric gene is sufficient to cause the disease with a clearly defined Mendelian pattern of inheritance. However, the variable phenotypic expression of HCM pointed towards to existence of additional environmental and genetic modifiers and HCM is currently considered a complex disease. In the present study we investigated whether various genes within the RAAS contribute to the development of hypertrophy in HCM.

4.5.1 AT₂ receptor

The main effector molecule of the RAAS, Ang II, when bound to the AT₁ and AT₂ receptors influences cardiac hypertrophy, remodelling and contraction in multiple BP-independent ways. Binding of Ang II to the AT₁ receptors activates multiple intracellular pathways that include phospholipids, calcium, reactive oxygen species (ROS) and kinases (Booz 2004). These AT₁ receptor-mediated pathways elicit cardiovascular hypertrophic effects that are well documented including vasoconstriction, aldosterone release and growth stimulation (Dostal and Baker, 1992; Hoffmann et al., 2001a; Hoffmann, 2005). Large clinical trials have concluded that AT₁ receptor antagonists reduce LVH and other cardiac morbidities (Dahlof et al., 2002; Okin et al., 2003). However, the exact role of the AT₂ receptor in the heart is not as clear.

Cardiac expression of the AT₂ receptor is upregulated in HF, myocardial infarction and cardiac remodelling (Nio et al., 1995; Ohkubo et al., 1997; Van Kesteren et al., 1997). Previous studies in adult rat hearts have suggested that the AT₂ receptors have antihypertrophic effects on the heart that counterbalance the hypertrophic effects of the AT₁ receptors (Booz and Baker, 1996; Mukawa et al., 2003). In a study on adult rat hearts, Bartunek et al. (1999) demonstrated that AT₂ receptor inhibition amplifies LVH in response to Ang II. They perfused normal and hypertrophied hearts with Ang II or Ang II with an AT₂ receptor blocker and measured new LV protein synthesis. AT₂ receptor

blocade in Ang II treated rats resulted in an amplified LV growth response to Ang II, which was coupled with reduced LV cGMP content and enhanced membrane protein kinase C translocation.

Zhang et al. (2006) reported that an rs5193/rs5194 haplotype in the AT₂ receptor gene is associated with a cardioprotective role in Cantonese patients with essential hypertension. A commonly occurring AT₂ receptor rs1403543 polymorphism, designated as -1332 G/A or +1675 G/A (Erdmann et al., 2000; Alfakih et al., 2004) has also been associated with the progression of LVH in previous studies. Schmieder and colleagues (2001) found that this polymorphism is significantly associated with echocardiographically determined LVM and relative LVWT in young mildly hypertensive males. This was confirmed by Alfakih et al. (2004) who reported an association between LVH and the rs1403543 polymorphism in patients with systemic hypertension.

The AT₂ receptor gene is located on the X-chromosome and consists of three exons and two introns and the entire open reading frame of the gene is situated in the third exon. The rs1403543 polymorphism is located at a lariat branch-point in the first intron, 29 bp before exon 2 in a region that is important for transcriptional activity (Warnecke et al., 1999; Erdmann et al., 2000). Nishimura et al. (1999) postulated that this polymorphism is functional and may affect pre-mRNA splicing, although a study by Warnecke et al. (2005) provided evidence that it modulates AT₂ receptor protein expression, but not mRNA splicing. Warnecke et al. (2005) concluded that the G-allele is associated with increased AT₂ receptor protein levels, which may be protective in LVH development.

The present study supports recent evidence that the AT₂ receptor modulates the development of hypertrophy. Highly significant evidence for association between the AT₂ receptor rs1403543, but not the rs5194 and rs11091046 variants, and heritable hypertrophy traits was found in the present HCM cohort. The A-allele of the rs1403543 polymorphism was associated with a marked decrease in echocardiographically determined LVM, mIVST and mLVWT as well as 13 other hypertrophy indices, independent of BP and other known hypertrophy covariates (table 3.5). It is therefore

possible that the A-allele may be cardioprotective, given the proven functionality of the rs1403543 polymorphism. Our results are therefore in keeping with the hypothesis that at least one form of the AT₂ receptor counteracts hypertrophic responses.

4.5.2 Renin and renin-associated genes

Renin is a rate-limiting component of the RAAS as it controls the initial conversion of angiotensinogen to Ang I and is traditionally viewed as a candidate gene for hypertension due to its crucial role in the regulation of BP (West et al., 1992; Hasimu et al., 2003; Gradman and Kad, 2008). However, studies in animal models suggest that renin also has cardiac effects independent of its effect on BP (Veniant et al., 1996; Saris et al., 2006).

Renin is initially synthesized as an enzymatically inactive prohormone, prorenin, in the juxtaglomerular cells of the kidney. Prorenin is subsequently converted to the active renin via proteolytic and nonproteolytic activation processes (Derckx et al., 1992; Reudelhuber et al., 1994). Interestingly, the plasma concentration of prorenin is ten times greater than that of renin (Danser et al., 1998).

Veniant and colleagues (1996) developed a transgenic rat line that expresses prorenin exclusively in the liver. These rats demonstrated a 400-fold increase in plasma prorenin, but exhibited normal plasma renin levels and BP. However, these animals developed severe liver fibrosis as well as cardiac and aortic hypertrophy. This study gained more attention with the recent cloning of the (pro)renin receptor (Nguyen et al., 2002). Renin and prorenin bound to this receptor displays a five-fold increase in angiotensin to Ang I conversion and exerts physiological effects that are completely independent of Ang II generation (Nguyen et al., 2003; Oliver 2006). In a study on neonatal rat cardiomyocytes, Saris et al. (2006) demonstrated that prorenin bound to the (pro)renin receptor activated the p38 MAPK/HSP27 pathway and they postulated that this activation is responsible for the severe hypertrophy observed by Veniant et al. (1996).

Similarly renin and/or prorenin has been proven to induce DNA synthesis, activate the p42/p44 MAPK intracellular pathways and stimulate the release of plasminogen activator

inhibitor (PAI)-1 and transforming growth factor (TGF) (Ichihara et al., 2006; Huang et al., 2006; Nguyen and Danser, 2006). These and other studies (Nguyen et al., 1996; Methot et al., 1999; Prescott et al., 2002) provide evidence that renin *per se* exerts hypertrophic cellular effects, independent of Ang II generation.

In addition, Takahashi et al. (1983) reported another protein that was capable of forming a complex with renin which they named RnBP. Further *in vitro* studies showed that this protein is able to form a heterodimer with renin and subsequently inhibit its activity (Takahashi et al., 1994). This protein was later found to be identical to the enzyme N-acetyl-D-glucosamine 2-epimerase (NAGE) (Takahashi et al., 1999). In a study on RnBP-knockout mice, Schmitz et al. (2002) were unable to detect any effect of RnBP deficiency on renal and circulating RAAS or BP, leading the authors to speculate that RnBP does not play a role in the regulation of plasma renin and RAAS activity.

However, Bohlmeier and colleagues (2003) investigated the expression of RnBP in failing human hearts with end-stage idiopathic dilated cardiomyopathy. They found that RnBP expression was restricted to endothelial cells in the non-failing hearts, while RnBP gene and protein expression was selectively activated in the ventricular cardiomyocytes of failing hearts. Interestingly, they reported that the highest RnBP mRNA levels were detected in a subject with significant LVH. Additionally, RnBP was redistributed from a cytosolic to a sarcolemmal/sarcomeric fraction, which led the authors to conclude that RnBP may be involved in the modification of cardiac cytoskeletal proteins.

The present study demonstrates for the first time that polymorphisms in the renin and RnBP genes play a BP-independent role in modulating hypertrophy in HCM, independent of BP. We found significant evidence for association between all the variants studied in renin and a number of heritable hypertrophy traits. In particular, the G-allele of the *REN* rs1464816 was found to significantly decrease LVM and mPWT as well as six other hypertrophy traits (table 3.7). Previously, Schoenhard et al. (2008) reported that this polymorphism is associated with plasma tissue-type plasminogen activator (t-PA) and PAI-1 levels in an urban West African population cohort consisting of 992 individuals,

leading the authors to speculate that this polymorphism might influence fibrosis and cardiovascular disease.

Furthermore, rs11571082 in *REN* was found to be associated with seven hypertrophy traits, while rs5705 was associated with five and rs10900555 with two hypertrophy traits. No published information could be found on the functionality of these SNPs. Additionally, rs1464816 and rs11571082 was found to be significantly associated with the score obtained from the principal component analysis.

Significant evidence for association was also found between variants in the RnBP gene and hypertrophy traits in the present cohort. The A-allele of the rs762656 polymorphism was found to significantly decrease 11 hypertrophy traits, including LVM and mPWT. The rs2269372 polymorphism was also found to significantly decrease mPWT and the rs2269370 polymorphism was found to increase two hypertrophy measurements at the apex level. However, no association was found between variants in the (pro)renin receptor gene and hypertrophy traits in this study cohort.

The present results provide the first evidence of a role for renin and the RnBP in hypertrophy development in HCM and are consistent with previous reports that link these genes to hypertrophy and therefore support the further investigation of renin and RnBP in the development of hypertrophy. However, we fail to report an association between (pro)renin receptor gene variants and hypertrophy, contrasting previous reports on animal models.

4.5.3 MR

Schunkert and colleagues (1997) reported that serum aldosterone levels modulate LVM in a population-based cohort of 615 middle-aged individuals. This effect was observed in both the hypertensive and normotensive individuals in the cohort. A case-control study by Malmqvist et al. (2002) found that PRA and serum aldosterone levels were elevated in hypertensive patients with LVH. Both PRA and serum aldosterone was significantly associated with LVM index, independent of BP and BSA. Similarly, Matsumura et al.

(2006) was significantly associated with LVM index in patients with primary aldosteronism, independent of BP and other known hypertrophy covariates.

Variants in the aldosterone synthase gene (*CYP11B2*) have been investigated intensively in the progression of LVH. One variant in particular, +344 C/T, significantly affects circulating aldosterone levels (Brand et al., 1998; Hautanena et al., 1998) and is significantly associated with LVM (Stella et al., 2004). This polymorphism was also previously associated with LVH in HCM patients (Chai et al., 2006). Mayosi et al. (2003) reported that polymorphisms and haplotypes in *CYP11B2* are associated with cardiac septal wall thickness and LV cavity size in a cohort of 955 British Caucasian individuals from 229 families. Additionally, previous studies revealed that the rs3097 polymorphism in *CYP11B2* was found to be significantly associated with hypertrophy traits in the present HCM cohort (Cloete REA, M.Sc).

Aldosterone exerts its cellular effects by binding to the MR. The MR is a member of the steroid/thyroid/retinoid/orphan receptor family of transcription factors and MR has been identified in cardiac tissue in previous studies (Lombes et al., 1995). MR antagonists were shown to reduce ventricular remodelling, SCD and myocardial fibrosis in the RALES and EPHEBUS trials, independent of the antagonist's effect on BP, providing concrete evidence that MR blockade offers cardioprotective effects in patients with HF and systolic left ventricular dysfunction (Pitt et al., 1999; Pitt et al., 2003).

Tsybouleva and colleagues (2004) investigated the effect of MR blockade in a transgenic mouse model of human HCM (cTnT-Q92). They were able to demonstrate that the MR blocker Spironolactone reduced myocyte disarray and interstitial fibrosis and improved diastolic function. They concluded that aldosterone significantly affects the relationship between sarcomeric dysfunction and the cardiac phenotype of HCM. In another mouse hypertrophy model, MR blockade was shown to reduce the expression of TGF- β and significantly reduce LVH and cardiac fibrosis (Zhang et al., 2008).

In the present study, we first performed a preliminary association study using an AGAT repeat microsatellite marker because the MR gene is relatively large (363.60 kb). We failed to find conclusive evidence for association between this AGAT repeat in the MR gene and hypertrophy and therefore decided not to follow with a multi-SNP based association study. Munoz-Brauning et al. (2005) previously reported that this AGAT repeat in intron 2 of the MR gene significantly affected PRA in an essential hypertensive population. They concluded that this polymorphism plays a role in the control of the MR gene expression and BP. In the present study, we were interested in the BP-independent effects of RAAS genes on hypertrophy and all analyses were therefore adjusted for BP. It is then tempting to speculate that the biological effects of the AGAT repeat microsatellite is BP dependent. However, these data do not provide conclusive evidence to confirm nor deny the involvement of the MR in hypertrophy development.

4.5.4 Na⁺/K⁺-ATPase subunits

Various studies have implicated increased intracellular Na⁺ in hypertrophy (Pogwizd et al., 2003; Verdonck et al., 2003). The Na⁺/K⁺-ATPase is one of the downstream effectors of the aldosterone/MR complex and is responsible for maintaining the transmembrane gradients of Na⁺ and K⁺. The Na⁺/K⁺-ATPase is a heteromeric protein that consists of α - and β -subunits (Kaplan, 2002). The α -subunit is a polytopic membrane protein that confers the catalytic activity of the enzyme and binding sites for Na⁺, K⁺ and ATP (Shull et al., 1985). The β -subunit modulates the pump function and is important for the efficient translation of the α -subunit on the endoplasmic reticulum, membrane insertion and correct folding of the α -subunit as well as the expression of the enzyme on the plasma membrane (Rajasekaran et al., 2005).

To date, four isoforms of the α -subunit (α 1, α 2, α 3 and α 4) and three isoforms of the β -subunit (β 1, β 2 and β 3) have been described in mammals, which exhibit tissue-specific expression (Blanco and Mercer, 1998). Previous studies have confirmed the expression of the α 1, α 2, α 3, β 1, β 2 and β 3 subunits in human hearts (Wang et al., 1996; Malik et al., 1998; Schwinger et al., 1999).

Allen et al. (1992) published the first report on Na⁺/K⁺-ATPase isoform expression in the myocardium of normal and failing human hearts. They reported that none of the three α -subunits showed altered expression in the left ventricles of normal and failing hearts. Later, Shamraj et al. (1993) reported that Na⁺/K⁺-ATPase isoform expression is indeed altered in failing compared to nonfailing human hearts, which was subsequently corroborated by other groups (Schwinger et al., 1999; Muller-Ehmsen et al., 2001). The α 1-isoform expression was decreased in human heart failure (Borlak and Thum, 2003), but increased in hypertrophic rat hearts (Zwadlo and Borlak, 2005). Previous studies in different rat hypertrophy models also provided clear evidence that α 2-isoform expression is increased in LVH (Baek and Weiss, 2005).

The Na⁺/K⁺-ATPase also serves as a receptor for ouabain and other related cardiac glycosides. Previous investigations have established that the positive inotropic effects of cardiac glycosides on the myocardium is due to partial inhibition of the cardiac Na⁺/K⁺-ATPase, which causes a small increase in intracellular Na⁺ and in turn affects the Na⁺/Ca²⁺ exchanger, ultimately leading to increased intracellular Ca²⁺ and contraction force (Akera and Ng, 1991; Huang et al., 1997). Studies on α 1- α 2 knockout mice provided clear evidence that the Na⁺/K⁺-ATPase is a regulator of cardiac contractility (Dostanic et al., 2004).

Huang et al. (1997) demonstrated that partial inhibition of the Na⁺/K⁺-ATPase by ouabain in cultured neonatal rat cardiomyocytes induced hypertrophic growth, which was coupled with increased expression of TGF- β and other late response genes that are markers of cardiac hypertrophy. Further studies by the same group showed that the hypertrophic response of Na⁺/K⁺-ATPase inhibition was also associated with p42/44 MAPK and ROS-dependent pathways (Kometiani et al., 1998; Xie et al., 1999).

In the present study, we found significant evidence for association between two Na⁺/K⁺-ATPase subunit genes and hypertrophy. The A-allele of rs850609 in the Na⁺/K⁺-ATPase α 1-subunit gene significantly increased IWmit and LWpap, while the C-allele of rs1200130 in the Na⁺/K⁺-ATPase β 1-subunit gene significantly decreased IWmit and

PWmit. There are some concerns about the interpretation of these associations as it is only with a few hypertrophy traits. Additionally, these traits are not ones that are conventionally used as measurements of the extent of hypertrophy. However, there is prior reason to think that the Na^+/K^+ -ATPase gene products affect LVH, due to the previous studies mentioned earlier and these results can therefore not be ignored.

Due to the nature of association studies it is possible that these variants or other genetic variants in LD with these variants may influence the hypertrophic phenotype of HCM. Given the known influence of the Na^+/K^+ -ATPase on hypertrophy and these results it should be interesting to determine whether these variants are indeed functional or not. However, it must be emphasized that these results do not provide concrete evidence for the involvement of the Na^+/K^+ -ATPase in hypertrophy development and more studies are therefore needed in this respect.

4.5.5 ENaC subunits

Further downstream effectors of the aldosterone/MR complex are the ENaCs. The ENaCs are important regulators of intracellular Na^+ as they are responsible for the electrodiffusion of Na^+ through epithelial cells. Each ENaC consists of three homologous subunits, i.e. an α -, β -, and a γ -subunit (Canessa et al., 1994).

The fact that intracellular Na^+ is increased in hypertrophy and HF (Pogwizd et al., 2003; Verdonck et al., 2003), warrants the investigation of ENaCs as potential modifiers of hypertrophy as they are crucial regulators of intracellular Na^+ homeostasis. Liddle syndrome is a rare condition caused by activating mutations in ENaC subunits. These mutations prevent the degradation of ENaCs, resulting in excessive Na^+ absorption, K^+ wasting, systemic hypertension as well as a high incidence of early cardiovascular disease (Hansson et al., 1995; Jeunemaitre et al., 1997). Certain autosomal recessive mutations in genes encoding ENaC subunits can also result in a second rare condition called Pseudohypoaldosteronism type I, which is characterized by unresponsiveness to aldosterone, severe salt wasting, extreme hyperkalaemia and elevated PRA (Edelheit et al., 2005).

The role of ENaC mutations in hypertension is well documented and the antihypertensive properties of the ENaC inhibitor amiloride have long been known (Gombos et al., 1966; Su and Menon, 2001). However, studies in animal models of hypertension have shown that low doses of amiloride reduce renal and cardiovascular disease, despite elevated BP (Campbell et al., 1993; Mirkovic et al., 2002; Sepehrdad et al., 2003; Sepehrdad et al., 2004). These effects occurred independently of changes on serum K^+ . These and other studies highlight the potential cardiovascular benefit of ENaC inhibition (Teiwes and Toto, 2007).

The association of the ubiquitin ligase Nedd4-2 with an ENaC leads to ubiquitination of the ENaC and its removal from the plasma membrane. Nedd4-2 is therefore vital to the activity and regulation of ENaCs. In a study on Nedd4-2 knockout mice, Shi and colleagues (2008) demonstrated these mice have elevated BP and impaired ENaC activity, which was aggravated by a high salt diet. Ultimately, these animals developed cardiac hypertrophy and cardiac systolic dysfunction.

A single polymorphism in the ENaC α -subunit gene, rs2286600, was associated with a modest decrease in IWmit in the present HCM study. Additionally, rs1107455 in the ENaC β -subunit gene was found to decrease five hypertrophy traits while the rs9930640 polymorphism within the same gene was significantly associated with an increase in mLVWTpap, aIVSpap and LWpap. No association was found between variants in the ENaC γ -subunit gene and hypertrophy traits. Again it might be possible that these variants are in LD with a functional allele or that these variants *per se* influence hypertrophy development. Currently, no information exists on the functionality of these polymorphisms, so it is difficult to speculate on this matter. However, the current findings and previous evidence for the involvement of the ENaCs in cardiovascular phenotypes, suggest that the ENaC β -subunit gene should be further investigated as a potential modifier of hypertrophy.

4.6 GENE-GENE INTERACTION ANALYSIS

The present study was conducted as an explorative study to identify possible modifiers of hypertrophy within the context of HCM. In complex diseases such as HCM, a lot of factors contribute to the eventual phenotype. Genes do not generally act in a simple additive manner, but rather through complex networks that involve gene-environment as well as gene-gene interactions (epistasis) (Colhoun et al., 2003). In the present study, we employed statistical methods to investigate the gene-gene interactions between the genes studied in an attempt to better understand the contribution of each gene to the complex HCM phenotype.

However, it must be mentioned that statistical estimates of interaction does have limitations. Statistical interaction does not necessarily imply interaction between genes on a mechanistic or biological level. It may point to but not absolutely predict true biological interaction; that is a question that will be answered best by molecular, rather than statistical studies (Cordell, 2002).

4.6.1 Renin and RnBP

We identified a highly significant interaction between the rs2269370 polymorphism in *RENBP* and the rs1464816 polymorphism in *REN*. These two SNPs were found to significantly interact to influence five hypertrophy traits, including mLVWT and mIVST. This interaction is intriguing, as previous studies have provided evidence that RnBP is able to form a heterodimer with renin and subsequently inhibit its activity (Takahashi et al., 1994). This interaction as well as the statistical association between *REN* and *RENBP* polymorphisms and hypertrophy traits certainly warrants the further investigation of these genes in the development of hypertrophy.

4.6.2 Renin and the ENaC β -subunit

Highly significant interaction between rs10900555 in *REN* and rs2303153 in the ENaC β -subunit gene, *SCNN1B*, was found to influence ten hypertrophy traits, including mIVST and mLVWT. Renin is a rate-limiting component of the RAAS and the ENaCs are partially responsible for the downstream effects of the RAAS, such as BP regulation and

intracellular Na^+ concentrations. Interestingly, certain mutations in ENaC subunit genes cause Liddle syndrome and Pseudohypoaldosteronism type I, which is associated with elevated PRA. It is therefore conceivable that these two genes should interact at a mechanistic level, but more studies are needed to confirm this interaction.

4.6.3 Renin and the Na^+/K^+ -ATPase β 1-subunit

The interactions that influenced the highest number of hypertrophy traits in the present study was between the rs1040503 polymorphism in the Na^+/K^+ -ATPase β 1-subunit gene, *ATP1B1*, and two polymorphisms in *REN*. Highly significant interaction between rs1040503 in *ATP1B1* and rs1464816 in *REN* was found to influence 18 hypertrophy traits, including LVM, mIVST and mLVT. Similarly, significant interaction was also found between rs1040503 in *ATP1B1* and rs5705 in *REN*, which influenced 22 hypertrophy traits including LVM, mIVST, mLVT and mPWT.

As for the renin-ENaC interaction discussed previously, it is possible that these interactions may point toward a mechanistic interaction as renin is a rate-limiting component of the RAAS and the Na^+/K^+ -ATPase contributes to the downstream effects of the RAAS. It is, indeed, remarkable that renin should show significant statistical interaction with both the downstream effectors of the RAAS.

4.6.4 (Pro)renin receptor and the ENaC β -subunit

An interaction between rs2968917 in the (pro)renin receptor gene, *ATP6AP2*, and rs250563 in the ENaC β -subunit gene, *SCNN1B*, was found to influence five hypertrophy traits. This interaction is interesting as we did not find any significant evidence for association between either of these variants and hypertrophy and further studies are therefore needed to confirm and explain these findings.

4.6.5 ENaC subunits

Three highly significant interactions were observed between the ENaC subunit genes. The rs2303153 variant in *SCNN1B* showed evidence for interaction with the rs11614164 and rs378726 variants in *SCNN1A* to influence 16 and 12 hypertrophy traits, respectively.

Moreover, interaction was also found between rs250563 in *SCNN1B* and rs5735 in *SCNN1G* to influence nine hypertrophy traits. A strong possibility exists indeed that this statistical interaction is indicative of the true biological interaction between the ENaC subunits.

4.6.6 Na⁺/K⁺-ATPase and ENaC subunits

In total, we observed five significant interactions between β -subunit isoforms of the Na⁺/K⁺-ATPase and ENaC subunits. The rs1358714 polymorphism in the Na⁺/K⁺-ATPase β 1-subunit gene showed significant interaction with the rs11614164 and rs3782726 polymorphisms in the ENaC α -subunit gene to particularly influence LVM and mIVST. Additionally, the rs2068230 variant in the Na⁺/K⁺-ATPase β 3-subunit gene showed highly significant evidence for interaction with one variant in the ENaC α -subunit gene (rs11614164) and two variants in the ENaC β -subunit gene (rs238547 and rs250563). It is noteworthy that both Na⁺/K⁺-ATPase β -subunit genes showed significant interaction with the same polymorphism in the ENaC α -subunit gene, i.e. rs11614164.

Both the Na⁺/K⁺-ATPase and ENaCs are important downstream effectors and regulators of intracellular Na⁺ homeostasis. It is therefore possible that this statistical interaction might reflect the true biological interaction between them due to their overlapping biological functions.

4.7 FUTURE STUDIES

As this study is the first to report association between variants in renin and RnBP and hypertrophy, we recommend that efforts should be made to elucidate the role of the renin and RnBP in the progression of hypertrophy in general and in HCM, specifically. This includes determining the functionality of the renin and RnBP variants as well as genetic association studies in other models of hypertrophy. More research is also needed to determine the functionality of significant RAAS variants identified in the present study and to further explore the gene-gene interactions observed.

The present study forms part of a larger research study of which the ultimate aim is to identify genes that modulate the development of hypertrophy in a South African HCM cohort. The effect of the 11 β -HSD2 enzyme on hypertrophy was not investigated in the present study as ABI TaqMan Validated SNP Genotyping Assays could not be found to adequately cover this gene. However, variant in this enzyme have been associated with hypertension and –associated cardiovascular effects and should therefore be investigated as a possible modifier of hypertrophy, for instance by designing and validating appropriate in-house TaqMan genotyping assays.

Previous studies have suggested an association between the Na⁺/K⁺-ATPase and the Na⁺/Ca²⁺ exchanger. As the Na⁺/Ca²⁺ exchanger has been implicated in the progression of hypertrophy (reviewed in Sipido et al., 2002), it might be possible that the Na⁺/Ca²⁺ exchanger could influence hypertrophy in HCM, and thus the Na⁺/Ca²⁺ exchanger gene, *NCX3*, would be a good candidate for further research.

4.8 CONCLUSION

The present explorative study confirmed the involvement of the AT₂ receptor in hypertrophy in HCM and demonstrates for the first time that variations in the renin and RnBP genes play a role in modulating hypertrophy in HCM, independent of BP. Additionally we report an association between Na⁺/K⁺-ATPase α 1- and β 1-subunits as well as the ENaC α - and β -subunits and hypertrophy. However, we did not find any significant evidence for association between hypertrophy and the (pro)renin receptor, MR, Na⁺/K⁺-ATPase α 2- and β 3-subunits or the ENaC γ -subunit. Significant evidence for epistasis was found between renin and downstream RAAS effectors, suggesting a complex interplay between these RAAS variants and the hypertrophic phenotype in HCM. The identification of such modifiers for HCM may offer novel targets for hypertrophy research and ultimately anti-hypertrophic therapy.

APPENDIX I
SOLUTIONS, BUFFERS, AND MARKERS

1. DNA EXTRACTION SOLUTIONS

Cell lysis buffer

Sucrose	0.32 M
Triton-X-100	1%
MgCl ₂	5 mM
Tris-HCl	10 mM
H ₂ O	1 l

3 M Sodium Acetate

Sodium Acetate (Merck (Pty) Ltd, RSA)	40.81 g
H ₂ O	50 ml

Adjust pH to 5.2 with glacial acetic acid (Merck (Pty) Ltd, RSA) and adjust volume to 100 ml with ddH₂O

Na-EDTA solution

NaCl (Merck (Pty) Ltd, RSA)	18.75 ml of 4 mM stock solution
EDTA (B & M Scientific)	250 ml of 100 mM stock solution
Mix well	

Phenol/Chloroform

Phenol (saturated with 1x TE) (Merck (Pty) Ltd, RSA)	50 ml
Chloroform (Merck (Pty) Ltd, RSA)	48 ml
8-hydroxyquinone (Merck (Pty) Ltd, RSA)	2 ml
Mix well, store at 4°C	

Chloroform/octanol (24:1)

Chloroform (Merck (Pty) Ltd, RSA) 96 ml

Octanol (Merck (Pty) Ltd, RSA) 4 ml

Mix well, store at 4°C

TE-buffer (10x stock solution)

TrisOH 0.1 M (pH 8.00)

EDTA 0.01 M (pH 8.00)

H₂O 150 ml

Mix well

2. ELECTROPHORESIS STOCK SOLUTIONS**SB Buffer (20x stock)**

Di-sodium tetraborate decahydrate 38.137g/mol

Add ddH₂O to a final volume of 1 l

Bromophenol blue

Bromophenol blue (Merck (Pty) Ltd, RSA) 0.2 % (w/v)

Glycerol 50%

Tris (pH 8.00) 10 mM

Ethidium Bromide

Ethidium Bromide 500 mg

ddH₂O 50 ml

APPENDIX II
P-VALUES FOR THE GENE-GENE INTERACTION ANALYSIS BETWEEN
THE VARIOUS SNPS AND HYPERTROPHY TRAITS

Table II.2. Results from the gene-gene interaction analysis between all the SNPs for mIVST. Significant interactions are indicated in bold red.

	ATP1A2		ATP1B1		REN		ATP1A1		ATP1B3		SCNN1A		SCNN1G		SCNN1B		AGTR2		RENBP		ATP6AP2																		
rs7548116	0.74	0.69	0.64	0.27	0.23	0.42	0.97	0.15	0.28	0.12	0.71	0.22	0.03	0.51	0.65	0.76	0.95	0.58	0.46	0.70	0.77	0.92	0.67	0.08	0.50	0.15	0.26	0.09	0.11	0.11	0.37	0.72	0.64	0.76	0.85	rs7548116	ATP1A2		
rs11585375																																					rs11585375	ATP1A2	
rs1200130	0.29	0.28	0.87	0.79	0.30	0.18	0.91	0.56	0.90	0.32	0.55	0.46	0.91	0.10	0.20	0.58	0.43	0.98	0.01	0.35	0.07	0.15	0.87	0.09	0.50	0.68	0.68	0.66	0.12	0.50	0.56	0.54	0.99	0.55	rs1200130	ATP1B1			
rs1358714																																					rs1358714	ATP1B1	
rs1040503																																					rs1040503	ATP1B1	
rs1464816																																					rs1464816	REN	
rs11571082																																					rs11571082	REN	
rs5705																																						rs5705	REN
rs10900555																																						rs10900555	REN
rs10924074																																						rs10924074	ATP1A1
rs850609																																						rs850609	ATP1A1
rs2068230																																						rs2068230	ATP1B3
rs11614164																																						rs11614164	ATP1B3
rs3782726																																						rs3782726	SCNN1A
rs7973914																																						rs7973914	SCNN1A
rs10849446																																						rs10849446	SCNN1A
rs2286600																																						rs2286600	SCNN1G
rs5735																																						rs5735	SCNN1G
rs4247210																																						rs4247210	SCNN1G
rs11074555																																						rs11074555	SCNN1B
rs9930640																																						rs9930640	SCNN1B
rs239345																																						rs239345	SCNN1B
rs238547																																						rs238547	SCNN1B
rs8044970																																						rs8044970	SCNN1B
rs152740																																						rs152740	SCNN1B
rs250563																																						rs250563	AGTR2
rs2303153																																						rs2303153	AGTR2
rs1403543																																						rs1403543	AGTR2
rs5194																																						rs5194	AGTR2
rs11091046																																						rs11091046	RENBP
rs2269370																																						rs2269370	RENBP
rs2269372																																						rs2269372	RENBP
rs762656																																						rs762656	RENBP
rs2968915																																						rs2968915	ATP6AP2
rs2968917																																						rs2968917	ATP6AP2
rs10536																																						rs10536	ATP6AP2

Table II.3. Results from the gene-gene interaction analysis between all the SNPs for mLVWT. Significant interactions are indicated in bold red.

	ATPIA2		ATPIB1		REN		ATPIA1		ATPIB3		SCNN1A		SCNN1G		SCNN1B		AGTR2		RENBP		ATP6AP2		
rs7548116																							
rs11585375	0.52																						
rs1200130	0.56	0.25																					
rs1358714	0.54	0.25	0.88																				
rs1040503	0.28	0.70	0.16	0.34																			
rs1464816	0.28	1.00	0.34	0.14	0.46																		
rs11571082	0.11	0.36	0.14	0.46	0.62	0.39	0.26	0.70	0.78	0.79	0.97	0.93	0.78	0.45	0.13	0.76	0.44	0.80	0.55	0.89	0.07	0.78	0.82
rs5705	0.47	0.14	0.46	0.62	0.39	0.26	0.70	0.78	0.79	0.97	0.93	0.78	0.45	0.13	0.76	0.44	0.80	0.55	0.89	0.07	0.78	0.82	
rs10900555	0.75	0.36	0.14	0.46	0.62	0.39	0.26	0.70	0.78	0.79	0.97	0.93	0.78	0.45	0.13	0.76	0.44	0.80	0.55	0.89	0.07	0.78	0.82
rs10924074	0.10	0.47	0.31	0.38	0.66	0.90	0.01	0.01	0.07	0.24	0.23	0.51	0.58	0.99	0.15	0.50	0.33	0.35	0.71	0.67	0.74	0.53	0.07
rs850609	0.15	0.36	0.14	0.46	0.62	0.39	0.26	0.70	0.78	0.79	0.97	0.93	0.78	0.45	0.13	0.76	0.44	0.80	0.55	0.89	0.07	0.78	0.82
rs2068230	0.28	0.96	0.21	0.43	0.32	0.78	0.09	0.17	0.43	0.47	0.83	0.03	0.36	0.06	0.12	0.88	0.07	0.46	0.44	0.31	0.32	0.09	0.21
rs11614164	0.69	0.46	0.10	0.58	0.81	0.71	0.99	0.37	0.34	0.78	0.88	0.91	0.52	0.10	0.35	0.17	0.07	0.03	0.04	0.08	0.58	0.22	0.92
rs3782726	0.10	0.32	0.78	0.09	0.17	0.43	0.47	0.83	0.03	0.36	0.06	0.12	0.88	0.07	0.46	0.44	0.31	0.32	0.09	0.21	0.30	0.35	0.87
rs7973914	0.58	0.09	0.17	0.43	0.47	0.83	0.03	0.36	0.06	0.12	0.88	0.07	0.46	0.44	0.31	0.32	0.09	0.21	0.30	0.35	0.87	0.35	0.35
rs10849446	0.81	0.09	0.17	0.43	0.47	0.83	0.03	0.36	0.06	0.12	0.88	0.07	0.46	0.44	0.31	0.32	0.09	0.21	0.30	0.35	0.87	0.35	0.35
rs2286600	0.71	0.17	0.43	0.47	0.83	0.03	0.36	0.06	0.12	0.88	0.07	0.46	0.44	0.31	0.32	0.09	0.21	0.30	0.35	0.87	0.35	0.35	0.35
rs5735	0.99	0.43	0.47	0.83	0.03	0.36	0.06	0.12	0.88	0.07	0.46	0.44	0.31	0.32	0.09	0.21	0.30	0.35	0.87	0.35	0.35	0.35	0.35
rs4247210	0.37	0.43	0.47	0.83	0.03	0.36	0.06	0.12	0.88	0.07	0.46	0.44	0.31	0.32	0.09	0.21	0.30	0.35	0.87	0.35	0.35	0.35	0.35
rs11074555	0.34	0.78	0.88	0.91	0.52	0.10	0.35	0.17	0.07	0.03	0.04	0.08	0.58	0.22	0.92	0.36	rs7548116	ATPIA2					
rs9930640	0.78	0.88	0.91	0.52	0.10	0.35	0.17	0.07	0.03	0.04	0.08	0.58	0.22	0.92	0.36	rs11585375	ATPIA2						
rs239345	0.88	0.91	0.52	0.10	0.35	0.17	0.07	0.03	0.04	0.08	0.58	0.22	0.92	0.36	rs1200130	ATPIA2							
rs238547	0.91	0.52	0.10	0.35	0.17	0.07	0.03	0.04	0.08	0.58	0.22	0.92	0.36	rs1358714	ATPIB1								
rs8044970	0.52	0.10	0.35	0.17	0.07	0.03	0.04	0.08	0.58	0.22	0.92	0.36	rs1040503	ATPIB1									
rs152740	0.10	0.35	0.17	0.07	0.03	0.04	0.08	0.58	0.22	0.92	0.36	rs1464816	REN										
rs250563	0.35	0.17	0.07	0.03	0.04	0.08	0.58	0.22	0.92	0.36	rs11571082	REN											
rs2303153	0.17	0.07	0.03	0.04	0.08	0.58	0.22	0.92	0.36	rs5705	REN												
rs1403543	0.07	0.03	0.04	0.08	0.58	0.22	0.92	0.36	rs10900555	ATPIA1													
rs5194	0.03	0.04	0.08	0.58	0.22	0.92	0.36	rs10924074	ATPIA1														
rs11091046	0.04	0.08	0.58	0.22	0.92	0.36	rs850609	ATPIA1															
rs2269370	0.08	0.58	0.22	0.92	0.36	rs2068230	ATPIB3																
rs2269372	0.58	0.22	0.92	0.36	rs11614164	ATPIB3																	
rs762656	0.83	0.22	0.92	0.36	rs3782726	SCNN1A																	
rs2968915	0.22	0.92	0.36	rs7973914	SCNN1A																		
rs2968917	0.92	0.36	rs10849446	SCNN1A																			
rs10536	0.36	rs2286600	SCNN1G																				
	0.22	0.92	0.36	rs5735	SCNN1G																		
	0.92	0.36	rs11074555	SCNN1G																			
	0.36	rs9930640	SCNN1B																				
	0.36	rs239345	SCNN1B																				
	0.36	rs238547	SCNN1B																				
	0.36	rs8044970	SCNN1B																				
	0.36	rs152740	AGTR2																				
	0.36	rs250563	AGTR2																				
	0.36	rs2303153	AGTR2																				
	0.36	rs1403543	AGTR2																				
	0.36	rs5194	AGTR2																				
	0.36	rs11091046	AGTR2																				
	0.36	rs2269370	RENBP																				
	0.36	rs2269372	RENBP																				
	0.36	rs762656	RENBP																				
	0.36	rs2968915	ATP6AP2																				
	0.36	rs2968917	ATP6AP2																				
	0.36	rs10536	ATP6AP2																				

Table II.6. Results from the gene-gene interaction analysis between all the SNPs for the CWT score. Significant interactions are indicated in bold red.

ATPIA2		ATPIB1		REN		ATPIA1		ATPIB3		SCNN1A		SCNN1G		SCNN1B		AGTR2		RENBP		ATP6AP2																	
rs7548116																																					
rs11585375	0.85	0.76	0.48	0.49	0.31	0.26	0.89	0.31	0.07	0.36	0.92	0.23	0.05	0.90	0.81	0.94	0.89	0.37	0.15	0.91	0.85	0.99	0.54	0.28	0.44	0.02	0.17	0.10	0.13	0.13	0.25	0.34	0.50	0.97	0.84	rs7548116	ATPIA2
rs1200130	0.26	0.63	0.95	0.97	0.73	0.38	0.46	1.00	0.52	1.00	0.29	0.36	0.82	0.09	0.14	0.88	0.50	0.82	0.07	0.29	0.11	0.20	0.77	0.19	0.95	0.80	0.32	0.34	0.14	0.33	0.49	0.85	0.97	0.84	rs11585375	ATPIA2	
rs1358714	0.46	0.43	0.87	0.26	0.65	0.87	0.90	0.22	0.61	0.81	0.62	0.85	0.75	0.49	0.45	0.21	0.47	0.83	0.57	0.54	0.87	0.09	0.45	0.52	0.65	0.29	0.38	0.22	0.79	0.74	0.49	0.93	0.58	rs1200130	ATPIB1		
rs1040503	0.33	0.27	0.39	0.32	0.64	0.32	0.82	0.64	0.02	0.03	0.12	0.40	0.43	0.69	0.99	0.73	0.27	0.72	0.03	0.35	0.82	0.53	0.89	0.33	0.01	0.02	0.63	0.45	0.26	0.40	0.93	0.89	rs1358714	ATPIB1			
rs1464816	0.00	0.00	0.00	0.07	0.38	0.77	0.15	0.32	0.21	0.19	0.57	0.30	0.83	0.99	0.87	0.58	0.20	0.39	0.86	0.96	0.82	0.58	0.81	0.46	0.57	0.80	0.35	0.80	0.96	0.72	0.81	rs1040503	REN				
rs11571082	0.64	0.65	0.26	0.63	0.74	0.79	0.18	0.23	0.55	0.60	0.37	0.25	0.39	0.48	0.36	0.37	0.66	0.50	0.85	0.64	0.89	0.46	0.44	0.52	0.04	0.04	0.09	0.14	0.75	0.45	0.66	rs1464816	REN				
rs5705	0.40	0.52	0.88	0.10	0.14	0.92	0.87	0.90	0.87	0.65	0.16	0.50	0.07	0.02	0.98	0.79	0.88	0.26	0.86	0.96	0.99	0.48	0.54	0.65	0.03	0.19	0.06	0.63	0.46	0.63	0.46	rs11571082	REN				
rs10900555	0.31	0.71	0.68	0.14	0.82	0.82	0.84	0.69	0.71	0.76	0.36	0.09	0.15	0.62	0.65	0.30	0.41	0.67	0.56	0.93	0.54	0.61	0.57	0.08	0.33	0.23	0.59	0.88	0.97	rs5705	REN						
rs10924074	0.75	0.41	0.03	0.77	0.82	0.42	0.85	0.54	0.70	0.66	0.72	0.73	0.31	0.03	0.07	0.08	0.68	0.04	0.64	0.66	0.57	0.50	0.49	0.88	0.92	0.88	0.97	rs10900555	ATPIA1								
rs850609	0.82	0.90	0.71	0.60	0.56	0.64	0.50	0.97	0.62	0.73	0.32	0.56	0.18	0.99	0.31	0.42	0.19	0.16	0.51	0.48	0.03	0.08	0.19	0.46	0.95	0.06	0.95	0.06	0.95	0.06	rs10924074	ATPIA1					
rs2068230	0.63	0.54	0.69	0.19	0.61	0.65	0.40	0.69	0.14	0.97	0.10	0.06	0.53	0.99	0.28	0.43	0.65	0.92	0.98	0.65	0.68	0.93	0.29	0.41	0.86	rs850609	ATPIA1										
rs11614164	0.06	0.29	0.66	0.11	0.21	0.51	0.74	0.04	0.45	0.06	0.00	0.20	0.11	0.01	0.36	0.47	0.22	0.36	0.74	0.01	0.06	0.45	0.76	0.82	rs2068230	ATPIB3											
rs3782726	0.13	0.60	0.67	0.33	0.45	0.67	0.91	0.79	0.30	0.02	0.69	0.29	0.85	0.00	0.80	0.17	0.16	0.42	0.38	0.16	0.70	0.83	0.88	0.88	rs11614164	SCNN1A											
rs7973914	0.36	0.64	0.45	0.48	0.76	0.55	0.97	0.60	0.02	0.93	0.34	0.97	0.00	0.77	0.17	0.27	0.45	0.22	0.86	0.98	0.60	0.98	0.60	rs3782726	SCNN1A												
rs10849446	0.98	0.94	0.49	0.16	0.69	0.67	0.45	0.03	0.79	0.25	0.38	0.38	0.93	0.23	0.30	0.48	0.04	0.01	0.10	0.70	0.75	rs7973914	SCNN1A														
rs2286600	0.17	0.68	0.57	0.97	0.06	0.86	0.25	0.46	0.41	0.06	0.63	0.18	0.71	0.75	0.59	0.93	0.61	0.81	0.55	0.20	0.81	0.55	0.20	rs10849446	SCNN1A												
rs5735	0.44	0.44	0.79	0.05	0.84	0.06	0.16	0.39	0.17	0.83	0.26	0.80	0.84	0.63	0.38	0.73	0.80	0.95	0.30	0.65	0.43	0.65	rs5735	SCNN1G													
rs4247210	0.29	0.52	0.25	0.79	0.12	0.59	0.42	0.05	0.02	0.04	0.04	0.05	0.10	0.47	0.56	0.53	0.43	0.65	0.70	0.02	rs4247210	SCNN1G															
rs11074555	0.65	0.55	0.56	0.85	0.64	0.50	0.21	0.70	0.87	0.55	0.50	0.68	0.22	0.57	0.45	0.41	0.50	0.68	0.22	0.57	0.45	0.41	0.50	rs11074555	SCNN1G												
rs9930640	0.23	0.53	0.23	0.56	0.76	0.42	0.60	0.27	0.59	0.56	0.82	0.89	0.77	0.65	0.70	0.02	rs9930640	SCNN1G																			
rs239345	0.82	0.57	0.71	0.68	0.60	0.17	0.44	0.94	0.91	0.29	0.43	0.45	0.99	0.43	0.11	rs239345	SCNN1G																				
rs238547	0.12	0.87	0.88	0.76	0.58	0.11	0.15	0.14	0.15	0.44	0.45	0.49	0.29	0.75	rs238547	SCNN1B																					
rs8044970	0.30	0.22	0.07	0.42	0.95	0.56	0.53	0.62	0.46	0.21	0.63	0.94	0.72	0.63	0.94	0.72	rs8044970	SCNN1B																			
rs152740	0.47	0.06	0.92	0.89	0.71	0.65	0.66	0.87	0.81	0.51	0.86	0.95	rs152740	SCNN1B																							
rs250563	0.02	0.21	0.61	0.37	0.39	0.62	0.47	0.43	0.25	0.57	0.06	rs250563	SCNN1B																								
rs2303153	0.64	0.66	0.08	0.09	0.31	0.86	0.78	0.04	0.01	0.47	rs2303153	SCNN1B																									
rs1403543	0.21	0.72	0.78	0.28	0.72	0.46	0.67	0.68	0.43	rs1403543	AGTR2																										
rs5194	0.85	0.80	0.25	0.38	0.24	0.55	0.71	0.20	0.38	0.24	0.55	0.71	0.20	0.38	0.24	0.55	0.71	0.20	0.38	0.24	0.55	0.71	rs5194	AGTR2													
rs11091046	0.35	0.20	0.10	0.09	0.46	0.61	0.97	rs11091046	AGTR2																												
rs2269370	0.23	0.10	0.09	0.52	0.55	0.98	rs2269370	AGTR2																													
rs2269372	0.84	0.83	0.67	0.25	0.81	rs2269372	RENBP																														
rs762656	0.92	0.11	0.04	0.62	rs762656	RENBP																															
rs2968915	0.19	0.07	0.89	rs2968915	ATP6AP2																																
rs2968917	0.72	0.46	rs2968917	ATP6AP2																																	
rs10536	0.09	rs10536	ATP6AP2																																		

Table II.7. Results from the gene-gene interaction analysis between all the SNPs for the mLVWTmit. Significant interactions are indicated in bold red.

rs7548116	rs11585375	rs1200130	rs1358714	rs1040503	rs1464816	rs11571082	rs5705	rs10900555	rs10924074	rs850609	rs2068230	rs11614164	rs3782726	rs7973914	rs10849446	rs2286600	rs5735	rs4247210	rs11074555	rs9930640	rs239345	rs238547	rs8044970	rs152740	rs250563	rs2303153	rs1403543	rs5194	rs11091046	rs2269370	rs2269372	rs762656	rs2968915	rs2968917	rs10536		
	0.28	0.71	0.81	0.29	0.15	0.69	1.00	0.09	0.08	0.70	0.73	0.21	0.05	0.80	0.97	0.96	0.91	0.36	0.63	0.89	0.74	0.73	0.38	0.31	0.22	0.09	0.07	0.03	0.04	0.03	0.47	0.69	0.39	0.83	0.80	rs7548116	ATP1A2
		0.53	0.38	0.84	0.78	0.42	0.11	0.34	0.78	0.57	0.30	0.63	0.76	0.88	0.16	0.24	0.53	0.74	0.74	0.08	0.60	0.05	0.16	0.56	0.31	0.55	0.45	0.43	0.40	0.16	0.59	0.84	0.38	0.90	0.47	rs11585375	ATP1A2
			0.56	0.09	0.46	0.19	0.46	0.75	0.63	0.31	0.93	0.75	0.97	0.97	0.98	0.82	0.22	0.21	0.87	0.34	0.78	0.41	0.68	0.05	0.95	0.48	0.59	0.15	0.15	0.16	0.90	0.81	0.27	0.41	0.82	rs1200130	ATP1B1
				0.42	0.41	0.33	0.23	0.41	0.66	0.92	0.91	0.01	0.01	0.28	0.33	0.25	0.50	0.48	0.74	0.11	0.31	0.11	0.15	0.98	0.79	0.89	0.40	0.05	0.09	0.79	0.78	0.94	0.32	0.75	0.77	rs1358714	ATP1B1
					0.00	0.04	0.00	0.03	0.44	0.62	0.14	0.90	0.72	0.65	0.53	0.35	0.86	0.74	0.80	0.72	0.23	0.36	0.97	0.85	0.56	0.39	0.57	1.00	0.98	0.62	0.71	0.85	0.97	0.80	0.33	rs1040503	ATP1B1
						0.74	0.68	0.57	0.48	0.64	0.69	0.12	0.21	0.34	0.70	0.99	0.35	0.32	0.87	0.92	0.92	0.43	0.68	0.40	0.54	0.48	0.60	0.68	0.03	0.22	0.24	0.43	0.30	0.73	rs1464816	REN	
							0.29	1.00	0.55	0.17	0.21	0.80	0.51	0.97	0.99	0.48	0.26	0.49	0.13	0.21	0.87	0.93	0.74	0.16	0.81	0.75	0.75	0.72	0.78	0.84	0.03	0.27	0.27	0.71	0.73	rs11571082	REN
								0.60	0.48	0.92	0.14	0.76	0.88	0.75	0.60	0.97	0.73	0.59	0.14	0.32	0.48	0.56	0.35	0.24	0.60	0.88	0.96	0.48	0.47	0.84	0.33	0.82	0.48	0.98	0.80	rs5705	REN
									0.63	0.70	0.06	0.31	0.54	0.39	0.99	0.75	0.64	0.38	0.58	0.97	0.11	0.05	0.25	0.62	0.43	0.01	0.65	0.47	0.43	0.62	0.88	0.52	0.94	0.95	0.70	rs10900555	REN
										0.76	0.88	0.88	0.36	0.80	0.73	0.27	0.74	0.27	0.70	0.93	0.41	0.61	0.81	0.41	0.76	0.34	0.02	0.42	0.40	0.35	0.02	0.03	0.44	0.49	0.04	rs10924074	ATP1A1
											0.81	0.88	0.99	0.10	0.57	0.64	0.64	0.55	0.59	0.86	0.23	0.04	0.52	0.62	0.11	0.56	0.83	0.88	0.92	0.23	0.37	0.59	0.79	0.92	0.51	rs850609	ATP1A1
												0.03	0.11	0.34	0.20	0.28	0.38	0.66	0.07	0.57	0.05	0.00	0.35	0.51	0.05	0.07	0.35	0.44	0.60	0.93	0.09	0.36	0.21	0.45	0.83	rs2068230	ATP1B3
													0.08	0.24	0.61	0.88	0.70	0.31	0.80	0.32	0.18	0.26	0.63	0.93	0.78	0.02	0.82	0.39	0.42	0.83	0.96	0.79	0.70	0.38	0.71	rs11614164	ATP1A1
														0.11	0.41	0.66	0.79	0.44	0.58	0.40	0.56	0.08	0.94	0.89	0.35	0.08	0.76	0.20	0.21	0.56	0.76	0.53	0.25	0.17	0.58	rs3782726	SCNN1A
															0.97	0.83	0.46	0.17	0.99	0.95	0.33	0.17	0.75	0.40	0.64	0.93	0.74	0.50	0.46	0.43	0.27	0.14	0.03	0.58	0.46	rs7973914	SCNN1A
																0.51	0.19	0.64	0.31	0.19	0.24	0.06	0.59	0.46	0.02	0.49	0.01	0.12	0.12	0.41	0.50	0.95	0.50	0.28	0.15	rs10849446	SCNN1A
																	0.09	0.46	0.33	0.06	0.22	0.01	0.48	0.54	0.06	0.31	0.04	0.16	0.15	0.68	0.15	0.42	0.67	0.76	0.51	rs2286600	SCNN1G
																		0.49	0.54	0.43	0.27	0.56	0.87	0.32	0.12	0.40	0.14	0.34	0.32	0.11	0.23	0.30	0.89	0.73	0.16	rs5735	SCNN1G
																			0.27	0.12	0.88	0.47	0.72	0.25	0.49	0.57	0.32	0.20	0.18	0.64	0.03	0.09	0.26	0.79	0.45	rs4247210	SCNN1G
																				0.94	0.26	0.63	0.57	0.51	0.75	0.68	0.08	0.42	0.38	0.48	0.58	0.95	0.46	0.31	0.05	rs11074555	SCNN1G
																					0.64	0.61	0.55	0.52	0.77	0.50	0.30	0.13	0.14	0.44	0.36	0.50	0.34	0.48	0.56	rs9930640	SCNN1B
																																				rs239345	SCNN1B
																																				rs238547	SCNN1B
																																				rs8044970	SCNN1B
																																				rs152740	SCNN1B
																																				rs250563	SCNN1B
																																				rs2303153	SCNN1B
																																				rs1403543	AGTR2
																																				rs5194	AGTR2
																																				rs11091046	AGTR2
																																				rs2269370	RENBP
																																				rs2269372	RENBP
																																				rs762656	RENBP
																																				rs2968915	ATP6AP2
																																				rs2968917	ATP6AP2
																																				rs10536	ATP6AP2

Table II.9. Results from the gene-gene interaction analysis between all the SNPs for the pIVSmit. Significant interactions are indicated in bold red.

	ATP1A2		ATP1B1		REN		ATP1A1		ATP1B3		SCNN1A		SCNN1G		SCNN1B		AGTR2		RENBP		ATP6AP2																	
rs7548116	0.80	0.51	0.93	0.63	0.23	0.20	0.88	0.28	0.11	0.49	0.77	0.54	0.27	0.58	0.68	0.90	0.47	0.27	0.19	0.98	0.70	0.83	0.33	0.15	0.24	0.04	0.55	0.21	0.27	0.05	0.50	0.84	0.80	0.46	0.96	rs7548116	ATP1A2	
rs11585375		0.93	0.32	0.87	0.67	0.33	0.08	0.64	0.98	0.43	0.33	0.79	0.69	0.88	0.04	0.07	0.56	0.30	0.97	0.23	0.68	0.11	0.20	0.47	0.75	0.84	0.68	0.77	0.75	0.04	0.61	0.70	0.95	0.60	0.76	rs11585375	ATP1A2	
rs1200130			0.40	0.26	0.57	0.19	0.57	0.75	0.83	0.35	0.76	0.88	0.70	0.88	0.79	0.83	0.44	0.23	0.87	0.34	0.63	0.49	0.50	0.13	0.90	0.22	0.69	0.08	0.10	0.19	0.84	0.88	0.78	1.00	0.76	rs1200130	ATP1B1	
rs1358714				0.18	0.56	0.16	0.07	0.36	0.95	0.89	0.88	0.00	0.00	0.12	0.44	0.71	1.00	0.75	0.73	0.17	0.25	0.14	0.15	0.97	0.80	0.52	0.77	0.14	0.24	0.68	0.83	0.99	0.21	0.42	0.63	rs1358714	ATP1B1	
rs1040503					0.18	0.56	0.16	0.07	0.36	0.95	0.89	0.88	0.00	0.00	0.12	0.44	0.71	1.00	0.75	0.73	0.17	0.25	0.14	0.15	0.97	0.80	0.52	0.77	0.14	0.24	0.68	0.83	0.99	0.21	0.42	0.63	rs1040503	ATP1B1
rs1464816					0.00	0.01	0.00	0.01	0.91	0.91	0.16	0.40	0.30	0.61	0.68	0.32	0.56	0.92	0.40	0.97	0.09	0.68	0.91	0.90	0.50	0.71	0.76	0.29	0.33	0.32	0.81	0.50	0.98	0.91	0.41	rs1464816	REN	
rs11571082					0.00	0.01	0.00	0.01	0.91	0.91	0.16	0.40	0.30	0.61	0.68	0.32	0.56	0.92	0.40	0.97	0.09	0.68	0.91	0.90	0.50	0.71	0.76	0.29	0.33	0.32	0.81	0.50	0.98	0.91	0.41	rs11571082	REN	
rs5705						0.14	0.18	0.35	0.13	0.62	0.89	0.18	0.19	0.33	0.98	0.80	0.11	0.37	0.70	0.99	0.93	0.99	0.30	0.14	0.49	0.62	0.53	0.56	0.63	0.01	0.39	0.31	0.48	0.54	0.48	rs1464816	REN	
rs10900555						0.48	0.34	0.98	0.05	0.30	0.74	0.85	0.98	0.62	0.78	0.67	0.83	0.22	0.46	0.56	0.98	0.85	0.25	0.94	0.79	0.43	0.41	0.49	0.66	0.14	0.74	0.07	0.47	0.73	rs11571082	REN		
rs10924074							0.13	0.73	0.71	0.27	0.87	0.91	0.81	0.28	0.46	0.81	0.58	0.38	0.77	0.74	0.57	0.89	0.43	0.61	0.78	0.91	0.21	0.24	0.75	0.82	0.51	0.16	0.58	0.59	rs5705	REN		
rs850609								0.20	0.19	0.01	0.35	0.30	0.35	0.99	0.77	0.06	0.83	0.43	0.60	0.65	0.21	0.04	0.37	0.89	0.14	0.80	0.84	0.96	0.46	0.61	0.29	0.69	0.72	0.29	rs10900555	ATP1A1		
rs2068230									0.58	0.73	0.73	0.62	0.18	0.87	0.07	0.77	0.95	0.76	0.75	0.24	0.22	0.48	0.17	0.97	0.78	0.05	0.98	0.94	0.17	0.03	0.02	0.16	0.37	0.09	rs10924074	ATP1A1		
rs11614164										0.77	0.63	1.00	0.08	0.45	0.52	0.42	0.93	0.31	0.86	0.24	0.45	0.95	0.76	0.29	0.69	0.63	0.85	0.78	0.56	0.45	0.60	0.79	0.54	0.93	rs850609	ATP1A1		
rs3782726										0.01	0.03	0.27	0.06	0.08	0.26	0.85	0.12	0.49	0.05	0.01	0.54	0.20	0.01	0.71	0.69	0.19	0.33	0.89	0.16	0.46	0.70	0.83	0.63	rs2068230	ATP1B3			
rs7973914											0.18	0.23	0.72	0.62	0.94	0.34	0.71	0.69	0.14	0.24	0.96	0.80	0.94	0.02	0.80	0.68	0.70	0.89	0.91	0.63	0.42	0.19	0.95	rs11614164	ATP1B3			
rs10849446											0.26	0.81	0.72	0.90	0.55	0.80	0.81	0.48	0.11	0.63	0.69	0.41	0.06	0.94	0.66	0.66	0.80	0.80	0.57	0.18	0.11	0.85	rs3782726	SCNN1A				
rs2286600												0.24	0.41	0.60	0.21	0.38	0.52	0.07	0.68	0.83	0.47	0.22	0.96	0.60	0.10	0.13	0.74	0.31	0.17	0.20	0.70	0.42	rs7973914	SCNN1A				
rs5735													0.32	0.22	0.76	0.84	0.20	0.85	0.45	0.52	0.57	0.02	0.86	0.16	0.41	0.42	0.62	0.62	0.85	0.41	0.28	0.15	rs10849446	SCNN1A				
rs4247210														0.05	0.39	0.83	0.09	0.70	0.12	0.33	0.51	0.13	0.52	0.24	0.26	0.25	0.70	0.27	0.55	0.72	0.61	0.61	rs2286600	SCNN1G				
rs11074555															0.24	0.64	0.38	0.67	0.52	0.72	0.60	0.11	0.26	0.09	0.32	0.33	0.39	0.13	0.11	0.70	0.40	0.45	rs5735	SCNN1G				
rs9930640																0.23	0.12	0.57	0.75	0.68	0.44	0.15	0.80	0.94	0.78	0.69	0.80	0.15	0.30	0.42	0.77	0.48	rs4247210	SCNN1G				
rs239345																	0.82	0.23	0.15	0.17	0.53	0.17	0.19	0.19	0.36	0.33	0.69	0.45	0.52	0.50	0.47	0.11	rs11074555	SCNN1B				
rs238547																		0.57	0.03	0.99	0.39	0.22	0.07	0.96	0.27	0.30	0.27	0.37	0.56	0.86	0.86	0.89	rs9930640	SCNN1B				
rs8044970																				0.10	0.39	0.38	0.50	0.57	0.06	0.04	0.05	0.07	0.56	0.37	0.25	0.36	0.56	rs239345	SCNN1B			
rs152740																					0.06	0.89	0.11	0.85	0.50	1.00	0.99	0.65	0.13	0.10	0.49	0.71	0.13	rs238547	SCNN1B			
rs250563																						0.24	0.15	0.96	0.65	0.55	0.53	0.89	0.33	0.35	0.25	0.73	0.66	rs8044970	SCNN1B			
rs2303153																							0.08	0.89	0.94	0.55	0.62	0.61	0.30	0.40	0.38	0.96	0.41	rs152740	SCNN1B			
rs1403543																								0.64	0.96	0.61	0.67	0.24	0.93	0.86	0.03	0.09	0.83	rs250563	SCNN1B			
AGTR2																									0.42	0.55	0.57	0.49	0.24	0.22	0.29	0.10	0.07	rs2303153	AGTR2			
RENBP																											0.51	0.56	0.20	0.31	0.14	0.33	0.70	0.73	rs1403543	AGTR2		
ATP6AP2																												0.78	0.11	0.24	0.17	0.14	0.44	0.30	rs5194	AGTR2		
																													0.12	0.26	0.18	0.15	0.48	0.35	rs11091046	AGTR2		
																														0.67	0.96	0.76	0.28	0.80	rs2269370	RENBP		
																															0.56	0.13	0.18	0.85	rs2269372	RENBP		
																																0.13	0.14	0.81	rs762656	RENBP		
																																0.99	0.07	rs2968915	ATP6AP2			
																																0.02	rs2968917	ATP6AP2				
																																		rs10536	ATP6AP2			

Table II.10. Results from the gene-gene interaction analysis between all the SNPs for the aIVSmit. Significant interactions are indicated in bold red.

rs7548116	rs1158537	rs1200130	rs1358714	rs1040503	rs1464816	rs1157108	rs5705	rs1090055	rs1092407	rs850609	rs2068230	rs1161416	rs3782726	rs7973914	rs1084944	rs2286600	rs5735	rs4247210	rs1107455	rs9930640	rs239345	rs238547	rs8044970	rs152740	rs250563	rs2303153	rs1403543	rs5194	rs1109104	rs2269370	rs2269372	rs762656	rs2968915	rs2968917	rs10536		
	1.00	0.86	0.85	0.80	0.48	0.98	0.65	0.44	0.67	0.86	0.32	0.03	0.01	0.94	0.70	0.76	0.60	0.67	0.30	0.91	0.90	0.74	0.21	0.26	0.49	0.12	0.20	0.08	0.10	0.01	0.56	0.84	0.61	0.72	0.33	rs7548116	
		0.23	0.54	0.77	0.80	0.85	0.36	0.91	0.65	0.75	0.32	0.37	0.77	0.97	0.38	0.86	0.38	0.74	0.54	0.09	0.29	0.06	0.36	0.70	0.14	0.38	0.52	0.53	0.49	0.19	0.96	0.63	0.46	0.74	0.49	rs11585375	ATP1A2
			0.70	0.05	0.33	0.62	0.97	0.47	0.37	0.27	0.82	0.54	0.49	0.89	0.90	0.86	0.06	0.24	0.76	0.45	0.83	0.35	0.84	0.13	0.35	0.77	0.27	0.12	0.13	0.11	0.48	0.53	0.34	0.75	0.48	rs1200130	
				0.59	0.52	0.25	0.12	0.65	0.23	0.88	0.85	0.00	0.00	0.22	0.29	0.24	0.53	0.74	0.59	0.17	0.78	0.05	0.15	0.64	0.91	0.63	0.16	0.02	0.03	0.57	0.68	0.57	0.32	0.88	0.95	rs1358714	ATP1B1
					0.00	0.11	0.00	0.03	0.17	0.99	0.25	0.71	0.53	0.64	0.54	0.23	0.86	0.70	0.59	0.42	0.67	0.28	0.92	0.54	0.90	0.60	0.20	0.90	0.89	0.72	0.60	0.43	0.88	0.99	0.57	rs1040503	
						0.95	0.93	0.86	0.63	0.34	0.47	0.08	0.14	0.60	0.80	0.99	0.72	0.39	0.54	0.81	0.40	0.67	0.74	0.40	0.39	0.32	0.57	0.88	0.84	0.05	0.11	0.09	0.51	0.27	0.77	rs1464816	
							0.25	0.84	0.57	0.30	0.24	0.72	0.50	0.79	0.98	0.26	0.15	0.38	0.12	0.20	0.82	0.70	0.98	0.21	0.37	0.96	0.70	0.62	0.67	0.49	0.05	0.24	0.44	0.83	0.40	rs11571082	REN
								0.96	0.62	0.92	0.17	0.98	0.82	0.70	0.50	0.67	0.50	0.22	0.16	0.32	0.80	0.96	0.69	0.14	0.30	0.73	0.78	0.72	0.70	0.56	0.24	0.57	0.99	0.64	0.89	rs5705	
									0.92	0.50	0.09	0.50	0.89	0.49	0.76	0.63	0.98	0.23	0.66	0.54	0.34	0.12	0.50	0.77	0.39	0.00	0.80	0.29	0.27	0.85	0.97	0.70	0.79	0.80	0.87	rs10900555	
										0.54	0.89	0.57	0.21	0.70	0.92	0.59	0.39	0.16	0.53	0.81	0.43	0.99	0.64	0.22	0.92	0.62	0.05	0.31	0.30	0.52	0.06	0.05	0.49	0.51	0.05	rs10924074	ATP1A1
											0.89	0.90	0.74	0.34	0.55	0.53	0.86	0.69	0.95	0.89	0.53	0.03	0.43	0.35	0.31	0.94	0.62	0.68	0.71	0.23	0.69	0.98	0.69	0.75	0.86	rs850609	ATP1A1
												0.04	0.07	0.60	0.18	0.26	0.76	0.70	0.10	0.41	0.06	0.00	0.55	0.30	0.06	0.10	0.62	0.53	0.70	1.00	0.25	0.49	0.11	0.30	0.67	rs2068230	ATP1B3
													0.10	0.42	0.81	0.90	0.37	0.59	0.93	0.18	0.52	0.21	0.80	0.38	0.45	0.01	0.93	0.54	0.56	0.42	0.87	0.85	0.29	0.20	0.68	rs11614164	
														0.24	0.66	0.79	0.40	0.41	0.61	0.30	0.59	0.15	0.91	0.64	0.53	0.03	0.49	0.13	0.14	0.20	0.68	0.54	0.25	0.21	0.47	rs3782726	
															0.36	0.45	0.70	0.27	0.61	0.88	0.47	0.25	0.83	0.82	0.63	0.92	0.90	0.98	0.90	0.34	0.29	0.29	0.17	0.81	0.39	rs7973914	SCNN1A
																0.25	0.29	0.55	0.46	0.14	0.29	0.07	0.58	0.49	0.04	0.77	0.05	0.15	0.15	0.13	0.20	0.66	0.26	0.24	0.09	rs10849446	
																	0.21	0.40	0.26	0.08	0.23	0.01	0.64	0.60	0.03	0.69	0.19	0.39	0.37	0.31	0.13	0.42	0.49	0.69	0.27	rs2286600	
																		0.83	0.52	0.34	0.44	0.66	0.80	0.52	0.06	0.42	0.10	0.11	0.10	0.09	0.31	0.24	0.17	0.13	0.23	rs5735	SCNN1G
																			0.42	0.17	0.92	0.44	0.89	0.21	0.27	0.59	0.29	0.31	0.28	0.94	0.11	0.33	0.23	0.93	0.49	rs4247210	
																				0.76	0.31	0.56	0.79	0.66	0.93	0.76	0.11	0.41	0.38	0.69	0.64	0.93	0.32	0.23	0.03	rs11074555	
																					0.72	0.53	0.87	0.66	0.79	0.39	0.33	0.10	0.10	0.07	0.43	0.52	0.30	0.26	0.54	rs9930640	
																						0.46	0.77	0.72	0.65	0.55	0.01	0.03	0.04	0.10	0.13	0.11	0.57	0.38	0.78	rs239345	
																						0.05	0.31	0.18	0.55	0.40	0.94	0.91	0.89	0.34	0.25	0.15	0.36	0.90	rs238547	SCNN1B	
																							0.28	0.19	0.54	0.56	0.96	0.94	0.66	0.55	0.77	0.09	0.36	0.90	rs8044970		
																									0.14	0.64	0.96	0.66	0.71	0.52	0.27	0.35	0.10	0.42	0.07	rs152740	
																									0.74	0.95	0.27	0.37	0.15	0.97	0.92	0.04	0.01	0.61	rs250563		
																									0.72	0.68	0.67	0.17	0.18	0.19	0.66	0.32	0.42	0.42	0.81	rs2303153	
																										0.48	0.46	0.13	0.16	0.07	0.72	0.56	0.81	rs1403543			
																											0.13	0.18	0.05	0.02	0.34	0.95	0.41	rs5194	AGTR2		
																													0.18	0.05	0.02	0.34	0.96	0.43	rs11091046		
																														0.71	0.56	0.87	0.46	0.63	rs2269370		
																															0.29	0.59	0.26	0.26	rs2269372	RENBP	
																															0.62	0.25	rs762656				
																																0.71	0.10	rs2968915			
																																	0.02	rs2968917	ATP6AP2		
																																			rs10536		

Table II.16. Results from the gene-gene interaction analysis between all the SNPs for the mIVSTpap. Significant interactions are indicated in bold red.

rs7548116	rs11585375	rs1200130	rs1358714	rs1040503	rs1464816	rs11571082	rs5705	rs10900555	rs10924074	rs850609	rs2068230	rs11614164	rs3782726	rs7973914	rs10849446	rs2286600	rs5735	rs4247210	rs11074555	rs9930640	rs239345	rs238547	rs8044970	rs152740	rs250563	rs2303153	rs1403543	rs5194	rs11091046	rs2269370	rs2269372	rs762656	rs2968915	rs2968917	rs10536		
	0.93	0.38	0.59	0.71	0.40	0.50	0.63	0.51	0.11	0.29	0.70	0.51	0.14	0.43	0.54	0.73	0.73	0.42	0.50	0.96	0.68	0.83	0.99	0.21	0.82	0.12	0.12	0.03	0.04	0.08	0.69	0.79	0.31	0.53	0.72	rs7548116	ATP1A2
		0.45	0.26	0.71	0.72	0.72	0.30	0.91	0.89	0.96	0.40	0.55	0.39	0.56	0.08	0.30	0.59	0.60	0.87	0.04	0.80	0.04	0.13	0.50	0.10	0.46	0.31	0.31	0.29	0.12	0.40	0.56	0.88	0.78	0.86	rs11585375	ATP1A2
			0.94	0.16	0.38	0.28	0.61	0.56	0.67	0.25	0.72	0.67	0.92	0.99	0.44	0.34	0.66	0.05	0.71	0.85	0.47	0.69	0.90	0.40	0.62	0.53	0.69	0.16	0.18	0.31	0.89	0.64	0.55	0.79	0.87	rs1200130	ATP1B1
			0.78	0.19	0.98	0.85	0.57	0.47	0.85	0.72	0.03	0.04	0.10	0.41	0.43	0.69	0.77	0.97	0.16	0.48	0.33	0.49	0.90	0.45	0.62	0.94	0.10	0.18	0.82	0.62	0.80	0.22	0.82	0.97	rs1358714	ATP1B1	
				0.00	0.03	0.00	0.01	0.49	0.59	0.08	0.46	0.22	0.56	0.95	0.50	0.75	0.44	0.79	0.49	0.14	0.74	0.44	0.22	0.98	0.62	0.25	0.83	0.89	0.85	0.71	0.35	0.76	0.95	0.88	rs1040503	ATP1B1	
				0.86	0.72	0.89	0.74	0.19	0.48	0.05	0.15	0.52	0.92	0.58	0.64	0.79	0.94	0.29	0.66	0.30	0.23	0.63	0.68	0.37	0.40	0.44	0.50	0.01	0.22	0.20	0.58	0.35	0.87	rs1464816	ATP1B1		
					0.17	0.62	0.69	0.16	0.15	0.37	0.97	0.42	0.97	0.31	0.41	0.84	0.03	0.03	0.65	0.78	0.65	0.39	0.87	0.94	0.88	0.38	0.46	0.69	0.17	0.64	0.14	0.74	0.84	rs11571082	REN		
						0.83	0.87	0.86	0.26	0.30	0.81	0.42	0.53	0.63	0.90	0.85	0.10	0.15	0.96	0.51	0.21	0.43	0.42	0.82	0.69	0.38	0.41	0.85	0.74	0.71	0.41	0.91	0.72	rs5705	REN		
							0.14	0.27	0.02	0.18	0.72	0.49	0.89	0.49	0.45	0.80	0.54	0.67	0.32	0.05	0.26	0.51	0.68	0.00	0.72	0.88	0.77	0.23	0.73	0.84	0.76	0.71	0.21	0.21	rs10900555	REN	
								0.90	0.39	0.90	0.33	0.89	0.73	0.21	0.97	0.98	0.74	0.55	0.10	0.54	0.79	0.40	0.83	0.71	0.46	0.48	0.45	0.04	0.34	0.45	0.99	0.45	0.36	rs10924074	ATP1A1		
									0.94	0.65	0.72	0.09	0.95	0.80	0.62	0.74	0.58	0.70	0.29	0.04	0.34	0.43	0.30	0.24	0.78	0.76	0.84	0.38	0.57	0.95	0.33	0.33	0.91	rs850609	ATP1A1		
											0.01	0.03	0.22	0.17	0.25	0.99	0.85	0.08	0.70	0.13	0.03	0.57	0.74	0.01	0.24	0.96	0.51	0.75	0.72	0.17	0.25	0.20	0.30	0.64	rs2068230	ATP1B3	
												0.10	0.45	0.38	0.33	0.59	0.81	0.44	0.94	0.93	0.06	0.77	0.85	0.63	0.01	0.85	0.54	0.55	0.62	0.34	0.20	0.59	0.47	0.97	rs11614164	ATP1B3	
													0.11	0.35	0.28	0.48	0.97	0.21	0.88	0.66	0.02	0.81	0.69	0.95	0.01	0.79	0.60	0.61	0.49	0.49	0.35	0.25	0.18	0.65	rs3782726	SCNN1A	
													0.72	0.75	0.54	0.04	0.32	0.72	0.40	0.22	0.56	0.36	0.49	0.98	0.99	0.38	0.42	0.26	0.23	0.18	0.24	0.72	0.31	rs7973914	SCNN1A		
														0.06	0.56	0.25	0.39	0.05	0.30	0.19	0.86	0.89	0.05	0.73	0.42	0.69	0.69	0.90	0.27	0.58	0.97	0.75	0.21	rs10849446	SCNN1A		
															0.26	0.16	0.39	0.04	0.46	0.04	0.33	0.73	0.17	0.70	0.60	0.62	0.60	0.92	0.06	0.16	0.49	0.60	0.77	rs2286600	SCNN1A		
																0.33	0.63	0.18	0.55	0.27	0.82	0.14	0.11	0.11	0.21	0.19	0.19	0.07	0.06	0.09	0.25	0.14	0.36	rs5735	SCNN1G		
																			0.53	0.27	0.66	0.69	0.68	0.54	0.33	0.72	0.86	0.95	0.85	0.79	0.02	0.08	0.09	0.77	0.59	rs4247210	SCNN1G
																				0.71	0.22	0.94	0.57	0.51	0.16	0.65	0.98	0.86	0.93	0.84	0.82	0.44	0.79	0.67	0.06	rs11074555	SCNN1G
																					0.46	0.10	0.80	0.47	0.44	0.26	0.20	0.89	0.94	0.24	0.07	0.07	0.26	0.93	0.49	rs9930640	SCNN1G
																						0.68	0.93	0.21	0.30	0.89	0.61	0.55	0.55	0.10	0.51	0.77	0.81	0.78	0.48	rs239345	SCNN1G
																							0.17	0.28	0.10	0.98	0.54	0.99	0.99	0.62	0.13	0.07	0.14	0.29	0.86	rs238547	SCNN1B
																							0.27	0.12	0.76	0.96	0.75	0.74	0.81	0.63	0.95	0.21	0.59	0.64	rs8044970	SCNN1B	
																								0.09	0.34	0.95	0.48	0.55	0.67	0.23	0.26	0.01	0.09	0.02	0.64	rs152740	SCNN1B
																									0.92	0.65	0.10	0.17	0.28	0.91	0.96	0.03	0.01	0.64	rs250563	SCNN1B	
																										0.09	0.18	0.19	0.92	0.69	0.73	0.80	0.48	0.22	rs2303153	SCNN1B	
																											0.73	0.67	0.19	0.69	0.87	0.66	0.28	0.41	rs1403543	SCNN1B	
																												0.28	0.15	0.48	0.31	0.71	0.13	0.33	rs5194	AGTR2	
																													0.16	0.51	0.32	0.68	0.12	0.37	rs11091046	AGTR2	
																													0.86	0.95	0.71	0.27	0.96	rs2269370	RENBP		
																														0.40	0.52	0.38	0.98	rs2269372	RENBP		
																															0.65	0.41	0.73	rs762656	RENBP		
																																0.52	0.43	rs2968915	RENBP		
																																	0.11	rs2968917	ATP6AP2		
																																			rs10536	ATP6AP2	

Table II.17. Results from the gene-gene interaction analysis between all the SNPs for the pIVSpap. Significant interactions are indicated in bold red.

rs7548116	rs11585375	rs1200130	rs1358714	rs1040503	rs1464816	rs11571082	rs5705	rs10900555	rs10924074	rs850609	rs2068230	rs11614164	rs3782726	rs7973914	rs10849446	rs2286600	rs5735	rs4247210	rs11074555	rs9930640	rs239345	rs238547	rs8044970	rs152740	rs250563	rs2303153	rs1403543	rs5194	rs11091046	rs2269370	rs2269372	rs762656	rs2968915	rs2968917	rs10536		
	0.64	0.69	0.79	0.72	0.57	0.31	0.71	0.64	0.09	0.30	0.39	0.95	0.38	0.37	0.82	0.89	0.82	0.59	0.54	0.80	0.46	0.93	0.67	0.21	0.92	0.29	0.16	0.03	0.06	0.17	0.57	0.76	0.52	0.80	0.97	rs7548116	ATP1A2
		0.54	0.31	0.50	0.81	0.71	0.22	0.98	0.93	0.77	0.18	0.66	0.35	0.85	0.10	0.21	0.79	0.26	0.98	0.12	0.68	0.10	0.09	0.40	0.56	0.42	0.14	0.19	0.18	0.12	0.35	0.46	0.73	0.37	0.89	rs11585375	ATP1A2
			0.89	0.16	0.47	0.11	0.38	0.91	0.31	0.40	0.63	0.66	1.00	0.82	0.19	0.08	0.80	0.08	0.76	0.53	0.48	0.68	0.61	0.47	0.74	0.39	0.59	0.27	0.27	0.21	0.28	0.16	0.49	0.62	0.73	rs1200130	ATP1B1
				0.55	0.57	0.84	0.63	0.27	0.60	0.97	0.41	0.02	0.03	0.12	0.43	0.67	0.61	0.88	0.90	0.21	0.64	0.27	0.91	0.88	0.45	0.48	0.85	0.19	0.36	0.51	0.78	0.92	0.11	0.52	0.91	rs1358714	ATP1B1
					0.01	0.02	0.00	0.04	0.83	0.47	0.20	0.23	0.06	0.52	0.75	0.84	0.61	0.55	0.47	0.45	0.15	0.59	0.61	0.24	0.92	0.61	0.79	0.68	0.76	0.52	0.73	0.25	0.86	0.95	0.62	rs1040503	REN
						0.82	0.56	0.63	0.97	0.29	0.74	0.13	0.41	0.77	0.74	0.86	0.57	0.55	0.64	0.46	0.42	0.40	0.13	0.90	0.63	0.55	0.37	0.34	0.42	0.01	0.40	0.38	0.64	0.52	0.96	rs1464816	REN
							0.22	0.77	0.62	0.15	0.33	0.17	0.93	0.30	0.75	0.51	0.25	0.76	0.09	0.14	0.25	0.98	0.80	0.28	0.91	0.86	0.93	0.12	0.17	0.40	0.11	0.46	0.08	0.54	0.95	rs11571082	REN
								0.54	0.93	0.77	0.33	0.17	0.94	0.25	0.69	0.93	0.77	0.84	0.24	0.34	0.43	0.77	0.46	0.40	0.63	0.64	0.36	0.09	0.11	0.49	0.57	0.80	0.21	0.67	0.75	rs5705	REN
									0.36	0.33	0.11	0.21	0.95	0.55	0.77	0.69	0.29	0.65	0.77	0.76	0.65	0.13	0.08	0.47	0.79	0.01	0.64	0.94	0.90	0.43	0.70	0.31	0.91	0.73	0.44	rs10900555	REN
									0.99	0.56	0.95	0.22	0.79	0.44	0.11	0.39	0.47	0.84	0.86	0.24	0.37	0.92	0.30	0.97	0.89	0.12	0.88	0.82	0.02	0.04	0.07	0.70	0.67	0.19	0.52	rs10924074	ATP1A1
										0.94	0.71	0.97	0.24	0.58	0.62	0.62	0.83	0.93	0.90	0.66	0.16	0.20	0.46	0.33	0.30	0.99	0.68	0.78	0.67	0.79	0.83	0.28	0.24	0.98	rs850609	ATP1A1	
											0.06	0.16	0.23	0.11	0.27	0.94	0.79	0.12	0.94	0.19	0.01	0.21	0.44	0.01	0.43	0.45	0.10	0.24	0.51	0.04	0.08	0.32	0.51	0.63	rs2068230	ATP1B3	
													0.20	0.68	0.25	0.38	0.98	0.79	0.24	0.62	0.89	0.08	0.66	0.68	0.58	0.01	0.50	0.78	0.79	0.26	0.16	0.07	0.57	0.48	0.81	rs11614164	ATP1B3
														0.19	0.14	0.16	0.83	0.91	0.14	0.40	0.50	0.02	0.74	0.36	0.85	0.02	0.95	0.57	0.58	0.14	0.10	0.05	0.15	0.09	0.78	rs3782726	SCNN1A
															0.74	0.75	0.88	0.08	0.23	0.66	0.43	0.32	0.19	0.60	0.28	0.83	0.77	0.40	0.48	0.17	0.24	0.12	0.08	0.96	0.13	rs7973914	SCNN1A
																0.15	0.86	0.39	0.89	0.04	0.73	0.17	0.56	0.39	0.04	0.81	0.14	0.33	0.33	0.80	0.58	0.99	0.92	0.74	0.34	rs10849446	SCNN1A
																	0.54	0.29	0.84	0.02	0.86	0.03	0.21	0.33	0.14	0.90	0.26	0.34	0.33	0.69	0.24	0.50	0.58	0.87	0.89	rs2286600	SCNN1G
																		0.18	0.36	0.06	0.39	0.19	0.62	0.10	0.24	0.13	0.12	0.11	0.11	0.17	0.03	0.05	0.41	0.22	0.13	rs5735	SCNN1G
																			0.51	0.17	0.63	0.68	0.92	0.40	0.28	0.36	0.77	0.39	0.31	0.80	0.05	0.15	0.13	0.89	0.52	rs4247210	SCNN1G
																				0.67	0.20	0.64	0.40	0.91	0.05	0.85	0.42	0.73	0.66	0.86	0.79	0.77	0.59	0.44	0.02	rs11074555	SCNN1G
																					0.41	0.10	0.69	0.59	0.33	0.52	0.24	0.91	0.97	0.18	0.19	0.15	0.68	0.78	0.25	rs9930640	SCNN1B
																						0.33	0.98	0.35	0.30	0.61	0.12	0.10	0.11	0.07	0.27	0.48	0.28	0.42	0.73	rs239345	SCNN1B
																							0.33	0.34	0.08	0.82	0.51	0.78	0.77	0.81	0.10	0.04	0.34	0.56	0.45	rs238547	SCNN1B
																							0.26	0.20	0.43	0.84	0.93	0.96	0.64	0.71	0.92	0.37	0.97	0.50	rs8044970	SCNN1B	
																								0.11	0.32	0.51	0.26	0.32	0.92	0.14	0.14	0.03	0.25	0.06	0.97	rs152740	SCNN1B
																										0.93	0.97	0.26	0.36	0.23	0.98	0.89	0.01	0.04	0.97	rs250563	SCNN1B
																											0.07	0.33	0.36	0.79	0.67	0.61	0.65	0.37	0.38	rs2303153	SCNN1B
																												0.72	0.81	0.09	0.74	0.44	0.96	0.75	0.92	rs1403543	AGTR2
																													0.79	0.04	0.16	0.10	0.76	0.51	0.19	rs5194	AGTR2
																														0.05	0.18	0.11	0.81	0.46	0.23	rs11091046	AGTR2
																														0.99	0.97	0.63	0.25	0.86	rs2269370	RENBP	
																															0.59	0.46	0.34	0.65	rs2269372	RENBP	
																																0.59	0.37	0.84	rs762656	RENBP	
																																	0.79	0.36	rs2968915	ATP6AP2	
																																		0.12	rs2968917	ATP6AP2	
																																				rs10536	ATP6AP2

Table II.19. Results from the gene-gene interaction analysis between all the SNPs for the AWpap. Significant interactions are indicated in bold red.

	ATPIA2		ATPIB1		REN		ATPIA1		ATPIB3		SCNN1A		SCNN1G		SCNN1B		AGTR2		RENBP		ATP6AP2																		
rs7548116																																							
rs11585375	0.67	0.74	0.21	0.51	0.30	0.47	0.66	0.51	0.12	0.18	0.81	0.40	0.14	0.25	0.68	0.77	0.82	0.47	0.17	0.65	0.86	0.55	0.89	0.42	0.83	0.26	0.08	0.10	0.16	0.11	0.44	0.68	0.18	0.95	0.45	rs7548116	ATPIA2		
rs1200130		0.36	0.32	0.60	0.52	0.64	0.31	0.89	0.51	0.65	0.46	0.44	0.62	0.94	0.02	0.12	0.65	0.52	0.55	0.03	0.32	0.02	0.10	0.42	0.07	0.62	0.31	0.17	0.16	0.11	0.41	0.44	0.28	0.69	0.46	rs11585375	ATPIA2		
rs1358714			0.85	0.39	0.83	0.64	0.95	0.62	0.86	0.29	0.64	0.99	0.96	0.58	0.63	0.64	0.88	0.02	0.80	0.90	0.63	0.35	0.61	0.13	0.70	0.61	0.48	0.37	0.38	0.17	0.92	0.87	0.25	0.67	0.46	rs1200130	ATPIB1		
rs1040503				0.41	0.93	0.92	0.49	0.43	0.67	0.34	0.94	0.02	0.02	0.19	0.98	0.98	0.91	0.54	0.76	0.72	0.68	0.17	0.28	0.63	0.07	0.31	0.91	0.05	0.12	0.67	0.72	0.72	0.43	0.93	0.82	rs1358714	ATPIB1		
rs1464816					0.07	0.03	0.01	0.16	0.83	0.60	0.14	0.94	0.49	0.95	0.72	0.76	0.84	0.92	0.59	0.45	0.35	0.87	0.43	0.50	0.24	0.20	0.82	0.70	0.79	0.59	0.82	0.93	0.75	0.66	0.28	rs1040503	ATPIB1		
rs11571082						0.31	0.60	0.36	0.38	0.26	0.98	0.06	0.15	0.19	0.86	0.40	0.48	0.49	0.81	0.75	0.49	0.62	0.47	0.10	0.63	0.28	0.68	0.88	0.72	0.18	0.43	0.40	0.58	0.66	0.47	rs1464816	REN		
rs5705							0.14	0.74	0.94	0.02	0.53	0.33	0.75	0.36	0.81	0.32	0.23	0.59	0.08	0.05	0.36	0.45	0.96	0.06	0.42	0.43	0.88	0.89	0.98	0.82	0.15	0.58	0.16	0.79	0.39	rs11571082	REN		
rs1090555								0.71	0.59	0.30	0.28	0.44	0.76	0.33	0.86	0.30	0.66	0.35	0.19	0.15	0.72	0.71	0.55	0.13	0.46	0.64	0.82	0.67	0.74	0.90	0.56	0.80	0.38	0.87	1.00	rs5705	REN		
rs10924074									0.28	0.06	0.05	0.53	0.71	0.19	0.67	0.59	0.86	0.65	0.51	0.28	0.40	0.17	0.18	0.63	0.52	0.06	0.83	0.45	0.34	0.47	0.80	0.77	0.50	0.80	0.57	rs1090555	ATPIA1		
rs850609										0.45	0.94	0.94	0.19	0.93	0.48	0.14	0.82	0.80	0.99	0.89	0.38	0.64	0.96	0.76	0.35	0.53	0.05	0.16	0.14	0.40	0.16	0.28	0.76	0.69	0.02	rs10924074	ATPIA1		
rs2068230											0.50	0.57	0.70	0.04	0.28	0.67	0.85	0.73	0.73	0.34	0.40	0.10	0.69	0.83	0.27	0.90	0.41	0.73	0.63	0.95	0.33	0.49	0.61	0.60	0.88	rs850609	ATPIA1		
rs1614164												0.00	0.01	0.13	0.65	0.67	0.60	0.73	0.05	0.50	0.06	0.01	0.28	0.31	0.03	0.46	0.46	0.21	0.39	0.69	0.01	0.03	0.48	0.89	0.92	rs2068230	ATPIB3		
rs782726													0.04	0.96	0.39	0.35	0.78	0.74	0.40	0.27	0.89	0.07	0.38	0.32	0.38	0.01	0.74	0.75	0.75	0.76	0.81	0.50	0.98	0.72	0.61	rs1614164	ATPIB3		
rs7973914														0.63	0.13	0.20	0.36	0.74	0.07	0.25	0.76	0.02	0.59	0.24	0.43	0.01	0.78	0.30	0.30	0.48	0.62	0.40	0.62	0.54	0.50	rs782726	SCNN1A		
rs10849446															0.30	0.49	0.31	0.02	0.79	0.79	0.27	0.76	0.66	0.24	0.55	0.67	0.43	0.95	0.93	0.85	0.87	0.45	0.10	0.72	0.33	rs7973914	SCNN1A		
rs2286600																0.27	0.78	0.16	0.82	0.04	0.58	0.51	0.74	0.71	0.31	0.63	0.22	0.80	0.84	0.88	1.00	0.66	0.49	1.00	0.14	rs10849446	SCNN1A		
rs735																0.68	0.13	0.97	0.03	0.60	0.78	0.80	0.67	0.41	0.58	0.31	0.90	0.90	0.68	0.63	0.86	0.16	0.24	0.82	0.82	0.54	0.50	rs2286600	SCNN1G
rs4247210																	0.40	0.50	0.85	0.80	0.08	0.98	0.45	0.83	0.39	0.26	0.22	0.26	0.38	0.46	0.35	0.68	0.54	0.26	rs735	SCNN1G			
rs11074555																		0.88	0.66	0.60	0.77	0.75	0.76	1.00	0.85	0.49	0.89	0.77	0.48	0.04	0.15	0.13	0.60	0.20	rs4247210	SCNN1G			
rs9930640																			0.46	0.35	0.87	0.64	0.62	0.10	0.83	0.24	0.85	0.91	0.30	0.77	0.82	0.81	1.00	0.03	rs11074555	SCNN1G			
rs239345																				0.97	0.48	0.36	0.24	0.76	0.55	0.51	0.93	0.87	0.91	0.09	0.21	0.52	0.73	0.32	rs9930640	SCNN1G			
rs238547																					0.78	0.62	0.40	0.51	0.21	0.12	0.31	0.31	0.52	0.36	0.23	0.76	0.67	0.40	rs239345	SCNN1B			
rs8044970																						0.21	0.40	0.04	0.55	0.94	0.50	0.50	0.72	0.17	0.13	0.08	0.11	0.64	rs238547	SCNN1B			
rs152740																						0.25	0.16	0.66	0.59	0.66	0.62	0.39	0.63	0.86	0.13	0.42	0.55	rs8044970	SCNN1B				
rs250563																							0.16	0.30	0.79	0.39	0.46	0.72	0.38	0.34	0.06	0.14	0.04	0.89	rs152740	SCNN1B			
rs2303153																								0.36	0.53	0.38	0.45	0.37	0.42	0.49	0.01	0.01	0.89	rs250563	SCNN1B				
rs1403543																									0.07	0.27	0.30	0.92	0.84	0.54	0.93	0.73	0.51	rs2303153	SCNN1B				
rs5194																										0.49	0.57	0.82	0.63	0.26	0.64	0.10	0.71	rs1403543	AGTR2				
rs11091046																											0.51	0.89	0.19	0.16	0.99	0.25	0.82	rs5194	AGTR2				
rs2269370																												0.93	0.21	0.18	0.96	0.22	0.72	rs11091046	AGTR2				
rs2269372																													0.93	0.69	0.88	0.43	0.42	rs2269370	RENBP				
rs762656																														0.70	0.48	0.66	0.96	rs2269372	RENBP				
rs2968915																															0.62	0.77	0.76	rs762656	RENBP				
rs2968917																															0.44	0.39	rs2968915	ATP6AP2					
rs10536																															0.16	rs2968917	ATP6AP2						
																																					rs10536	ATP6AP2	

Table II.20. Results from the gene-gene interaction analysis between all the SNPs for the LWpap. Significant interactions are indicated in bold red.

ATPIA2		ATPIB1		REN		ATPIA1		ATPIB3		SCNN1A		SCNN1G		SCNN1B		AGTR2		RENBP		ATP6AP2																	
rs7548116																																					
rs11585375	0.46	0.53	0.81	0.92	0.30	0.59	0.22	0.43	0.03	0.33	0.74	0.41	0.06	0.18	0.82	0.33	0.78	0.49	0.52	0.78	0.73	0.43	0.43	0.50	0.68	0.21	0.04	0.06	0.05	0.13	0.38	0.50	0.91	0.85	0.31	rs7548116	ATPIA2
rs1200130	0.48	0.74	0.27	0.70	0.45	0.38	0.63	0.94	0.20	0.65	0.13	0.06	0.05	0.77	0.96	0.98	0.71	0.15	0.71	0.09	0.04	0.33	0.82	0.07	0.58	0.41	0.32	0.31	0.12	0.05	0.18	0.81	0.72	0.80	rs11585375	ATPIA2	
rs1358714	0.48	0.84	0.77	0.57	0.43	0.85	0.62	0.56	0.41	0.87	0.36	0.19	0.33	0.28	0.93	0.28	0.53	0.61	0.46	0.14	0.13	0.03	0.35	0.46	0.67	0.93	0.89	0.05	0.53	0.25	0.94	0.51	0.83	rs1200130	ATPIB1		
rs1040503	0.16	0.74	0.53	0.92	0.27	0.53	0.51	0.19	0.03	0.05	0.27	0.97	0.84	0.86	0.55	0.86	0.61	0.36	0.55	0.75	0.84	0.44	0.45	0.96	0.55	0.51	0.51	0.58	0.92	0.55	0.88	0.78	rs1358714	ATPIB1			
rs1464816	0.00	0.04	0.01	0.26	0.39	0.84	0.50	0.44	0.26	0.27	0.23	0.10	0.61	0.43	0.65	0.26	0.02	0.29	0.59	0.62	0.35	0.55	0.41	0.25	0.21	0.74	0.15	0.28	0.27	0.45	1.00	rs1040503	ATPIB1				
rs11571082	0.57	0.43	0.60	0.95	0.65	0.83	0.32	0.46	0.14	0.22	0.02	0.46	0.63	0.80	0.65	0.71	0.39	0.25	0.82	0.61	0.52	0.16	0.59	0.46	0.04	0.15	0.21	0.21	0.12	0.49	rs1464816	REN					
rs5705	0.25	0.79	0.69	0.28	0.85	0.57	0.92	0.50	0.77	0.42	0.17	0.82	0.32	0.31	0.76	0.92	0.83	0.17	0.95	0.93	0.25	0.13	0.11	0.80	0.04	0.08	0.06	0.53	0.88	rs11571082	REN						
rs10900555	0.59	0.82	0.49	0.72	0.39	0.78	0.52	0.99	0.35	0.35	0.75	0.40	0.23	0.77	0.81	0.55	0.47	0.93	0.80	0.33	0.25	0.23	0.85	0.20	0.41	0.26	0.62	0.41	0.62	0.41	0.62	0.41	rs5705	REN			
rs10924074	0.25	0.63	0.09	0.57	0.28	0.13	0.33	0.02	0.77	0.49	0.81	0.19	0.34	0.01	0.01	0.01	0.30	0.70	0.73	0.55	0.63	0.75	0.78	0.94	0.76	0.28	0.77	rs10900555	ATPIA1								
rs850609	0.95	0.58	0.76	0.18	0.57	0.59	0.41	0.88	0.86	0.52	0.03	0.84	0.04	0.53	0.29	0.14	0.59	0.47	0.28	0.29	0.07	0.08	0.30	0.38	0.83	0.06	0.66	0.66	0.66	0.66	0.66	rs10924074	ATPIA1				
rs2068230	0.06	0.74	0.80	0.07	0.08	0.15	0.52	0.99	0.14	0.93	0.03	0.53	0.75	0.61	0.25	0.63	0.76	0.76	0.73	0.77	0.31	0.56	0.39	0.39	0.95	rs850609	ATPIA1										
rs11614164	0.51	0.66	0.59	0.44	0.62	0.02	0.85	0.37	0.52	0.44	0.08	0.74	0.13	0.04	0.90	0.85	0.31	0.29	0.89	0.30	0.49	0.65	0.58	0.91	rs2068230	ATPIB3											
rs3782726	0.03	0.29	0.49	0.07	0.97	0.15	0.42	0.82	0.05	0.66	0.38	0.13	0.00	0.39	0.99	0.98	0.35	0.60	0.46	0.55	0.38	0.79	rs3782726	SCNN1A													
rs7973914	0.52	0.73	0.63	0.12	0.39	0.81	0.31	0.19	0.81	0.29	0.70	0.16	0.39	0.56	0.70	0.70	0.20	0.10	0.10	0.73	0.54	rs7973914	SCNN1A														
rs10849446	0.32	0.24	0.78	0.89	0.33	0.49	0.32	0.62	0.52	0.21	0.70	0.70	0.96	0.98	0.85	0.86	0.70	0.42	0.14	0.94	rs10849446	SCNN1A															
rs2286600	0.66	0.45	0.94	0.30	0.98	0.13	0.33	0.60	0.86	0.57	0.47	0.68	0.68	0.75	0.37	0.69	0.81	0.60	0.53	rs2286600	SCNN1A																
rs5735	0.40	0.78	0.02	0.89	0.48	0.83	0.98	0.01	0.07	0.07	0.04	0.01	0.01	0.03	0.33	0.24	0.56	0.19	0.99	rs5735	SCNN1G																
rs4247210	0.79	0.23	0.71	0.96	0.88	0.04	0.92	0.25	0.70	0.66	0.75	0.15	0.56	0.79	0.99	0.45	rs4247210	SCNN1G																			
rs11074555	0.95	0.35	0.91	0.72	0.42	0.15	0.16	0.27	0.39	0.41	0.47	0.31	0.53	0.93	0.55	0.16	rs11074555	SCNN1G																			
rs9930640	0.90	0.79	0.23	0.11	0.67	0.79	0.51	0.28	0.31	0.15	0.97	0.95	0.92	0.70	0.09	rs9930640	SCNN1B																				
rs239345	0.63	0.73	0.13	0.38	0.11	0.06	0.06	0.06	0.07	0.17	0.17	0.52	0.86	0.26	rs239345	SCNN1B																					
rs238547	0.34	0.34	0.09	0.35	0.41	0.17	0.19	0.76	0.10	0.03	0.66	0.61	0.93	rs238547	SCNN1B																						
rs8044970	0.54	0.07	0.74	0.36	0.15	0.17	0.82	0.44	0.73	0.84	0.40	0.24	rs8044970	SCNN1B																							
rs152740	0.13	0.73	0.09	0.01	0.01	0.54	0.20	0.15	0.23	0.43	0.03	rs152740	SCNN1B																								
rs250563	0.96	0.12	0.07	0.09	0.34	0.83	0.87	0.07	0.17	0.29	rs250563	SCNN1B																									
rs2303153	0.46	0.57	0.56	0.21	0.11	0.02	0.37	0.67	0.59	rs2303153	SCNN1B																										
rs1403543	0.95	0.99	0.44	0.85	0.72	0.46	0.04	0.77	rs1403543	AGTR2																											
rs5194	0.32	0.21	0.35	0.31	0.16	0.02	0.83	rs5194	AGTR2																												
rs11091046	0.21	0.33	0.29	0.18	0.02	0.79	rs11091046	AGTR2																													
rs2269370	0.44	0.55	0.50	0.12	0.81	rs2269370	RENBP																														
rs2269372	0.59	0.30	0.22	0.36	rs2269372	RENBP																															
rs762656	0.50	0.38	0.54	rs762656	RENBP																																
rs2968915	0.22	0.80	rs2968915	ATP6AP2																																	
rs2968917	0.35	rs2968917	ATP6AP2																																		
rs10536	rs10536	ATP6AP2																																			

Table II.22. Results from the gene-gene interaction analysis between all the SNPs for the PWpap. Significant interactions are indicated in bold red.

	ATP1A2		ATP1B1		REN		ATP1A1		ATP1B3		SCNN1A		SCNN1G		SCNN1B		AGTR2		RENBP		ATP6AP2																	
rs7548116																																						
rs11585375	0.22	0.40				0.04	0.47	0.71	0.05	0.05	0.24	0.83	0.94	0.86	0.37	0.15	0.96	0.91	0.42	0.60	0.40	0.91	0.84	0.41	0.15	0.29	0.92	0.42	0.39	0.26	0.11	0.16	0.70	0.45	0.68	rs7548116	ATP1A2	
rs1200130		0.52	0.66	0.55	0.86	0.08	0.35	0.85	0.56	0.80	0.77	0.81	0.63	0.96	0.97	0.95	0.86	0.64	0.98	0.53	0.82	0.54	0.88	0.70	0.89	0.54	0.55	0.55	0.55	0.67	0.82	1.00	0.26	0.27	0.30	rs11585375		
rs1358714			0.23	0.91	0.54	0.16	0.26	0.48	0.18	0.02	0.02	0.34	0.37	0.17	0.36	0.92	0.54	0.69	0.49	0.36	0.33	0.69	0.34	0.92	0.97	0.17	0.91	0.72	0.67	0.98	0.30	0.43	0.62	0.46	0.98	rs1200130	ATP1B1	
rs1040503				0.13	0.80	0.64	0.88	0.34	0.24	0.26	0.75	0.01	0.05	0.22	0.67	0.86	0.38	0.57	0.70	0.29	0.94	0.91	0.67	0.78	1.00	0.24	0.49	0.15	0.18	0.70	0.89	0.80	0.67	0.84	0.82	rs1358714		
rs1464816					0.14	0.20	0.12	0.81	0.55	0.70	0.58	0.16	0.22	0.30	0.99	0.17	0.84	0.88	0.54	0.96	0.36	0.62	0.92	0.55	0.76	0.87	0.98	0.42	0.39	0.92	0.86	0.59	0.83	0.98	0.66	rs1040503		
rs11571082						0.76	0.98	0.88	0.61	0.34	0.79	0.14	0.37	0.38	0.73	0.72	0.09	0.49	0.87	0.35	0.44	0.61	0.82	0.59	0.47	0.45	0.98	0.52	0.54	0.36	0.15	0.22	0.35	0.14	0.23	rs1464816		
rs5705							0.23	0.36	0.30	0.41	0.14	0.95	0.60	0.67	0.34	0.37	0.32	0.71	0.93	0.34	0.53	0.61	0.33	0.96	0.55	0.81	0.83	0.73	0.78	0.26	0.19	0.35	0.88	0.91	0.96	rs11571082	REN	
rs10900555								0.57	0.77	0.94	0.28	0.78	0.76	0.73	0.08	0.24	0.23	0.81	0.49	0.03	0.76	0.41	0.37	0.53	0.15	0.47	0.49	0.74	0.72	0.06	0.19	0.31	0.90	0.70	0.93	rs5705		
rs10924074									1.00	0.79	0.09	0.67	0.83	0.96	0.88	0.45	0.85	0.81	0.52	0.11	0.75	0.75	0.03	0.26	0.51	0.68	0.63	0.17	0.15	0.42	0.62	0.75	0.76	0.58	0.72	rs10900555		
rs850609										0.07	0.47	0.21	0.03	0.39	0.04	0.43	0.91	0.46	0.54	0.69	0.54	0.09	0.87	0.11	0.04	0.64	0.06	0.29	0.28	0.92	0.36	0.28	0.23	0.43	0.01	rs10924074	ATP1A1	
rs2068230											0.03	0.38	0.54	0.36	0.45	0.65	0.22	0.85	0.03	0.20	0.02	0.29	0.32	0.72	0.10	0.34	0.79	0.57	0.60	0.95	0.47	0.37	0.77	0.99	0.54	rs850609		
rs11614164											0.49	0.64	0.95	0.57	0.49	0.30	0.50	0.17	0.03	0.05	0.06	0.44	0.13	0.04	0.03	0.06	0.26	0.32	0.65	0.42	0.96	0.45	0.31	0.34	rs2068230	ATP1B3		
rs3782726												0.27	0.41	0.83	0.46	0.54	0.41	0.27	0.87	0.32	0.99	0.17	0.35	0.54	0.03	0.83	0.04	0.04	0.55	0.86	0.71	0.32	0.11	0.39	rs11614164			
rs7973914													0.47	0.41	0.74	0.78	0.65	0.42	0.74	0.53	0.90	0.07	0.64	0.57	0.01	0.89	0.13	0.13	0.08	0.87	0.92	0.55	0.27	0.12	0.12	rs3782726	SCNN1A	
rs10849446														0.74	0.75	0.85	0.39	0.98	0.07	0.05	0.77	0.38	0.66	0.05	0.93	0.27	0.08	0.08	0.47	0.54	0.20	0.20	0.21	0.98	rs7973914			
rs2286600															0.07	0.30	0.63	0.64	0.12	0.85	0.61	0.53	0.99	0.09	0.40	0.32	0.40	0.41	0.80	1.00	0.86	0.39	0.68	0.04	rs10849446			
rs735																0.66	0.59	0.52	0.07	0.51	0.17	0.18	0.84	0.41	0.55	0.90	0.13	0.14	0.56	0.48	0.42	0.72	0.34	0.25	rs2286600			
rs4247210																	0.88	0.39	0.78	0.19	0.65	0.82	0.81	0.00	0.02	0.41	0.48	0.51	0.34	0.89	0.93	0.63	0.93	0.39	0.39	rs735	SCNN1G	
rs11074555																		0.92	0.19	0.77	0.38	0.53	0.22	0.16	0.90	0.12	0.69	0.73	0.32	0.34	0.50	0.92	0.56	0.17	rs4247210			
rs9930640																			0.50	0.61	0.52	0.55	0.86	0.69	0.29	0.28	0.98	0.96	0.95	0.56	0.71	0.91	0.73	0.11	rs11074555			
rs239345																					0.99	0.63	0.22	0.50	0.34	0.34	0.69	0.65	0.66	0.74	0.15	0.44	0.46	0.62	0.26	0.26	rs9930640	
rs238547																						0.07	0.37	0.54	0.99	0.96	0.18	0.06	0.06	0.93	0.77	0.84	0.50	0.49	0.51	rs239345		
rs8044970																							0.57	0.53	0.30	0.73	0.42	0.43	0.44	0.64	0.64	0.51	1.00	0.82	0.83	rs238547	SCNN1B	
rs152740																								0.31	0.06	0.42	0.61	0.48	0.47	0.41	0.42	0.29	0.80	0.64	0.60	rs8044970		
rs250563																									0.08	0.70	0.06	0.18	0.20	0.39	0.93	0.95	0.71	0.93	0.29	0.29	rs152740	
rs2303153																										0.59	0.61	0.28	0.30	0.50	0.81	0.93	0.33	0.04	0.77	rs250563		
rs1403543																											0.95	0.57	0.56	0.57	0.35	0.13	0.96	0.95	0.39	0.39	rs2303153	
rs5194																												0.88	0.86	0.99	0.36	0.29	0.31	0.79	0.55	rs1403543	AGTR2	
rs11091046																													0.75	0.76	0.74	0.51	0.49	0.90	0.29	rs5194		
rs2269370																														0.75	0.72	0.50	0.51	0.92	0.27	rs11091046		
rs2269372																															0.68	0.42	0.25	0.55	0.28	rs2269370		
rs762656																																0.36	0.62	1.00	0.76	rs2269372	RENBP	
rs2968915																																	0.72	0.94	rs762656			
rs2968917																																	0.93	0.51	rs2968915			
rs10536																																	0.57	rs2968917	ATP6AP2			
																																					rs10536	

Table II.23. Results from the gene-gene interaction analysis between all the SNPs for the mLVWTapx. Significant interactions are indicated in bold red.

	ATP1A2		ATP1B1		REN		ATP1A1		ATP1B3		SCNN1A		SCNN1G		SCNN1B		AGTR2		RENBP		ATP6AP2																
rs7548116																																					
rs11585375	0.90	0.90	0.25	0.26	0.19	0.14	0.30	0.12	0.25	0.96	0.33	0.39	0.10	0.63	0.47	0.62	0.86	0.22	0.24	0.92	0.62	0.32	0.72	0.53	0.29	0.04	0.12	0.08	0.09	0.09	0.91	0.76	0.39	1.00	0.42	rs7548116	ATP1A2
rs1200130	0.09	0.09	0.39	0.64	0.77	0.40	0.49	0.73	0.94	0.93	0.50	0.39	0.78	0.06	0.10	0.90	0.38	0.52	0.02	0.72	0.04	0.10	0.45	0.17	0.74	0.62	0.38	0.42	0.16	0.38	0.43	0.49	0.62	0.59	rs11585375	ATP1A2	
rs1358714			0.94	0.45	0.52	0.09	0.59	0.87	0.95	0.05	0.87	0.53	0.90	0.97	0.90	0.48	0.25	0.11	0.70	0.77	0.72	0.31	0.44	0.03	0.59	0.90	0.67	0.56	0.72	0.14	0.56	0.42	0.15	0.54	0.44	rs1200130	ATP1B1
rs1040503			0.40	0.15	0.35	0.54	0.55	0.33	0.95	0.98	0.03	0.04	0.06	0.24	0.51	0.97	0.90	0.88	0.39	0.85	0.12	0.81	0.88	0.39	0.77	0.66	0.12	0.15	0.30	0.53	0.47	0.04	0.40	0.97	rs1358714	ATP1B1	
rs1464816					0.00	0.01	0.00	0.03	0.85	0.82	0.65	0.47	0.36	0.56	0.65	0.35	0.48	0.46	0.36	0.89	0.36	0.82	0.71	0.92	0.86	0.45	0.35	0.87	0.73	0.79	0.69	0.90	0.78	0.78	0.30	rs1040503	ATP1B1
rs11571082					0.67	0.35	0.15	0.39	0.38	0.26	0.01	0.02	0.04	0.90	0.72	0.16	0.89	0.49	0.22	0.63	0.80	0.64	0.77	0.49	0.98	0.34	0.37	0.47	0.03	0.08	0.08	0.53	0.70	0.91	rs1464816	ATP1B1	
rs5705					0.48	0.91	0.33	0.18	0.16	0.18	0.39	0.45	0.69	0.93	0.20	0.77	0.01	0.02	0.49	0.78	0.61	0.15	0.96	0.75	0.27	0.77	0.76	0.52	0.09	0.35	0.01	0.38	0.22	0.85	rs11571082	REN	
rs10900555					0.50	0.29	0.67	0.16	0.13	0.26	0.42	0.67	0.93	0.99	0.88	0.04	0.27	0.33	0.56	0.43	0.37	0.48	0.56	0.48	0.79	0.70	0.47	0.13	0.49	0.03	0.28	0.60	0.85	rs5705	REN		
rs10924074					0.92	0.43	0.21	0.50	0.97	0.17	0.71	0.91	0.15	0.86	0.65	0.97	0.53	0.22	0.30	0.39	0.95	0.01	0.98	0.50	0.44	0.21	0.76	0.89	0.80	0.72	0.85	0.60	rs10900555	ATP1A1			
rs850609					0.63	0.62	0.45	0.77	0.82	0.68	0.40	0.81	0.85	0.83	0.97	0.50	0.59	0.59	0.79	0.44	0.42	0.20	0.23	0.23	0.12	0.14	0.30	0.52	0.96	0.09	0.91	0.91	0.88	rs10924074	ATP1A1		
rs2068230					0.81	0.76	0.77	0.10	1.00	0.93	0.89	0.96	0.67	0.84	0.30	0.02	0.38	0.27	0.20	0.34	0.75	0.97	0.95	0.55	0.45	0.65	0.62	0.74	0.88	0.88	0.88	0.88	0.88	rs850609	ATP1A1		
rs11614164					0.03	0.19	0.28	0.23	0.19	0.77	1.00	0.01	0.30	0.02	0.00	0.26	0.34	0.00	0.29	0.79	0.38	0.48	0.61	0.02	0.05	0.10	0.20	0.70	0.20	0.70	0.20	0.70	0.20	rs2068230	ATP1B3		
rs3782726					0.09	0.95	0.75	0.99	0.60	0.63	0.95	0.63	0.40	0.27	0.75	0.87	0.48	0.00	0.90	0.29	0.26	0.69	0.38	0.16	0.98	0.69	0.89	0.69	0.89	0.69	0.89	0.69	0.89	rs11614164	ATP1B3		
rs7973914									0.54	0.82	0.83	0.67	0.58	0.68	0.90	0.87	0.06	0.83	0.71	0.76	0.00	0.86	0.48	0.44	0.47	0.31	0.21	0.94	0.62	0.67	0.67	0.67	0.67	rs3782726	SCNN1A		
rs10849446									0.74	0.83	0.43	0.06	0.98	1.00	0.49	0.41	0.55	0.67	0.34	0.49	0.94	0.55	0.68	0.94	0.39	0.18	0.30	0.47	0.20	0.20	0.20	0.20	rs7973914	SCNN1A			
rs2286600									0.21	0.75	0.32	0.85	0.22	0.81	0.61	0.69	0.95	0.01	0.57	0.19	0.61	0.68	0.87	0.39	0.21	0.84	0.52	0.32	0.32	0.32	0.32	0.32	rs10849446	SCNN1A			
rs5735									0.85	0.15	0.69	0.08	0.71	0.09	0.17	0.74	0.04	0.75	0.47	0.83	0.91	0.84	0.97	0.88	0.65	0.94	0.57	0.65	0.94	0.57	0.65	0.94	0.57	rs2286600	SCNN1G		
rs4247210									0.33	0.58	0.35	0.97	0.21	0.55	0.41	0.08	0.10	0.02	0.01	0.01	0.07	0.16	0.13	0.58	0.56	0.21	0.58	0.56	0.21	0.58	0.56	0.21	rs5735	SCNN1G			
rs11074555									0.92	0.73	0.43	0.99	0.95	0.29	0.31	0.74	0.60	0.83	0.81	0.52	0.18	0.36	0.45	0.35	0.60	0.60	0.60	0.60	0.60	0.60	0.60	0.60	0.60	rs4247210	SCNN1G		
rs9930640									0.27	0.37	0.85	0.98	0.64	0.32	0.96	0.34	0.98	0.96	0.95	0.98	0.80	0.64	0.67	0.05	0.98	0.80	0.64	0.67	0.05	0.98	0.80	0.64	0.67	0.05	rs11074555	SCNN1G	
rs239345									0.62	0.28	0.89	0.90	0.61	0.37	0.55	0.88	0.87	0.22	0.84	0.88	0.82	0.49	0.14	rs9930640	SCNN1B												
rs238547									0.29	0.70	0.80	0.58	0.79	0.51	0.48	0.43	0.26	0.55	0.53	0.40	0.17	0.81	rs239345	SCNN1B													
rs8044970									0.56	0.08	0.05	0.76	0.99	0.85	0.79	0.88	0.30	0.12	0.61	1.00	0.80	rs238547	SCNN1B														
rs152740									0.52	0.01	0.92	0.87	0.93	0.86	0.83	0.82	0.81	0.77	0.44	0.83	rs8044970	SCNN1B															
rs250563									0.00	0.38	0.87	0.84	0.81	0.92	0.69	0.53	0.36	0.61	0.24	rs152740	SCNN1B																
rs2303153									0.51	0.42	0.04	0.03	0.58	0.72	0.78	0.05	0.01	0.41	rs250563	SCNN1B																	
rs1403543									0.11	0.67	0.73	0.19	0.27	0.20	0.33	0.29	0.57	rs2303153	AGTR2																		
rs5194									0.57	0.56	0.41	0.86	0.76	0.87	0.19	0.16	rs1403543	AGTR2																			
rs11091046									0.39	0.31	0.29	0.24	0.54	0.36	0.62	rs5194	AGTR2																				
rs2269370									0.38	0.29	0.24	0.63	0.30	0.61	rs11091046	RENBP																					
rs2269372									0.82	0.68	0.23	0.04	0.73	rs2269370	RENBP																						
rs762656									0.52	0.12	0.10	0.28	rs2269372	RENBP																							
rs2968915									0.19	0.15	0.54	rs762656	ATP6AP2																								
rs2968917									0.97	0.43	rs2968915	ATP6AP2																									
rs10536									0.04	rs2968917	ATP6AP2																										

Table II.25. Results from the gene-gene interaction analysis between all the SNPs for the AWapx. Significant interactions are indicated in bold red.

ATPIA2		ATPIB1		REN		ATPIA1		ATPIB3		SCNN1A		SCNN1G		SCNN1B		AGTR2		RENBP		ATP6AP2																	
rs7548116	0.73	0.90	0.15	0.27	0.14	0.25	0.47	0.12	0.19	0.65	0.63	0.05	0.01	0.96	0.66	0.87	0.96	0.34	0.07	0.39	0.82	0.77	0.12	0.37	0.56	0.21	0.20	0.13	0.16	0.04	0.99	0.90	0.76	0.64	0.38	rs7548116	ATPIA2
rs11585375	0.14	0.46	0.41	0.90	0.75	0.49	0.58	0.85	0.72	0.38	0.18	0.20	0.43	0.10	0.30	0.82	0.89	0.74	0.10	0.42	0.06	0.21	0.91	0.09	0.85	0.29	0.28	0.33	0.41	0.83	0.91	0.74	0.95	0.48	rs11585375	ATPIA2	
rs1200130	0.91	0.32	0.60	0.19	0.94	0.41	0.98	0.00	0.47	0.76	0.44	0.93	0.47	0.36	0.85	0.04	0.19	0.56	0.84	0.49	0.99	0.04	0.35	0.57	0.50	0.47	0.65	0.13	0.90	0.72	0.33	0.52	0.47	rs1200130	ATPIA2		
rs1358714	0.58	0.38	0.18	0.22	0.76	0.62	0.85	0.73	0.09	0.14	0.09	0.17	0.26	0.62	0.94	0.62	0.36	0.36	0.18	0.66	0.57	0.16	0.55	0.84	0.05	0.08	0.20	0.56	0.44	0.16	0.64	0.69	rs1358714	ATPIB1			
rs1040503	0.10	0.07	0.00	0.19	0.72	0.99	0.29	0.51	0.42	0.73	0.62	0.70	0.76	0.31	0.18	0.78	0.53	0.65	0.80	0.86	0.54	0.73	0.12	0.46	0.35	0.56	0.79	0.68	0.80	0.85	0.46	rs1040503	ATPIB1				
rs1464816	0.82	0.40	0.08	0.44	0.06	0.49	0.04	0.49	0.04	0.22	0.04	0.44	0.35	0.15	0.66	0.76	0.07	0.96	0.38	0.42	0.33	0.93	0.62	0.64	0.70	0.93	0.12	0.45	0.53	0.26	0.23	0.99	rs1464816	REN			
rs11571082	0.05	0.99	0.49	0.17	0.22	0.68	0.90	0.90	0.53	0.92	0.38	0.98	0.00	0.03	0.70	0.69	0.81	0.11	0.88	0.74	0.09	0.70	0.65	0.72	0.21	0.63	0.07	0.38	0.58	rs11571082	REN						
rs5705	0.34	0.30	0.63	0.12	0.43	0.57	0.90	0.66	0.99	0.57	0.76	0.00	0.21	0.34	0.59	0.60	0.23	0.55	0.94	0.34	0.80	0.69	0.56	0.31	0.84	0.09	0.36	0.92	0.52	rs5705	REN						
rs10900555	0.56	0.21	0.13	0.87	0.48	0.23	0.49	0.65	0.08	0.26	0.17	0.63	0.09	0.09	0.38	0.54	0.68	0.05	0.87	0.42	0.32	0.48	0.88	0.64	0.97	0.67	0.52	rs10900555	ATPIA1								
rs10924074	0.65	0.87	0.57	0.58	0.51	0.86	0.92	0.64	0.89	0.97	0.39	0.88	0.51	0.59	0.75	0.29	0.11	0.41	0.28	0.26	0.21	0.42	0.78	0.85	0.76	0.42	0.85	0.76	0.42	rs10924074	ATPIA1						
rs850609	0.75	0.10	0.46	0.29	0.95	0.72	0.81	0.85	0.73	0.70	0.37	0.00	0.48	0.12	0.47	0.25	0.48	0.92	0.86	0.33	0.57	0.83	0.33	0.60	0.43	rs850609	ATPIA1										
rs2068230	0.01	0.11	0.17	0.93	0.63	0.84	0.51	0.07	0.54	0.07	0.00	0.47	0.29	0.01	0.47	0.95	0.40	0.56	0.76	0.02	0.08	0.18	0.29	0.54	0.54	0.29	0.54	0.54	0.63	rs2068230	ATPIB3						
rs11614164	0.21	0.36	0.67	0.46	0.29	0.95	0.69	0.65	0.54	0.21	0.77	0.70	0.44	0.00	0.81	0.23	0.20	0.44	0.82	0.64	0.85	0.81	0.63	0.81	0.63	rs11614164	ATPIB3										
rs3782726	0.73	0.54	0.29	0.26	0.93	0.99	0.94	0.75	0.05	0.71	0.41	0.46	0.01	0.42	0.15	0.13	0.69	0.98	0.64	0.90	0.96	0.54	rs3782726	SCNN1A													
rs7973914	0.54	0.83	0.17	0.16	0.92	0.81	0.75	0.50	0.24	0.67	0.23	0.89	0.75	0.14	0.28	0.71	0.75	0.41	0.34	0.98	0.77	rs7973914	SCNN1A														
rs10849446	0.22	0.53	0.41	0.88	0.27	0.82	0.69	0.98	0.87	0.21	0.50	0.69	0.67	0.59	0.80	0.70	0.32	0.58	0.74	0.20	0.20	0.58	0.74	0.20	rs10849446	SCNN1A											
rs2286600	0.78	0.26	0.43	0.03	0.75	0.42	0.50	0.55	0.44	0.58	0.49	0.69	0.61	0.47	0.39	0.62	0.35	0.26	0.09	rs2286600	SCNN1G																
rs5735	0.18	0.44	0.25	0.46	0.20	0.82	0.21	0.13	0.04	0.13	0.13	0.18	0.11	0.34	0.30	0.36	0.34	0.38	rs5735	SCNN1G																	
rs4247210	0.70	0.98	0.27	0.85	0.83	0.45	0.26	0.47	0.51	0.82	0.78	0.82	0.09	0.29	0.73	0.18	1.00	rs4247210	SCNN1G																		
rs11074555	0.41	0.80	0.52	0.56	0.76	0.17	0.76	0.39	0.68	0.65	0.90	0.51	0.34	0.92	0.96	0.09	rs11074555	SCNN1B																			
rs9930640	0.63	0.83	0.74	0.59	0.67	0.98	0.42	0.73	0.71	0.11	0.88	0.82	0.59	0.44	0.05	rs9930640	SCNN1B																				
rs239345	0.39	0.99	0.79	0.53	0.36	0.48	0.54	0.49	0.44	0.79	0.79	0.36	0.24	0.86	rs239345	SCNN1B																					
rs238547	0.25	0.11	0.03	0.77	0.82	0.86	0.78	0.83	0.32	0.12	0.46	0.57	0.69	rs238547	SCNN1B																						
rs8044970	0.41	0.02	0.70	0.65	0.59	0.52	0.58	0.74	0.82	0.74	0.70	0.76	rs8044970	SCNN1B																							
rs152740	0.00	0.35	0.95	0.66	0.63	0.50	0.93	0.84	0.43	0.56	0.41	rs152740	SCNN1B																								
rs250563	0.27	0.65	0.05	0.05	0.70	0.67	0.55	0.07	0.02	0.27	rs250563	SCNN1B																									
rs2303153	0.08	0.92	0.98	0.80	0.95	0.73	0.49	0.32	0.62	rs2303153	SCNN1B																										
rs1403543	0.75	0.72	0.63	0.78	0.73	0.66	0.32	0.14	rs1403543	AGTR2																											
rs5194	0.32	0.39	0.44	0.39	0.97	0.28	0.95	rs5194	AGTR2																												
rs11091046	0.49	0.46	0.41	0.84	0.21	0.92	rs11091046	AGTR2																													
rs2269370	0.39	0.49	0.02	0.01	0.27	rs2269370	RENBP																														
rs2269372	0.15	0.01	0.02	0.76	rs2269372	RENBP																															
rs762656	0.04	0.05	0.51	rs762656	RENBP																																
rs2968915	0.79	0.44	rs2968915	ATP6AP2																																	
rs2968917	0.12	rs2968917	ATP6AP2																																		
rs10536	rs10536	ATP6AP2																																			

Table II.26. Results from the gene-gene interaction analysis between all the SNPs for the LWapx. Significant interactions are indicated in bold red.

ATPIA2		ATPIB1		REN		ATPIA1		ATPIB3		SCNN1A		SCNN1G		SCNN1B		AGTR2		RENBP		ATP6AP2																	
rs7548116																																					
rs11585375	0.82	0.95	0.30	0.48	0.57	0.22	0.35	0.24	0.18	0.42	0.38	0.66	0.51	0.64	0.26	0.24	0.50	0.16	0.04	0.20	0.16	0.08	0.38	0.88	0.37	0.05	0.14	0.26	0.32	0.04	0.69	0.67	0.91	0.16	0.47	rs7548116	ATPIA2
rs1200130	0.78	0.47	0.87	0.54	0.55	0.35	0.51	0.95	0.77	0.62	0.34	0.47	0.42	0.54	0.60	0.61	0.96	0.26	0.90	0.08	0.05	0.23	0.34	0.20	0.76	0.66	0.71	0.66	0.13	0.13	0.21	0.33	0.13	0.52	rs11585375	ATPIA2	
rs1358714	0.21	0.45	0.54	0.22	0.58	0.76	0.92	0.15	0.49	0.48	0.27	0.87	0.29	0.30	0.37	0.36	0.26	0.79	0.56	0.53	0.49	0.35	0.93	0.98	0.14	0.38	0.42	0.01	0.34	0.32	0.84	0.80	0.67	rs1200130	ATPIB1		
rs1040503	0.46	0.08	0.25	0.69	0.82	0.80	0.37	0.58	0.14	0.32	0.07	0.30	0.19	0.17	0.88	0.33	0.58	0.08	0.91	0.99	0.78	0.74	0.66	0.75	0.33	0.43	0.08	0.11	0.16	0.16	0.11	0.61	rs1358714	ATPIB1			
rs1464816	0.11	0.15	0.03	0.33	0.97	0.93	0.49	0.24	0.34	0.52	0.94	0.68	0.13	0.27	0.28	0.25	0.08	0.70	0.22	0.43	0.74	0.44	0.83	0.89	0.94	0.56	0.27	0.47	0.79	0.72	0.52	rs1040503	ATPIB1				
rs11571082	0.64	0.53	0.16	0.12	0.66	0.95	0.64	0.86	0.50	0.82	0.51	0.54	0.68	0.45	0.21	0.80	0.81	0.82	0.61	0.82	0.81	0.70	0.51	0.49	0.45	0.42	0.56	0.95	0.98	0.46	rs1464816	ATPIB1					
rs5705	0.23	0.28	0.91	0.21	0.07	0.92	0.72	0.59	0.32	1.00	0.03	0.83	0.38	0.22	0.62	0.15	0.59	0.64	0.71	0.96	0.23	0.52	0.49	0.91	0.08	0.34	0.06	0.34	0.32	rs11571082	REN						
rs10900555	0.88	0.78	0.95	0.11	0.71	0.78	0.93	0.58	0.69	0.18	0.81	0.45	0.81	0.29	0.16	0.20	0.84	0.96	0.97	0.59	0.84	0.84	0.53	0.06	0.26	0.16	0.44	0.93	rs5705	REN							
rs10924074	0.69	0.49	0.44	0.99	0.57	0.59	0.40	1.00	0.86	0.40	0.75	0.23	0.73	0.13	0.06	0.19	0.93	0.23	0.46	0.29	0.28	0.23	0.53	0.79	0.91	0.94	0.73	rs10900555	REN								
rs850609	0.74	0.52	0.95	0.26	0.80	0.99	0.45	0.83	0.82	0.41	0.16	0.21	0.08	0.16	0.79	0.65	0.12	0.29	0.27	0.26	0.26	0.22	0.49	0.60	0.52	0.15	rs10924074	ATPIA1									
rs2068230	0.80	0.81	0.77	0.31	0.54	0.63	0.83	0.53	0.11	0.50	0.07	0.11	0.55	0.36	0.37	0.15	0.65	0.60	0.78	0.55	0.72	0.32	0.30	0.65	0.72	0.32	0.30	0.65	rs850609	ATPIA1							
rs11614164	0.17	0.42	0.05	0.20	0.60	0.44	0.94	0.01	0.35	0.07	0.00	0.39	0.44	0.16	0.07	0.09	0.03	0.07	0.33	0.07	0.19	0.40	0.85	0.87	rs2068230	ATPIB3											
rs3782726	0.06	0.42	0.21	0.26	0.07	0.48	0.94	0.73	0.03	0.24	0.39	0.31	0.87	0.03	0.77	0.22	0.24	0.51	0.95	0.73	0.88	0.99	0.76	rs11614164	ATPIB3												
rs7973914	0.63	0.33	0.11	0.12	0.48	0.56	0.93	0.21	0.09	0.46	0.49	0.89	0.02	0.88	0.51	0.54	0.91	0.80	0.55	0.91	0.79	0.40	0.55	0.91	0.79	0.40	rs3782726	SCNN1A									
rs10849446	0.26	0.25	0.12	0.11	0.66	0.22	0.33	0.49	0.96	0.61	0.68	0.63	0.37	0.69	0.82	0.25	1.00	0.67	0.86	0.52	0.24	rs7973914	SCNN1A														
rs2286600	0.06	0.24	0.91	0.27	0.88	0.13	0.12	0.73	0.91	0.36	0.02	0.11	0.32	0.32	0.27	0.08	0.03	0.44	0.33	0.95	rs10849446	SCNN1A															
rs735	0.43	0.68	0.47	0.30	0.38	0.23	0.60	0.83	0.49	0.04	0.07	0.39	0.38	0.50	0.25	0.13	0.65	0.47	0.76	rs2286600	SCNN1G																
rs4247210	0.20	0.81	0.59	0.68	0.49	0.24	0.66	0.19	0.58	0.05	0.02	0.02	0.03	0.07	0.08	0.41	0.90	0.23	rs735	SCNN1G																	
rs11074555	0.60	0.35	0.97	0.76	0.25	0.60	0.76	0.85	0.66	0.65	0.70	0.72	0.28	0.53	0.50	0.50	0.61	0.50	0.61	rs4247210	SCNN1G																
rs9930640	0.86	0.68	0.61	0.29	0.38	0.76	0.42	0.09	0.18	0.18	0.41	0.23	0.28	0.08	0.38	0.28	rs11074555	SCNN1B																			
rs239345	0.51	0.63	0.17	0.14	0.93	1.00	0.80	0.63	0.61	0.72	0.89	0.87	0.06	0.94	0.19	rs9930640	SCNN1B																				
rs238547	0.17	0.45	0.43	0.86	0.94	0.40	0.13	0.15	0.08	0.26	0.26	0.05	0.02	0.64	rs239345	SCNN1B																					
rs8044970	0.25	0.18	0.53	0.75	0.06	0.06	0.06	0.70	0.65	0.45	0.56	0.81	0.19	rs238547	SCNN1B																						
rs152740	0.43	0.21	0.47	0.27	0.14	0.15	0.30	0.10	0.07	0.82	0.46	0.58	rs8044970	SCNN1B																							
rs250563	0.26	0.72	0.15	0.05	0.06	0.67	0.47	0.44	0.41	0.37	0.10	rs152740	SCNN1B																								
rs2303153	0.96	0.54	0.15	0.19	0.98	0.54	0.41	0.67	0.18	0.53	rs250563	SCNN1B																									
rs1403543	0.87	0.24	0.27	0.05	0.06	0.03	0.27	0.40	0.97	rs2303153	SCNN1B																										
rs194	0.97	0.99	0.43	0.42	0.35	0.97	0.14	0.18	rs1403543	AGTR2																											
rs11091046	0.76	0.36	0.25	0.33	0.88	0.45	0.55	rs194	AGTR2																												
rs2269370	0.35	0.27	0.34	0.85	0.47	0.52	rs11091046	AGTR2																													
rs2269372	0.55	0.48	0.15	0.03	0.36	rs2269370	RENBP																														
rs762656	0.06	0.03	0.10	0.32	rs2269372	RENBP																															
rs2968915	0.07	0.20	0.72	rs762656	RENBP																																
rs2968917	0.85	0.24	rs2968915	ATP6AP2																																	
rs10536	0.14	rs2968917	ATP6AP2																																		
	rs10536																																				

Table II.28. Results from the gene-gene interaction analysis between all the SNPs for Comp1. Significant interactions are indicated in bold red.

ATP1A2		ATP1B1		REN		ATP1A1		ATP1B3		SCNN1A		SCNN1G		SCNN1B		AGTR2		RENBP		ATP6AP2																	
rs7548116																																					
	0.79	0.99	0.64	0.61	0.36	0.12	0.75	0.44	0.03	0.13	0.98	0.24	0.08	0.91	0.87	0.75	0.75	0.43	0.20	0.85	0.96	0.61	0.86	0.50	0.38	0.05	0.17	0.17	0.21	0.18	0.25	0.36	0.75	0.67	0.78	rs7548116	ATP1A2
		0.58	0.45	0.83	0.86	0.53	0.35	0.82	0.80	0.84	0.60	0.56	0.77	0.96	0.26	0.34	0.93	0.53	0.90	0.16	0.35	0.04	0.12	0.52	0.24	0.89	0.72	0.19	0.19	0.16	0.42	0.66	0.57	0.83	0.91	rs11585375	ATP1A2
			0.42	0.53	0.98	0.31	0.65	0.70	0.52	0.06	0.45	0.68	0.46	0.73	0.72	0.39	0.41	0.20	0.69	0.82	0.80	0.77	0.88	0.17	0.63	0.56	0.85	0.45	0.54	0.19	0.46	0.44	0.68	0.85	0.64	rs1200130	ATP1B1
			0.39	0.47	0.41	0.51	0.43	0.37	0.72	0.87	0.01	0.02	0.08	0.26	0.45	0.80	0.80	0.88	0.32	0.63	0.27	0.56	0.68	0.48	0.74	0.56	0.05	0.09	0.90	0.87	0.85	0.31	0.75	0.79	rs1358714	ATP1B1	
				0.00	0.01	0.00	0.10	0.62	0.58	0.15	0.47	0.30	0.52	0.62	0.33	0.88	0.64	0.96	0.95	0.11	0.67	0.78	0.87	0.97	0.53	0.32	0.92	0.99	0.97	0.76	0.75	0.84	0.97	0.83	rs1040503	ATP1B1	
					0.61	0.72	0.44	0.54	0.69	0.88	0.09	0.13	0.39	0.57	0.30	0.35	0.81	0.52	0.44	0.43	0.59	0.39	0.95	0.70	0.98	0.74	0.59	0.63	0.09	0.20	0.27	0.84	0.63	0.69	rs1464816	REN	
					0.25	0.51	0.67	0.04	0.11	0.89	0.76	0.89	0.64	0.84	0.12	0.90	0.07	0.03	0.91	0.71	0.63	0.31	0.91	0.87	0.96	0.56	0.62	0.69	0.04	0.20	0.17	0.94	0.55	rs11571082	REN		
					0.34	0.67	0.46	0.20	0.69	0.74	0.98	0.48	0.83	0.54	0.71	0.11	0.13	0.68	0.67	0.28	0.43	0.99	0.80	0.99	0.60	0.65	0.38	0.07	0.28	0.58	0.95	0.61	rs5705	REN			
							0.99	0.02	0.68	0.88	0.59	0.83	0.38	0.75	0.87	0.47	0.58	0.26	0.02	0.02	0.07	0.95	0.06	0.96	0.38	0.33	0.51	0.70	0.92	0.91	0.91	0.98	rs10900555	ATP1A1			
							0.81	0.53	0.99	0.16	0.70	0.87	0.87	0.82	0.75	0.94	0.26	0.78	0.10	0.88	0.36	0.21	0.36	0.28	0.36	0.34	0.06	0.41	0.68	0.71	0.80	0.06	rs10924074	ATP1A1			
							0.44	0.41	0.61	0.18	0.77	0.74	0.50	0.68	0.06	0.83	0.03	0.00	0.23	0.58	0.22	0.45	0.43	0.88	0.83	0.50	0.32	0.48	0.35	0.50	0.65	rs850609	ATP1A1				
								0.02	0.22	0.18	0.17	0.25	0.51	0.95	0.02	0.27	0.02	0.00	0.30	0.22	0.01	0.12	0.52	0.21	0.33	0.82	0.07	0.24	0.34	0.68	0.76	rs2068230	ATP1B3				
									0.12	0.33	0.78	0.69	0.39	0.80	0.64	0.85	0.26	0.07	0.92	0.58	0.80	0.00	0.71	0.13	0.13	0.54	0.61	0.30	0.78	0.84	0.98	rs11614164	ATP1B3				
									0.16	0.84	0.61	0.43	0.95	0.28	1.00	0.62	0.05	0.70	0.75	0.91	0.00	0.56	0.12	0.13	0.29	0.78	0.46	0.97	0.92	0.64	rs3782726	SCNN1A					
									0.54	0.63	0.58	0.11	0.67	0.78	0.56	0.20	0.67	0.73	0.36	0.67	0.70	0.52	0.55	0.94	0.31	0.14	0.25	0.97	0.69	rs7973914	SCNN1A						
									0.15	0.97	0.43	0.91	0.09	0.98	0.36	0.54	0.55	0.05	0.98	0.33	0.95	0.97	0.72	0.91	0.60	0.88	0.81	0.23	rs10849446	SCNN1A							
									0.60	0.31	0.43	0.04	0.64	0.10	0.24	0.48	0.20	0.95	0.49	0.81	0.80	0.74	0.29	0.57	0.54	0.64	0.27	rs2286600	SCNN1G								
									0.23	0.98	0.15	0.91	0.47	0.82	0.90	0.00	0.02	0.01	0.02	0.02	0.06	0.21	0.24	0.62	0.30	0.22	rs5735	SCNN1G									
									0.46	0.75	0.80	0.73	0.82	0.66	0.11	0.83	0.60	0.95	0.90	0.83	0.09	0.31	0.54	0.64	0.88	0.04	0.70	0.99	0.67	0.86	0.04	rs11074555	SCNN1G				
									0.51	0.34	0.52	0.70	0.70	0.54	0.74	0.16	0.44	0.42	0.78	0.70	0.99	0.67	0.86	0.04	0.70	0.99	0.67	0.86	0.04	rs11074555	SCNN1G						
										0.56	0.41	0.62	0.76	0.78	0.08	0.50	0.91	0.88	0.23	0.47	0.53	0.76	0.54	0.06	rs9930640	SCNN1B											
											0.26	0.88	0.32	0.77	0.83	0.09	0.07	0.07	0.10	0.26	0.25	0.44	0.28	0.79	rs239345	SCNN1B											
											0.23	0.27	0.10	0.89	1.00	0.48	0.46	0.65	0.28	0.09	0.36	0.47	0.39	rs238547	SCNN1B												
											0.37	0.04	0.93	0.85	0.58	0.55	0.57	0.91	0.64	0.58	0.93	0.96	rs8044970	SCNN1B													
												0.04	0.41	0.55	0.29	0.31	0.38	0.58	0.52	0.19	0.39	0.10	rs152740	SCNN1B													
													0.71	0.60	0.06	0.07	0.61	0.94	0.80	0.03	0.01	0.23	rs250563	SCNN1B													
														0.14	0.60	0.64	0.16	0.40	0.22	0.51	0.59	0.39	rs2303153	SCNN1B													
															0.68	0.64	0.31	0.56	0.40	0.99	0.24	0.21	rs1403543	AGTR2													
															0.40	0.22	0.18	0.17	0.87	0.23	0.96	rs5194	AGTR2														
																0.25	0.19	0.18	0.92	0.21	0.91	rs11091046	AGTR2														
																	0.77	0.78	0.95	0.53	0.73	rs2269370	RENBP														
																		0.76	0.30	0.25	0.76	rs2269372	RENBP														
																			0.48	0.37	0.98	rs762656	RENBP														
																				0.73	0.50	rs2968915	ATP6AP2														
																				0.20	rs2968917	ATP6AP2															
																						rs10536	ATP6AP2														

REFERENCES

- Abecasis GR, Cookson WO, Cardon LR. 2000. Pedigree tests for transmission disequilibrium. *Eur J Hum Genet.* 8:545-551
- Adams TD, Yanowitz FG, Fisher AG, Ridges JD, Nelson AG, Hagan AD, Williams RR, Hunt SC. 1985. Heritability of cardiac size: an echocardiographic and electrocardiographic study of monozygotic and dizygotic twins. *Circulation* 71:39-44
- Ahmad U, Saleheen D, Bokhari A, Frossard PM. 2005. Strong association of a renin intronic dimorphism with essential hypertension. *Hypertens Res.* 28:339-344
- Akera T, Ng, YC. 1991. Digitalis sensitivity of Na⁺,K⁺-ATPase, myocytes and the heart. *Life Sci.* 48:97-106
- Alcalai R, Seidman JG, Seidman CE. 2008. Genetic basis of hypertrophic cardiomyopathy: from bench to the clinics. *J Cardiovasc Electrophysiol* 19:104-110
- Allen PD, Schmidt TA, Marsh JD, Kjeldsen K. 1992. Na,K-ATPase expression in normal and failing human left ventricle. *Basic Res Cardiol.* 87 Suppl 1:87-94
- Ambrosius WT, Bloem LJ, Zhou L, Rebhun JF, Snyder PM, Wagner MA, Guo C, Pratt JH. 1999. Genetic variants in the epithelial sodium channel in relation to aldosterone and potassium excretion and risk for hypertension. *Hypertension* 34:631-637
- Anan R, Greve G, Thierfelder L. 1994. Prognostic implications of novel beta-cardiac myosin heavy chain gene mutations that cause familial hypertrophic cardiomyopathy. *J Clin Invest.* 93:280-285
- Andersen PS, Havndrup O, Hougs L, Sorensen KM, Jensen M, Larsen LA, Hedley P, Thomsen ARB, Moolman-Smook J, Christiansen M, Bundgaard H. 2008. Diagnostic yield, interpretation,

and clinical utility of mutation screening of sarcomere encoding genes in Danish hypertrophic cardiomyopathy patients and relatives. *Hum Mutat.* 0:1-8 (Epub ahead of print)

Arad M, Seidman JG, Seidman CE. 2002. Phenotypic diversity in hypertrophic cardiomyopathy. *Hum Mol Genet.* 11:2499-2506

Arad M, Maron BJ, Gorham JM, Johnson WH, Saul JP, Perez-Atayde AR, Spirito P, Wright GB, Kanter RJ, Seidman CE, Seidman JG. Glycogen storage diseases presenting as hypertrophic cardiomyopathy. *N Engl J Med.* 352:362-372

Baek M, Weiss M. 2005. Down-regulation of Na⁺ pump α_2 isoform in isoprenaline-induced cardiac hypertrophy in rat: evidence for increased receptor binding affinity but reduced inotropic potency of digoxin. *J Pharmacol Exp Ther.* 313:731-739

Baker KM, Aceto JF. 1990. Angiotensin II stimulation of protein synthesis and cell growth in chick heart cells. *Am J Physiol.* 259:H610-H618

Bartunek J, Weinberg EO, Tajima M, Rohrbach S, Lorrel BH. 1999. Angiotensin II type 2 receptor blockade amplifies the early signals of cardiac growth response to angiotensin II in hypertrophied hearts. *Circulation* 99:22-25

Berry CR, Touyz AF, Dominiczak RC, Webb JDG. 2001. Angiotensin receptors: signaling, vascular pathophysiology, and interactions with ceramide. *Am J Physiol Heart Circ Physiol.* 281:H2337-H2365

Blanco G, Mercer RW. 1998. Isozymes of the Na-K-ATPase: heterogeneity in structure, diversity in function. *Am J Physiol.* 275:F633-F650

Bohlmeyer T, Ferdensi A, Bristow MR, Takahashi S, Zisman LS. 2003. Selective activation of N-Acyl-D-Glucosamine 2-Epimerase expression in failing human heart ventricular myocytes. *J Card Fail.* 9:59-68

Bonvalet JP, Alfaidy N, Farman N, Lombes M. 1995. Aldosterone: intracellular receptors in human heart. *Eur Heart J.* 16 Suppl N:92-97

Booz GW, Baker KM. 1996. Role of type 1 and type 2 angiotensin receptors in angiotensin II-induced cardiomyocyte hypertrophy. *Hypertension* 28:635-640

Booz GW. 2004. Cardiac Angiotensin AT₂ receptor: what exactly does it do? *Hypertension* 43:1162-1163

Borlak J, Thum T. 2003. Hallmarks of ion channel gene expression in end-stage heart failure. *FASEB J.* 17:1592-1608

Brand E, Chatelain N, Mulatero P, Fery I, Curnow K, Jeunemaitre X, Corvol P, Pascoe L, Soubrier F. 1998. Structural analysis and evaluation of the aldosterone synthase gene in hypertension. *Hypertension* 32:198-204

Burckle CA, Danser AHJ, Müller DN, Garrelds IM, Gasc J, Popova E, Plehm R, Peters J, Bader M, Nguyen G. 2006. Elevated blood pressure and heart rate in human renin receptor transgenic rats. *Hypertension* 47:552-556

Campbell SE, Janicki JS, Matsubara BB, Weber KT. 1993. Myocardial fibrosis in the rat with mineralocorticoid excess. Prevention of scarring by amiloride. *Am J Hypertens.* 6:487-495

Campbell H, Rudan I. 2002. Interpretation of genetic association studies in complex disease. *Pharmacogenomics J.* 2:349-360

Canessa CM, Schild L, Buell G, Thorens B, Gautschi I, Horisberger J-D, Rossier BC. 1994. Amiloride-sensitive epithelial Na⁺ channel is made of three homologous subunits. *Nature* 367:463-467

Cardon LR, Palmer LJ. 2003. Population stratification and spurious allelic association. *Lancet* 361:598-604

Catanzaro DF. 2005. Physiological relevance of renin/prorenin binding and uptake. *Hypertens Res.* 28: 97–105

Chai W, Danser AHJ. 2006. Why are mineralocorticoid receptor antagonists cardioprotective? *Naunyn-Schmiedeberg's Arch Pharmacol.* 374:153–162

Chai W, Hoedemaekers Y, van Schaik RH, van Fessem M, Garrelds IM, Saris JJ, Dooijes D, ten Cate FJ, Kofflard MM, Danser AH. 2006. Cardiac aldosterone in subjects with hypertrophic cardiomyopathy. *J Renin Angiotensin Aldosterone Syst.* 7:225-230

Chang YC, Liu X, Kim JDO, Ikeda MA, Layton MR, Weder AB, Cooper RS, Kardia SLR, Rao DC, Hunt SC, Luke A, Boerwinkle E, Chakravarti A. 2007. Multiple genes for essential-hypertension susceptibility on chromosome 1q. *Am J Hum Genet.* 80:253-264

Charron P, Dubourg O, Desnos M, Isnard R, Hagege A, Bonne G, Carrier L, Tesson F, Bouhour JB, Buzzi JC, Feingold J, Schwartz K, Komajda M. 1998. Genotype-phenotype correlations in familial hypertrophic cardiomyopathy. A comparison between mutations in the cardiac protein-C and the beta-myosin heavy chain genes. *Eur Heart J.* 19:139-145

Chung M, Tsoutsman T, Semsarian C. 2003. Hypertrophic cardiomyopathy: from gene defect to clinical disease. *Cell Research* 13:9-20

Colhoun HM, McKeigue PM, Smith GD. 2003. Problems of reporting genetic associations with complex outcomes. *Lancet* 361:865-872

Collins A, Lau W, De La Vega FM. 2004. Mapping Genes for Common Diseases: The Case for Genetic (LD) Maps. *Hum hered.* 58:2-9

Cordell HJ. 2002. Epistasis: what it means, what it doesn't mean, and statistical methods to detect it in humans. *Hum Mol Genet.* 11:2463-2468

Corfield VA, Moolman JC, Martell R, Brink PA. 1993. Polymerase chain reaction-based detection of MN blood group-specific sequences in the human genome. *Transfusion* 33:119-124

Dahlof B, Devereux RB, Kjeldsen SE, Julius S, Beevers G, de Faire U, Fyhrquist F, Ibsen H, Kristiansson K, Lederballe-Pedersen O, Lindholm LH, Nieminen MS, Omvik P, Poaril S, Wedel H, Losartan Intervention for Endpoint reduction in hypertension Study Investigators. 2002. Cardiovascular morbidity and mortality in the Losartan Intervention For Endpoint reduction in hypertension study (LIFE): a randomised trial against atenolol. *Lancet* 359:995-1003

Danser AHJ, Derkx FHM, Schalekamp MADH, Hense HW, Riegger GAJ, Schunkert H. 1998. Determinants of interindividual variation of renin and pro-renin concentrations: evidence for a sexual dimorphism of (pro)renin levels in humans. *J Hypertens.* 16:853– 62

Danser AHJ, Saris JJ. 2002. Prorenin uptake in the heart: a prerequisite for local angiotensin generation? *J Mol Cell Cardiol.* 34:1463–1472

De Gasparo M, Catt KJ, Inagami T, Wright JW, Unger TH. 2002 International Union of Pharmacology. XXIII. The Angiotensin II Receptors. *Pharmacol Rev.* 52:415–472

Deinum J, van Gool JMG, Kofflard MJM, ten Cate FJ, Danser AHJ. 2001. Angiotensin II type 2 receptors and cardiac hypertrophy in women with hypertrophic cardiomyopathy. *Hypertension* 38:1278-1281

De Lannoy LM, Danser AH, van Kats JP, Schoemaker RG, Saxena PR, Schalekamp MA. 1997. Renin-angiotensin system components in the interstitial fluid of the isolated perfused rat heart: local production of angiotensin I. *Hypertension* 29:1111–1117

De La Vega FM, Isaac HI, Scafe CR. 2006. A tool for selecting SNPs for association studies based on observed linkage disequilibrium patterns. *Pac Symp Biocomput.* 487-498

De La Vega FM. 2007. Selecting single-nucleotide polymorphisms for association studies with SNPbrowser software. *Methods Mol Biol.* 376:177-193

Delles C, Erdmann J, Jacobo J, Hilgers KF, Fleck E, Regitz-Zagrosek V. 2001. Aldosterone synthase (CYP11B2)-344 C/T polymorphism is associated with left ventricular structure in human arterial hypertension. *J Am Coll Cardiol.* 37:878-884

Derkx FH, Deinum J, Lipovski M, Verhaar M, Fischli W, Schalekamp MADH. 1992. Nonproteolytic “activation” of pro-renin by active site-directed renin inhibitors as demonstrated by renin-specific monoclonal antibody. *J Biol Chem.* 267:22837– 22842

Devereux RB, Roman MJ. 1993. Inter-relationships between hypertension, left ventricular hypertrophy and coronary heart disease. *J Hypertens.* 11:3-9

Devereux RB, Palmieri V, Sharpe N, De Quattro V, Bella JN, Di Simone G, Walker JF, Hahn RT, Dahlof B. 2001. Effects of once daily angiotensin converting enzyme inhibition and calcium channel blockade-based antihypertensive treatment regimens on left ventricular hypertrophy and diastolic filling in hypertension: the prospective randomized enalapril study evaluating regression of ventricular enlargement (preserve) trial. *Circulation* 104:1248-1254

Devereux RB, Wachtell K, Gerds E, Bosman K, Nieminen MS, Papademetriou V, Rokkedal J, Harris K, Aurup P, Dahlof B. 2004. Prognostic significance of left ventricular mass change during treatment of hypertension. *JAMA* 292:2350

Domenighetti AA, Wang Q, Egger M, Richards SM, Pedrazzini T, Delbridge LM. 2005. Angiotensin II-mediated phenotypic cardiomyocyte remodeling leads to age-dependent cardiac dysfunction and failure. *Hypertension* 46:426–432

Donahue MP, Allen AS. 2005. Genetic association studies in cardiology. *Am Heart J.* 149:964-970

Doris PA. 2002. Hypertension genetics, single nucleotide polymorphisms, and the common disease: common variant hypothesis. *Hypertension* 39:323-336

Dostal DE, Baker KM. 1992. Angiotensin II stimulation of left ventricular hypertrophy in adult rat heart. Mediation by the AT1 receptor. *Am J Hypertens.* 5:576-280

Dostal DE, Rothblum KN, Chernin MI, Cooper GR, Baker KM. 1992. Intracardiac detection of angiotensinogen and renin: a localized renin-angiotensin system in neonatal rat heart. *Am J Physiol.* 363:C838-C850

Dostanic I, Schultz JEJ, Lorenz JN, Lingrel JB. 2004. The alpha 1 isoform of Na,K-ATPase regulates cardiac contractility and functionally interacts and co-localizes with the Na/Ca exchanger in heart. *J Biol Chem.* 279:54053-54061

Dzau VJ, Re RN. 1987. Evidence for the existence of renin in the heart. *Circulation* 75(suppl I):I134-I136

Eaton DC, Malik B, Saxena NC, Al-Khalili OK, Yue G. 2001. Mechanisms of aldosterone's action on epithelial Na⁺ transport. *J Membrane Biol.* 184:313-319

Edelheit O, Hanukoglu I, Gizewska M, Kandemir N, Tenenbaum-Rakover Y, Yurdakok M, Zajaczek S, Hanukoglu A. 2005. Novel mutations in epithelial sodium channel (ENaC) subunit genes and phenotypic expression of multisystem pseudohypoaldosteronism. *Clin Endocrin.* 62:547-553

Epstein ND, Cohn GM, Cyran F, Fananapazir L. 1992. Differences in clinical expression of hypertrophic cardiomyopathy associated with two distinct mutations in the β -myosin heavy chain gene: a 908^{Leu→Val} mutation and a 403^{Arg→Gln} mutation. *Circulation* 86:345-352

Erdmann J, Guse M, Kallisch H, Fleck E, Regitz-Zagrosek V. 2000. Novel intronic polymorphism (+1675G/A) in the human angiotensin II subtype 2 receptor gene. *Hum Mutat.* 15:487

Erdmann J, Raible J, Maki-Abedi J, Hummel M, Hammann J, Wollnik B, Frantz E, Fleck E, Hetzer R, Regitz-Zagrosek V. 2001. Spectrum of clinical phenotypes and gene variants in cardiac myosin-binding protein C mutation carriers with hypertrophic cardiomyopathy. *J Am Coll Cardiol.* 38:322-330

Fananapazir L, Epstein ND. 1994. Genotype-phenotype correlations in hypertrophic cardiomyopathy. Insights provided by comparisons of kindreds with distinct and identical beta-myosin heavy chain gene mutations. *Circulation* 89:22-32

Forissier JF, Charron P, Tezenas du Montcel S, Hagege A, Isnard R, Carrier L, Richard P, Desnos M, Bouhour JB, Schwartz K, Komajda M, Dubourg O. 2005. Diagnostic accuracy of a 2D left ventricle hypertrophy score for familial hypertrophic cardiomyopathy. *Eur Heart J.* 26:1882-1886

Gabriel SB, Schaffner SF, Nguyen H, Moore JM, Roy J, Blumenstiel B, Higgins J, DeFelice M, Lochner A, Faggart M, Liu-Cordero SN, Rotimi C, Adeyemo A, Cooper R, Ward R, Lander ES, Daly MJ, Altshuler D. 2002. The structure of haplotype blocks in the human genome. *Science* 296:2225-2229

Geier C, Perrot A, Ozcelik C, Binner P, Counsell D, Hoffmann K, Pilz B, Martiniak Y, Gehmlich K, Van Der Ven PF, Furst DO, Vornwald A, Von Hodenberg E, Nurnberg P, Scheffold T, Dietz R, Osterziel KJ. 2003. Mutations in the human muscle LIM protein gene in families with hypertrophic cardiomyopathy. *Circulation* 107:1390-1395

Geisterfer-Lowrance AA, Kass S, Tanigawa G, Vosberg HP, McKenna W, Seidman CE, Seidman JG. 1990. A molecular basis for familial hypertrophic cardiomyopathy: a beta myosin heavy chain gene missense mutation. *Cell* 62:999-1006

Geisterfer-Lowrance AA, Christe M, Conner DA, Ingwall JS, Schoen FJ, Seidman CE, Seidman JG. 1996. A mouse model of familial hypertrophic cardiomyopathy. *Science* 272: 731-734

Geller DS, Farhi A, Pinkerton N, Fradley M, Motitz M, Spitzer A, Meinke G, Tsai FTF, Sigler PB, Lifton RP. 2000. Activating mineralocorticoid receptor mutation in hypertension exacerbated by pregnancy. *Science* 289:119-123\

Gombos EA, Freis ED, Moghadam A. 1966. Effects of MK-870 in normal subjects and hypertensive patients *N Eng J Med.* 275:1215-1220

Gordon D, Finch SJ. 2005. Factors affecting statistical power in the detection of genetic association. *J Clin Invest.* 115:1408–1418

Gradman AH, Kad R. 2008. Renin inhibition in hypertension. *J Am Coll Cardiol.* 51:519-528

GriendlingKK, Murphy TJ, Alexander RW. 1993. Molecular biology of the renin-angiotensin system. *Circulation* 87:1816-1828

Haider AW, Larson MG, Benjamin EJ, Levy D. 1998. Increased left ventricular mass and hypertrophy are associated with increased risk for sudden death. *J Am Coll Cardiol.* 32:1454-1462

Hansson JH, Schild L, Lu Y, Wilson TA, Gautschi I, Shimkets R, Nelson-Williams C, Rossier BC, Lifton RP. 1995. A de novo missense mutation of the beta subunit of the epithelial sodium channel causes hypertension and Liddle syndrome, identifying a proline-rich segment critical for regulation of channel activity. *Proc Natl Acad Sci USA.* 92:11495-11499

Harrap SB, Dominiczak AF, Fraser R, Lever AF, Morton JJ, Foy CJ, Watt GCM. 1996. Plasma angiotensin II, predisposition to hypertension, and left ventricular size in healthy young adults. *Circulation* 93:1148-1154

Harshfield GA, Grim CE, Hwang C, Savage DD, Anderson SJ. 1990. Genetic and environmental influences on echocardiographically determined left ventricular mass in black twins. *Am J Hypertens.* 3:538-543

Hasimu B, Nakayama T, Mizutani Y, Izumi Y, Asai S, Soma M, Kokubun S, Ozawa Y. 2003. Haplotype analysis of the human renin gene and essential hypertension. *Hypertension* 41:308-312

Hautanena A, Lankinen L, Kupari M, Janne OA, Adlercreutz H, Nikkila H, White PC. 1998. Associations between aldosterone synthase gene polymorphism and the adrenocortical function in males. *J Intern Med.* 244:11-18

Herrmann S, Nicaud V, Schmidt-Petersen K, Pfeifer J, Erdmann J, McDonagh T, Dargie HJ, Paul M, Regitz-Zagrosek. 2002. Angiotensin II type 2 receptor gene polymorphism and cardiovascular phenotypes: the GLAECO and GLAOLD studies. *Eur J Heart Fail.* 4:707-712

Ho CY, Lever HM, DeSanctis R, Farver CF, Seidman JG, Seidman CE. 2000. Homozygous mutation in cardiac troponin T: Implications for hypertrophic cardiomyopathy. *Circulation* 102:1950-1955

Hoffmann B, Schmidt-Traub H, Perrot A, Osterziel KJ, Gessner R. 2001. First mutation in cardiac troponin C, L29Q, in a patient with hypertrophic cardiomyopathy. *Hum Mutat.* 17:524

Hoffmann S, Krause T, van Geel PP, Willenbrock R, Pagel I, Pinto Y, Buikema H, van Gilst WH, Lindschau C, Paul M, Inagami T, Ganten D, Urata H. 2001a. Overexpression of the human angiotensin II type 1 receptor in the rat heart augments load induced cardiac hypertrophy. *J Mol Med.* 79:601-608

Hoffmann S. 2005. Cardiac-specific overexpression of angiotensin II type 1 receptor in transgenic rats. *Methods Mol Med.* 112:389–403

Huang L, Li H, Xie Z. 1997. Ouabain-induced hypertrophy in cultured cardiac myocytes is accompanied by changes in expression of several late response genes. *J Mol Cell Cardiol.* 29:429-437

Huang Y, Wongamorntham S, Kasting J, McQuillan D, Owens RT, Yu L, Noble NA, Border W. 2006. Renin increases mesangial cell transforming growth factor- β 1 and matrix proteins through receptor-mediated, angiotensin II-independent mechanisms. *Kidney Int.* 69:105-113

Ichihara A, Suzuki F, Nakagawa T, Kaneshiro Y, Takemitsu T, Sakoda M, Nabi AH, Nishiyama A, Sugaya T, Hayashi M, Inagami T. 2006. Pro-renin receptor blockade inhibits development of glomerulosclerosis in diabetic angiotensin II type 1a receptor-deficient mice. *J Am Soc Nephrol.* 17:1950-1961

Iles MM. Linkage and association: The transmission/disequilibrium test for QTLs. In: *Quantitative Trait Loci: methods and protocols.* New Jersey, Pa: Humana Press Inc. 2002. 101-138

Ishanov A, Okamoto H, Yoneya K, Watanabe M, Nakagawa I, Machida M, Onozuka H, Mikami T, Kawaguchi H, Hata A, Kondo K, Kitabatake A. 1997. Angiotensinogen gene polymorphism in Japanese patients with hypertrophic cardiomyopathy. *Am Heart J.* 133:184-189

Innes BA, McLaughlin MG, Kapuscinski MK, Jacob HJ, Harrap SB. 1998. Independent genetic susceptibility to cardiac hypertrophy in inherited hypertension. *Hypertension* 31:741-746

Iwai N, Ohmichi N, Nakamura Y, Kinoshita M. 1994. DD genotype of the angiotensin-converting enzyme gene is a risk factor for left ventricular hypertrophy. *Circulation* 90:2622-2628

Iwai N, Baba S, Mannami T, Ogihara T, Ogata J. 2002. Association of a sodium channel α subunit promoter variant with blood pressure. *J Am Soc Nephrol.* 13:80-85

Jeunemaitre X, Bassilana F, Persu A, Dumont C, Champigny G, Lazdunski M, Corvol P, Barbry P. 1997. Genotype-phenotype analysis of a newly discovered family with Liddle's syndrome. *J Hypertension.* 15:1091-1100

Johnson GCL, Esposito L, Barratt BJ, Smith AN, Heward J, Di Genova G, Ueda H, Cordell HJ, Eaves IA, Dudbridge F, Twells RC, Payne F, Hughes W, Nutland S, Stevens H, Carr P, Tuomilehto-Wolf E, Tuomilehto J, Gough SC, Clayton DG, Todd JA. 2001. Haplotype tagging for the identification of common disease genes. *Nat Genet.* 29:233-837

Kaderali L. 2007. Primer design for multiplexed genotyping. *Methods Mol Biol.* 402:269-286

Kamynina E, Staub O. 2002. Concerted action of ENaC, Nedd4-2, and Sgk1 in transepithelial Na⁺ transport. *Am J PhysiolRenal Physiol.* 283:F377-F387

Kaplan JH. 2002. Biochemistry of Na,K-ATPase. *Annu Rev Biochem.* 71:511-535

Kato N, Hyne G, Bihoreau MT, Gauguier D, Lathrop GM, Rapp JP. 1999. Complete genome searches for quantitative trait loci controlling blood pressure and related traits in four segregating populations derived from Dahl hypertensive rats. *Mamm Genome* 10:259-265

Kaufman BD, Auerbach S, Sushma R, Manlhiot C, Deng L, Prakash A, Printz BF, Gruber D, Papavassiliou DP, Hsu DT, Sehnert AJ, Chung WK, Mital S. 2007. RAAS gene polymorphisms influence progression of paediatric hypertrophic cardiomyopathy. *Hum Genet.* 122:515-523

Kimura A, Harada H, Park JE, Nishi H, Satoh M, Takahashi M, Hiroi S, Sasaoka T, Ohbuchi N, Nakamura T, Koyanagi T, Hwang TH, Choo JA, Chung KS, Hasegawa A, Nagai R, Okazaki O, Nakamura H, Matsuzaki M, Sakamoto T, Toshima H, Koga Y, Imaizumi T, Sasazuki T. 1997.

Mutations in the cardiac troponin I gene associated with hypertrophic cardiomyopathy. *Nat Genet.* 16:379-3825

Kometiani P, Li J, Gnudi L, Kahn BB, Askari A, Xie Z. 1998. Multiple signal transduction pathways link Na⁺/K⁺-ATPase to growth-related genes in cardiac myocytes. The roles of Ras and mitogen-activated protein kinases. *J Biol Chem.* 273:15249-15256

Koren MJ, Devereux RB, Casale PN, Savage DD, Laragh JH. 1991. Relation of left ventricular mass and geometry to morbidity and mortality in uncomplicated essential hypertension. *Ann Intern Med.* 114:345-352

Klues HG, Schiffers A, Maron BJ. 1995. Phenotypic spectrum and patterns of left ventricular hypertrophy in hypertrophic cardiomyopathy: morphologic observations and significance as assessed by two-dimensional echocardiography in 600 patients. *J Am Coll Cardiol.* 26:1699-708

Kristensen VN, Kelefiotis D, Kristensen T, Borrensens-Dale L. 2001. High-throughput methods for detection of genetic variation. *BioTechniques* 30:318-332

Kunz R, Kreutz R, Beige J, Distler A, Sharma AM. 1997. Association between the angiotensinogen 235-T variant and essential hypertension in whites: a systematic review and methodological appraisal. *Hypertension* 30:1331-1337

Kuo TY, Lau W, Collins AR. 2007. LDMAP: the construction of high-resolution linkage disequilibrium maps of the human genome. *Methods Mol Biol.* 376:47-57

Kutyavin IV, Afonina IA, Mills A, Gorn VV, Lukhtanov EA, Belousov ES, Singer MJ, Walburger DK, Lokhov SG, Gall AA, Dempcy R, Reed MW, Meyer RB, Hedgpeth J. 2000. 3'-minor groove binder-DNA probes increase sequence specificity at PCR extension temperatures. *Nucleic Acids Res.* 28:655-661

Lechin M, Quinones MA, Omran A, Hill R, Yu QT, Rakowski H, Wigle D, Liew CC, Sole M, Roberts R. 1995. Angiotensin-I converting enzyme genotypes and left ventricular hypertrophy in patients with hypertrophic cardiomyopathy. *Circulation* 92:1808-1812

Lekanne Deprez RH, Muurling-Vlietman JJ, Hruđa J, Baars MJ, Wijnaendts LC, Stolke-Dijkstra I, Alders M, Van Hagen JM. 2006. Two cases of severe neonatal hypertrophic cardiomyopathy caused by compound heterozygous mutations in the MYBPC3 gene. *J Med Genet.* 43:829-832

Lemarié CA, Paradis P, Schiffrin EL. 2008. New insights on signaling cascades induced by cross-talk between angiotensin II and aldosterone. *J Mol Med.* 86:673–678

Levy D, Labib SB, Anderson KM, Christiansen JC, Kannel WB, Castelli WP. 1990. Determinants of sensitivity and specificity of electrocardiographic criteria for left ventricular hypertrophy. *Circulation* 81:815-820

Lieb W, Graf J, Gotz A, Koning AR, Mayer B, Fisher M, Stritzke J, Hengstenberg C, Holmer SR, Doring A, Lowel H, Schunkert H, Erdmann J. 2006. Association of angiotensin-converting enzyme 2 (ACE2) gene polymorphisms with parameters of left ventricular hypertrophy in men. Results from the MONICA Augsburg echocardiographic study. *J Mol Med.* 84:88-96

Lijnen P, Petrov V. 1999. Renin-angiotensin system, hypertrophy and gene expression in cardiac myocytes. *J Mol Cell Cardiol.* 31:949-970

Lindpaintner K, Jin M, Niedermeier N, Wilhelm MJ, Ganten D. 1990. Cardiac angiotensinogen and its local activation in the isolated perfused beating heart. *Circ Res.* 67:564-573

Lombes M, Alfaidy N, Emmanuel E, Alessandro L, Farman N, Bonvalet JP. 1995. Molecular and Cellular Cardiology: Prerequisite for Cardiac Aldosterone Action: Mineralocorticoid Receptor and 11 beta -Hydroxysteroid Dehydrogenase in the Human Heart. *Circulation* 92:175-182

Makridakis NM, Reichardt JK. 2001. Multiplex automated primer extension analysis: simultaneous genotyping of several polymorphisms. *BioTechniques* 31:1374-1380

Malik N, Canfield V, Sanchez-Watts G, Watts AG, Scherer S, Beatty BG, Gros P, Levenson R. 1998. Structural organization and chromosomal localization of the human Na,K-ATPase beta 3 subunit gene and pseudogene. *Mamm Genome*. 9:136-143

Malmqvist K, Ohman KP, Lind L, Nystrom F, Kahan T. 2002. Relationships between left ventricular mass and the renin-angiotensin system, catecholamines, insulin and leptin. *J Intern Med*. 252:430-439

Maniatis N, Collins A, Gibson J, Zhang W, Tapper W, Morton NE. 2004. Positional cloning by linkage disequilibrium. *Am J Hum Genet*. 75:846-855

Maniatis N, Morton NE, Gibson J, Xu C-F, Hosking LK, Collins A. 2005. The optimal measure of linkage disequilibrium reduces error in association mapping of affection status. *Hum Mol Genet*. 14:145-153

Marian AJ. 2001. On genetic and phenotypic variability of hypertrophic cardiomyopathy: nature versus nurture. *J Am Coll Cardiol*. 38:331-334

Marian AJ. 2002. Modifier genes for hypertrophic cardiomyopathy. *Curr Opin Cardiol*. 17:242-252

Marian AJ, Yu Q, Workman R, Greve G, Roberts. 1993. Angiotensin-converting enzyme polymorphism in hypertrophic cardiomyopathy and sudden cardiac death. *Lancet* 342:1085-1086

Marian AJ, Mares A Jr, Kelly DP, Yu Q-T, Abchee AB, Hill R, Roberts R. 1995. Sudden cardiac death in hypertrophic cardiomyopathy: variability in phenotypic expression of beta-myosin heavy chain mutations. *Eur Heart J*. 16:368-376

Marian AJ, Roberts R. 1998. Molecular genetic basis of hypertrophic cardiomyopathy: genetic markers for sudden cardiac death. *J Cardiovasc Electrophysiol.* 9:88-99

Maron BJ, Bonow RO, Cannon RO, Leon MB, Epstein SE. 1987. Hypertrophic cardiomyopathy: interrelation of clinical manifestations, pathophysiology, and therapy. *N Engl J Med.* 316:780-789

Maron BJ, Gardin JM, Flack JM, Gidding SS, Kurosaki TT, Bild DE. 1995. Prevalence of hypertrophic cardiomyopathy in a general population of young adults. Echocardiographic analysis of 4111 subjects in the CARDIA study. *Circulation* 92:785-789

Maron BJ. 2002. Hypertrophic cardiomyopathy: a systematic review. *JAMA* 287:1308-1320

Maron BJ, McKenna WJ, Danielson GK, Kappenberger LJ, Kuhn HJ, Seidman CE, Shah PM, Spencer WH, Spirito P, Ten Cate FJ, Wigle ED. 2003. ACC/ESC clinical expert consensus document on hypertrophic cardiomyopathy: a report of the American College of Cardiology Task Force on Clinical Expert Consensus Documents and the European Society of Cardiology Committee for Practise Guidelines (Committee to Develop an Expert Consensus Document on Hypertrophic Cardiomyopathy). *Eur Heart J.* 24:1965-1991

Marrero MB, Schieffer B, Paxton WG, Heerdt L, Berk BC, Delafontaine P, Bernstein KE. 1995. Direct stimulation of Jak/STAT pathway by the angiotensin II AT1 receptor. *Nature* 375:247-250

Mathew J, Lonn E, Johnstone D. 2000. Left ventricular hypertrophy by electrocardiogram predicts death and development of heart failure in high-risk patients without systolic dysfunction. *J Am Coll Cardiol.* 35(suppl A):212A

Mathew J, Sleight P, Lonn E, Johnstone D, Pogue J, Yi Q, Bosch J, Sussex B, Probstfield J, Yusuf S, Heart Outcomes Prevention Evaluation (HOPE) Investigators. 2001. Reduction of

cardiovascular risk by regression of electrocardiographic markers of left ventricular hypertrophy by the angiotensin-converting enzyme inhibitor ramipril. *Circulation* 104:1615

Matsubara H. 1998. Pathophysiological role of Angiotensin II Type 2 Receptor in cardiovascular and renal diseases. *Circ Res.* 83:1182-1191

Matsumura K, Fujii K, Oniki H, Oka M, Iida M. 2006. Role of aldosterone in left ventricular hypertrophy in hypertension. *Am J Hyper.* 19:13-18

Mayosi BM, Keavney B, Watkins H, Farrall M. 2003. Measured haplotype analysis of the aldosterone synthase gene and heart size. *Eur J Hum Genet.* 11:395-401

McIntyre LM, Martin ER, Simonsen KL, Kaplan NL. 2000. Circumventing multiple testing: a multilocus monte carlo approach to testing for association. *Genet Epidemiol.* 19:18–29

McLenachan JM, Henderson E, Morris KI, Dargie HJ. 1987. Ventricular arrhythmias in patients with hypertensive left ventricular hypertrophy. *N Engl J Med.* 317:787-792

Mehta PK, Griendling KK. 2007. Angiotensin II cell signaling: physiological and pathological effects in the cardiovascular system. *Am J Physiol Cell Physiol.* 292:C82–C97

Messerli FH, Schmieder RE, Weir MR. Salt. 1997. A perpetrator of hypertensive target organ disease? *Arch Intern Med.* 157:2449-2452

Methot D, Silversides DW, Reudelhuber TL. 1999. In vivo enzymatic assay reveals catalytic activity of the human renin precursor in tissues. *Circ Res.* 84:1067-1072

Mirkovic S, Seymour AM, Fenning A, Strachan A, Margolin SB, Taylor SM, Brown L. 2002. Attenuation of cardiac fibrosis by pirfenidone and amiloride in DOCA-salt hypertensive rats. *Br J Pharmacol.* 135:961-968

Mogensen J, Klausen IC, Pedersen AK, Egeblad H, Bross P, Kruse TA, Gregersen N, Hansen PS, Baandrup U, Borglum AD. 1999. α -cardiac actin is a novel disease gene in familial hypertrophic cardiomyopathy. *J Clin Invest.* 103:R39-R43

Mohidden SA, Begley DA, McLam E, Cardoso JP, Winkler JB, Sellers JR, Fananapazir L. Utility of genetic screening in hypertrophic cardiomyopathy: Prevalence and significance of novel and double (homozygous and heterozygous) beta-myosin mutations. *Genet Test.* 7:21-27

Moolman JC, Corfield VA, Posen B, Ngumbela K, Seidman C, Brink PA, Watkins H. 1997. Sudden death due to troponin T mutations. *J Am Coll Cardiol.* 29:549-555

Moolman-Smook JC, De Lange WJ, Bruwer EC, Brink PA, Corfield VA. 1999. The origins of hypertrophic cardiomyopathy-causing mutations in two South African subpopulations: a unique profile of both independent and founder events. *Am J Hum Genet.* 65:1308-1320

Mottl AK, Shoham DA, North KE. 2008. Angiotensin II type 1 receptor polymorphisms and susceptibility to hypertension: a HuGE review. *Genet Med.* 10:560-574

Mukawa H, Yoki Y, Miyazaki Y, Matsui H, Okumura K, Ito T. 2003. Angiotensin II type 2 receptor blockade partially negates antihypertrophic effects of type 1 receptor blockade on pressure-overload rat cardiac hypertrophy. *Hypertens Res.* 26:89-95

Muller DN, Fischli W, Clozel J, Hilgers KF, Bohlender J, Menard J, Busjahn A, Ganten D, Luft FC. 1998. Local angiotensin II generation in the rat heart. Role of renin uptake. *Circ Res* 82:13-20

Muller-Ehmsen J, Wang J, Schwinger RHG, McDonough. 2001. Region specific regulation of sodium pump isoform and Na,Ca-exchanger expression in the failing human heart--right atrium vs left ventricle. *Cell Mol Biol.* 47:373-381

Munoz-Brauning CR, Carvajal CA, Mosso LM, Valdivia G, Fardella CE. 2005. Satellite marker AGAT of the mineralocorticoid receptor gene is associated with plasma renin activity in patients with essential hypertension. *Rev Med Chile*. 133:1415-1423

Nagata K, Obata K, Xu J, Ichihara S, Noda A, Kimata H, Kato T, Izawa H, Murohara T, Yokota M. 2006. Mineralocorticoid receptor antagonism attenuates cardiac hypertrophy and failure in low-aldosterone hypertensive rats. *Hypertension* 47:656-664

Neal B, MacMahon S, Chapman N. 2000. Effects of ACE inhibitors, calcium antagonists, and other blood-pressure-lowering drugs: results of prospectively designed overviews of randomized trials: Blood Pressure Lowering Treatment Trialists' Collaboration. *Lancet* 356:1955–1964

Neitzel H. 1986. A routine method for the establishment of permanent growing lymphoblastoid cell lines. *Hum Genet*. 73:320-326

Nguyen G, Delarue F, Berrou J, Rondeau E, Sraer JD. 1996. Specific receptor binding of renin on human mesangial cells in culture increases plasminogen activator inhibitor-1 antigen. *Kidney Int*. 50:1897-1903

Nguyen G, Delarue F, Burcklé C, Bouzahir L, Giller T, Sraer J-D. 2002. Pivotal role of the renin/pro-renin receptor in angiotensin II production and cellular responses to renin. *J Clin Invest*. 109:1417–1427

Nguyen G, Burckle C, Sraer J-D. 2003. The renin receptor: the facts, the promise and the hope. *Curr Opin Nephrol Hypertens*. 12:51-55

Nguyen G, Burckle CA, Sraer JD. 2004. Renin/prorenin-receptor biochemistry and functional significance. *Curr Hypertens Rep*. 6:129–132

Nguyen G, Danser AHJ. 2006. The (pro)renin receptor: therapeutic consequences. *Expert Opin Investig Drugs*. 15:1131–1135

Niimura H, Bachinski LL, Sangwatanaroj S, Watkins H, Chudley AE, McKenna W, Kristinsson A, Roberts R, Sole M, Maron BJ, Seidman JG, Seidman CE. 1998. Mutations in the gene for cardiac myosin-binding protein C and late-onset familial hypertrophic cardiomyopathy. *N Engl J Med.* 338:1248-1257

Niimura H, Patton KK, McKenna WJ, Soultis J, Maron BJ, Seidman JG, Seidman CE. 2002. Sarcomere protein gene mutations in hypertrophic cardiomyopathy of the elderly. *Circulation* 105:446-451

Nio Y, Matsubara H, Murasawa S, Kanasaki M, Inada M. 1995. Regulation of gene transcription of angiotensin II receptor subtypes in myocardial infarction. *J Clin Invest.* 95:46-54

O'Donnell CJ, Lindpaintner K, Larson MG, Rao VS, Ordovas JM, Schaefer EJ, Myers RH, Levy D. 1998. Evidence for association and genetic linkage of the angiotensin-converting enzyme locus with hypertension and blood pressure in men but not women in the Framingham heart study. *Circulation* 97:1766-1772.

Ohkubo N, Matsubara H, Nozawa Y, Mori Y, Murasawa S, Kijima K, Maruyama K, Masaki H, Tsutumi Y, Shibasaki Y, Iwasaka T, Inada M. 1997. Angiotensin type 2 receptors are reexpressed by cardiac fibroblasts from failing myopathic hamster hearts and inhibit cell growth and fibrillar collagen metabolism. *Circulation* 96:3954-3962

Okin PM, Devereux RB, Jern S, Kjeldsen SE, Julius S, Nieminen MS, Snapinn S, Harris KE, Aurup P, Edelman JM, Dahlof B. Losartan Intervention for Endpoint reduction in hypertension Study Investigators. 2003. Regression of electrocardiographic left ventricular hypertrophy by losartan versus atenolol: The Losartan Intervention for Endpoint reduction in Hypertension (LIFE) Study. *Circulation* 108:684-690

Oliver JA. 2006. Receptor mediated actions of renin and pro-renin. *Kidney Int.* 69:13-15

Osio A, Tan L, Chen SN, Lombardi R, Nagueh SF, Shete S, Roberts R, Willerson JT, Marian AJ. Myozenin 2 is a novel gene for human hypertrophic cardiomyopathy. *Circ Res.* 100:766-768

Osterop APRM, Kofflard MJM, Sandkuijl LA, ten Cate FJ, Krams R, Schalekamp MADH, Danser AHJ. 1998. AT1 receptor A/C1166 polymorphism contributes to cardiac hypertrophy in subjects with hypertrophic cardiomyopathy. *Hypertension* 32:825-830

Palmieri V, Devereux RB. 2002. Angiotensin converting enzyme inhibition and dihydropyridine calcium channel blockade in the treatment of left ventricular hypertrophy in arterial hypertension. *Minerva Cardioangiol.* 50:169-174

Patil N, Berno AJ, Hinds DA, Barrett WA, Doshi JM, Hacker CR, Kautzer CR, Lee DH, Marjoribanks C, McDonough DP, Nguyen BT, Norris MC, Sheehan JB, Shen N, Stern D, Stokowski RP, Thomas DJ, Trulson MO, Vyas KR, Frazer KA, Fodor SP, Cox DR. 2001. Blocks of limited haplotype diversity revealed by high-resolution scanning of human chromosome 21. *Science* 294:1719-1723

Paul M, Schunkert H, Allen P, Dzau VJ. 1990. Widespread distribution of angiotensin converting enzyme mRNA in human tissues. *J Hypertens.* 8(suppl 3):S36

Paul M, Wagner J, Dzau VJ. 1993. Gene expression of the components of the renin-angiotensin system in human tissues: quantitative analysis by the polymerase chain reaction. *J Clin Invest.* 91:2058–2064

Paul M, Stoll M, Falkenhahn M Kreutz R. 1996. Cellular localization of angiotensin converting enzyme gene expression in the heart. *Basic Res Cardiol.* 91:57–65

Paul M, Mehr A, Kreutz R. 2006. Physiology of local renin-angiotensin systems. *Physiol Rev.* 86:747-803

Perkins MJ, Van Driest SL, Ellsworth EG, Will ML, Gersh BJ, Ommen SR, Ackerman MJ. 2005. Gene-specific modifying effects of pro-LVH polymorphisms involving the renin-angiotensin-aldosterone system among 389 unrelated patients with hypertrophic cardiomyopathy. *Eur Heart J*. 26:2457-2462

Perneger TV. 1998. What's wrong with Bonferroni adjustments. *BMJ* 316:1236-1238

Pfeufer A, Osterziel KJ, Urata H, Brock G, Schuster H, Wienker T, Dietz R, Luft FC. 1996. Angiotensin-converting enzyme and heart chymase gene polymorphisms in hypertrophic cardiomyopathy. *Am J Cardiol*. 78:362-364

Pilia G, Chen WM, Scuteri A, Orru M, Albai G, Dei M, Lai S, Usala G, Lai M, Loi P, Mameli C, Vacca L, Deiana M, Olla N, Masala M, Cao A, Najjar SS, Terracciano A, Nedorezov T, Sharov A, Zonderman AB, Abecasis GR, Costa P, Lakatta E, Schlessinger D. 2006. Heritability of cardiovascular and personality traits in 6 148 Sardinians. *PLoS Genet*. 2:e132

Pitt B, Zannad F, Remme WJ, Cody R, Castaigne A, Perez A, Palensky J, Wittes J. 1999. The effect of spironolactone on morbidity and mortality in patients with severe heart failure. Randomized Aldactone Evaluation Study Investigators. *N Engl J Med*. 341:709-717

Pitt B, Remme W, Zannad F, Neaton J, Martinez F, Roniker B, Bittman R, Hurley S, Kleiman J, Gatlin M. 2003. Eplerenone, a selective aldosterone blocker, in patients with left ventricular dysfunction after myocardial infarction. *N Engl J Med*. 348:1309-1321

Poch E, González D, Giner V, Bragulat E, Coca A, De la Sierra A. 2001. Molecular basis of salt sensitivity in human hypertension: evaluation of renin-angiotensin-aldosterone system gene polymorphisms. *Hypertension* 38:1204-1209

Poetter K, Jiang H, Hassanzadeh S, Master SR, Chang A, Dalakas MC, Rayment I, Sellers JR, Fananapazir L, Epstein ND. 1996. Mutations in either the essential or regulatory light chains of

myosin are associated with a rare myopathy in human heart and skeletal muscle. *Nat Genet.* 13:63-69

Pogwizd SM, Sipido KR, Verdonck F, Bers, DM. 2003. Intracellular Na in animal models of hypertrophy and heart failure: contractile function and arrhythmogenesis. *Cardiovasc Res.* 57:887-896

Pokharel S, van Geel PP, Sharma UC, Cleutjens JP, Bohnemeier H, Tian XL, Schunkert H, Crijns HJ, Paul M, Pinto YM. 2004. Increased myocardial collagen content in transgenic rats overexpressing cardiac angiotensin-converting enzyme is related to enhanced breakdown of *N*-acetyl-Ser-Asp-Lys-Pro and increased phosphorylation of Smad2/3. *Circulation* 110:3129–3135

Posen BM, Moolman JC, Corfield VA, Brink PA. 1995. Clinical and prognostic evaluation of familial hypertrophic cardiomyopathy in two South African families with different cardiac beta myosin heavy chain gene mutations. *Br Heart J.* 74:40-46

Pravenec M, Gauguier D, Schott JJ, Buard J, Kren V, Bila V, Szpirer C, Szpirer J, Wang JM, Huang H. 1995. Mapping of quantitative trait loci for blood pressure and cardiac mass in the rat by genome scanning of recombinant inbred strains. *J Clin Invest.* 96:1973–1978

Prescott G, Silversides DW, Reudelhuber TL. 2002. Tissue activity of circulating prorenin. *Am J Hypertens.* 15:280-285

Rajasekaran SA, Barwe SP, Rajasekaran AK. 2005. Multiple functions of Na,K-ATPase in epithelial cells. *Semin Nephrol.* 25:328-334

Ram CV. 2008. Angiotensin receptor blockers: current status and future prospects. *Am J Med.* 121:656-663

Reudelhuber TL, Ramla D, Chiu L, Mercure C, Seidah NG. 1994. Proteolytic processing of human pro-renin in renal and non-renal tissues. *Kidney Int.* 46:1522– 1524

Richard P, Charron P, Carrier L, Ledeuil C, Cheav T, Pichereau C, Benaiche A, Isnard R, Dubourgh O, Burban M, Gueffet JP, Millaire A, Desnos M, Schwartz K, Hainque B, Komajda M. 2003. Hypertrophic cardiomyopathy: distribution of disease genes, spectrum of mutations and implications for a molecular diagnosis strategy. *Circulation* 107:2227-2232

Ritchie RH, Schiebinger RJ, La Pointe MC, March JD. 1998. Angiotensin II-induced hypertrophy of adult rat cardiomyocytes is blocked by nitric oxide. *Am J Physiol.* 275:H1370-H1374

Rogers TB, Gaa ST, Allen IS. 1986. Identification and characterization of functional angiotensin II receptors on cultured heart myocytes. *J Pharmacol Exp Ther.* 236:438-444

Rossier BC, Pradervand S, Schild L, Hummler E. 2002. Epithelial sodium channel and the control of sodium balance: interaction between genetic and environmental factors. *Annu Rev Physiol.* 64:877-897

Sadoshima J, Izumo S. 1993. Molecular characterization of angiotensin II-induced hypertrophy of cardiac myocytes and hyperplasia of cardiac fibroblasts: critical role of the AT1 receptor subtype. *Circ Res.* 73:413-423

Saris JJ, Derkx FH, Lamers JM, Saxena PR, Schalekamp MA, Danser AH. 2001. Cardiomyocytes bind and activate native human prorenin: role of soluble mannose 6-phosphate receptors. *Hypertension* 37:710-715

Saris JJ, 't Hoen PAC, Garrelds IM, Dekkers DHW, den Dunnen JT, Lamers JMJ, Danser AHJ. 2006. Prorenin induces intracellular signaling in cardiomyocytes independently of angiotensin II. *Hypertension* 48:564-571

Satoh M, Takahashi M, Sakamoto T, Hirle M, Marumo F, Kimura A. 1999. Structural analysis of the titin gene in HCM: identification of a novel disease gene. *Biochem Biophys Res Commun.* 262:411-417

Schieffer B, Drexler H, Ling BN, Marrero MB. 1997. G proteincoupled receptors control vascular smooth muscle cell proliferation via pp60c-src and p21ras. *Am J Physiol Cell Physiol.* 272:C2019–C2030

Schiller NB, Shah PM, Crawford M, DeMaria A, Devereux R, Feigenbaum H, Gutgesell H, Reichek N, Sahn D, Schnittger I. 1989. Recommendations for quantitation of the left ventricle by two-dimensional echocardiography. American Society of Echocardiography Committee on Standards, Subcommittee on Quantitation of Two-Dimensional Echocardiograms. *J Am Soc Echocardiogr.* 2:358-367

Schmieder RE, Schlaich MP, Klingbeil AU, Martus P. 1998. Update on reversal of left ventricular hypertrophy in essential hypertension (a meta-analysis of all randomized double-blind studies until December 1996). *Nephrol Dial Transplant.* 13:564-569

Schmieder RE, Erdmann J, Delles C, Jacobi J, Fleck E, Hilgers K, Regitz-Zagrosek V. 2001. Effect of the angiotensin II type 2-receptor gene (+1675 G/A) on left ventricular structure in humans. *J Am Coll Cardiol.* 37:175-182

Schmitz C, Gotthardt M, Hinderlich S, Leheste JR, Gross V, Vorum H, Christensen EI, Luft FC, Takahashi S, Willnow TE. 2000. Normal blood pressure and plasma renin activity in mice lacking the renin-binding protein, a cellular renin inhibitor. *J Biol Chem.* 275:15357-15362

Schoenhard JA, Asselbergs FW, Poku KA, Stocki SA, Gordon S, Vaughan DE, Brown NJ, Moore JH, Williams SM. 2008. Male–female differences in the genetic regulation of t-PA and PAI-1 levels in a Ghanaian population. *Hum Genet.* Oct 25 (Epub ahead of print)

Schwinger RH, Wang J, Frank K, Muller-Ehmsen J, Brixius K, McDonough AA, Erdmann E. 1999. Reduced sodium pump alpha1, alpha3, and beta1-isoform protein levels and Na⁺,K⁺-ATPase activity but unchanged Na⁺-Ca²⁺ exchanger protein levels in human heart failure. *Circulation* 99:2105-2112

Schunkert H, Dzau VJ, Tang SS, Hirsch AT, Apstein CS, Lorell BH. 1990. Increased rat cardiac angiotensin converting enzyme activity and mRNA expression in pressure overload left ventricular hypertrophy. *J Clin Invest.* 86:1913–1920

Schunkert H, Hense HW, Holmar SR, Stender M, Perz S, Keil U, Lorell BH, Riegger GA. 1994. Association between a deletion polymorphism of the angiotensin-converting enzyme and left ventricular hypertrophy. *N Eng J Med.* 330:1634-1638

Schunkert H, Sadoshima J, Cornelius T, Kagaya Y, Weinberg EO, Izumo S, Riegger G, Lorell BH. 1995. Angiotensin II-induced growth responses in isolated adult rat hearts. Evidence for load-independent induction of cardiac protein synthesis by angiotensin II. *Circ Res.* 76:489-497

Schunkert H, Hense HW, Muscholl M, Luchner A, Kürzinger S, Danser AHJ, Riegger GA .1997. Associations between circulating components of the renin-angiotensin-aldosterone system and left ventricular mass. *Heart* 77:24–31

Schunkert H, Brockel U, Hengstenberg C, Luchner A, Muscholl MW, Kurzidim K, Kuch B, Doring A, Riegger GAJ, Hense H. 1999. Familial predisposition of left ventricular hypertrophy. *J Am Coll Cardiol.* 33:1685-1691

Schwinger RHG, Bundgaard H, Muller-Ehmsen J, Kjeldsen K. 2003. The Na, K-ATPase in the failing human heart. *Cardiovasc Res.* 57:913-920

Sebkhi A, Zhao L, Lu L, Haley CS, Nunez DJ, Wilkins MR. 1999. Genetic determination of cardiac mass in normotensive rats: results from an F344xWKY cross. *Hypertension* 33:949-953

Seidman JG, Seidman CE. 2001. The genetic basis for cardiomyopathy: from mutation identification to mechanistic paradigms. *Cell* 104:557-567

Semsarian C, Healey MJ, Fatkin D, Giewat M, Duffy C, Seidman CE, Seidman JG. 2001. A polymorphic modifier gene alters the hypertrophic response in a murine model of familial hypertrophic cardiomyopathy. *J Mol Cell Cardiol.* 33:2055-2060

Sepehrdad R, Chander PN, Oruene A, Rosenfeld L, Levine S, Stier CT. 2003. Amiloride reduces stroke and renal injury in stroke-prone hypertensive rats. *Am J Hypertens.* 16:312-318

Sepehrdad R, Chander PN, Singh G, Stier CT. 2004. Sodium transport antagonism reduces thrombotic microangiopathy in stroke-prone spontaneously hypertensive rats. *Am J Physiol Renal Physiol.* 286:1185-1192

Shamraj OI, Grupp IL, Grupp G, Melvin D, Gradoux N, Kremers W, Lingrel JB, De Pover A. 1993. Characterisation of Na/K-ATPase, its isoforms, and the inotropic response to ouabain in isolated failing human hearts. *Cardiovasc Res.* 27:2229-2237

Shi PP, Cao XR, Sweezer FM, Kinney TS, Williams NR, Husted RF, Nair R, Weiss RM, Williamson RA, Sigmund CD, Snyder PM, Staub O, Stokes JB, Yang B. 2008. Salt-sensitive hypertension and cardiac hypertrophy in mice deficient in the ubiquitin ligase Nedd4-2. *Am J Physiol Renal Physiol.* 295:F462-F470

Shull GE, Schwartz A, Lingrel JB. 1985. Amino-acid sequence of the catalytic subunit of the (Na⁺ + K⁺)ATPase deduced from a complementary DNA. *Nature* 316:691-695

Simon DK, Johns DR. 1999. Mitochondrial disorders: clinical and genetic features. *Annu Rev Med.* 50:111-127

Sipido KR, Volders PGA, Vos MA, Verdonck F. 2002. Altered Na/Ca exchange activity in cardiac hypertrophy and heart failure: a new target for therapy? *Cardiovas Res.* 53:782-805

Sobel E, Sengul H, Weeks DE. 2001. Multipoint estimation of identity-by-descent probabilities at arbitrary positions among marker loci on general pedigrees. *Hum Hered* 52:121-131

Solomon SD, Wolff SA, Watkins H, Ridker PM, Come P, McKenna WJ, Seidman CE, Lee RT. 1993. Left ventricular hypertrophy and morphology in familial hypertrophic cardiomyopathy associated with mutations of the beta-myosin heavy chain gene. *J Am Coll Cardiol*. 22:498-505

Spirito P, Maron BJ. 1989. Relation between extent of left ventricular hypertrophy and age in patients with hypertrophic cardiomyopathy. *J Am Coll Cardiol*. 13:820-823

Spirito P, Maron BJ. 1990. Relation between extent of left ventricular hypertrophy and diastolic filling abnormalities in hypertrophic cardiomyopathy. *J Am Coll Cardiol*. 15:808-813

Spirito P, Seidman CE, McKenna WJ, Maron BJ. 1997. The management of hypertrophic cardiomyopathy. *N Engl J Med*. 336:775-785

Stella P, Bigatti G, Tizzoni L, Barlassina C, Lanzani C, Bianchi G, Cusi D. 2004. Association between aldosterone synthase (CYP11B2) polymorphism and left ventricular mass in human essential hypertension. *J Am Coll Cardiol*. 43:265–270

Stockland JD. 2002. New ideas about aldosterone signaling in epithelia. *Am J Physiol Renal Physiol*. 282:F559–F576

Stowasser M, Gordon RD. 2006. Monogenic mineralocorticoid hypertension. *Best Pract Res Clin Endocrinol Metab*. 20:401-420

Su YR, Menon AG. 2001. Epithelial sodium channels and hypertension. *Drug Metab Dispos*. 29:553-556

Takahashi S, Ohsawa T, Miura R, Miyake Y. 1983. Purification of high molecular weight (HMW) renin from porcine kidney and direct evidence that the HMW renin is a complex of renin with renin binding protein (RnBP). *J Biochem.* 93:265-274

Takahashi S, Inoue H, Fukui K, Miyake Y. 1994. Structure and function of renin binding protein. *Kidney Int.* 46:1525-1527

Takahashi S, Takahashi K, Kaneko T, Ogasawara H, Shindo S, Kobayashi M. 1999. Human renin-binding protein is the enzyme N-acetyl-D-glucosamine 2-epimerase. *J Biochem.* 125:348-353

Tannin GM, Agarwal AK, Monder C, New MI, White PC. 1991. The human gene for 11 β - hydroxysteroid-dehydrogenase. Structure, tissue distribution, and chromosomal location. *J Biol Chem.* 266:16653-16658

Teiwes J, Toto RD. 2007. Epithelial sodium channel inhibition in cardiovascular disease. *Am J Hypertens.* 20:109-117

Thierfelder L, Watkins H, MacRae C, Lamas R, McKenna W, Vosberg HP, Seidman JG, Seidman CE. 1994. Alpha-tropomyosin and cardiac troponin T mutations cause familial hypertrophic cardiomyopathy: a disease of the sarcomere. *Cell* 77:701-712

Tian XL, Pinto YM, Costerousse O, Franz WM, Lippoldt A, Hoffmann S, Unger T, Paul M. 2004. Over-expression of angiotensin converting enzyme-1 augments cardiac hypertrophy in transgenic rats. *Hum Mol Genet.* 13:1441-1450

Tsoutsman T, Lam L, Semsarian C. 2006. Genes, calcium and modifying factors in hypertrophic cardiomyopathy. *Clin Exp Pharmacol Physiol.* 36:139-145

Tsujita Y, Iwai N, Tamaki S, Nakamura Y, Nishimura M, Kinoshita M. 2000. Genetic mapping of quantitative trait loci influencing left ventricular mass in rats. *Am J Physiol Heart Circ Physiol.* 279:2062-2067

Tsutumi Y, Matsubara H, Ohkubo N, Mori Y, Nozawa Y, Murasawa S, Kijima K, Maruyama K, Masaki H, Moriguchi Y, Shibasaki Y, Kamihata H, Inada M, Iwasaka T. 1998. Angiotensin II type 2 receptor is upregulated in human heart with interstitial fibrosis and cardiac fibroblasts are the major cell type for its expression. *Circ Res.* 83:1035-1046

Tsybouleva N, Zhang L, Chen S, Patel R, Lutucuta S, Nemoto S, De Freitas G, Entman M, Carabello BA, Roberts R, Marian AJ. 2004. Aldosterone, through novel signaling proteins, is a fundamental molecular bridge between the genetic defect and the cardiac phenotype of hypertrophic cardiomyopathy. *Circulation* 109:1284-1291

Unger T, Chung O, Csikos T, Culman J, Gallinat S, Gohlke P, Hohle S, Meffert S, Stoll M, Stroth U, and Zhu YZ. 1996. Angiotensin receptors. *J Hypertens Suppl.* 14:S95-S103

Unger T. 2002. The role of the renin-angiotensin system in the development of cardiovascular disease. *Am J Cardiol.* 89(suppl):3A-10A

Urata H, Healy B, Stewart RW, Bumpus FM, Husain A. 1989. Angiotensin II receptors in normal and failing human hearts. *J Clin Endocrinol Metab.* 69:54-66

Van der Merwe L, Cloete R, Revera M, Heradien M, Goosen A, Corfield V, Brink P, Moolman-Smook JC. 2008. Genetic variation in angiotensin-converting enzyme 2 gene is associated with extent of left ventricular hypertrophy in hypertrophic cardiomyopathy. *Hum Genet.* 124:57-61

Van Driest SL, Ommen SR, Tajik AJ, Gersh BJ, Ackerman MJ. 2005. Yield of genetic testing in hypertrophic cardiomyopathy. *Mayo Clin Proc.* 80:739-744

Van Kesteren CA, Van Heugten HA, Lamers JM, Saxena PR, Schalekamp MA, Danser AH. 1997. Angiotensin II-mediated growth and antigrowth effects in cultured neonatal rat cardiac myocytes and fibroblasts. *J Mol Cell Cardiol.* 29:2147-2157

Varnava AM, Elliot PM, Baboonian C, Davison F, Davies MJ, McKenna WJ. 2001. Hypertrophic cardiomyopathy: histopathological features of sudden death in cardiac troponin T disease. *Circulation* 104:1380-1384

Veniant M, Menard J, Bruneval P, Morley S, Gonzales MF, Mullins J. 1996. Vascular damage without hypertension in transgenic rats expressing prorenin exclusively in the liver. *J Clin Invest.* 98:1966-1970

Verdecchia P, Schillaci G, Borgioni C, Ciucci A, Gattobigio R, Zampi I, Reboldi G, Porcellati C. 1998. Prognostic significance of serial changes in left ventricular mass in essential hypertension. *Circulation* 97:48-54

Verdecchia P, Porcellati C, Reboldi G, Gattobigio R, Borgioni C, Pearson TA, Ambrosio G. 2001. Left ventricular hypertrophy as an independent predictor of acute cerebrovascular events in essential hypertension. *Circulation* 104:2039-2044

Verdonck F, Volders PGA, Vos MA, Sipido KR. 2003. Intracellular Na⁺ and altered Na⁺ transport mechanisms in cardiac hypertrophy and failure. *J Mol Cell Cardiol.* 35:5-25

Verhaaren HA, Schienken RM, Mosteller M, Hewitt JK, Eaves LJ, Nance WE. 1991. Bivariate genetic analysis of left ventricular mass and weight in pubertal twins (The Medical College of Virginia Twin Study). *Am J Cardiol.* 68:661-668.

Wada H, Zile MR, Ivester CT, Cooper GT, McDermott PJ. 1996. Comparative effects of contraction and angiotensin II on growth of adult feline cardiomyocytes in primary culture. *Am J Physiol.* 271:H29-H37

Wang J, Schwinger RH, Frank K, Muller-Ehmsen J, Martin-Vasallo P, Pressley TA, Xiang A, Erdmann E, McDonough AA. 1996. Regional expression of sodium pump subunits isoforms and Na⁺-Ca⁺⁺ exchanger in the human heart. *J Clin Invest.* 98:1650-1658

Warnecke C, Willich T, Holzmeister J, Bottari SP, Fleck E, Regitz-Zagrosek V. 1999. Efficient transcription of the human angiotensin II type 2 receptor gene requires intronic sequence elements. *Biochem J.* 340:17-24

Watkins H, Rosenzweig A, Hwang DS. 1992. Characteristics and prognostic implications of myosin missense mutations in familial hypertrophic cardiomyopathy. *N Engl J Med.* 326:1108-1114

Watkins H, Seidman JG, Seidman CE. 1995a. Familial hypertrophic cardiomyopathy: a genetic model of cardiac hypertrophy. *Hum Mol Genet.* 4:1721-1727

Watkins H, Conner D, Thierfelder J, Jarcho JA, MacRae C, McKenna WJ, Maron BJ, Seidman JG, Seidman CE. 1995b. Mutations in the cardiac myosin binding protein-C gene on chromosome 11 cause familial hypertrophic cardiomyopathy. *Nat Genet.* 11:434-437

Weinberg EO, Schoen FJ, George D, Kagaya Y, Douglas PS, Litwin SE, Schunkert H, Benedict CR, Lorell BH. 1994. Angiotensin converting enzyme inhibition prolongs survival and modifies the transition to heart failure in rats with pressure overload hypertrophy due to ascending aortic stenosis. *Circulation* 90:1410-1422

West MJ, Summers KM, Huggard PR. 1992. Polymorphisms of candidate genes in essential hypertension. *Clin Exp Pharmacol Physiol.* 19:315-318

Wharton J, Morgan K, Rutherford RAD, Catravas JD, Chester A, Whitehead BF, De Leval MR, Jacoub HM, Pollack JM. 1998. Differential distribution of AT₂ receptors in the normal and failing human heart. *J Pharmacol Exp Ther.* 284:323-336

Wigle ED. 1995. Novel insights into the clinical manifestations and treatment of hypertrophic cardiomyopathy. *Curr Opin Cardiol*.10:299-305

Wigle ED, Sasson Z, Henderson MA, Ruddy TD, Fulop J, Rakowski H, Williams WG. 1985. Hypertrophic cardiomyopathy. The importance of the site and the extent of hypertrophy. A review. *Prog Cardiovasc Dis*. 28:1-83

Wong ZYH, Stebbing M, Ellis JA, Lamantia A, Harrap SB. 1999. Genetic linkage of beta and gamma subunit of epithelial sodium channel to systolic blood pressure. *Lancet* 53:1222-1225

Xie Z, Kometiani P, Liu J, Li J, Shapiro JJ, Askari A. 1999. Intracellular reactive oxygen species mediate the linkage of Na⁺/K⁺-ATPase to hypertrophy and its marker genes in cardiac myocytes. *J Biol Chem*. 274:19323-19328

Zhang W, Collins A, Maniatis N, Tapper W, Morton NE. 2002. Properties of linkage disequilibrium (LD) maps. *Proc Natl Acad Sci USA*. 99:17004-17007

Zhang K, Calabrese P, Nordborg M, Sun F. 2002a. Haplotype block structure and its applications in association studies: Power and study design. *Am J Hum Genet*. 71:1386-1394

Zhang Y, Zhang K, Wang G, Huang W, Zhu D. 2003. Angiotensin II type 2 receptor gene polymorphisms and essential hypertension. *Acta Pharmacol Sin*. 24:1089-1093

Zhang K, Qin ZS, Liu JS, Chen T, Waterman MS, Sun F. 2004. Haplotype block partitioning and tag SNP selection using genotype data and their applications to association studies. *Genome Res*. 14:908-916

Zhang M, Ma H, Wang B, Zhao Y. 2006. Angiotensin II type 2 receptor gene polymorphisms and cardioprotective role in essential hypertension. *Heart Vessels* 21:95-101

Zhang Q, Saito Y, Naya N, Imagawa K, Somekawa S, Kawata H, Takeda Y, Uemura S, Kishimoto I, Nakao K. 2008. The specific mineralocorticoid receptor blocker eplerenone attenuates left ventricular remodeling in mice lacking the gene encoding Guanylyl Cyclase-A. *Hypertens Res.* 31:1251-1256

Zwandlo C, Borlak J. 2005. Disease-associated changes in the expression of ion channels, ion receptors, ion exchangers and Ca²⁺-handling proteins in heart hypertrophy. *Toxicol Appl Pharmacol.* 207:244-256